Universidad Autónoma de Madrid

Departamento de Bioquímica

microRNAs link the Germinal Center reaction and B cell lymphomagenesis

PhD Thesis

Nahikari Bartolomé Izquierdo

Madrid, 2016

Departamento de Bioquímica

Facultad de Medicina

Universidad Autónoma de Madrid

microRNAs link the Germinal Center reaction and B cell lymphomagenesis

Memoria presentada por la licenciada en Bioquímica

Nahikari Bartolomé Izquierdo

para optar al título de Doctor por la Universidad Autónoma de Madrid

Directores de tesis:

Dra. Almudena R. Ramiro

Dra. Virginia García de Yébenes

Este trabajo ha sido realizado en el laboratorio de Linfocitos B,

en Centro Nacional de Investigaciones Cardiovasculares (CNIC)

Madrid, 2016

ABSTRACT

Germinal centers (GC) are microstructures where B cells that have been activated by antigen undergo a developmental program that involves the somatic diversification of their immunoglobulin genes and intense proliferative activity coupled to apoptotic selective events. As a result, from GCs emerge plasma cells and memory B cells that bear immunoglobulins with higher affinity for the initiating antigen and with more versatile effector functions. While ensuring a competent humoral immune response, GCs are also a site particularly prone to neoplastic transformation. Indeed, the vast majority of human lymphomas arise from GC-experienced B cells.

MicroRNAs (miRNAs) are small non-coding RNA molecules that regulate gene expression post-transcriptionally. In the past years miRNAs have arisen as key regulators of the immune function, however little is known of their role in GC B cells. In this work, we have identified miR-217 and miR-28 as GC microRNAs and have explored their functional impact in GC events and in B cell lymphomagenesis.

We observed that miR-217 is a positive modulator of the GC response that boosts immunoglobulin diversification, i.e. the generation of class-switched antibodies and the frequency of somatic hypermutation. We found that miR-217 dampens the expression of a DNA damage response and repair gene network and in turn stabilizes Bcl-6 expression in GC B cells. Importantly, miR-217 overexpression also promotes mature B-cell lymphomagenesis; this is physiologically relevant as we find that miR-217 is overexpressed in aggressive human B-cell lymphomas.

In contrast, miR-28 acts as a negative regulator of the GC response that impairs B cell proliferation and survival through the regulation of a BCR signaling gene network. In addition, we found that miR-28 expression is lost in a wide range of GC-derived human malignancies. Further, miR-28 re-expression dramatically inhibits tumor growth in various lymphoma models, suggesting that miR-28 is a tumor suppressor for GC-derived neoplasias.

Together, we have found that miR-217 and miR-28 provide antagonistic regulatory roles of the GC reaction that are intimately intertwined with pathways leading to B cell transformation. In addition, our results open new perspectives for the development of a novel therapeutic strategy for the treatment of B cell tumors based on miR-28 replacement.

RESUMEN

Los centros germinales (CG) son microestructuras donde las células B que han sido activadas por antígeno llevan a cabo un programa madurativo que implica la diversificación somática de los genes de inmunoglobulinas y una intensa actividad proliferativa asociada con procesos de selección apoptóticos. Como resultado, de los CG emergen células plasmáticas y células B memoria que portan inmunoglobulinas con mayor afinidad por el antigeno iniciador, y con mayor versatilidad funcional. Aunque aseguran la eficiencia de la respuesta inmune humoral, los CG son también un entorno particularmente propenso a la transformación maligna. De hecho, la inmensa mayoría de los linfomas humanos tienen su origen en células B que han pasado por un CG.

Los microRNAs (miRNAs) son moléculas de RNAs pequeñas y no codificantes que regulan la expresión génica post-transcripcionalmente. En los últimos años los miRNAs han surgido como reguladores clave de la función inmune, pero se sabe muy poco de su función en células B de CGs. En este trabajo hemos identificado a miR-217 y miR-28 como miRNAs de CG y hemos explorado su impacto funcional en los procesos asociados a CGs y a la linfomagénesis B.

Observamos que miR-217 es un modulador positivo de la respuesta de CG que aumenta la diversificación de anticuerpos, es decir, la generación de cambio de isotipo y la hipermutación somática. Encontramos que miR-217 amortigua la expresión de una red de genes implicados en la respuesta al daño y la reparación del DNA y a su vez estabiliza la expresión de Bcl-6 en células B de CG. Además, la sobreexpresión de miR-217 induce la generación de linfomas B; esta observación es relevante fisiológicamente porque encontramos que miR-217 está sobre-expresado en ciertos linfomas B humanos.

Por el contrario, miR-28 actúa como un regulador negativo de la respuesta de CG, que disminuye la proliferación y la supervivencia de las células B mediante la regulación de la señalización a través del BCR. También encontramos que la expresión de miR-28 se pierde en un amplio espectro de neoplasias derivadas de CGs. Finalmente, la re-expresión de miR-28 produce una inhibición dramática en el crecimiento tumoral en diversos modelos de linfoma, lo que sugiere que miR-28 es un supresor de tumores en neoplasias derivadas de CG.

En conjunto, hemos encontrado que miR-217 y miR-28 tienen funciones antagónicas en la regulación del CG y que estas están íntimamente relacionadas con los mecanismos que dan lugar a la transformación de las células B . Además, nuestros resultados abren nuevas posibilidades para el desarrollo de estrategias terapéuticas para el tratamiento de linfomas B, basadas en la re-expresión de miR-28.

INDEX

Abbreviation	Full name
ABC-DLBCL	Activated B cell like Diffuse Large B cell lymphoma
AID	Activation Induced cytidine Deaminase
Bcl-2	B-cell lymphoma 2
Bcl-6	B-cell lymphoma 6
BCR	B cell receptor
BL	Burkitt Lymphoma
BLIMP1	B-lymphocyte-induced maturation protein1
CD3	Cluster of differentiation 3
CLL	Chronic lymphocytic leukemia
CSR	Class Switch Recombination
DLBCL	Diffuse Large B Cell Lymphoma
DOX	Doxycycline
DZ	Dark Zone
ERK	Extracellular Signal-Regulated Kinase
FL	Follicular Lymphoma
GC	Germinal Center
GC-DLBCL	Germinal Center B cell like Diffuse large B cell lymphoma
GFP	Green fluorescent protein
GO	Gene Ontology
H&E	Hematoxilin and eosin
Ig	Inmunoglobulin
IKKB	Inhibitor of Nuclear Factor Kappa-B Kinase Subunit Beta
IL4	Interleuchine four
IRES	Internal ribosome entry site
IRF4	Interferon responding factor four
LPS	Lipopolisacharide
LZ	Light Zone
MCL	Mantle cell lymphoma
miRNA	microRNA
MZL	Marginal Zone B cell lymphoma
NF-KB	Nuclear Factor Kappa-B
NGS	Next generation sequencing
NP-CGG	nitrophenyl hapten-coupled chicken gamma-globulin
NSG	NOD Scid Gamma
ORF	Open reeding frame
PAX5	Paired box 5
PCT	Plasmacytoma
PI	Proliferation index
RFP	Red fluoresecent protein
SBL	Small B cell lymphoma
SHM	Somatic Hyper Mutation
SRBC	Sheep red blood cells
T_{FH}	T follicular helper
UTR	Untranslated region
XBP1	X-Box Binding Protein 1

INTRODUCTION

1. B cell differentiation and function

1.1. Immune system: innate immunity and adaptive immunity

The immune system is composed of the cells and molecules in charge of defending the organism against infection. There are two fundamental arms in the immune system. Innate (natural) immunity provides a first line of rapid response against common microorganisms; it does not require previous exposure to the infectious agent and it does not evolve with subsequent infections. Innate immunity involves phagocytic cells, cells that release inflammatory mediators and natural killer cells, as well as the complement system, acute-phase proteins, and cytokines such as the interferons. In contrast, acquired (adaptive) immunity occurs during the lifetime of an individual as an adaptation to infection with any given pathogen; it is thus a more specialized barrier against infection and confers immunological memory. B and T lymphocytes are the effector cells in adaptive immunity. Their activity relies on the expression of surface receptors that can recognize specific molecular structures present on the pathogens, called antigens. In the case of T cells the antigen receptor is called T cell receptor (TCR) and in the case of B cells the receptor is called B cell receptor (BCR). While T cells mediate cellular immunity against intracellular pathogens, B cells are specialized in generating antibodies –the secreted form of the BCR- and thus mount humoral responses against extracellular pathogens.

1.2. B cell differentiation and antibody diversification

Each individual B cell expresses a single BCR with unique antigen specificity such that the pool of mature B cells is capable of producing antibodies that specifically recognize and respond to virtually any foreign antigen. The generation of this hugely diverse repertoire of BCR specificities is achieved through the somatic diversification of immunoglobulin genes during B cell differentiation in the bone marrow, and is subsequently completed as a consequence of antigen encounter in Germinal Centers (GC).

The BCR is composed of two identical immunoglobulin heavy (IgH) chains and two identical immunoglobulin light (IgL) chains. The N-terminus of IgH and IgL encode the variable region of the immunoglobulins and is responsible of the antigenic recognition. The C-terminus of IgH encodes the constant region, which determines the antigen clearance via. The BCR receptor is the main modulator of B cell physiology, and the engagement of an antigen into the BCR can lead to different responses, including proliferation, cell death or further differentiation depending of the signal strength and spatial-temporal contexts (Niiro and Clark 2002).

1.2.1- Early B cell differentiation and primary antibody diversification

The genes encoding antibody variable regions are composed of groups of gene segments called *Variable* (V), *Diversity* (D), and *Joining* (J) for the IgH locus or V and J for the IgL locus. During B-cell differentiation, a segment from each V (D) and J group is assembled to give rise to a specific VDJ (or VJ) rearrangement; this combinatorial event generates the diversity of the primary antibody repertoire. Assembly of antibody genes takes place through a process of site-specific recombination called V(D)J recombination that involves the introduction of DNA double-strand breaks (DSBs) at specific recognition signal sequences (RSS) flanking the V, D, and J elements by recombination activating genes (RAG1 and RAG2), followed by repair. Developing B cells in the bone marrow (or fetal liver) first assemble their IgH locus in two successive steps, D_HJ_H and $V_HD_HJ_H$, at the so-called progenitor B (pro-B) stage. Pro-B cells that achieve a productive IgH rearrangement express an Igμ chain together with the surrogate chains λ5 and VpreB (pre-BCR). pre-BCR expression leads to a phase of vigorous clonal cell expansion of precursor B (pre-B) cells and the subsequent rearrangement of the IgL locus by an analogous VDJ recombination event. As a result, a mature BCR is expressed for the first time in immature B cells, which are then ready to leave the bone marrow and join the peripheral pool of functional B cells.

Given the stochastic nature of V(D)J recombination, this developmental process is coupled to selective events that guarantee that only cells where a rearrangement has given rise to a functional pre-BCR and BCR receive the appropriate survival signals, whereas the rest undergo apoptosis. In addition, central and peripheral tolerance checkpoints ensure the elimination or inactivation of B cells expressing BCRs with self-reactive specificities (Rajewsky 1996).

1.2.2- The Germinal Center reaction and secondary antibody diversification

Unlike T cells, B cells have a second opportunity to further diversify their primary antibody repertoire after antigen encounter. When a mature B cell in the periphery encounters an antigen, it can engage in the Germinal Center (GC) reaction, a complex biological process that is absolutely required to generate antibody secreting plasma cells (PC) and long lived memory B cells that are highly specific for the antigen that elicited the response. GCs are transient microstructures that form within B-cell follicles of secondary lymphoid tissues to enable immunoglobulin affinity maturation in response to T-cell-dependent antigens. Within GCs, B cells undergo clonal expansion and two molecular processes named somatic hypermutation (SHM) and class switch recombination (CSR). SHM involves the introduction of mutations, usually single-nucleotide substitutions, in the V(D)J rearranged variable region of the IgH and IgL chains, thus allowing the production of BCRs with a higher affinity for antigen. Only those B cells in which SHM results in the generation of BCRs with improved affinity for their cognate antigen survive

and proliferate. CSR is a region-specific recombination reaction that replaces the primary μ constant region with a downstream constant region, giving rise to antibodies with different isotypes and therefore new capabilities for antigen removal.

SHM and CSR are both initiated by activation-induced deaminase (AID), which deaminates cytosines on the immunoglobulin locus (Fig. 1). This initial lesion on DNA is subsequently processed by DNA repair and recombination factors to allow the fixation of a mutation, in the case of SHM, or the generation of a DNA double-strand break and a recombination reaction, in the case of CSR (reviewed in (Stavnezer, Guikema et al. 2008) (Peled, Kuang et al. 2008) (de Yebenes and Ramiro 2006) (Di Noia and Neuberger 2007). Once these processes are completed, B cells expressing high affinity immunoglobulins are selected for terminal differentiation into antibody secreting PCs (PC) cells or long-lived memory B cells. The efficiency of the GC reaction is facilitated by the specialized GC microenvironment that supports the close interaction and the rapid movements of various cell types in a confined space.

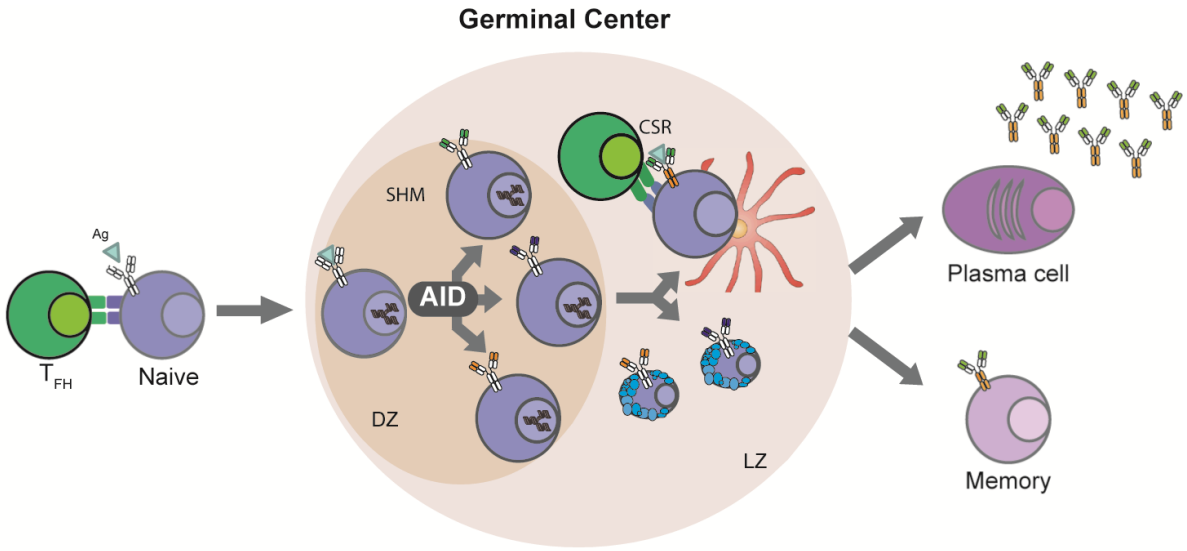

Figure 1. The GC reaction: B cells that have successfully undergone V(D)J recombination and that express functional BCRs migrate as naive B cells from the bone marrow to the secondary lymphoid organs. Upon encounter with an antigen (Ag), naive B cells become activated by interaction with $CD4^+$ T follicular helper (T_{FH}) cells and aggregate into primary follicles to form Germinal Centers (GCs). In the GC, B cells undergo secondary antibody diversification through somatic hypermutation (SHM) and class switch recombination (CSR) reactions. Both reactions are initiated by the activity of activation induced deaminase (AID), which deaminates cytosines on the immunoglobulin gene locus to initiate either a mutation (in SHM) or a recombination reaction (in CSR) and serve to generate cells with high-affinity antibodies and different effector functions. The outcome of the GC reaction is the generation of plasma cells (PC) and long-lived memory B cells with high affinity for the antigen that elicited the response. GCs comprise a dark zone (DZ), where SHM takes place and B cells divide rapidly, and a light zone (LZ) where B cells are in contact with follicular dendritic cells, T cells and macrophages and are selected on the basis of the affinity of their BCRs.

The GC is anatomically divided into a Dark Zone (DZ) and a Light Zone (LZ). In the DZ B cells divide rapidly, upregulate AID expression and undergo SHM of immunoglobulin variable regions generating mutants with altered antibody affinity. In the LZ B cell capture antigen from follicular dendritic cells and compete for limiting T follicular helper cells. Higher affinity cells survive and either re-enter DZ or are exported out of the GC as PC or memory B cell. Lower-affinity GC B cells die by apoptosis and are cleared by macrophages. Thus the GC promotes several interactive rounds of mutation and selection and, following differentiation into post-GC cells, produces a stepwise increase in the antigen affinity of secreted antibodies (De Silva and Klein 2015).

1.3. The GC transcriptional program

The GC reaction is regulated by a number of key transcription regulators that establish a GC specific genetic program and control the timing of the transition from GC B cells to terminal B cell differentiation.

Bcl-6

This BTB-zinc finger transcriptional repressor is considered a master regulator of the GC response. Bcl-6 protein is highly upregulated in GC B cells, where it regulates a broad network of direct target genes involved in various cellular processes. Upregulation of Bcl-6 is essential for initiation of the GC reaction as Bcl-6 deficient GC precursor B cells fail to enter the follicle (Kitano, Moriyama et al. 2011). Conversely, Bcl-6 downregulation by the transcription factor IRF4 (which is induced by NF-κB) represses Bcl-6 (Saito, Gao et al. 2007) to exit the GC reaction and to allow PC differentiation. A critical biological function of Bcl-6 in GC B cells is to facilitate rapid replication and tolerance to the genomic damage occurring during clonal expansion and SHM by directly repressing DNA damage sensing genes and checkpoint genes such as ATR and TP53 and modulating apoptosis in GC B cells (Ranuncolo, Polo et al. 2007) (Phan and Dalla-Favera 2004). Thus, Bcl-6 provides a permissive environment for physiological AID mediated DNA remodeling to occur. Bcl-6 orchestrates other genes to inhibit cell cycle arrest and prevents premature exit from the GC stage by repressing Blimp-1 (Basso and Dalla-Favera 2010) (Basso and Dalla -Favera 2012). In agreement with these functions Bcl-6 deregulation is associated with a fraction of mature B cell neoplasms (see below).

Myc

Myc is a transcription factor with a crucial role in almost all proliferating cells. Myc supports robust proliferation by regulating diverse processes including cell cycle progression, metabolism and telomere maintenance (Dang 2012). Likewise, Myc deregulated expression is oncogenic and has been shown to

be sufficient for the generation of GC-derived lymphoma in a mouse model (Erikson, ar-Rushdi et al. 1983).

Within GCs, c-Myc has been shown to be required for both the formation and maintenance of GCs (Calado, Sasaki et al. 2012) (Dominguez-Sola, Victora et al. 2012). After GC establishment, Myc expression is silenced as a result of transcriptional repression by Bcl-6 (Dominguez-Sola, Victora et al. 2012) (Calado, Sasaki et al. 2012), and Myc expression is almost entirely absent in the proliferating B centroblast until it is re-expressed in a subpopulation of LZ B cells destined to DZ re-entry in established GCs (Basso and Dalla-Favera 2015).

NF-κB

Nuclear factor-κB (NF-κB) is a family of transcription factors that play a pivotal role in regulating B cell survival and proliferation and whose constitutive activation is recurrently found in B cell malignancies. NF-κB activation in B cells occurs transiently downstream of numerous receptors, including the BCR, CD40, the BAFF receptor and various Toll-like receptors. NF-κB transcription factors are formed by homo- and heterodimerization of the subunits p50 (encoded by NF-κB1), p52 (encoded by NF-κB2), p65 (Rel-A), Rel-B, and c-Rel. These factors shuttle between the cytoplasm and the nucleus in a fashion that is regulated by diverse intracellular signaling events. Within GCs NF-κB signaling is required for GC maintenance (Kitano, Moriyama et al. 2011) (Dominguez-Sola, Victora et al. 2012) (Heise, De Silva et al. 2014) and plays an important role in LZ B cells, were NF-κB-mediated upregulation of IRF4 expression results in the repression of Bcl-6 transcription and the termination of the GC-associated transcription program (Saito, Gao et al. 2007), giving rise to terminal B cell differentiation.

IRF4

IRF4 is a member of the interferon regulatory factor superfamily of transcription factors that shows a bimodal pattern of expression during GC reaction. IRF4 expression is induced upon BCR ligation and is required to initiate the GC program (Klein, Casola et al. 2006) (Sciammas, Shaffer et al. 2006). Additionally, IRF4 is needed for isotype switching, as IRF4 deficient mice fail to induce AID and promote CSR (Sciammas, Shaffer et al. 2006) (Klein, Casola et al. 2006). However, IRF4 it is not required for GC maintenance, as deletion in latter points does not impact GC structure (Klein, Casola et al. 2006). Importantly, IRF4 is one of the factors that initiates PC differentiation program, repressing Bcl-6 and inducing Blimp-1. Indeed IRF4 lacking mice fail to generate terminally differentiated PCs (Sciammas, Shaffer et al. 2006).

Blimp-1 and XBP1

Two transcription factors are essential to orchestrate PC differentiation, Blimp-1 (encoded by the gene

PRDM1) and XBP1. Blimp-1 is a transcriptional repressor exclusively expressed in antibody secreting plasmablasts and PCs that shuts down all the transcription factors that were relevant during the previous stages of B cell differentiation and arrests cell cycle to exit GC program (Turner, Mack et al. 1994) (Shaffer, Lin et al. 2002) (Shapiro-Shelef, Lin et al. 2003) (Shapiro-Shelef, Lin et al. 2005). XBP1 acts downstream of Blimp-1 and is not completely required to allow PC generation (Todd, McHeyzer-Williams et al. 2009). Instead, XBP1 provokes the necessary changes in the B cell metabolism and cellular structures to allow the secretion of huge quantities of Ig in the PC by inducing endoplasmic reticulum remodeling, autophagic pathways and the induction of the unfolded protein response (Shaffer, Shapiro-Shelef et al. 2004) (Engel and Barton 2010).

1.4. B cell lymphomas

1.4.1- Classification and etiology

Lymphomas are hematological tumors that have their origin in B or T lymphocytes. The World Health Organization (WHO) established a classification of two main groups of lymphomas: Hodking lymphoma (HL) and non-Hodking lymphoma (NHL). About 90% of the lymphomas are NHLs, comprising a heterogeneous group of malignancies of different biology and prognosis. However, the majority of NHLs are from B cell origin, and more specifically the vast majority of B-NHLs arise from mature antigen experienced GC B cells (Table 1). B cell NHL subtypes include low grade (indolent) slow growing lymphomas and high grade (aggressive), quickly growing lymphomas. Low grade B cell NHLs include follicular lymphoma (FL), mantle cell lymphoma (MCL), marginal zone lymphoma (MZL) and small lymphocytic lymphoma (SLL) B-NHLs. High grade B cell NHLs include Burkitt lymphoma (BL) and diffuse large B cell lymphoma (DLBCL). Based on different molecular characteristics DLBCL are subdivided in two major subtypes; a germinal center B-cell-like subtype (GC-DLBCL) and an activated B-cell-like subtype (ABC-DLBCL). DLBC are the most prevalent form of NHLs, representing one third of all NHLs cases (Staudt and Wilson 2002).

One signature of the GC origin of mature B cell lymphomas is the presence of mutations in the V gene segments of immunoglobulin genes (Klein, Klein et al. 1995) (Rockwood, Torrey et al. 2002) (Greeve, Philipsen et al. 2003) (Basso and Dalla-Favera 2015). However, the major hallmark of mature B-cell lymphomas is the presence of recurrent chromosome translocations that juxtapose one of the Ig loci and a proto-oncogene; such as c-Myc in BL, Bcl-6 in DLBCL or Bcl-2 in FL (Basso and Dalla-Favera 2015) (Table 1). These translocations have been shown to be dependent on AID activity, as they are absent in $AID^{-/-}$ B cells (Ramiro, Jankovic et al. 2004) (Robbiani, Bothmer et al. 2008). As a result of the translocation, expression of the proto-oncogene is deregulated, usually as a consequence of the

transcription driven by Ig regulatory elements. Therefore, translocation events driven by AID are not mere markers of B GC neoplasia; indeed deregulated proto-oncogene expression is critical for the etiology of neoplasia generation (Kovalchuk, Qi et al. 2000) (Cattoretti, Pasqualucci et al. 2005). Thus, AID activity establishes one direct connection between the GC reaction and lymphomagenic transformation.

Table 1. B cell NHL classification and etiology

B cell NHL	Frequency (%)	Origin	Diagnostic molecular features	Genetic aberration	Deregulated pathway	Malignant phenotype
MCL	8	Pre-GC	CyclinD1 t(11;14)	CyclinD1 t(11;14), BMI1, TP53, CDKN2A, Ink4a/ARF, ATM	Bcl-2	S, P, DDR
CLL/SLL	9	Pre-GC and **Post-GC**[ŧ]	ZAP70[¥]	NOTCH1, Myd88, TP53, ATM, miR-15 - miR-16,	BCR, Bcl-2	S, P, DDR, MS, BD
FL	28	**GC**	Bcl-2 t(14;18)	Bcl-2 t(14;18), EZH2, TNFRSF14, Fas, MEF2B, MEF2C, CREBBP; EP300, MLL	BCR	S, P, DDR, MS, BD
BL	1	**GC**	Myc t(8;14)	Myc, miR-17-92, CDKN2A, Ink4a/ARF, TP53		S, P, DDR, MS
ABC-DLBCL	17	**Post-GC**	Gene expression profiling	Myd88, CD79 A and B, Bcl-6 t(3;x), CARD11, Myc, Bcl-2, TP53, CDKN2A, Ink4a/ARF,TNFAIP3, PRDM1	NF-κB, IRF4, Myc, BCR, TLR-Myd88, IL-6;10-JAK/STAT3, IFN1, Bcl-6, Blimp-1	S, P, DDR, MS, BD, IM
GC-DLBCL	19	**GC**	Gene expression profiling	Bcl-2 t(14;18), EZH2, Bcl-6 t(3;x), MDM2, miR-17-92, Myc, MYD88, PTEN, Fas, MEF2B, MEF2C, TP53, MLL2, CREBBP;EP300	Bcl-6, Myc	S, P, DDR, MS, BD, IM
MZL (MALT*)	10	**Post-GC**	AP12-MALT1 t(11;18)	cIAP2-MALT1 t(11;18), MALT t(14;18), Bcl-10, FoxP1, CDKN2A, INK4a/ARF	NF-κB, Chronic infection	S, P, DDR, IM
HCL	1	**Post-GC**	BRAF V600E	BRAF		S, P
PMBL	7	Thymic B cell	Gene expression profiling	JAK2; JMJD2D, PDC1LG2, SOCS1, CIITA, TP53, TNFAIP3,	IL-13-JAK2, NF-κB, Myc	S, DDR, MS, IM

MCL: Mantle cell lymphoma
CLL/SLL: Chronic lymphocytic lymphoma / Small B cell lymphoma
FL: Follicular lymphoma
BL: Burkitt lymphoma
DLBCL-ABC: Diffuse Large B cell lymphoma - Activated cell type
DLBCL-ABC: Diffuse Large B cell lymphoma - Germinal Center cell type
MZL: Marginal zone lymphoma (MALT is mucosal associated lymphoid tissue lymphoma, which is the most common type)*
HCL: Hairy cell leukemia
PMBL: Primary mediastinal B cell lymphoma
¥: ZAP70 is expressed in 50% of CLL/SLL cases.
Ŧ: The origin of CLL is an antigen experienced B cell, that can be mutated (Post-GC origin) or unmutated (Pre-GC origin) in the Ig V region.

Green: Cell cycle regulator
Light blue: Apoptosis
Brown: Genomic integrity
Red: miRNAs
Purple: Epigenetic modifier
Black: Signaling factor
Yellow: Immune regulator
Grey: Transcription factor

S: Survival
P: Proliferation
DDR: DNA damage response
MS: Metabolic switch
BD: Block in differentiation
IM: Immune modulation

1.4.2- Oncogenic signaling

Besides the AID's contribution to genomic instability in GC B cells, very often the mechanisms that drive normal B cell differentiation and activation are frequently subverted by B cell lymphomas for their unlimited growth and survival. The signaling pathways that a normal B cell utilizes to sense antigens are frequently derailed in B cell malignancies, leading to constitutive activation of prosurvival pathways through different molecular mechanisms. In addition, these malignancies co-opt transcriptional regulatory systems that characterize their normal B cell counterparts and frequently alter epigenetic regulators of chromatin structure and gene expression (Table 1).

B cell receptor (BCR) signaling

One of the signaling pathways that has more impact in B cell physiology is BCR signaling. Im-

portantly, key signaling pathways downstream the BCR contribute not only to B cell homeostasis, but also to transformed B cell survival (Sander, Calado et al. 2012). Thus, normal BCR signaling pathways can be hijacked by tumoral B cells to ensure their uncontrolled growth and survival (Küppers 2005) (Rickert 2013) (Young, Shaffer et al. 2015).

Physiological signaling trough the BCR is initiated when the Ig binds the antigen, triggering the phosphorylation of the Immunoreceptor Tyrosine-based Activation Motifs (ITAMs) in the cytoplasmic domains of Igα/Igβ (also known as CD79A and CD79B) and the activation of three kinases: Syk, Lyn and Btk. Adaptor molecules such as BLNK and BAM32 modulate the progression of the signaling pathway with other downstream effector molecules, most notably phosphatidylinositol 3-kinase (PI3K) and phospholipase C gamma 2 (PLCgamma2). In this way, PI3K activation results in the formation of phosphatidylinositol-3,4,5-trisphosphate (PtdInsP3), which, in turn, recruits the protein serine/threonine kinase AKT and the phosphoinositide-dependent kinase 1 (PDK1), to the membrane. Subsequently AKT phosphorylates several substrates, including mTORC1 and forkhead/winged helix box class O (FOXO) proteins (Werner, Hobeika et al. 2010) with the net effect of enhancing growth and suppression of apoptosis (Marshall, Niiro et al. 2000). On the other hand, PLCgamma2 generates inositol-1,4,5-trisphosphate (IP3), and diacylglycerol (DAG), which increase intracellular Ca^{2+} concentration and activates protein kinase C (PKC). This leads in turn to the activation of MAPKs, specifically, ERK, JNK and p38 MAPK, and activation of transcription factors such as NFAT and NF-κB, which have important regulatory functions in B-cell activation, maturation and survival (Fig. 2). Overall, these different activation routes are responsible of different biological outcomes that can be modulated by the BCR (Niiro and Clark 2002) (Rickert 2013).

Signals stemming from the BCR can drive malignant transformation (Rickert 2013) and can involve both tonic (independent of ligand) and antigen-dependent BCR signaling. Human malignant B cells typically maintain expression of the BCR on the cell surface, suggesting that they may utilize the ability of the BCR to engage downstream proliferation and survival pathways (reviewed in (Shaffer, Young et al. 2012)). Notably, pathogenic BCR signaling in lymphoma has a major impact on the ABC subtype of DLBCL, which utilizes a chronic active form of BCR signaling and is dependent on BCR signaling for survival. Abrogation of BCR signaling in ABC-DLBCL impairs lymphoma growth by diminishing NF-κB, AKT, ERK, MAP and NF-AT signaling, in keeping with the known activities of the BCR in normal B cells (Davis, Ngo et al. 2010). Interestingly, many subtypes of B cell NHL also rely (although in a lower grade) in uncontrolled BCR signaling to maintain their viability (Woyach, Johnson et al. 2012) (Blum 2015) (Table 1).

The most common path taken by lymphoid malignancies to avoid cell death is constitutive activation of the NF-κB pathway. The lymphoid malignancies that have been associated with a higher frequency

with an altered NF-κB signaling are ABC-DLBCL, HL and multiple myeloma. NF-κB pathway activates the transcription of an antiapoptotic module, including Bcl-2 family members. NF-κB pathway deregulation in lymphoma occurs through different mechanisms that include activating mutations in the BCR subunits CD79A and CD79B, somatic mutations targeting MyD88 (an adaptor protein in the Toll-like receptor (TLR) pathway), activating mutations in the scaffold protein CARD11 and also hyperactivation of IKKs, which phosphorylate IκBα (that masks the nuclear localization signal (NLS) of NF-κB), thereby promoting its degradation and allowing NF-κB transcription factors to enter the nucleus and exert their function (Staudt 2010) (Davis, Ngo et al. 2010) (Lenz, Davis et al. 2008). Indeed, ABC-DLBCL cells are addicted to constitutive activity of IKKs in such a way that its inhibition is lethal (Lam, Davis et al. 2005) (Ceribelli, Kelly et al. 2014).

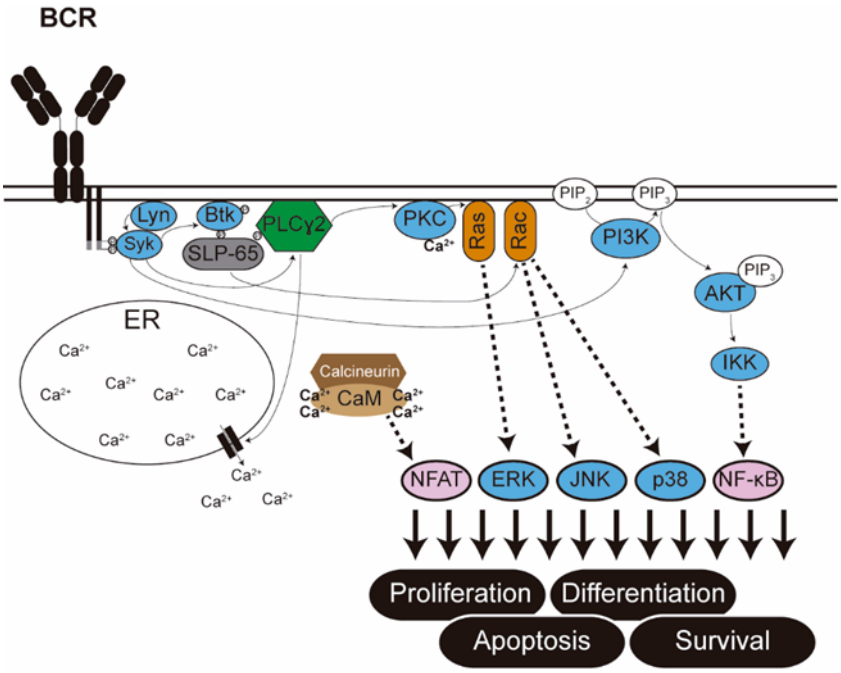

Figure 2. BCR signaling controls B cell physiology: The binding of antigen to the BCR leads to the phosphorylation of three kinases: Syk, Lyn and Btk, which activate different signaling pathways by phosphorylating different substrates. These signaling pathways determine the outcome of the B cell by controlling a myriad of biological functions. PI3K produces PIP3, which leads to AKT recruitment, activating the NF-κB pathway. Phosphorylation of PLCγ2 induces calcium release from the endoplasmic reticulum, which produces the activation of the NFAT TF, PKC and Ras, which at the same time induce the activation of ERK. PLCγ2 activates Rac trough SLP-65, which produces the activation of JNK and p38. Colored in blue are depicted the kinases, in orange GTPases, in green phospholipases, in grey adaptor molecules and in pink transcription factors.

1.4.3- Transcriptional regulators and lymphomagenesis

Transcriptions factors play a key role in a variety of B cell responses that include proliferation, migration, differentiation and cell death, and consequently, they are exploited by B cell malignancies.

As it was noticed in the previous point, deregulated signaling pathways end up with an excess of activation of the NF-kB transcription factor, which activates transcription of antiapoptotic genes. Another very frequently altered transcriptional regulator in B cell malignancies is Bcl-6, the master regulator of GC transcriptional program whose activity is dysregulated by translocation or mutation in a remarkably high proportion of DLBCL cases (50%) and in a subset of FL (10%) (reviewed in (Basso and Dalla-Favera 2010) (Table 1). Constitutive Bcl-6 expression is oncogenic for B cells, as shown in a mouse knockin model in which Bcl-6 expression is driven by the I_{μ} promoter in the IgH locus that results in the generation of a B cell malignancy akin to human DLBCL (Cattoretti, Pasqualucci et al. 2005). Blimp-1 acts as a tumor suppressor in ABC-DLBCL (Pasqualucci, Compagno et al. 2006) (Mandelbaum, Bhagat et al. 2010) and in a fraction of ABC-DLBCL tumors, the PRDM1 gene encoding Blimp-1 is disrupted by truncation, deletion, and mutation, or it is epigenetically silenced. Accordingly, deletion of PRDM1 in mouse GC B cells results in a lymphoproliferative disease that gives rise to DLBCLs with a long latency (Mandelbaum, Bhagat et al. 2010) (Calado, Zhang et al. 2010). IRF4 is required for the survival of several post-GC malignancies (Shaffer, Young et al. 2012). Finally, a cytogenetic hallmark for BL is the Myc-IgH translocation t(8;14) (q24;q32) and its variants, which juxtapose the Myc oncogene with one of the three immunoglobulin loci. Consequently, Myc is deregulated, resulting in massive perturbation of gene expression and uncontrolled growth. Importantly, this translocation has been shown to be completely AID dependent (Ramiro, Jankovic et al. 2004) (Table 1).

1.4.4- B cell lymphoma treatment

In general, chemotherapy and radiation therapy are the principal forms of treatment for B-NHL, although radiation is many times used to complement other therapeutic strategies. Nowadays, the chemotherapy of choice for many cases is called R-CHOP and consists of a combination of 5 drugs: 1) Rituximab, is an antibody that recognizes CD20, a molecule expressed by B cells, thereby promoting their elimination; 2) cyclophosphamide, which interferes with DNA replication; 3) doxorubicin, a DNA intercalating drug; 4) Oncovin, an inhibitor of mitosis; and 5) prednisone, an immunosuppressant. This multidrug therapy can be very effective, but it has a number of limitations: i) a fraction of the cases is resistant to the treatment (in the case of DLBCL, the most prevalent of aggressive lymphomas, around 40 -45% of patients do not respond to R-CHOP, thus becoming refractory; ii) a proportion of patients relapse after R-CHOP treatment; iii) treatment is highly intensive, which precludes the use in the elderly and has a high toxicity including immunosuppression and heart damage. Therefore, there is great interest in the development of novel alternative or complementary therapeutic approaches that allow to target better the uncontrolled survival of the lymphoma cells, and to treat refractory and relapsed cases (Lam, Davis et al. 2005) (Wilson, Young et al. 2015).

2. miRNA control of the B cell physiology

2.1. Bases of miRNA biology

microRNAs (miRNAs) are 21- to 24-nucleotide long single strand RNA molecules that are processed from longer RNA precursors and do not encode a protein product, but instead they are biologically active as RNA molecules. They function as negative regulators of gene expression by affecting either the stability or the translation efficiency of their target mRNAs. miRNA activity on its target mRNAs typically results in a relatively mild (<two fold) reduction in protein levels, which has led to the view that miRNAs act primarily as reinforcers of transcriptional programs conferring robustness to biological processes (Ebert and Sharp 2012). However, the regulatory activity of miRNAs is in many aspects similar to that of s and transcriptional repressors. Thus, like transcriptional regulators, a single miRNA can potentially regulate many targets to provide coordinated and simultaneous regulation of a network of genes in a particular tissue or at a specific developmental stage.

miRNAs are processed from longer RNA precursors (pri-miRNAs). Pri-miRNAs are either transcribed as independent genes or are included within intronic sequences of other genes. Pri-miRNAs fold into hairpins that are sequentially cleaved by two RNAseIII endonucleases, called Drosha and Dicer. Drosha cleavage generates a ≈ 70-nucleotide long pre-miRNA that is exported to the cytoplasm, where Dicer further processes it into a 20–25 bp RNA duplex. One strand of this duplex is the mature miRNA, which is loaded onto the miRNA-induced silencing complex (RISC). The main components of the RISC complex are Argonaute (AGO) proteins, which pair with the mature miRNA and guide it to its targets. miRNA-RISC complexes bind to their target mRNAs and they induce their degradation or block the target translation (Bartel 2009). The most important motif in a mature miRNA for determining target specificity resides in the 5’ end, particularly in the stretch from nucleotides 2–7, called the seed. The seed region of the miRNA binds to the 3’ untranslated region (UTR) of the target mRNA, which results in the downregulation of its expression (Fig. 3). However, sequence complementarity alone is not stringent enough to faithfully predict miRNA targets. Indeed, numerous algorithms and predictive tools have been developed to aid in this task, which incorporate both sequence complementarity and evolutionary conservation criteria.

Experimental approaches to decode miRNA-target interactions include chromatin immunoprecipitation of the RISC components, followed by sequencing (HITS-CLIP and PARP-CLIP) (Grosswendt, Filipchyk et al. 2014) and high-throughput studies of the shift in gene expression induced by the miRNA (by RNA-Seq and/or quantitative proteomics).These analysis have shown that individual miRNAs can promote the downregulation of hundreds of genes, a large fraction of which are potential direct targets

(Selbach, Schwanhäusser et al. 2008) (Mihailovich, Bremang et al. 2015).

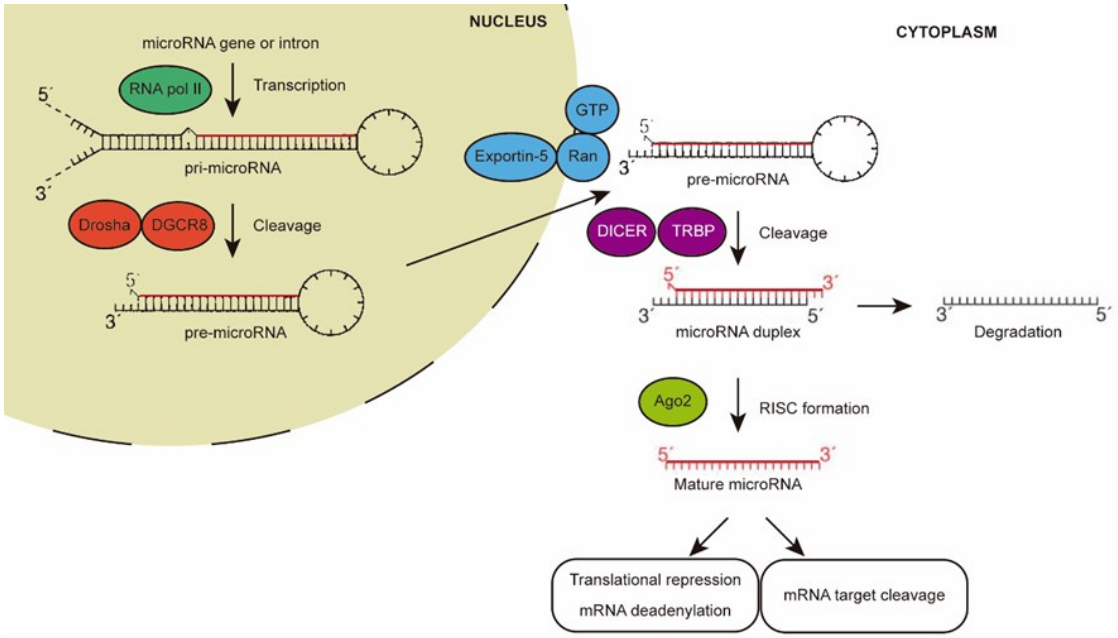

Figure 3: miRNA biogenesis and mechanism of action: miRNA maturation starts in the nucleus with the production of the primary miRNA transcript (pri-miRNA) by RNA polymerase II or III and cleavage of the pri-miRNA by the microprocessor complex Drosha–DGCR8 (Pasha) in the nucleus. The resulting precursor hairpin, the pre-miRNA, is exported from the nucleus by Exportin-5–Ran-GTP. In the cytoplasm, the RNase Dicer in complex with the double-stranded RNA-binding protein TRBP cleaves the pre-miRNA hairpin to its mature length. The functional strand of the mature miRNA is loaded together with Argonaute (Ago2) proteins into the RNA-induced silencing complex (RISC), where it guides RISC to silence target mRNAs through mRNA cleavage or translational repression, whereas the passenger strand (black) is degraded.

Specific expression or regulation of miRNA levels in a particular cell context is considered a faithful indication of miRNA biological relevance. In this regard, different studies have analyzed miRNA expression profiles in distinct B cell subsets by small RNA library sequencing (Landgraf, Rusu et al. 2007) (Basso, Sumazin et al. 2009) and miRNA next-generation sequencing techniques (Kuchen, Resch et al. 2010) providing valuable data resources. Functional validation of miRNAs involve relatively standard gain and loss of function analysis, like viral transduction or generation of mouse models, and more particular ones, like the use of antagomir or sponge approaches for miRNA inhibition (Gentner, Schira et al. 2009) (de Yebenes, Bartolome-Izquierdo et al. 2013).

2.2. miRNA control of B cell function

The global function of miRNAs in B cell differentiation has been addressed in several works where the generation of mature miRNAs is abrogated by the deletion of Dicer or Drosha endonucleases. Thus, when B cells are deprived of miRNAs at a very early stage of differentiation using the mb1 -Cre driver for Dicer deletion, a dramatic block at the pro-B- to pre-B transition ensues, revealing that miRNAs are essential for B cells to transit to further stages of differentiation (Koralov, Muljo et al.

2008). A later deletion of Dicer with the CD19-Cre driver, showed that late B cell differentiation and the establishment of immune tolerance are also dependent on miRNAs (Belver, de Yébenes et al. 2010). Finally, Dicer deletion in GC B cells impaired the GC response and the generation of memory B and PCs (Xu, Guo et al. 2012).

In addition, a number of studies have contributed to identify and characterize individual miRNAs that play key roles in B cell development and function. miRNAs have been shown to act as positive (miR17-92) (Xiao, Srinivasan et al. 2008) or negative (miR34a (Rao, O'Connell et al. 2010), miR-150 (Xiao, Calado et al. 2007), miR-125 (Chaudhuri, So et al. 2012)) regulators of B-cell generation in the bone marrow (see Fig. 4). These works have also revealed the intimate connection between transcription factors and miRNAs, making the regulatory loops more complex. This could reflect the need of subtle changes in the expression of master regulators of the B cell program. Interestingly, alterations in the expression of these miRNAs in the bone marrow appear to principally affect the pro-B to pre-B transition, probably reflecting the importance of an optimal balance between proliferation and cell death at the developmental checkpoint governed by pre-BCR expression (Fig. 4).

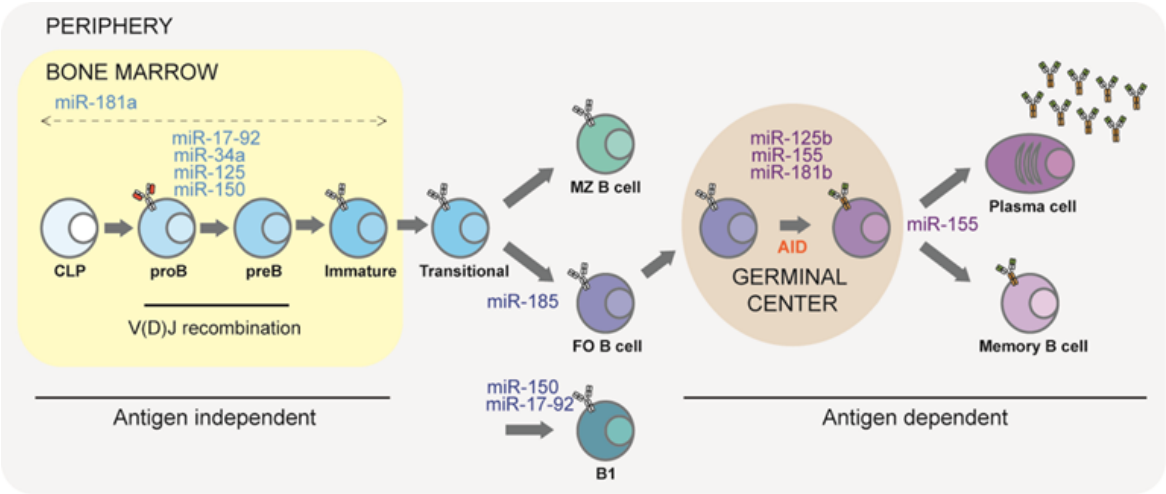

Figure 4. miRNAs play crucial roles in B-cell development. Scheme depicting the developmental Stages of B-cell differentiation in which particular miRNAs have been shown to play a role.

Regarding mature B-cell biology, miR-181b and miR-155, have been linked to the GC reaction. Interestingly, both miR-181b and miR-155 can target the SHM and CSR initiating enzyme, AID. miR-181b was identified in our group through a functional screening of a miRNA library. We found that ectopic expression of miR-181b during B-cell activation decreased the CSR rate through the direct targeting of AID mRNA (de Yebenes, Belver et al. 2008).

miR-155 is upregulated in GC B cells and is required for the GC response (Tam 2001) (Thai, Calado et

al. 2007) (Rodriguez, Vigorito et al. 2007) (Vigorito, Perks et al. 2007) (Basso, Sumazin et al. 2009) (Kuchen, Resch et al. 2010). miR-155-germline-deficient mice have an impaired humoral response to immunization (Rodriguez, Vigorito et al. 2007) (Thai, Calado et al. 2007), and conversely mice that conditionally overexpress miR-155 in mature B cells had increased numbers of GC B cells and showed high antigen-specific antibody secretion upon T-cell dependent immunization (Thai, Calado et al. 2007). Two of the confirmed putative miR-155 targets are PU.1 (Vigorito, Perks et al. 2007) and AID (Dorsett, McBride et al. 2008). miR-125b, expressed by a subset of GC B cells (Gururajan, Haga et al. 2010), was shown to directly target Blimp-1 and IRF4, two transcription factors essential for post-GC plasma B-cell differentiation (Gururajan, Haga et al. 2010). Accordingly, overexpression of miR-125b in B cells inhibited plasma B-cell differentiation and Ig secretion in vitro (Gururajan, Haga et al. 2010).

Overall, these studies indicate that AID levels in B cells are controlled by different miRNAs with non-overlapping functions. Thus, whereas miR-181b would prevent premature AID activity in resting B cells and allow proper AID transcriptional activation upon stimulation, miR-155 would prevent excessive accumulation of AID transcripts in activated B cells. In addition, miRNAs can also control the time window of the GC reaction, preventing premature exit from GC by inhibition of the PC program, as it is the case of miR-125b in B cells.

2.3. miRNAs in mature B cell lymphomagenesis

Deregulation of miRNA expression is a common event in cancer, including B-cell lymphomas, and miRNA profiling is increasingly recognized as a valuable tool for cancer classification (Lu, Getz et al. 2005) (Volinia, Calin et al. 2006) (Calin and Croce 2006). Different studies have contributed to identify the gene pathways and critical targets affected by miRNA deregulation in B cells lymphomas (reviewed in Table 2). These include increase in BCR signaling and the PI3K/AKT pathway, the inhibition of pro-apoptotic genes, the increase in proliferation and the deregulated expression of key transcription factors.

Table 2: Deregulated miRNAs in human B cell malignancies

miRNA	Disregulation	Lymphoma type	Targeted genes / Pathways	Referencies
miR-155	Upregulated	DLBCL / FL / MCL / CLL	AID / PU.1 / SHIP-1 / Increase PI3K/AKT pathway	Eis P, PNAS 2005 / Costinean S, Blood 2009
miR-21	Upregulated	DLBCL / FL	PTEN / PDCD4 / Increase PI3K/AKT pathway	Lawrie C, Int J Cancer 2007 / Medina P, Nature 2010
miR-17-92	Upregulated	DLBCL / FL / MCL / BL	BIM / PTEN / E2F1 / Increase PI3K/AKT pathway	O'Donnell KA, Nature 2005, Ventura A, Cell 2008 / Xiao C, Nat Immunol. 2008
miR-150	Downregulated	DLBCL / FL / MCL / CLL	MYB	Xiao C, Cell 2007 / Malumbres R, Blood 2009
miR-15a-16-1	Downregulated	CLL / DLBCL / MCL	Bcl-2 / TP53	Calin GA, PNAS 2002 / Cimmino A, PNAS 2005 / Eis P, PNAS 2005
miR-181b	Downregulated	CLL	AID / Bcl-2 / MCL1 / TCL1	de Yébenes VG, J Exp Med 2008 / Bisone R, Blood 2011
miR-34a	Downregulated	DLBCL / MALT / FL / CLL	FOXP1 / Axl / Bcl-2 / Bcl-6 / B-MYB / CDK6 / Sirt1	Zenz T, Blood 2009 / Zenz T, Blood 2009 / / Yamakuchi M, PNAS 2008 / Craig VJ, Blood 2011

Nevertheless, formal proof of the direct role of miRNAs in tumor development involves the generation of animal models in which alterations to miRNA expression levels has an impact on the incidence of the neoplasia under study. These studies have fostered the concepts of oncogenic (oncomiRs) and tumor suppressor miRNAs. However, very few miRNAs until the beginning of this work have been demonstrated to play a direct role in de development of mature B cell lymphomagenesis (see Table 3). The development of miRNA overexpressing mouse models has allowed to stablish that miR-155, miR-21, miR-29 and miR-125b are oncomiRs for B cell lymphocytes that when overexpressed lead to the generation of B cell leukemia or inmature B cell lymphoma. miR-15a-16-1 has been shown to be a tumor suppressor miRNA, whose deletion leads to B cell leukemia development. However, until the beginning of this work they were no miRNA shown to be oncomiRs or tumor suppressors for mature GC derived B cell lymphoma.

Table 3: miRNAs whose genetic deregulation causes B cell neoplasms.

microRNA	miRNA porperties	Mouse model	B cell neoplasia	Subtype	Referencies
miR-155	OncomiR	Eμ/V_H miR-155	Inmature lymphoma	ALL/high-grade lymphoma	Costinean S. PNAS 2006 / Costinean S. Blood 2009
miR-21	OncomiR	NesCre8/miR-21$^{LSL\text{-}Tet\text{-}off}$	Inmature lymphoma	Pre-B expansion	Medina P, Nature 2010
miR-29	OncomiR	Eμ/VH miR-29	Leukemia	CLL	Santanam U, PNAS, 2010
miR-125b	OncomiR	Eμ/VH miR-125b	Leukemia	CLL	Enomoto Y, Leukemia, 2011
miR-15a-16-1	Tumor supressor	MDR ko	Leukemia	CLL	Klein U, Cancer Cell, 2010

2.4. miRNA mediated therapeutics

miRNA therapeutics is based on the finding that some of the aberrantly expressed miRNAs play key roles in the development of human disease, and on the rationale that correcting these miRNA alterations by either antagonizing or restoring miRNA function may provide a therapeutic benefit (Sibley, Seow et al. 2010). miRNAs possess several advantages to be exploited as therapeutic tools: they are short, easy to be chemically modified and very importantly, they are able to target multiple genes. This last property allows a single therapeutic agent to target at the very same time various signaling cascades that contribute to the illness onset and maintenance. Moreover, miRNA therapy (both restoring and inhibiting endogenous miRNAs) has another yet and fundamental benefit, which is that nonspecific off-target effects are unlikely as miRNAs are expected to behave like the natural counterpart for which the proper miRNA-mRNA interactions have evolved over a billion years.

Although naked delivery of the therapeutic RNA molecules is possible, various non-viral vectors can be used to deliver small RNA, including small interfering RNA (siRNA) and miRNAs and miRNA

inhibitors (Yin, Kanasty et al. 2014). This vectors aim to improve the targeted delivery of the miRNA or the miRNA inhibitor by encapsulation in different types of nanoparticles, such as lipidic particles or charged nanoparticles (Yin, Kanasty et al. 2014). Exosomal delivery is also started to be explored as a more physiological way of delivering miRNAs into immune cells (Momen-Heravi, Bala et al. 2014).

Synthetic miRNA inhibitors are single stranded reverse complement sequences of the mature targeted miRNA that have different types of chemical modifications that prevent RISC-induced cleavage, enhance binding affinity and provide resistance to nucleolytic degradation (Krützfeldt, Rajewsky et al. 2005) (Esau 2008) (Davis, Propp et al. 2009). When delivered to a cell, binding of endogenous mature miRNAs to these complementary synthetic target sites is thought to be irreversible, thus these inhibitors are presumed to sequester the endogenous miRNA, making it unavailable for normal function (Davis, Propp et al. 2009). The delivery of synthetic anti-miRNAs inhibitors is being successfully used as a novel therapeutic approach to inhibit the expression of oncomiRs in hepatocellular carcinoma (Kota, Chivukula et al. 2009) (Elmen, Lindow et al. 2008) and precursor B cell lymphomas (Babar, Cheng et al. 2012) (Cheng, Bahal et al. 2015).

miRNA replacement can technically be achieved by viral or synthetic miRNA mimic administration (Bader, Brown et al. 2010). These approaches are especially attractive to re-express tumor suppressor miRNAs whose expression is lost in specific neoplasias. The biggest difference among the mechanism of action between miRNA inhibitors and mimics is that unlike miRNA inhibitors, miRNA mimics are double stranded RNAs that require integration into the RNAi machinery (Søkilde, Newie et al. 2015). If they are not loaded into the RISC they are not functional. Although miRNA repalcement is being currently developed for the treatment of solid tumors (Daige, Wiggins et al. 2014), its application for B cell lymphoma treatment is starting to be explored nowadays.

To sum up, the current knowledge of the field suggests that deregulation of certain miRNAs could have great impact in the outcome of the GC reaction and in consequence in B cell lymphomagenesis. In this way, understanding miRNA mediated regulation of the GC reaction could help to the diagnosis and prognosis of certain subtypes of B cell lymphomas. Importantly, this knowledge could potentially be used to develop new treatment possibilities for GC derived B cell lymphomas based on the manipulation of key miRNAs in vivo.

OBJECTIVES

OBJECTIVES

This work focused on the identification and characterization of microRNAs that could act as regulators of germinal centers (GC). Based on expression-profiling criteria we selected miR-217 and miR-28 to pursue their functional impact on the biology of GC B cells with the following specific objectives,

1-Role of miR-217 in GC reaction and in B cell lymphomagenesis

-Generate mouse models for B cell specific miR-217 overexpression.

-Analyze miR-217 function in GC B cells by using gain and loss of function approaches.

-Identify miR-217 targets by transcriptome analysis and characterize molecular mechanisms of miR-217 activity.

-Assess the contribution of miR-217 to B cell lymphomagenesis.

2- Role of miR-28 in GC reaction and in B cell lymphomagenesis

- Analyze miR-28 function in GC B cells by using gain and loss of function approaches.

-Characterize the molecular mechanisms of miR-28 activity by combining transcriptome and proteome profiling.

- Characterize the tumor suppressor potential of miR-28 in GC B cells.

MATERIALS & METHODS

Human lymphomas and control samples

Samples of human BL and DLBCL were collected before patients received therapy and diagnosed by a panel of three hematopathologists (Di Lisio, Sánchez-Beato et al. 2012). Control samples included tonsils, lymph nodes and isolated $CD19^+$ B cells from peripheral blood of healthy donors. The project was approved by the ethics committee of the Instituto de Salud Carlos III (ISCIII).

Mice

To generate miR-217^{TG} mice, a construct encoding the mouse miR-217 precursor, IRES and GFP was inserted within regulatory elements of the IgK gene. The miR-217 precursor genomic sequence was PCR-amplified from C57BL/6 mouse genomic DNA with the primers: forward 5'-ttggatcctatatttggggagtttggggg-3'and reverse 5'-aactcgagaataaagatagctgctttagt-3', subcloned into the pGEMT vector (Promega) and inserted into the BamHI/XhoI site of pMX-PIE vector 3. The miR-217 precursor-IRES-GFP fragment was PCR amplified with the primers: forward 5'-aaggcgcgcctatatttggggagtttggggg-3' and reverse 5'-agttaattaattacttgtacagctcgtccat-3' and subcloned into Asc/Pac sites a modified Igκ vector (Robbiani, Colon et al. 2005). The plasmid backbone was removed with MluI and NotI prior to pronuclear injection into C57BL/6 × (C57BL/6 × CBA) oocytes.

miR-217^{KI} mice were generated by insertion of a construct encoding mouse miR-217 precursor into the Rosa26 IRES-GFP targeting vector (Nyabi, Naessens et al. 2009). miR-217 precursor sequence was PCR amplified from C57BL/6 mouse genomic DNA with the primers: forward 5'-aactcgaggaaaaagtaaaagagaatgcgttg-3'; reverse 5'-gtgaattcaaagttccaggctaataaagatag-3', cloned into the pENTR/D-TOPO Gateway vector (Invitrogen), and recombined into the Rosa26 targeting vector. The construct was electroporated into hybrid 129/C57BL/6 ES cells and positive clones were identified by Southern blot of EcoRV-digested genomic DNA hybridized with a 5'-arm Rosa26 probe. miR217^{KI} mice were crossed with CD19 $Cre^{KI/+}$mice (Rickert, Roes et al. 1997) to promote expression of miR-217 in B cells.

For tumor suppressor pathways studies, miR-217^{KI} mice were breed with Ink4A/ARF^{KO} and $p53^{KO}$ mice, kindly provided by Dr. M. Serrano. λ-MYC transgenic mice (Kovalchuk, Qi et al. 2000) were kindly provided by Dr. Miguel Campanero. NOD/SCID/IL-2rgnull (NSG) mice, C57BL/6 (Harlan) mice and CD45.1 C57BL/6 were provided and maintained by the animal facility.

miR-217 SPG or miR-28 SPG mouse chimeras were generated by retroviral transduction of bone marrow cells (see technical details below) from $CD45.1^+$ C57BL/6 mice with miR-217 sponge / miR-28

sponge or a control GFP retroviral vector, and transferring these cells to lethally irradiated CD45.2$^+$ C57BL/6 mice.

All the mice were bred in house under pathogen-free conditions and all procedures are conformed to European Union Directive 2010/63EU and Recommendation 2007/526/EC regarding the protection of animals used for experimental and other scientific purposes, enforced in Spanish law under Real Decreto 1201/2005.

Isolation and analysis of B cell subsets

To obtain lymphoid tissue, mice were sacrificed under hypoxic conditions in a CO_2 chamber and the spleen, lymph nodes, Peyer's patches and femurs were extracted. The organs were maintained on ice in the presence of RPMI-1460 medium (Sigma-Aldrich) supplemented with 10% fetal calf serum (FCS), penicillin (50 U/ml) and streptomycin (50 ug/ml) antibiotics, which is called RPMI complete medium. Spleens, lymph nodes and Peyer's patches were mechanically desegregated in a 70 µm cell strainer to obtain a cell suspension. After centrifugation (10' / 400 x g / 4ºC), the cells from organs with low erythrocyte presence (lymph nodes and Peyer's patches) were resuspended in PBS with 10%FCS. Splenic B cells were treated with ACK erythrocyte lysis buffer (Biowhittaker) for 4 minutes at room temperature and washed with cooled complete RPMI medium to stop the lysis. After recovering the cells by centrifugation (10' / 400 x g / 4ºC) the cells were resuspended in PBS 1% FCS. To obtain bone marrow cells, the femurs were perfused with the help of a syringe. After centrifugation erythrocytes were lysed as described before and resuspended in PBS 1%FCS.

Mouse primary B cells were purified from spleens of 6-8 weeks C57/BL6 mice by anti-CD43 immunomagnetic depletion (Miltenyi Biotech) and recovering the negative fraction, following the manufacturer instructions. To isolate B cell subsets ex-vivo, flow-activated cell sorting in a FACS Aria cell sorter (BD Biosciences) was used. GC B cells and naïve B cells were obtained from immunized spleens or Peyer's patches by staining the cells with the appropriate antibody combination (see below) and separating by sorting the naive cells (CD19$^+$Fas$^-$GL7$^-$) and GC B cells (CD19$^+$Fas$^+$GL7$^+$). Transduced cells were also separated from the total population in cell culture by using GFP or RFP reporter genes.

Analysis of lymphoid populations from bone marrow, lymph nodes, spleen and Peyer's patches was performed by preparing suspensions of live cells and incubating the cells with unlabeled anti-mouse CD16/CD32 antibodies (BD Pharmingen) to block Fc receptors. The cells were then labeled with specific combinations of the following antibodies and analyzed as soon as possible to maintain cell viability.

Table 4. Antibodies conjugated to flurochromes

ANTIBODY	REACTIVITY	COMPANY	FLUROCHROME
B220 (CD45R)	Mouse	BD Biosciencies	BV421
GL7	Mouse	BD Biosciencies	FITC
IgD	Mouse	BD Biosciencies	FITC
Igλ	Mouse	BD Biosciencies	FITC
CD21	Mouse	BD Biosciencies	PE
CD138	Mouse	BD Biosciencies	PE
IgM	Mouse	Invitrogen	PE
Fas	Mouse	BD Biosciencies	PE
IgM	Human	BD Biosciencies	PE
Igκ	Mouse	BD Biosciencies	PE
CD45.2	Mouse	BD Biosciencies	PerCpCy5.5
CD45.1	Mouse	BD Biosciencies	PerCpCy5.5
GL7	Mouse	BD Biosciencies	Alexa647
GL7	mouse & human	eBioscience	Alexa660
CD19	Mouse	BD Biosciencies	APC
CD3	Mouse	BD Biosciencies	APC
CD45 (total)	Mouse	BD Biosciencies	APC
CD93	Mouse	eBioscience	APC

Table 5. Antibodies conjugated to biotin

ANTIBODY	REACTIVITY	COMPANY
CD19	Mouse	BD Biosciencies
CD23	Mouse	BD Biosciencies
IgM	Mouse	BD Biosciencies
IgA	Mouse	BD Biosciencies
IgG1	Mouse	BD Biosciencies
IgD	Mouse	SouthernBiotech
CD43	Mouse	BD Biosciencies

Table 6. Avidins

ANTIBODY	COMPANY
PE-Cy7	BD Biosciencies
PE	BD Biosciencies
APC	BD Biosciencies
FITC	BD Biosciencies

Cell culture

Mouse primary B cells were cultured in RPMI-1460 medium (Sigma-Aldrich) supplemented with 10% fetal calf serum (FCS), penicillin (50 U/ml) and streptomycin (50 µg/ml) antibiotics, which is called RPMI complete medium complete, supplemented with 10mM Hepes (Gibco and 50 µM β-mercaptoethanol (Gibco). Activation of the cells in order to switch to IgG1 was obtained by culturing the primary B cells at a concentration of 1.3 x 10^6 cells/ml and by adding 25 µg/ml LPS (Sigma) and 10 ng/ml IL-4 (Peprotech) to the RPMI complete medium. To ensure the survival of the culture Blyss (R&D systems) was also added at a final concentration of 20 ng/ml. Switch was analyzed at different

time points depending on the experiment, but always between 2 and 5 days after activation.

Bone marrow cells were cultured at 1.1 x 10^6 cells/ml concentration in IMDM medium (Gibco) 20% FCS in the presence of penicillin (50 U/ml) and streptomycin (50 ug/ml) and supplemented with IL6 (20 ng/ml), IL-3 (50 ng/ml), SCF (50 ng/ml), β-mercaptoethanol (50 μM) and HEPES (10 μM) to maintain the stem cell potential of the hematopoietic progenitors.

The NIH-293T and 3T3 cell lines were cultured in DMEM (Gibco) containing 10% FCS in the presence of penicillin (50 U/ml) and streptomycin (50 ug/ml) antibiotics. The human B cell lymphoma cell lines (Ramos, Raji, Daudi, Farage, Riva, Namalwa, HBL1 and MD901) and the Jurkat T cell line were cultured in complete RPMI medium containing 10mM Hepes (Gibco) at a concentration of 200000 cells/ml.

Expression constructs and transductions

Retroviral constructs

For retroviral overexpression of miR-217 and miR-28, the DNA fragment containing their precursor sequence and their corresponding flanking 50-bp-long genomic context were cloned in XhoI-EcoRI sites of the pre-miRNA GFP vector, as previously described (de Yebenes, Belver et al. 2008). The empty p-miRNA Control vector was generated by liberating the insert, generating blunt ends with T4 polymerase and religating with T4 ligase. For retroviral inhibition of the endogenous miRNA, miR-217 and miR-28 sponges were generated. Briefly, 4 complementary sequences to the mature miR-217 5p or miR-28 5p were cloned in tandem within the 3'UTR of GFP into the MGP vector by annealing and subsequent extension with Klenow DNA polymerase (New England Biolabs) of two partially complementary oligonucleotides: For miR-217 sponge *(forward) 5'tcgactagctagaacgcggccgctccagtcagttcctgatgcagtagattccagtcagttcctgatgcagtaaccggttccagt-3'; (reverse) 5'gaagtcagtccgattctcgagtactgcatcaggaactgactggagtgatactgcatcaggaactgactggaaccggttactgcatc-3'. In the case of miR-28 sponge (forward) 5' tcgactagctagaacgcggccgcctcaatagactgtgagctccttcgatctcaatagactgtgagctccttaccggtctcaat-3'(reverse) 5'gaagtcagtccgattctcgagaaggagctcacagtctattgaggtgaaaggagctcacagtctattgagaccggtaaggagctc-3'*. Retroviral supernatants were produced by transient calcium phosphate transfection of NIH-293T cells with pCL-ECO (Imgenex) and the wanted p-miRNA or sponge retroviral vectors. Mouse splenic B cells and total bone marrows were transduced with retroviral supernatants for 16-20h in the presence of 8 μg/ml polybrene (Sigma-Aldrich).

Lentiviral constructs

For inducible expression of miR-28, its precursor sequence was cloned into the pTRIPZ vector (Thermo scientific) in a Tet-on configuration. The pre-miRNA sequence was replaced by a scramble sequence to

obtain the pTRIPZ scramble Control. Lentiviral supernatants were obtained by transient calcium phosphate transfection of NIH-293T cells with VSVG, Δ9.8 and pTRIPZ. Human lymphoma cell lines were transduced with lentiviral supernatants for 16h in the presence of 8 μg/ml polybrene. 48h later, selection of the infected cells was achieved by adding 0.4 μg/ml puromycin to the culture medium for 3 days. For the induction of miR-28 or the Scramble sequence 0.5 μg/ml doxycycline was added and RFP^+ was measured in a Facs Calibur cytometer.

Bone marrow reconstitution

$5x10^6$ total bone marrow cells from CD45.1 C57BL/6, donor mice were injected intravenously into 8- to 12-week-old CD45.2 C57BL/6 mice that had been lethally irradiated (2 x 550 cGy) 24hr before the reconstitution. Neomycin (2 mg/ml) was added in the drinking water of the mice until complete reconstitution.

Immunizations

T cell dependent immunizations were performed with two different immunogens; an NP (nytrophenil) hapten conjugated to chicken gamma globulin (CGG) via amide bonds to lysine (NP-CGG) or with sheep red blood cells (SRBC). In the case of NP-CGG, groups of 6-11 littermate mice were immunized by footpad injection with 50 μg of NP-CGG (Biosearch Technologies) in complete Freund's adjuvant. In secondary immunizations mice were reimmunized with 50 μg of NP-CGG in incomplete Freund's adjuvant. For immunizations with SRBC, 10^8 cells were intravenously injected in the tail vain of 6-11 littermate mice per group and mice were sacrificed between 3-14 days later, as indicated in the corresponding experiment. Mice injected with PBS were used as non-immunized controls.

Cellular assays

Apoptosis was measured using Annexin V eFluor450 kit (eBioscience) and anti- active Caspase-3 staining (conjugated to FITC, Clone C92-605) from BD Pharmingen. Proliferation was assessed with Cell Trace Violet or CFSE (both from Invitrogen) and analysis was performed using the FlowJo proliferation platform or by BrdU icorpation assays, using FITC-BrdU Flow Kit (BD Pharmingen). Cell cycle analysis was performed with propidium iodide or DAPI (1 μg/ml) staining. To induce genotoxic stress a range of 2 to 10 μM etoposide treatment was used for 6 hours and cell cycle was analyzed with DAPI afterword.

Immunoblotting (WB)

For immunoblotting, Ramos transduced cell pellets were incubated on ice for 20 min in lysis buffer containing 50 mM Tris, 150 mM NaCl, 0.1% SDS, 0.5% sodium deoxycholate and 1% RIPA in the presence of protease and phosphatase inhibitors (Roche and Cell signaling, respectively) and lysates were

cleared by centrifugation (15' / 16000 x g / 4ºC) . 5% β-mercaptoethanol was added. Total protein from a fraction of the lysate was sized-fractioned by SDS-PAGE on 10% acrylamide-bisa- crylamide gel and transferred to Protran nitrocellulose membrane (Whatman) in transfer buffer (0.19 M glycine, 25 mM Tris base, and 0.01% SDS) containing 20% methanol. Gels were transferred for 1hr at 0.4A. Membranes were probed with anti-human Bcl-6 (N-3; Santa Cruz Biotechnology), anti-human tubulin (Sigma-Aldrich), anti-human ERK1/2 (Cell signaling), anti-human p-ERK1/2 (Cell signaling) and anti-human p-AKT (Cell signaling). Then, membranes were incubated with corresponding secondary HRP-conjugated antibodies (Dako) and developed with Amersham ECL Western Blotting Detection reagent (Amersham). Band intensity was analyzed by Image-J program.

Bcl-6 protein detection by intracellular staining and FACS analysis

First, the cell suspension was membrane stained with surface antibodies to detect GC B cells ($CD19^+$, $GL7^+$, Fas^+, as described before). Next, intracellular flow cytometry staining of Bcl-6 was performed with anti-Bcl-6 antibody (clone K112-91, BD Pharmingen) after cell fixation and permeabilization with the Foxp3 staining kit from eBioscience. Bcl-6 positive cells were detected and gated within GC B Cells by analyzing them on a FACS Canto flow cytometer (BD Biosciences) with FACS Diva software.

AKT phosphorylation upon BCR stimulation

miR-28 transduced or scrambled transduced Ramos cells were in vitro activated with 10 µg/ml of soluble anti-human-IgM (Rockland) 5 minutes at 37ºC. Then, cooled complete RPMI medium was added to wash the cells and stop the stimulation. The cells were recovered by centrifugation (400 x g / 10' / 4ºC) and fixed and permeabilized with IC Fixation buffer and permeabilization buffer (eBioscience), following manufacturer instructions. Ramos cells were then labelled with anti-phospho-AKT (S473) (eBioscience) 20' in dark and at room temperature. After washing and recovering the cells, phospho-AKT levels upon BCR stimulation were analyzed FACS Canto flow cytometer (BD Biosciences) with FACS Diva software.

Somatic mutation analysis

For Sµ amplifications genomic DNA was amplified for 26 cycles with Pfu Ultra polymerase (Stratagene) with the primers (forward) 5'-aatggatacctcagtggtttttaatggtgggttta-3' and (reverse) 5'-gcggcccggctcattccagttcattacag-3'. For J_H4 intron mutations, DNA was amplified first for 11 cycles with the primers (forward) 5'-actatgctatggac-3' and (reverse) 5'-ctggactttcggtttggtg-3', and then for 19 cycles with the primers (forward) 5'-ggtcaaggaacctcagtca-3' and (reverse) 5'-tctctagacagcaactac-3', using Pfu Ultra polymerase (Stratagene).

V(D)J recombination analysis

Genomic DNA was isolated from total spleen of miR-217^{KI} mice with B-cell lymphomas, and the rearranged V_H sequences were amplified by PCR, using a degenerate forward primer that anneals to the framework region III of the most abundantly used V_HJ558 family (5'-(ag)gcctggg(ag)cttcagtgaag-3'), and a reverse primer that anneals immediately downstream of the J_H4 gene (5'-aggctctgagatccctagacag-3'). PCR products were gel purified, cloned in pGEM-T vector (Promega) and sequenced. >10 clones were sequenced per spleen sample. Assignment of V(D)J rearrangements was done with NCBI IgBLAST program (http://www.ncbi.nlm.nih.gov/igblast/data) using the IMGT V domain delineation system. Clonality was assigned when the same rearrangement, including its V(D)J junction, was repeatedly found in a significant fraction of the sequenced clones. Rearranged V(D)J genes were scored as SHM$^+$ when nucleotide substitutions were found in the V_H gene with respect to the assigned gene.

Analysis of mRNA expression levels by RT-qPCR

For the analysis of the expression levels of messenger RNAs, total RNA was extracted with Trizol (Invitrogen). 1 µg of the RNA was retrotranscribed to cDNA by using Random hexamers (Applied biosystems) as primers and the inverse retrotranscriptase Superscript II (Invitrogen), following manufacturer instructions. The obtained cDNA was next amplified by RT-qPCR using SYBER green PCR master mix (Applied Biosystems) and 0.4 mM of the specific pair of primers of the wanted messenger RNA target (reviewed in the table below). The obtained results were normalized to the expression of the housekeeping gene GAPDH. The amplification was performed in a 7900HT fast real-time PCR system (Applied Biosystems).

Table 7. Primers for mRNA amplification by q-RT-PCR

OLIGONUCLEOTIDE	SENSE	ANTISENSE	ORGANISM
GAPDH	5'-GAAGGTGAAGGTCGGAGTC-3'	5'-GAAGATGGTGATGGGATTTC-3'	human
GFP	5'-AGAAGAACGGCATCAAGGTGA-3'	5'-ATGTGATCGCGCTTCTCGT-3'	human
LIG4	5'-GCTGGGATTCTCTGGTTCACA-3'	5'-GCGGTGATGAATCTTCTCGTTT-3'	human
NBS1	5'-TGCACTCACCTTGTCATGGTATC-3'	5'-CGTCCACAAATGAGTGCACAT-3'	human
PDS5B	5'-AAGCCACTTTGGCAGTGCTACT-3'	5'-TTCCAGGCGGATTGGTACAT-3'	human
XRCC2	5'-AATCTGTTTGCTGATGAAGAT-3'	5'-CTGGGCCATGAAATTCAAGAA-3'	human
CCDC50	5'-GAAGAAGGATGAGGACATAGC-3'	5'-CTCTGGAAAGTGTTTCTTTCTC-3'	human
CD44	5'-CCAACTCTAATGTCAATCGTTCC-3'	5'-ATCAGCCATTCTGGAATTTGG-3'	human
CELSR3	5'-CAGAAAGCGAGGACAATGG-3'	5'-TTGCCATCCACATCTTTGG-3'	human
FOSB	5'-GAACGTCTGGAGTTTGTGC-3'	5'-AGGACTTGAACTTCCTCCG-3'	human
JAK3	5'-CTTCTTCTGCAAGGAGGTG-3'	5'-CAAAGTCCAGAGTGATGGG-3'	human
VAV3	5'-CTCTGCAGTTTCCATACAAGG-3'	5'-TTGGACTTAACAAGCTGTTGC-3'	human
NFKB2	5'-GTGCATAAACAGTATGCCA-3'	5'-CAGAAACACTGTTACAGGC-3'	human
BCL2	5'-GAGAACAGGGTACGATAACC-3'	5'-CTGCGACAGCTTATAATGG-3'	human
IKBKB	5'-AGACGGCAAGTTAAATGAG-3'	5'-AGATCTGAGTCTCATAGGTG-3'	human

miRNA detection by q-RT-PCR

RNA was extracted with Trizol (Invitrogen). For detection of mouse and human mature miR-217-5p and miR-28-5p by qRT-PCR, miRCURY LNA primers (Exiqon) were used with the sequences UACUG-CAUCAGGAACUGAUUGGA (product number 204010) and AAGGAGCUCACAGUCUAUUGAG (product number 204322), respectively. U6 amplification was used as normalization control. The amplification was performed in a 7900HT fast real-time PCR system (Applied Biosystems).

miR-217 RNAseq

GC ($CD19^{+}Fas^{+}GL7^{+}$) B cells from pooled Peyer's patches (4-6 animals per genotype) from control and miR-217^{TG} mice were isolated by cell sorting. Total RNA was extracted with Trizol (Invitrogen) and sequenced by RNAseq. RNA samples were processed through the "Ovation RNA-seq system" (NuGEN) and then retrotranscribed, and cDNA was amplified by the SPIA isothermal linear amplification procedure. The resulting ds-cDNA was fragmented to a range of 150-200bp in a Covaris S2 shearing instrument. cDNA (200ng of per sample) was processed through succeeding enzymatic treatments of end-repair, dA-tailing, and ligation to indexed adapters, according to "TruSeq DNA Sample Preparation Guide" (Illumina). Ligation products were purified with AMPure XP Beads. Adapter-ligated libraries were amplified by PCR with Illumina PE primers for 10 cycles. The resulting purified DNA libraries were applied to an Illumina flow cell for cluster generation, and sequenced on the Illumina Genome Analyzer IIx with SBS TruSeq v5 reagents. Sequences were converted to FASTQ read format, filtered with FastX Toolkit (http://hannonlab.cshl.edu/fastx_toolkit/index.html) and aligned with Tophat 2.0.4 (Kim, Pertea et al. 2013). Differential expression analysis was done using the edgeR package from Bioconductor (Gentleman, Leclercq et al. 2004) and genes with $p \leq 0.05$ were considered for analysis. Pathway analysis of the significantly up- and downregulated genes in miR-217^{TG} vs control GC B cells was performed by Ingenuity pathway analysis software (Ingenuity Systems). Significantly downregulated genes in miR-217^{TG} GC B cells were analyzed for the presence of 835 different miRNAs target sites based on predicted and experimentally validated miRNA-mRNA interactions. Scores for every predictive algorithm were normalized, and the compound score of predictive and experimental databases was calculated (Muniategui, Nogales-Cadenas et al. 2012).

miR-28 RNAseq

6 pairs of RFP^{+} sorted Ramos cells transduced with the miR-28 or Scrambled lentiviral construct in 3 independent infections were used for RNAseq analysis. Total RNA was extracted from 10^{7} Ramos transduced cells with Rneasy colums (Qiagen) and sequenced by RNAseq. For library preparation, 500 ng of total RNA were used to generate barcoded RNAseq libraries using the TruSeq RNA sample

preparation kit v2 (Illumina). Briefly, poly A^+ RNA was purified using poly-T oligo- attached magnetic beads using two rounds of purification followed by fragmentation and first and second cDNA strand synthesis. Next, cDNA 3' ends were adenylated and the adapters were ligated followed by PCR library amplification. Finally, the size of the libraries was checked using the Agilent 2100 Bioanalyzer DNA 1000 chip and their concentration was determined using the Qubit® fluorometer (Life Technologies). Libraries were sequenced on a HiSeq2500 (Illumina) to generate 60 bases single reads. FastQ files for each sample were obtained using CASAVA v1.8 software (Illumina).

Sequencing reads were pre-processed by means of a pipeline that used FastQC (Krueger, Andrews et al. 2011), to asses read quality, and Cutadapt v1.9 (Criscuolo and Brisse 2014) to trim sequencing reads, eliminating Illumina adaptor remains, and to discard reads that were shorter than 30 bp. The resulting reads were mapped against the human transcriptome (GRCh38, release 76; aug2014 archive) and quantified using RSEM v1.17 (Li and Dewey 2011). Data were then processed with a differential expression analysis pipeline that used Bioconductor package EdgeR (Robinson, McCarthy et al. 2010) for normalization and differential expression testing, taking into account the paired design of the experiment. 12725 genes were identified and of those 1202 were differentially expressed (568 downregulated and 634 upregulated) between miR-28 expressing and control cells, with a cut off-of $p \leq 0.05$ (non adjusted).

iTRAQ quantitative analysis

Sample preparation and peptide isobaric labelling

For proteomics analysis, eight Ramos cell pellets (10^7 cells; 4 pairs of miR-28 transduced and scrambled transduced samples, from 2 independent infections) were homogenized in Lysis Buffer (50 mM Tris-HCl pH 8.0 – 4% SDS – 50 mM DTT), boiled for 10 min, sonicated and lysed with agitation for 15 min at room temperature. Cell lysates were centrifuged (13000 g, 15 min) to eliminate cell debris at 13000g for 15 minutes, and protein concentration in the supernatant was determined by the DirectDetect IR spectrometer (Millipore). The cleared lysates were stored at -80ºC. The four biological replicates for each condition were independently analyzed by using an iTRAQ 8-plex experiment. For that end, 160 µg of total protein for each sample were digested using the FASP protocol as previously described (Cardona, Lopez et al. 2015), with minor modifications.

For stable isobaric labeling, the resulting tryptic peptides from the 4 pairs of biological replicates were dissolved in Triethylammonium bicarbonate (TEAB) buffer, and the concentration of peptides was determined by measuring amide bonds with the Direct Detect system (Millipore). Equal amounts of each peptide sample were labeled using the 8-plex iTRAQ Reagents Multiplex Kit (Applied Biosys-

tems, Foster City, CA, USA) according to manufacturer's protocol.

Identification by LC-MS/MS

Labeled peptides were loaded into the LC-MS/MS system for on-line desalting onto C18 cartridges and analyzing by LC-MS/MS using a C-18 reversed phase EASY nano-column (75 µm I.D. x 50 cm, 2 µm particle size, Acclaim PepMap RSLC, 100 C18; Thermo Fisher Scientific, USA) in a continuous acetonitrile gradient consisting of 0-30% B in 360 min, 50-90% B in 3 min (A= 0.5% formic acid; B=90% acetonitrile, 0.5% formic acid). A flow rate of 200 nl/min was used to elute peptides from the RP nano-column to an emitter nanospray needle for real time ionization and peptide fragmentation on a Q-Exactive mass spectrometer (Thermo Fisher). An enhanced FT-resolution spectrum (resolution=70.000) followed by the MS/MS spectra from the 15 most intense parent ions were analyzed along the chromatographic run. Dynamic exclusion was set at 40 s.

iTRAQ data analysis.

For peptide identification, all spectra were analyzed with Proteome Discoverer (version 1.4.0.29, Thermo Fisher Scientific) using SEQUEST-HT (Thermo Fisher Scientific). For database searching at the Uniprot database containing all sequences from human and crap contaminants (March 06, 2013; 70024 entries), the parameters were selected as follows: trypsin digestion with 2 maximum missed cleavage sites, precursor and fragment mass tolerances of 2 Da and 0.02 Da, respectively, carbamidomethyl cysteine, iTRAQ modifications at N-terminal and Lys residues as fixed modifications, and methionine oxidation as dynamic modification. Peptide identification was validated using the probability ratio method (Martinez-Bartolome, Navarro et al. 2008); false discovery rate (FDR) was calculated using inverted databases, and the refined method (Navarro and Vazquez 2009) with an additional filtering for precursor mass tolerance of 15 ppm (Bonzon-Kulichenko, Garcia-Marques et al. 2015).

Protein quantification from reporter ion intensities and statistical analysis of quantitative data were performed using QuiXoT based on the WSPP statistical model previously described (Navarro, Trevisan-Herraz et al. 2014). In this model protein log2-ratios are expressed in form of the standardized variables, i.e., in units of standard deviation according to their estimated variances (Zq values). From the 4 pairs of miR-28 transduced and scrambled transduced Ramos samples, 7324 proteins were identified with an FDR of 1%. From those, we stablished a cut off 10% FDR to group significantly changed proteins, obtaining 276 changed proteins (107 were downregulated and 169 upregulated by miR-28 expression).

Functional protein analysis and the systems biology triangle

The significantly changed 276 proteins found by ITRAQ were subjected to Ingenuity pathway analysis

(IPA) (Ficenec, Osborne et al. 2003), to uncover the relationships and pathways among the miR-28 regulated products.

To depict the sigmoid representation and apply the systems biology triangle, first proteins were annotated using Ingenuity Knowledge Database (IPA) (Ficenec, Osborne et al. 2003) (Calvano, Xiao et al. 2005), CORUM (Ruepp, Brauner et al. 2008) and DAVID (Huang da, Sherman et al. 2009). The latter repository included 15 functional databases, such as KEGG, REACTOME, Gene Ontology and Panther, among others. Analysis of altered categories was evaluated as described in (Cardona, Lopez et al. 2015). Alterations in the abundance of functional categories were visualized by comparing the cumulative frequency (sigmoid) plots of the standardized variable with that of the normal distribution, as in previous works (Cardona, Lopez et al. 2015) (Isern, Martin-Antonio et al. 2013). The system biology algorithsms was applied to determine the statistical significance that any protein belonging to a category deviates from the coordinated behavior of the rest of the proteins of the same category. This algorithm was developed by García-Marqués and colleagues in Jesus Vazquez's lab (Garcia-Marqués et al., Mol Cel Proteom, under first revision). Briefly, they developed a method that allows the detection of coordinated protein behaviors by applying sequentially the generic integration algorithm (GIA) (Navarro, Trevisan-Herraz et al. 2014) in a manner that discards the outliers. In this last integration, the category-all outliers correspond to the categories that are significantly altered by the perturbation as a consequence of the coordinated behavior of their proteins.

Lymphoma xenograft and allograft models

Subcutaneous xenografts

NOD Scid Gamma (NSG) mice (8-14 weeks) received subcutaneous flank injections of lymphoma cells (2 x 10^6 of WT non-transduced Ramos cells or 10^7 cells in the case of the lentiviraly transduced human tumoral B cells) resuspended in 100 µL PBS and mixed with 100 µl Matrigel (BD Biosciences) at 1:1 proportions. When the transduced cells were used, doxycycline (Sigma-Aldritch) was administered to the animals one week before the xenograft injection (tumor development experiment) or once the tumors reached 200 mm^3 (tumor regression experiments) at a concentration of 0.04% through their drinking water.

Subcutaneous primary lymphoma allografts

To establish subcutaneous λ-MYC primary tumors, first enlarged lymph nodes were extracted from 4-to-8 months-old λ-MYC sick animals and single cell suspensions were prepared in 1% FCS PBS using a cell strainer as previously described. The phenotype of the tumoral cells was analyzed by FACS and by immunohistochemistry staining before allograft injection. 10^7 mouse primary λ-MYC lymphoma cells

were subcutaneously injected in the 2 flanks of NSG mice. Tumor growth was measured 3 times per week with a digital caliper using the following formula: volume = $(width)^2$ x length/2. Animals were sacrificed if the tumor compromised their wellness (usually when tumor reached around 2000 mm^3). The tumors were extracted for further FACS and histopathological analysis.

Intravenous primary lymphoma allograft model

Primary Burkitt lymphoma cells were obtained from ill λ-MYC transgenic mice as described above. 2 x 10^6 of λ-MYC lymphoma cells were intravenously injected in the tail vain of receptor NSG mice. All the animals were sacrificed 17 days after the injection of the tumoral cells.

B cell lymphoma treatment by synthetic miR-28 mimic administration

miR-28 mimic (Ambion) was used in vivo to replace endogenous miR-28 function. From a stock solution of 1 mM mimic, the specific quantity of HPLC purified miR-28 mimic (Ambion) is mixed with RNAse free water to prepare a 3mg/ml solution. Then, this solution is mixed at 1:1 proportions in complexation buffer (Ambion) and the resulting solution with Invivofectamin (Ambion) in 1:1 proportions. The solution was incubated at 50ºC 30 minutes and dialyzed with a Por-Float-A-Lyzer cassette with an 8-10 KDa diameter pore, following manufacturer instructions. Then is diluted with RNAse free PBS (Lonza) to the needed final volume. For intratumoral treatment 0.1 nmoles or 0.5 nmoles were injected in 50 µl PBS per tumor, 3 times after tumor establishment separated by 3-4 days. Intravenous treatment was achieved by injecting in the tail vain two doses of 7 nmoles (in 100 µl PBS solution per mouse, which is equivalent to 5 mg/kg concentration), separated by 4 days.

Histopathology and toxicity studies

Organs were fixed in 10% buffered formalin and embedded in paraffin. Sections were stained with hematoxylin and eosin (Sigma), anti-Pax5 (Santa Cruz Biotechnology), anti-CD3ε (Santa Cruz Biotechnology), anti-KI-67 (Abcam), anti-Bcl-6 (Santa Cruz Biotechnology), anti-Bcl-2 (Dako) or anti Caspase-3 (RyD systems). Quantifications were performed using Image-J. Neoplasms where classified by a pathologist according to their histopathological and immunophenotypic profile following the criteria of the consensus international system. miR-28 related toxicity studies consisted in tissue damage analysis by immunihistochemistry and clinical biochemistry of the plasma of the treated mice. Tissue damage was assessed by H&E staining of kidney, liver, heart and spleen from treated mice. Clinical biochemistry included blood counts in the Abacus Junior hematology analyzer and biochemical profile of different indicators of liver, kidney and heart function. These indicators are AST/GOT, ALT/GPT, GGT, total cholesterol, alkaline phosphatase, triglycerides levels, glucose and albumin levels.

Statistical analysis

Cytometry results, RT-qPCR results, WB densitometry results, tumor volume and weight were analyzed with Student's T test. Survival curves were analyses by Kaplan-Meier curves and statistical significance was calculated with a long-Rank. All the analysis were performed using the Graphpad Software. Statistical significance was stablished at $p<0.05$. Statistical analysis of quantitative proteomics data were performed using QuiXoT based on the WSPP statistical model previously described (Navarro, Trevisan-Herraz et al. 2014). Differential expression in the RNAseqs was assessed for each gene using the Bioconductor EdgeR package, that uses an exact test analogous to Fisher's exact test, but adapted for overdispersed data (Robinson, McCarthy et al. 2010) (Robinson and Smyth 2008) (Gentleman, Carey et al. 2004) .

RESULTS

1. Role of miR-217 in Germinal Center reaction and in B cell lymphomagenesis

1.1. miR-217 expression is upregulated in activated B cells

To identify miRNAs that play a role during B-cell activation, we profiled miRNA expression in mature B cells during *in vitro* activation with lipopolysaccharide (LPS) + interleukin (IL) 4, which promotes AID expression, SHM in the switch regions, and CSR. Microarray analysis showed that one of the few miRNAs whose expression is upregulated during this process is miR-217 (de Yebenes, Belver et al. 2008). Induction of precursor and mature miR-217 during B-cell activation *in vitro* was confirmed by qRT-PCR (Fig. 5A). In addition, we generated GCs *in vivo* by immunizing mice with sheep red blood cells (SRBC) and conducted qRT-PCR on purified resting and GC B cells. miR-217 precursor and mature miR-217 expression increased by five- and eightfold, respectively, in GC cells (Fig. 5B). Similarly, we found that miR-217 expression is increased in GC human B cells compared with resting B cells (Fig. 5C). Together, these results show that miR-217 expression is induced during B-cell activation both in mouse and humans.

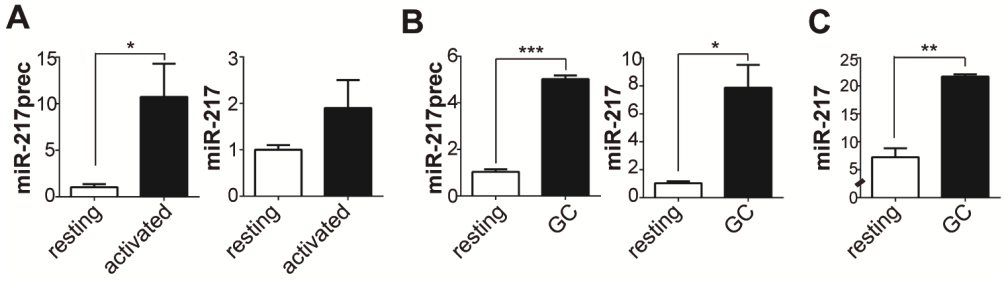

Figure 5. miR-217 expression is upregulated in activated B cells. (A) qRT-PCR analysis of the expression of the (left) miR-217 precursor and (right) mature miR-217 in B cells after 1 (open bars) and 3 days (filled bars) of activation with LPS + IL4. Data from 3 (miR-217 precursor) and 2 (mature miR-217) independent experiments are shown ($p = 0.05$ for miR-217 precursor and $p = 0.27$ for miR-217). Each experiment was performed with 2 individual mice. **(B)** qRT-PCR of miR-217 precursor (left) and mature miR-217 (right) in resting (open bars) or GC (filled bars) B cells isolated from spleens of wild-type C57BL/6 mice 10 days after immunization with sheep red blood cells (SRBC). Data are means 6 standard deviation from 2 independent experiments with 10 total immunized mice ($p = 0.0002$ for miR-217 precursor and $p = 0.01$ for miR-217). Two-tailed Student t test: p values: *p <0.05. **(C)** Quantification of miR-217 expression in human resting ($CD19^+CD27^+IgD^+$) and GC ($CD19^+CD10^+$) samples as measured by miRNA array hybridization (data were obtained from GSE29493, $p = 0.003$, 2-tailed Student t test).

1.2. Generation of B cell specific mouse models

To investigate the role of miR-217 during B-cell activation, we generated 2 independent mouse models of B cell-specific miR-217 overexpression. In the first, 4 independent transgenic mouse lines were generated with a construct encoding the miR-217 precursor and a GFP reporter gene under the control of regulatory elements of the mouse kappa light chain (Igκ) gene ($miR\text{-}217^{TG}$) (Fig. 6A, upper

construct). In the second strategy, the miR-217 precursor/GFP construct was preceded by a transcriptional stop cassette flanked by LoxP sites and inserted within the endogenous Rosa26 locus (ROSA26$^{miR217ki/+}$mice) (Fig. 6A, lower construct); specific expression of miR-217 in B cells was achieved by crossing ROSA26$^{miR217ki/+}$ mice with CD19-Cre$^{ki/+}$ mice (hereafter, miR-217^{KI} mice). ROSA26$^{miR217+/+}$ CD19-Cre$^{ki/+}$ mice were used as controls. B cells from miR-217^{TG} and miR-217^{KI} mice showed full GFP and miR-217 expression in mature splenic B cells (Fig. 6B-C). GFP expression was not detected in non-B-cell lineages, such as T, myeloid, or epithelial cells (data not shown). The proportions and absolute numbers of bone marrow and peripheral B cells in the miR-217^{TG} and miR-217^{KI} models were similar to those in wild-type littermate controls (Fig. 7), indicating that the miR-217^{TG} and miR-217^{KI} mouse models allow B cell-specific miR-217 overexpression without perturbing B-cell differentiation.

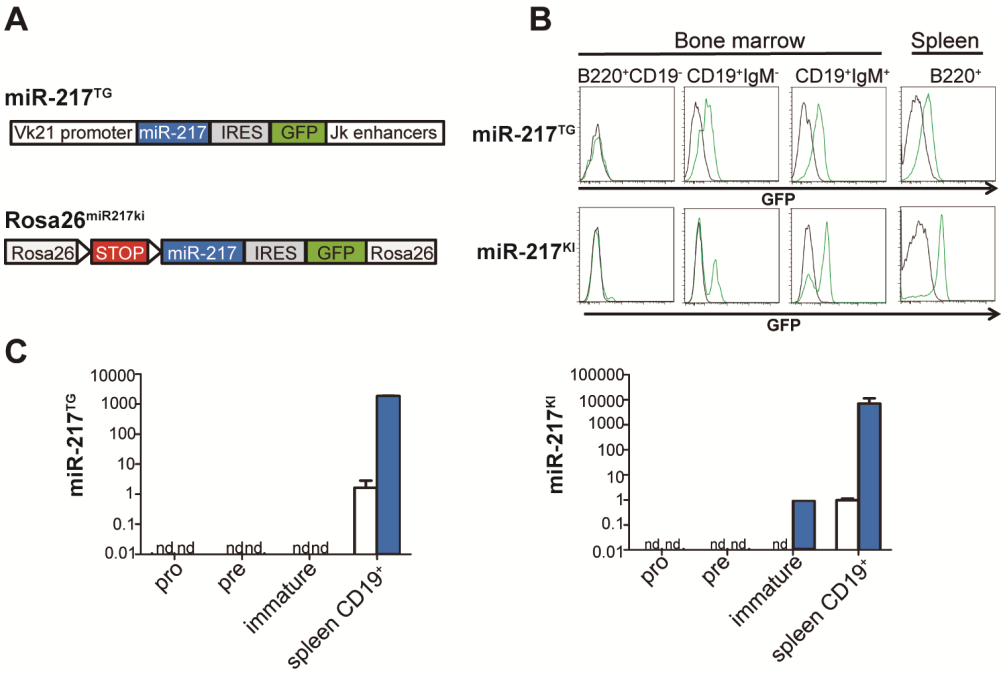

Figure 6. Generation of B cell specific mouse models. (A) Constructs used to generate the miR-217^{TG} and ROSA26miR217^{KI} specific mouse models. For miR-217^{TG} (represented in light blue), a construct encoding miR-217 precursor and GFP is expressed under the control of the Vκ21 promoter; for miR-217^{KI} (represented in dark blue), the miR-217 precursor construct is inserted within the Rosa26 locus, preceded by a transcriptional stop flanked by LoxP sites. miR-217^{KI} mice were crossed with CD19-Cre$^{KI/+}$ mice. **(B)** Representative FACS analysis of GFP expression in bone marrow and spleen B-cell subsets from control (black histograms) and miR-217^{TG} or miR-217^{KI} mice (green histograms). **(C)** q-RT-PCR quantification of miR-217 expression in bone marrow B cell precursors and splenic B cells isolated from control (open bars), miR-217^{TG} (filled light blue bars, left graph) and miR-217^{KI} mice (filled dark blue bars, right graph). Data are from three mice per genotype. n.d., not detectable.

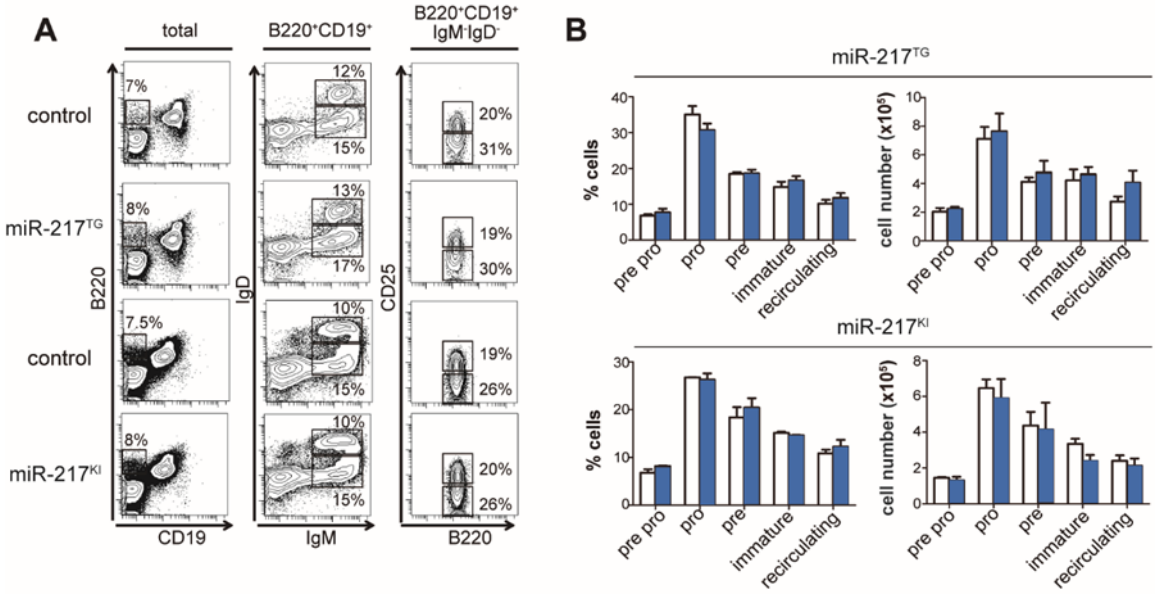

Figure 7. B cell specific miR-217 mouse models allow normal B cell development in the bone marrow. (A) Representative fluorescence-activated cells sorting (FACS) analysis of bone marrow from miR-217^{TG}, miR-217^{KI} and littermate control mice. Plots show the expression of B220/CD19 in total live lymphocytes (left), IgD/IgM gated in B220^{+}CD19^{+} cells (center), and CD25/B220 gated in B220^{+}CD19^{+}IgM^{+}IgD^{+} cells (right). The proportion of cells within B220^{+} cells is indicated in each gate. **(B)** Quantification of the proportions (left) and absolute cell numbers (right) of developing bone marrow B-cell subsets in control (open bars), miR-217^{TG} (light blue filled bars), and miR-217^{KI} mice (dark blue filled bars). The proportions of different B-cell subsets were quantified within the B220^{+} population.

1.3. miR-217 expression enhances the GC reaction

To address the role of miR-217 expression during B-cell activation in GCs, we analyzed the B-cell response to a T cell-dependent antigen in miR-217^{TG} mice. We first immunized miR-217^{TG} mice and wildtype littermate controls with NP-CGG. As an immunization control, mice were injected with phosphate-buffered saline (PBS). The lymph nodes of NP-CGG-immunized wild-type mice contained GC B cells (Fas^{+}GL7^{+}) and B cells that had undergone CSR (IgG1^{+}); but in miR-217^{TG} mice, the response to NP-CGG immunization was greater, with 22% more GC B cells ($p = 0.01$) and 20% more IgG1^{+} B cells ($p = 0.08$; Fig. 8). A similarly enhanced GC response to NP-CGG immunization was found in miR-217^{KI} mice (not shown).

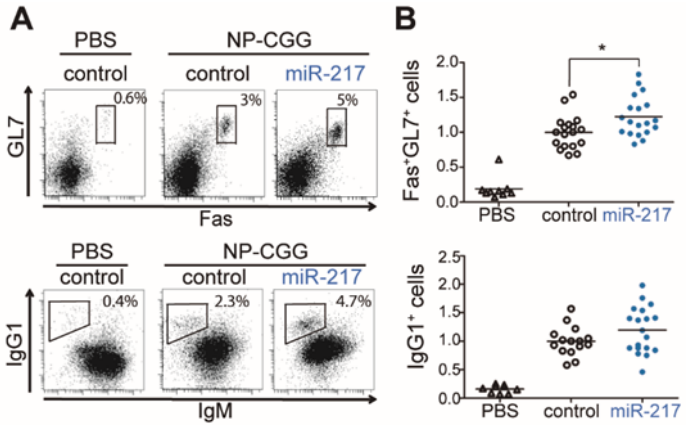

Figure 8. miR-217 expression in B cells enhances the GC response after primary immunization. (A) Representative FACS analysis of B220^{+} lymphocytes in lymph nodes after primary T cell dependent immunization with NP-CGG of miR-217^{TG} mice or littermate controls. **(B)** miR-217^{TG} mice (closed circles) or littermate controls (open circles) were immunized by subcutaneous injection of NP-CGG in complete Freund's adjuvant.

Figure 8 (continuation): 14 days after immunization, lymph nodes were analyzed for the presence of GC B cells (Fas^+GL7^+) and switched B cells ($IgG1^+$). Mice injected with PBS (open triangles) were used as non-immunized controls. Each symbol represents an individual mouse. Data were normalized to the mean value of control mice in each experiment; results are shown for a total of 4 experiments performed with 4 independent miR-217^{TG} mouse lines (p = 0.01 for GC B cells and p = 0 .08 for switched B cells).

We next analyzed the secondary B-cell immune response in control and miR-217^{TG} mice. The enhancement of the GC reaction in miR-217^{TG} mice was notably greater in secondary immunization assays, with 40% more Fas^+GL7^+ B cells and 60% more $IgG1^+$-switched B cells than controls (p = 0.019 and 0.018, respectively; Fig. 9. In addition, we found that the proportion of $CD138^+$ plasma cells is larger in miR-217^{TG} mice than in controls (not shown).

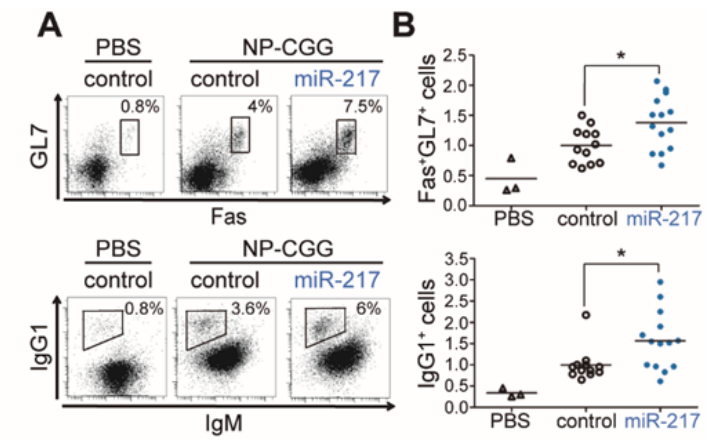

Figure 9. miR-217 expression in B cells enhances the GC response after secondary immunization. Fourteen days after primary immunization, miR-217^{TG} mice (closed circles) or littermate controls (open circles) were re-immunized by subcutaneous injection of NP-CGG and analyzed 7 days later. **(A)** Representative FACS analysis of $B220^+$ lymphocytes in lymph nodes after secondary NP-CGG immunization of miR-217^{TG} mice or littermate controls. **(B)** Quantification of the immunization response. Data from 2 independent experiments are normalized to the mean value of control mice in each experiment (p = 0.019 for GC and p = 0 .018 for switched B cells).

To analyze the influence of miR-217 overexpression on the long-lived memory B-cell compartment, we quantified $IgG1^+$ B cells in spleens from control and miR-217^{KI} mice 1 year after immunization. The proportion of memory B cells was 40% higher in miR-217^{KI} mice than in controls (p = 0.003; Fig. 10).

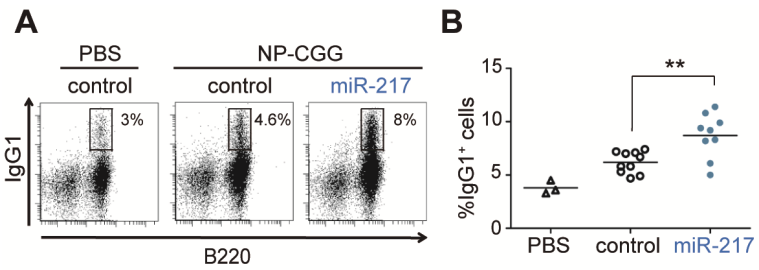

Figure 10. miR-217 expression increases the frequency of memory B cells after long term immunization. miR-217^{KI} mice or littermate controls were immunized with NP-CGG and immunization response was analyzed 1 year later. **(A)** Representative FACS plots showing the frequency of spleen memory $IgG1^+$ B cells gated within $B220^+$ cells. **(B)** Quantification of the proportion of memory B cells in the control group (open circles), miR-217^{KI} (closed circles) and in the non-immunized PBS injected (open triangles) group (p = 0.003).

To further characterize the role of miR-217 in the GC reaction, we examined the extent of SHM in miR-217^{TG} mice *in vivo*. We isolated Fas^{+} GL7^{+} GC B cells from Peyer's patches of control and miR-217^{TG} mice and quantified the mutation frequency in an intronic DNA region downstream of the J_H4 segment of the IgH locus, a region that accumulates mutations but cannot be subject to affinity maturation events (Fig. 11A). Conventional Sanger sequencing of the J_H4 intronic region showed that miR-217^{TG} B cells have a higher mutation load than wild type controls (control, 2.1 x 10^{-3}/bp and miR-217^{TG}, 3.7 x 10^{-3}/bp, p = 0.028; Fig. 11B). Likewise, GC B cells from miR-217^{KI} mice accumulated more mutations downstream of J_H4 than did wild-type controls (not shown). Similar results were obtained when we analyzed SHM frequency at the J_H4 intronic region by Next Generation Sequencing (NGS), which allows large numbers of mutations to be analyzed at very high depth (Perez-Duran, Belver et al. 2012). No mutations were detected in B cells isolated from AID$^{-/-}$ mice, used as negative control. We detected total mutation frequencies of 1.7 x 10^{-3}/bp in control animals and 3.7 x 10^{-3}/bp in miR-217^{TG} mice (p = 1.9 x 10^{-9}), a 2.2-fold difference (Fig. 11C). This difference was even higher (2.7-fold) when the analysis was limited to cytosines located in AID mutational hotspots RGYW/WRCY (where R = A/G, Y = C/T, and W = A/T) (5.8 X 10^{-3}/bp in controls vs 15.6 x 10^{-3}/bp in miR-217^{TG}; Fig. 11C), confirming that miR-217 overexpression in B cells increases the load of SHM in GCs. These results indicate that overexpression of miR-217 in B cells increases the efficiency of GC formation, CSR and SHM, and the generation of terminally differentiated B cells *in vivo*.

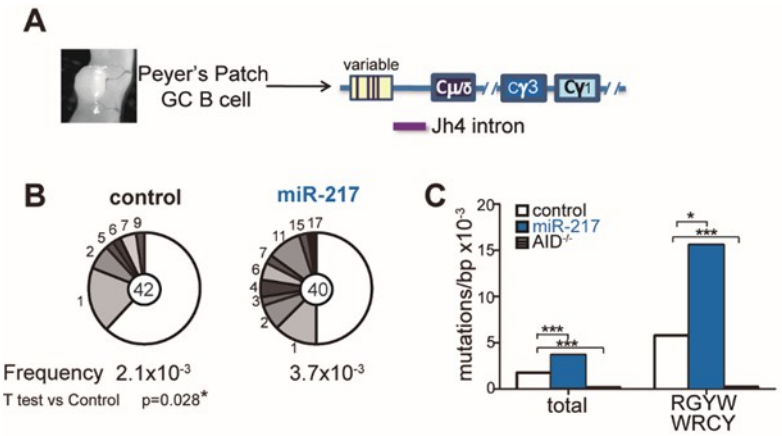

Figure 11. miR-217 expression in B cells enhances SHM. (A) SHM was quantified by sequencing the J_H4 intronic region of the IgH locus of GC B cells isolated from Peyer' patches. 6 control and 6 miR-217^{TG} mice were pooled to perform Sanger and NGS analyses. **(B)** Sanger sequencing analysis of SHM. Segment sizes in the pie charts are proportional to the number of sequences carrying the number of mutations indicated at the periphery. Mutation frequencies are indicated below each chart, and the total numbers of independent sequences analyzed are indicated in the chart centers. Statistical significance was determined by a 2-tailed Student t test (p = 0.028). **(C)** NGS quantification of the total J_H4 mutation frequency and of the mutation frequency at cytosines within the RGYW/WRCY AID hotspots in J_H4 sequences in GC B cells from control (open bars) and miR-217^{TG} mice (filled light blue bars). The mutation frequency in the J_H4 sequence of AID$^{-/-}$ splenic B cells is shown in hatched bars. A total of 300.000 kb/genotype was sequenced. Statistical significance of the mean mutation frequency at each position was determined by a paired Student t test (p = 1.9 x 10^{-9} for total mutation frequency and p = 0.002 for mutation frequency at WRCY hotspots).

1.4. Inhibition of endogenous miR-217 impairs the GC reaction *in vivo*

To address whether endogenous miR-217 expression plays a physiological role in GCs, we generated bone marrow mouse chimeras in which endogenous miR-217 expression was inhibited by the expression of a miR-217 sponge (miR-217 SPG) construct (Fig. 12A), where sequences complementary to miR-217 were cloned in tandem within the 3'untranslated region of a reporter gene and thus function as competitive inhibitors for the binding of the miRNA to its endogenous binding sites (Ebert, Neilson et al. 2007) (Rao, O'Connell et al. 2010). Bone marrow cells from wild-type mice were transduced with miR-217 SPG or control retroviruses and transferred into lethally irradiated CD45.1 congenic recipient mice and immunized 4 weeks later with NP-CGG (Fig. 12B). Chimeric mice injected with PBS were used as immunization negative controls.

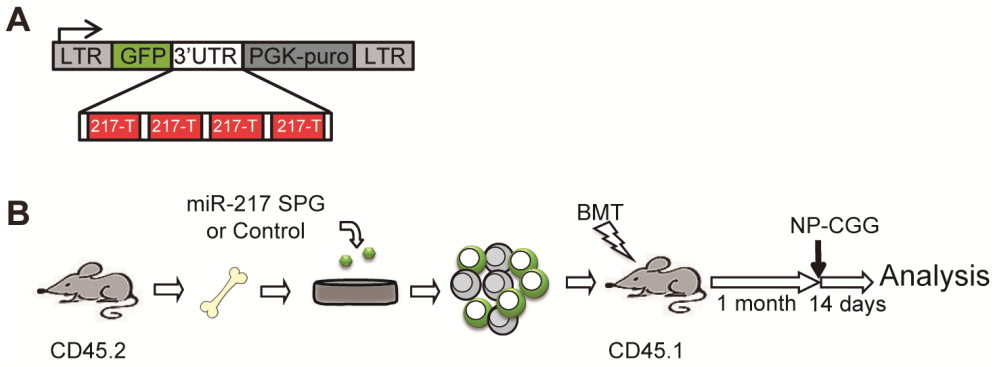

Figure 12. Schematic representation of the experimental approach used to inhibit endogenous miR-217 expression *in vivo*. (A) Retroviral construct used for miR-217 inhibition (miR-217 sponge (SPG)). Four miR-217 complementary sites (217-T) separated by 4-nt spacers were placed downstream of the GFP reporter gene in the MGP vector. **(B)** Generation of chimeric mice that lack endogenous miR-217. Bone marrow cells from CD45.2 mice were transduced with the miR-217 SPG or empty control vectors, and transferred into lethally irradiated CD45.1 recipient mice. After 1 month of reconstitution, chimeric mice were immunized with a T cell dependent antigen and the GC response was analyzed 14 days later.

When we analyzed the spleen and lymph nodes from immunized miR-217 SPG mice we noticed that they contained fewer GC and $IgG1^+$ switched B cells than immunized control chimeric mice, and indeed, the proportions of these cell subsets in immunized miR-217 SPG mice were as low as in PBS injected, non-immunized animals (Fig. 13).

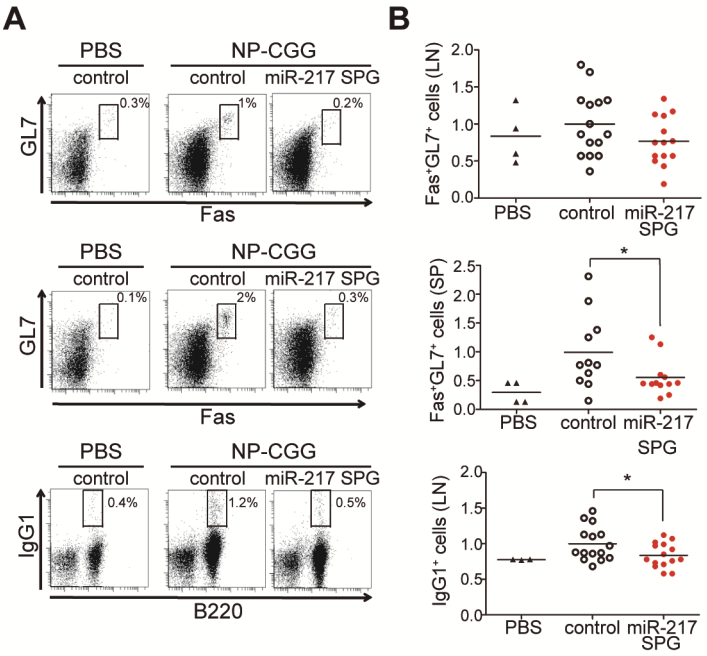

Figure 13. Inhibition of endogenous miR-217 expression in B cells impairs the GC response. Efficiency of GC (Fas^+GL7^+) and switched ($IgG1^+$) B cells isolated from lymph nodes 14 days after NP-GCC immunization of mouse chimeras reconstituted with control (open circles) or miR-217 SPG (in red) retrovirally transduced bone-marrow precursors. **(A)** Representative plots and **(B)** the respective quantifications are shown. Non-immunized mice injected with PBS (triangles) were included as immunization controls. Data are from two independent experiments, and are normalized to the mean response of control mice in each experiment. Statistical significance was determined by a two-tailed t test, *p < 0.05).

We next analyzed SHM in Peyer's patch GC B cells from miR-217 SPG and control chimeric mice by NGS. We found that miR-217 SPG GC B cells had a 25% lower mean mutation frequency than control B cells at the J_H4 intronic region ($p = 3.7 \times 10^{-5}$; Fig. 14). Very similar results were obtained when we analyzed the mutation load in a fragment of the μ switch region (Sμ) of IgH ($p = 4 \times 10^{-4}$), where mutations accumulate concomitantly with CSR (Fig. 14). These results thus show that inhibition of endogenous miR-217 attenuates the GC reaction and decreases the frequency of somatic mutations associated with both the SHM and the CSR reactions.

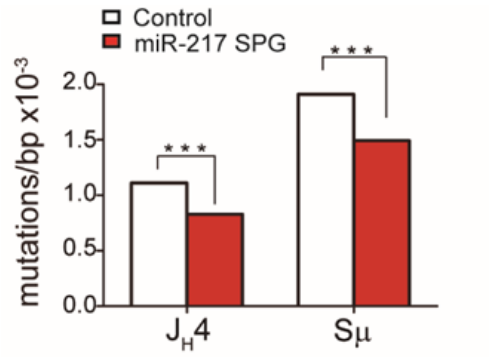

Figure 14. Inhibition of endogenous miR-217 impairs SHM. NGS quantification of mutations in J_H4 (left) and Sμ (right) sequences in $GFP^+CD45.1^+$ GC (Fas^+GL7^+) B cells isolated from pooled Peyer's of 8 control (open bars) and 8 miR-217^{SPG} (red bars) mouse chimeras. Data are from two (J_H4) and one (Sμ) independent experiments. At least 190 000 kb were sequenced per genotype. Statistical significance of the mean total mutation frequency at each position was determined by a paired Student t test ($p = 3.7 \times 10^{-5}$ for J_H4 SHM and $p = 4 \times 10^{-4}$ for Sμ SHM).

1.5. miR-217 regulates a DNA damage response and repair gene network and stabilizes Bcl-6 expression in GC B cells

1.5.1-Analysis of gene expression profile changes induced by miR-217 in GC B cells

To identify the genes regulated by miR-217 in activated B cells, we performed a genome-wide comparison of the gene expression profiles of miR-217^{TG} and wild-type GC B cells by RNAseq. Comparison of GC B cells from Peyer's patches of miR-217^{TG} and wild-type mice identified 1740 differentially expressed genes with $p \leq 0.05$ (see annex 1 to have the complete list of changed genes), 1236 of which were downregulated. This set of downregulated genes was significantly enriched in predicted miR-217 targets ($p = 9.75 \times 10^{-7}$; Fig. 15A), suggesting that a high proportion of the downregulated genes identified in miR-217^{TG} GC B cells are direct miR-217 targets. To identify the gene networks altered by miR-217 expression in GC B cells, we performed a bioinformatics analysis on the genes differentially expressed in miR-217^{TG} vs control GC (Fas^{+}GL7^{+}) B cells.

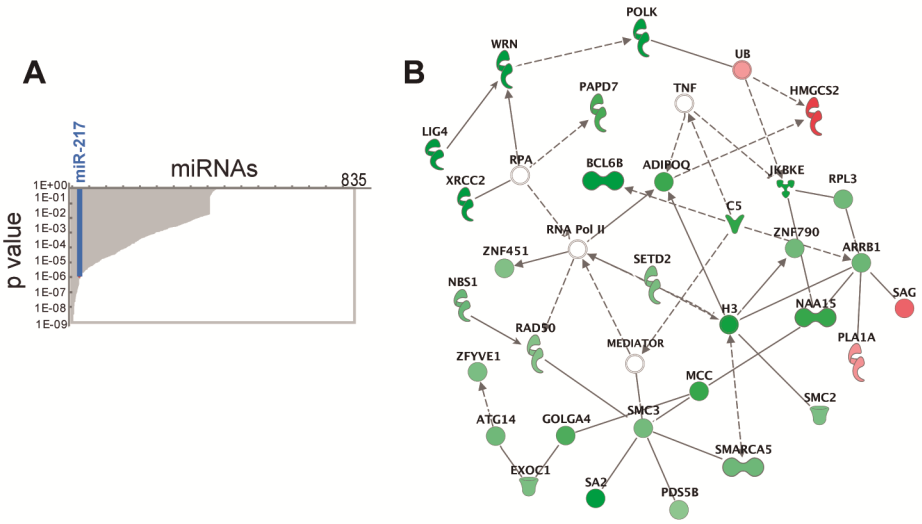

Figure 15. Identification of gene networks regulated by miR-217 in GC B cells. RNAseq analysis of genome-wide gene expression in control and miR-217^{TG} GC B cells isolated from Peyer's patches. **(A)** Enrichment in miR-217 predicted targets within the 1236 mRNAs whose expression was downregulated in miR-217^{TG} versus control GC B cells. **(B)** Ingenuity Pathway Analysis of the genes differentially expressed in control versus miR-217^{TG} GC B cells, showing enrichment for a DNA replication and repair gene network among the genes regulated by miR-217. Downregulated genes are shown in green, upregulated genes in red ($p < 0.001$).

Ingenuity Pathway Analysis revealed that miR-217 regulates a DNA damage response (DDR) and repair gene network in GC B cells ($p = 10^{-31}$; Fig. 15B). Interestingly, this gene network contained 2 main hubs, RNA pol II and replication protein A, which are directly linked to AID activity (Chaudhuri, Khuong et al. 2004) (Kenter 2012) (Nambu, Sugai et al. 2003) (Pavri, Gazumyan et al. 2010) (Vuong

and Chaudhuri 2012). The miR-217-regulated gene network included a number of genes linked to the DDR (Nbs1 and Rad50 components of the Mre11-Rad50-Nbs1 [MRN] complex) (Stracker and Petrini 2011) DNA repair and CSR (Wrn, Lig4, and Xrcc2) (Robbiani and Nussenzweig 2013) (Ramiro, Reina San-Martin et al. 2007) (Bothmer, Rommel et al. 2013) and genes of the cohesin complex (SMC2, SMC3, PDS5B, and SA2) involved in chromatid cohesion, as well as in DNA replication, transcription, recombination, and repair (Merkenschlager and Odom 2013) (Remeseiro and Losada 2013); all of them were downregulated by miR-217.

1.5.2-Analysis of the DNA damage response and Bcl-6 expression in miR-217 overexpressing B cells upon genotoxic stress

Bcl-6 expression is regulated by the DDR through a signaling pathway that promotes Bcl-6 degradation (Phan, Saito et al. 2007). As we found that miR-217 downregulates the expression of a number of genes involved in DDR and repair in GC B cells, we hypothesized that miR-217 could stabilize Bcl-6 expression in these cells. To test this hypothesis, we transduced Ramos cells, a human Burkitt lymphoma (BL) GC B-cell line, with miR-217-GFP and control retroviral vectors and analyzed Bcl-6 expression on genotoxic stress induction. We first verified that genes linked to the DDR and downregulated by miR-217 expression in mouse GC B cells (Nbs1, Xrcc2, Lig4, and Pds5b) were also downregulated by miR-217 in human Ramos cells (Fig. 16).

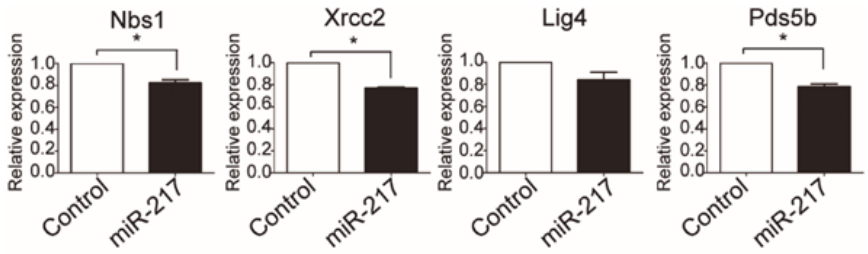

Figure 16. The DDR pathway is downregulated upon miR-217 expression in Ramos cells. Quantification of Nbs1, Xrcc2, Lig4, and Pds5b expression in Ramos cells transduced with control (open bars) or miR-217 (filled bars) retrovirus analyzed by q-RT-PCR. Two-tailed Student t test was used to calculate p values (*p ≤ 0.05).

To determine if miR-217 impacts on the response to genotoxic stress, we analyzed the effect of etoposide treatment on the cell cycle of control- and miR-217-transduced Ramos cells. Expectedly, we found that etoposide induced DDR promoted an increase in the fraction of cells in the S phase of the cell cycle, consistent with a replicative delay (Fig. 17). However, this S phase increase was milder in miR-217-transduced cells (Fig. 17B), which suggested that miR-217 may contribute to bypass the DDR response induced by etoposide.

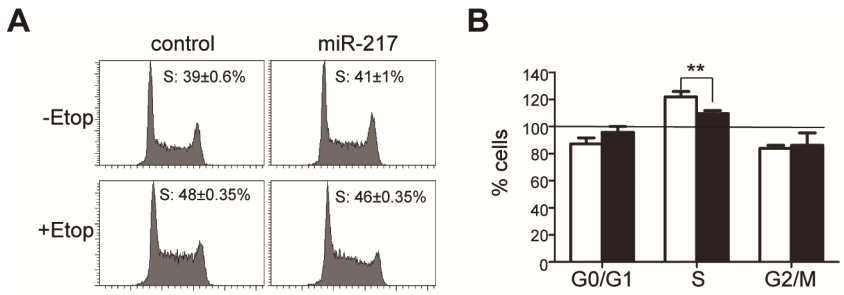

Figure 17. miR-217 expression attenuates the DDR response to etoposide-induced genotoxic stress. Cell cycle analysis of etoposide-treated control and miR-217- transduced Ramos cells. **(A)** Representative cell cycle plots of untreated (-Etop) or etoposide treated (6 hours, 10 mM) (+Etop) Ramos cells. The mean and standard deviation of the fraction of cells in S cycle are annotated in the plots. **(B)** Quantification of the change in the proportion of cells at each phase of cell cycle in response to etoposide treatment (open bars, control-transduced cells; black bars, miR-217-transduced cells). Bars represent means and standard deviations from 3 independent experiments (p = 0.004) (2-tailed Student t test).

Immunoblot analysis showed that etoposide treatment of control Ramos cells rapidly induced Bcl-6 degradation (Fig. 18), in agreement with previous results (Phan, Saito et al. 2007). However, Ramos cells overexpressing miR-217 were partially protected against genotoxic stress-induced Bcl-6 degradation and showed increased Bcl-6 expression levels (Fig. 18, upper panel). Caffeine treatment protected miR-217 Ramos cells from etoposide induced Bcl-6 degradation, indicating that an ataxia telangiectasia mutated/ataxia telangiectasia and Rad3-related–dependent pathway is involved in this process (Fig. 18, lower panels).

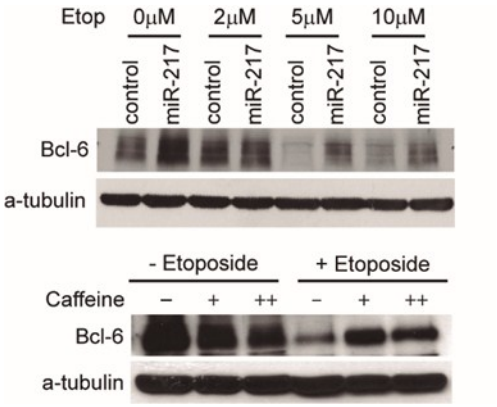

Figure 18. miR-217 dampens Bcl-6 degradation in GC B cells upon genotoxic stress. (Upper) Immunoblot of Bcl-6 in Ramos cells transduced with control or miR-217 retrovirus treated for 6 hours with the indicated doses of etoposide. (Lower) Immunoblot of Bcl-6 in miR-217-transduced cells left untreated (-Etoposide) or treated with 10 mM Etoposide for 6 hours (+Etoposide) in the presence of increases doses of caffeine (0 mM [-], 2 mM [+], and 5 mM [++]).

Analysis of Bcl-6 protein levels in GC B cells from control and miR-217^{KI} mice further confirmed that miR-217 expression promotes the accumulation of Bcl-6 (Fig. 19). Finally, quantification of Bcl-6 expression in spleens from miR-217^{TG} and control mice revealed that miR-217^{TG} mice have larger Bcl-6^{+} follicle areas in spleens (p = 0.0008; Fig. 20). Overall, these data indicate that miR-217 regulates the

GC reaction by modulating the expression levels of a gene network involved in DDR and repair and by dampening genotoxic stress-induced Bcl-6 degradation in GC B cells.

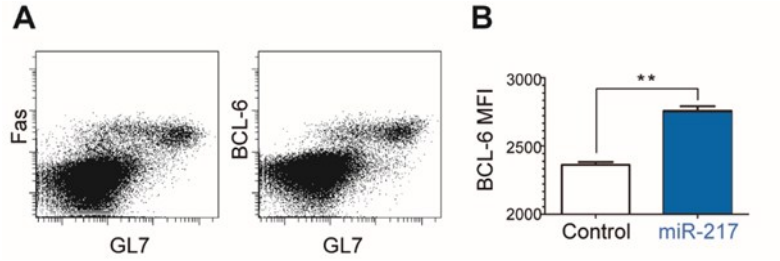

Figure 19. Analysis of Bcl-6 expression in miR-217^{KI} GC cells by flow cytometry. **(A)** Representative dot plots of Fas, GL7, and Bcl-6 staining of Peyer's patch B cells. **(B)** Quantification of Bcl-6 expression levels in B220^{+}Fas^{+}GL7^{+}GC B cells from Peyer's patches of littermate controls (white bar) and miR-217^{KI} mice (black bar) (MFI, mean fluorescence intensity; 3 mice per genotype, p = 0.0006, 2-tailed Student t test).

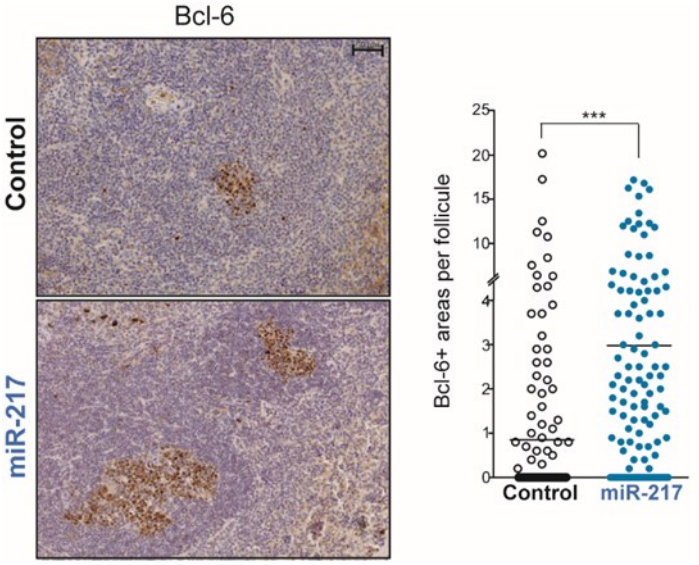

Figure 20. Aged miR-217^{TG} mice have bigger Bcl-6^{+} areas per follicle. Immunohistochemical analysis of the proportion of Bcl-6^{+} areas per follicles. 205 and 201 spleen follicles of control and 10 miR-217^{TG} mice were quantified, respectively. Statistical significance was determined by 2-tailed Student t test.

1.6. Deregulated miR-217 expression promotes mature B cell lymphomas

GC B cells are highly prone to oncogenic transformation. Our results show that miR-217 is a positive regulator of the GC reaction, presumably by downregulating the expression of DNA repair genes and by stabilizing Bcl-6 expression, which could enhance the susceptibility of these cells to oncogenic events. To test whether miR-217 overexpression in B cells affects the development of mature B-cell lymphomas, we monitored the incidence of B-cell lymphoma in a group of 34 control and 40 miR-217^{KI} mice. Mice were euthanized and analyzed at an end-point of 90 weeks or earlier if they showed signs of disease. miR-217^{KI} mice had larger spleens than control animals, with a fraction

showing clear splenomegaly (20% vs 0% spleens larger than 20 mm; Fisher's exact test, p = 0.0058; Fig. 21A; Table 8).

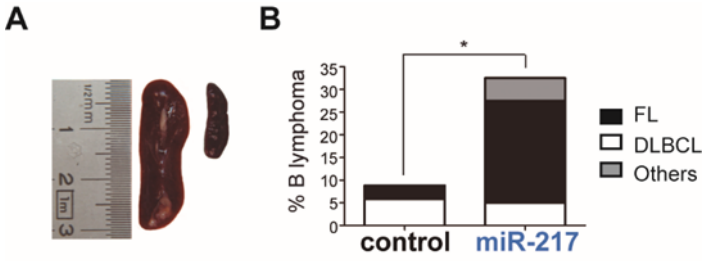

Figure 21. miR-217 overexpression promotes mature B cell lymphomas. 34 control and 40 miR-217^{KI} mice were monitored over 90 weeks for the appearance of B cell lymphoma. **(A)** Representative pictures of a non-tumoral control spleen (right) and a miR-217^{KI} spleen with splenomegaly (left). **(B)** Quantification of B cell lymphoma incidence in control mice (open bars) and miR-217^{KI} mice (filled bars). P value was determined by two-tailed t test (p = 0.028).

Histopathological evaluation of the spleens showed that a large proportion (33%) of miR-217^{KI} mice developed B-cell lymphoma (p = 0.028 vs control mice; Fig. 21B). We found that lymphomas in miR-217^{KI} mice had features of mature GC or post-GC B-cell origin. To classify the lymphomas, paraffin-embedded samples were stained with H&E and a B cell marker (Pax5), a T cell marker (CD3) and a GC marker (Bcl-6). Most neoplasias (70%) were classified as follicular lymphomas (FL), although we also observed other mature B-cell lymphomas, such as DLBCL and B-cell plasmacytomas (PCT) (Fig. 21B and Fig. 22; Table 8).

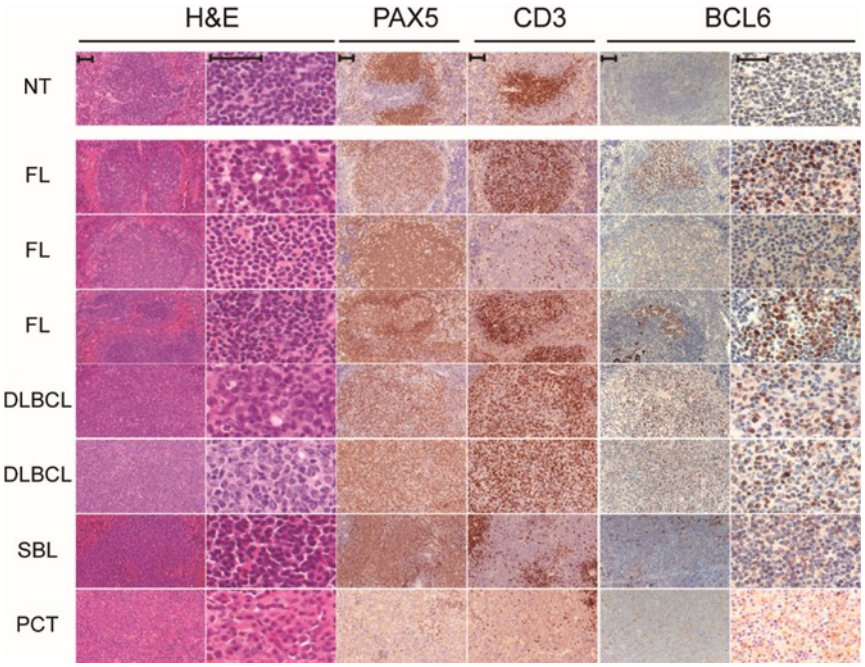

Figure 22. Immunohistochemical characterization of the B cell lymphomas found in miR-217^{KI} mice. All the tumors were stained for H&E (left), Pax5, CD3 and Bcl-6 and classified by a pathologist. Representative cases of the different B cell lymphomas generated are shown. Scale bar is 50 µm. NT, non-tumoral; SBL, small B-cell lymphoma.

Table 8. Characterization of B cell lymphomas in miR-217^{KI} mice

Mouse ID[a]	B cell lymphoma[b]	Grade[c]	Spleno-megaly[d]	Phenotype[e]
BPT048	FL			Mature B cell, B220^{+} CD19^{+} sIgM^{+} sIgκ^{+} Fas^{+}GL7^{+}, Pax5^{low} BCL-6^{+}; numerous infiltrating T cells.
BPT100	FL		Yes	Mature B cells, Pax5^{+} BCL-6^{-} and N/A
BPT105	FL			Mature B cell, B220^{+} CD19^{+} sIgM^{-} sIgκ^{+}, Pax5^{+} BCL-6^{+}
BPT106	FL			Mature B cell, B220^{+} CD19^{+} sIgM^{-} sIgκ^{+}, Pax5^{low} BCL-6^{+}
BPT109	PCT	Aggressive		Mature B cell, Pax5^{-} BCL-6^{-} and N/A
BPT124	FL	Aggressive		Mature B cell, B220^{low} CD19^{+} sIgM^{high} sIgκ^{+}, Pax5^{low} BCL-6^{-}
BPT137	FL			Mature B cell, B220^{+} CD19^{+} sIgM^{low} sIgκ^{+}, Pax5^{+} BCL-6^{-}
BPT148	DLBCL	Aggressive	Yes	Mature B cell, B220^{+} CD19^{+} sIgM^{low} sIgκ^{+}, Pax5^{low} BCL-6^{+}; numerous infiltrating T cells.
BPT224	DLBCL	Aggressive	Yes	Mature B cell, B220^{+} CD19^{+} sIgM^{low} sIgκ^{low}, Pax5^{low} BCL-6^{+}; numerous infiltrating T cells.
BPT226	FL	Aggressive	Yes	Mature B cell, B220^{+} CD19^{+} sIgM^{low} sIgκ^{low}, Pax5^{low} BCL-6^{+}; numerous infiltrating T cells.
BPT234	SBL			Mature B cell, B220^{+} CD19^{+} sIgM^{high} sIgκ^{+}, Pax5^{+} BCL-6^{-}
BPT263	FL		Yes	Mature B cell, B220^{high} CD19^{+} sIgM^{+} sIgκ^{+}, Pax5^{+} BCL-6^{+}
BPT266	FL	Aggressive		Mature B cell, B220^{+} CD19^{+} sIgM^{low} sIgκ^{+}, Pax5^{low} BCL-6^{-}

a: Mouse identification number
b: B cell lymphoma type: FL: follicular lymphoma; DLBCL: diffuse large B cell lymphoma; SBL: small B-cell lymphoma and PCT: plasmacytoma
c: Lymphoma classification grade
d: Splenomegaly: spleens larger than 20mm length.
e: Phenotype of tumoral cells determined by morphological features, flow cytometry and immunohistochemica stainings. N/A: not analyzed

Flow cytometry analysis of the spleens and lymph nodes showed that lymphomas from miR-217^{KI} mice presented frequent alterations in the expression of the B-cell surface molecules B220, IgD, IgM, and Igκ (Table 8). To further characterize the origin of these lymphomas, we performed molecular analysis of their V(D)J rearrangements by PCR amplification and sequencing. We found that a fraction of the lymphomas yielded unique amplification bands (Fig. 23), which were confirmed to correspond with single rearrangements (Table 8), thus providing proof of their clonal origin. In addition, all of the rearrangements subject to this analysis contained mutations (SHM^{+}) in their V genes (Table 9), confirming their GC/post-GC origin.

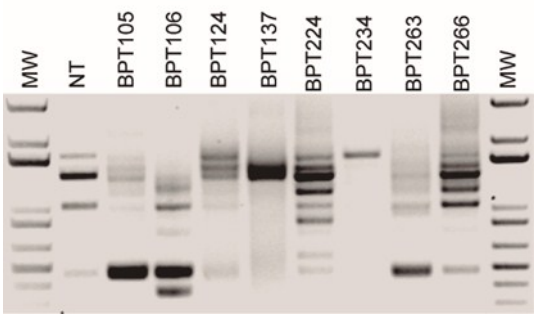

Figure 23. Evidences of clonality in miR-217 promoted B cell lymphomas. PCR analysis of V(D)J rearrangements in tumor samples from miR-217^{KI} mice. DNA was isolated from total spleen and amplified using a V-degenerate primer in combination with an antisense primer downstream of J_H4. Sequencing results are shown in Table 9. Mouse IDs are shown. MW, molecular weight marker.

Table 9. Analysis of VDJ gene rearrangements in clonal B-cell lymphomas of miR-217^{KI} mice

Mouse ID[a]	V gene[b]	D gene[b]	J gene[b]	V-D-J junction	SHM[c]
BPT105	IGHV1-66*01	IGHD2-5*01	IGHJ4*01	GGGGGCTATAGTCAAATGAGGGGG	+
BPT124	IGHV1S16*01	IGHD1-2*01	IGHJ2*01	GAGGGGATTACTACGGCTACC	+
BPT137	IGHV1S127*01	IGHD4-1*02	IGHJ2*01	GACTGGGACGTCGG	+
BPT234	IGHV1-47*01	IGHD2-4*01	IGHJ1*01	ATGATTACGACCACC	+

a: Mouse identification number
b: Assignment of V, D and J genes by NCBI/IGBLAST according to IMGT database.
c: Somatic hypermutation

1.6.1- Role of p53 and Ink4a/Arf tumor suppressors in miR-217 induced lymphomagenesis

To examine the contribution of tumor suppressor pathways to limiting the B-cell lymphomagenesis induced by miR-217, we analyzed the incidence of B-cell lymphoma in miR-217^{KI} mice in the Ink4a/Arf $^{-/-}$ and p53$^{-/-}$ backgrounds. Ink4a/Arf $^{-/-}$ and p53$^{-/-}$ mice often developed histiocytic sarcomas (40%) and T-cell lymphomas (70%), respectively (data not shown). In addition, we found that roughly 20% of both control Ink4a/Arf$^{-/-}$ and p53$^{-/-}$ tumor suppressor-deficient mice generated B-cell lymphomas. This incidence was not significantly altered by miR-217 overexpression in the p53$^{-/-}$ background, but in the Ink4a/Arf $^{-/-}$ background, miR-217 overexpression increased B-cell lymphoma incidence to 43% (Fig. 24A), although the mean survival of miR-217^{KI} Ink4a/Arf $^{-/-}$ mice was not significantly altered (Fig. 25). A similar molecular and histochemical characterization to that performed with miR-217^{KI} tumors was done with the Ink4a/Arf$^{-/-}$ tumors. B-cell lymphomas in miR-217^{KI} Ink4a/Arf $^{-/-}$ mice showed histopathological features of mature GC or post-GC B-cell lymphomas (Fig. 24B). These results suggest that the Ink4a/Arf, but not the p53, tumor suppressor pathway acts as a surveillance mechanism against the lymphomagenic events induced by miR-217 in mature B cells.

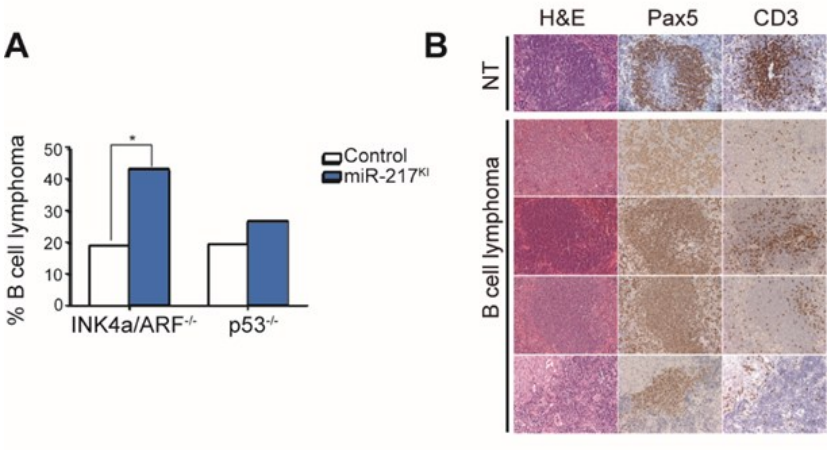

Figure 24. Loss of Ink4a/Arf but not p53 increases the frequency of the miR-217 induced B cell lymphomas. (A) Quantification of B-cell lymphoma incidence in control (open bars) and miR-217^{KI} (filled bars) Ink4a/Arf$^{-/-}$ and p53$^{-/-}$ mice. Statistical significance was determined by 2-tailed Student t test (p = 0.03 in miR217^{KI} Ink4a/Arf$^{-/-}$ vs control Ink4a/Arf$^{-/-}$ and p = 0.33 in miR217^{KI} p53$^{-/-}$ vs control p53$^{-/-}$). **(B)** Representative H&E and immunohistochemical stainings for Pax5 and CD3 from spleens of assorted to miR-217^{KI} Ink4a/Arf $^{-/-}$ lymphomas. Original pictures were taken at 40X.

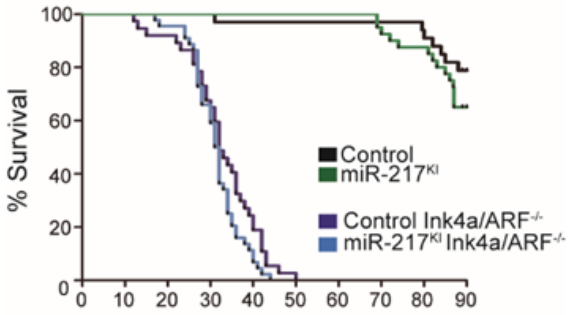

Figure 25. miR-217 does not affect overall survival of the Ink4a/Arf $^{-/-}$. Survival of control Ink4a/Arf $^{-/-}$ (37 mice, in dark blue) and miR-217^{KI} Ink4a/Arf$^{-/-}$ (44 mice, in light blue) mice and of control (33 mice, in dark green) and miR-217^{KI} mice (40 mice, in light green), observed for 90 weeks.

1.6.2- Alterations of miR-217 expression in human GC derived B cell lymphomas

To determine if miR-217 expression levels are altered in mature B-cell human lymphomas, we conducted a qRT-PCR analysis of miR-217 expression in a collection of BL and DLBCL samples. Expression of miR-217 was higher in BL and DLBCL than in control tonsil, lymph node, and peripheral blood B-cell samples (BL vs control, p = 0.05; Fig. 26). In agreement with these findings, analysis of published data of copy number variation in a cohort of DLBCL cases revealed that the genomic region that contains the miR-217 chromosomal location (MCR 1694) is amplified in a fraction of the cases (GSE111318) (Lenz, Wright et al. 2008). Together, these data indicate that miR-217 gain of function is associated with human mature B-cell lymphomas.

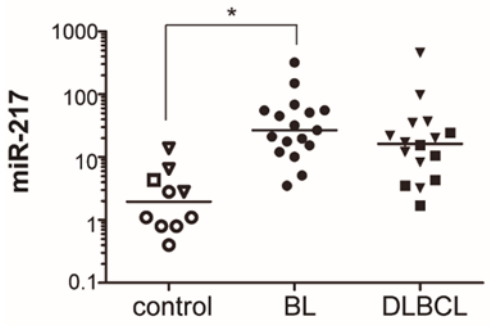

Figure 26. Increased miR-217 expression in human GC derived lymphomas. miR-217 relative expression in human control samples (open circles, peripheral blood CD19^{+} B cells; open squares, tonsils; open triangles, lymph nodes), in BL samples (closed circles) and in DLBCL samples (closed triangles, GC B GCB-DLBCL; closed squares, activated B cell, ABC-DLBCL) as determined by qRT-PCR. Statistical significance was determined by 2-tailed Student t test (p = 0.05 for BL).

Overall, our results identify miR-217 as a positive regulator of the GC reaction and as an oncogene in B cells that promotes B cell lymphomas of GC origin. miR-217 attenuates the DNA damage response stabilizing Bcl-6 and facilitating the molecular events that give rise to secondary antibody diversification. However, its upregulation promotes mature B cell lymphomagenesis. Importantly, we have found that there is an association between high miR-217 levels and human B cell lymphomas. Thus, miR-217 is a novel molecular link between the GC response and B-cell transformation and provides an *in vivo* model of mature B-cell lymphomagenesis.

2. Role of miR-28 in GC reaction and in B cell lymphomagenesis

2.1. miR-28 is a GC specific miRNA

Based on the hypothesis that significant miRNA expression in a particular tissue or at a specific differentiation stage very likely reflects functional relevance, we searched for GC specific miRNAs in databases that profile miRNA expression in lymphocyte subsets and found that miR-28 is expressed specifically in both mouse and human GC in B cells (Kuchen, Resch et al. 2010) (Schneider, Setty et al. 2014). Indeed, miR-28 expression is almost absent in other tissues except in *in vivo* GC B cells (Kuchen, Resch et al. 2010). To confirm this finding, we first analyzed miR-28 expression in GC B Cells by q-RT-PCR in naive pre-GC cells ($CD19^+Fas^-GL7^-IgA^-$), GC cells ($CD19^+Fas^+GL7^+IgA^-$) and in post-GC B cells ($CD19^+Fas^-GL7^-IgA^+$) sorted from Peyer's Patches of wild time C57BL/6 mice. We found that miR -28 is transiently induced in GC B cells (a 12.75-fold increase compared to the pre-GC naïve B cells) and downregulated immediately afterwards, in switched IgA^+ cells (Post-GC, Fig. 27A). Next, we performed miR-28 expression kinetics analysis upon in vivo B cell activation by immunizing C57BL/6 mice with SRBC and sorting splenic GC B cells at different time points after the immunization. miR-28 expression levels were measured by q-RT-PCR in early GC B cells (4-6 days after SRBC injection), and in late GC B cells (10-14 days after immunization). We found that miR-28 expression increases as the GC reaction progresses (7.45-fold increase at day 14 versus day 4) (Fig. 27B). These results demonstrate that miR-28 is upregulated upon in vivo B cell activation and that its expression is accumulated as the GC reaction progresses.

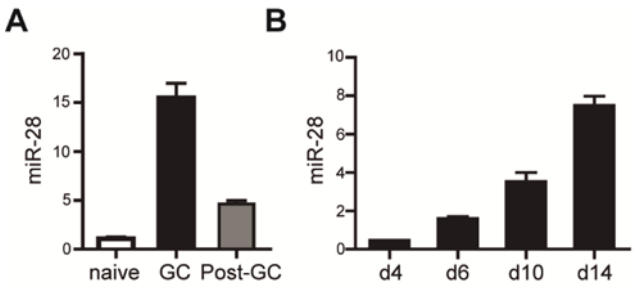

Figure 27. miR-28 is a GC specific miRNA. (A) miR-28 expression was assessed by qRT-PCR in naïve ($CD19^+Fas^-GL7^-IgA^-$), GC ($CD19^+Fas^+GL7^+$) and post-GC ($CD19^+Fas^-GL7^-IgA^+$) switched B cells from Peyer's patches (2 independent experiments) or **(B)** in splenic GC ($B220^+Fas^+GL7^+$) B cells at the indicated days after immunization with SRBC. Pools of at least 4 animals were used at each time point. Data from 2 independent experiments are shown .

2.2. miR-28 is a negative regulator of the GC reaction

To study the role of miR-28 during B cell activation, we first performed in vitro miR-28 gain of function experiments. Naïve B cells were isolated from spleens of C57BL/6 mice and were retrovirally transduced with a vector encoding miR-28 precursor and GFP or with an empty GFP control

and cultured in the presence of LPS and IL4. These culture conditions promote AID induction, CSR and induce proliferation of B cells, thus mimicking a physiological GC reaction. After transduction, CSR efficiency to IgG1 was assessed by flow cytometry within GFP^+, transduced cells. We found that miR-28 expressing B cells showed a mild but consistent reduction of CSR to IgG1 compared to the control GFP^+ cells ($p = 0.039$, Fig. 28). These results show that miR-28 impairs CSR to IgG1, suggesting that miR-28 is a negative regulator of the GC reaction.

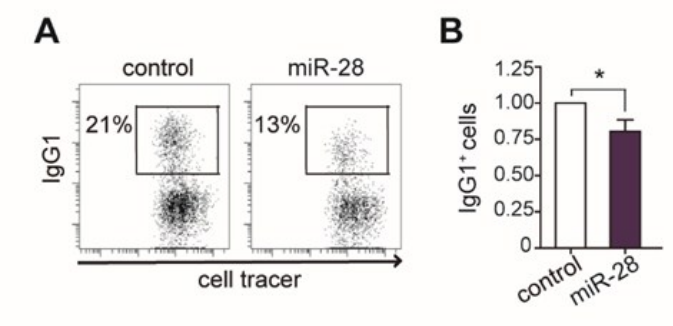

Figure 28. miR-28 impairs CSR. Spleen B cells were stimulated in the presence of LPS and IL4 and transduced with control or miR-28-containing retroviral constructs. CSR to IgG1 was assessed by FACS analysis 3 days after transduction. **(A)** Representative FACS plot; **(B)** quantification. Statistical significance was calculated with unpaired T test (*$p < 0.05$). Data from 5 independent experiments are shown.

To determine whether the role of miR-28 is physiologically relevant during a GC reaction *in vivo*, we inhibited endogenous miR-28 expression in GC B cells with a miR-28 sponge (miR-28 SPG) construct. We generated the miR-28 SPG construct (Fig. 29A) by cloning four complementary sequen-ces of miR-28 in tandem into the GFP-containing MGP vector. We then transduced CD45.1 bone marrow precursors with miR-28 SPG or with a control vector and performed bone marrow chimera experiments by injecting the transduced cells into lethally irradiated CD45.2 congenic receptor mice.

Four weeks after bone marrow transfer, we immunized the chimeric mice with SRBC and analyzed the immune response 7-9 days afterwards by flow cytometry. As an immunization control, mice were injected with PBS. We found that mice reconstituted with miR-28 SPG had a general increased response to immunization compared to control mice, with 34% more Fas+GL7+ GC B cells ($p = 0.015$) cells, 14% more IgG1+ switched B cells ($p = 0.027$) and 47% more CD138+ plasma B cells ($p = 0.024$) in the spleen (Fig. 29C). These results demonstrate that inhibition of endogenous miR-28 enhances the GC reaction, and therefore that miR-28 is a negative regulator of GCs.

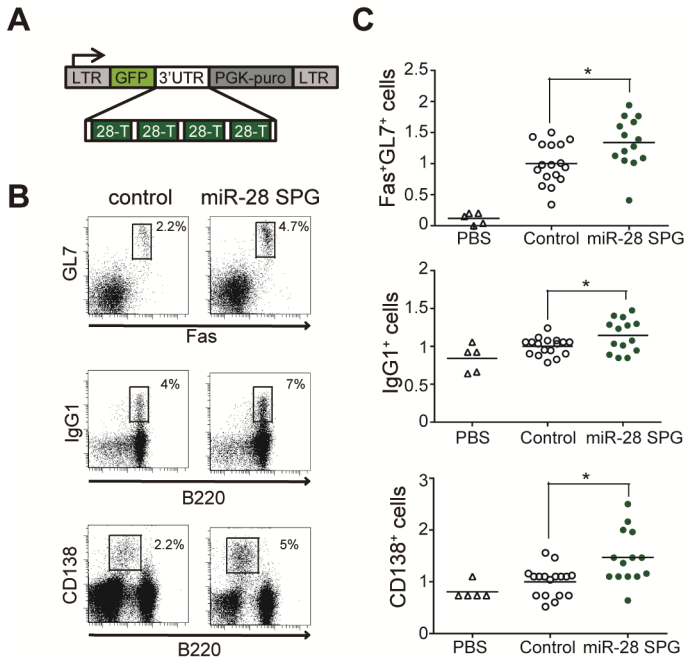

Figure 29. Inhibition of endogenous miR-28 boosts the GC reaction. (A) Scheme of the miR-28 sponge (miR-28 SPG) retroviral construct used for miR-28 inhibition. Four miR-28 complementary sites (28-T), separated by 4-nt spacers, were cloned downstream of GFP in the MGP vector. **(B)** and **(C)** miR-28 inhibition enhances the immunization response. Mouse chimeras of bone marrow cells transduced with miR-28 SPG or empty control vectors were analyzed by FACS 7-9 days after immunization with a T cell dependent antigen. Representative plots of GC B cells (B, upper panels), IgG1 switched B cells (middle panels) and plasma (bottom panels) cells are shown. **(C)** Quantification of FACS analysis shown in (B). Each symbol represents an individual mouse. PBS, non-immunized chimeric mice. Data are normalized to the response of PBS injected mice of 2 independent experiments. *p < 0.05, unpaired t test.

2.3. miR-28 expression is downregulated in GC derived B cell neoplams

The finding that miR-28 is a negative regulator of the GC reaction prompted us to explore the connection between miR-28 expression and B cell lymphomagenesis. Analysis of a miRNA expression dataset from human GC-derived B cell neoplasms (GSE 29493 (Di Lisio, Sánchez-Beato et al. 2012)) revealed that miR-28 expression is lost in various lymphoma subtypes, such as in BL ($p = 6.93 \times 10^{-11}$), DLBCL ($p = 2.64 \times 10^{-18}$), FL ($p = 9.25 \times 10^{-16}$) and in CLL leukemia, which is an heterogeneous malignancy with GC origin ($p = 1.65 \times 10^{-10}$) (Fig. 30A). miR-28 downregulation is also a common event in established GC derived B cell lines, such as the Ramos ($p = 0.0015$) and Raji BL cell lines ($p = 0.0012$) and the MD901 DLBCL cell line ($p = 0.0038$) (Fig. 30B). These data show that miR-28 downregulation is very frequently associated with GC B cell transformation, which could be suggestive of a tumor suppressor role of miR-28.

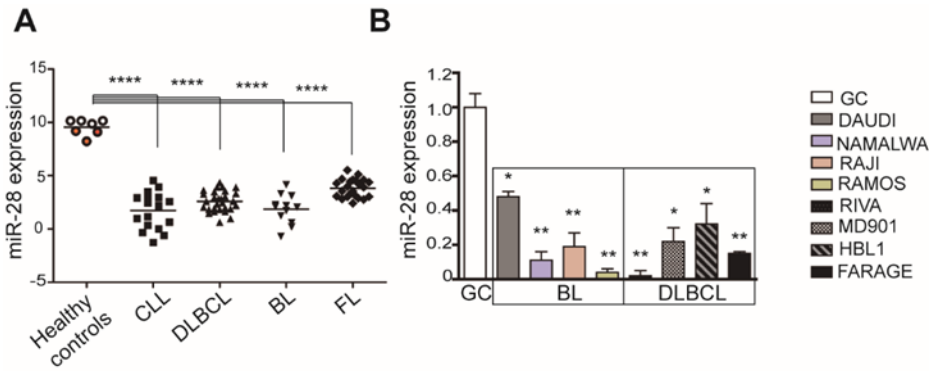

Figure 30. miR-28 is downregulated in human GC derived neoplasms. (A) Relative miR-28 expression in primary human B cell malignancies and **(B)** in immortalized human GC B cell lymphoma cell lines.

Figure 30 (continuation); (A) miR-28 microarray expression data (GSE29193) in cohorts of Chronic lymphocytic leukemia (CLL, 18 samples), Diffuse large B cell lymphoma (DLBCL, 29 samples), Burkitt lymphoma (BL, 12 samples) and Follicular lymphoma (FL, 23 samples). Human naive B cells ($CD19^+$ IgD^+ $CD27^-$) (3 samples, in orange) and human GC B cells ($CD10^+$ $CD19^+$) (4 samples, open circles) extracted from tonsils of healthy donors were used as controls. Adjusted P values are calculated with Benjamini & Hochberg. **(B)** q-RT-PCR analysis of miR-28 expression in a collection of human BL and DLBCL cell lines is represented relative to GC B cell levels (2 independent experiments). *$p < 0.05$, unpaired t test.

2.4. miR-28 expression regulates BCR signaling, proliferation and apoptosis in B cells

2.4.1- Quantitative proteomics and transcriptomics analysis upon miR-28 expression in BL cells

To identify the genes regulated by miR-28 in B cells, we performed transcriptome and proteome analysis in the human BL cell line Ramos, where miR-28 expression is greatly reduced compared to normal GC B cells (Fig 30B). To re-express miR-28 in Ramos cells we made use of a pTRIPZ lentiviral vector encoding miR-28 precursor along with "*red fluorescent protein*" (RFP) under a Tet-on promoter, which allows the induction of this cassette by doxycycline (Dox) treatment. In addition, transduced cells can be selected with puromycin (Fig. 31A). Ramos cells were transduced with either miR-28 or scrambled control pTRIPZ vectors, selected with puromycin, induced with Dox for 48 hours, and RFP+ cells were isolated by flow cytometry cell sorting. Cells were then subjected to RNAseq or iTRAQ analysis for transcriptome and proteome profiling, respectively (Fig. 31B).

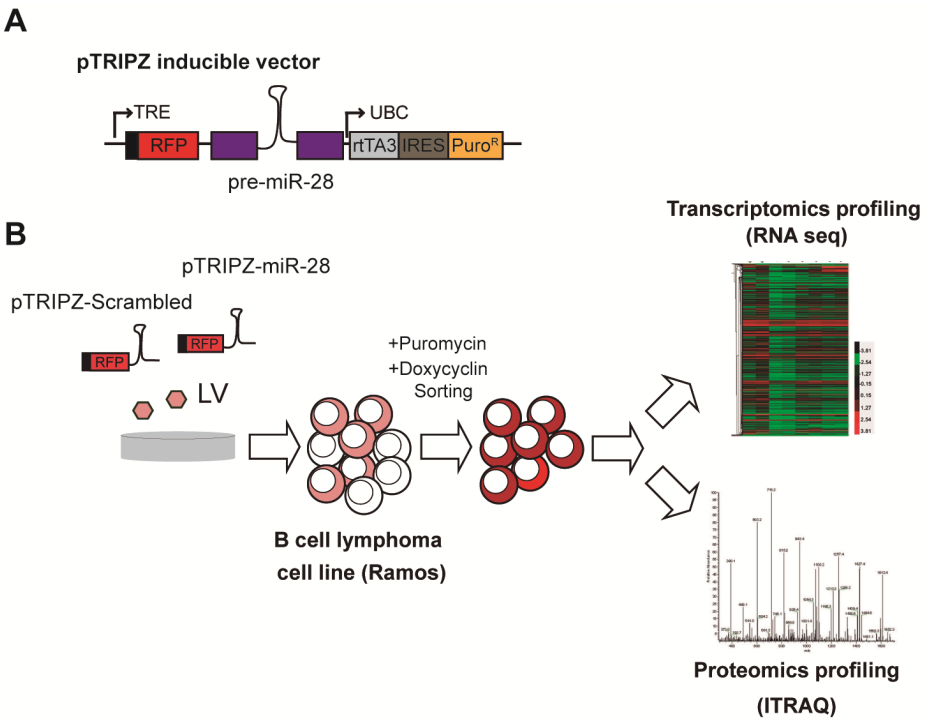

Figure 31. Pipeline used to identify miR-28 targets by quantitative proteomics and transcriptomic analysis. (A) Lentiviral constructs used to express miR-28 or a scrambled sequence.

Figure 31 (continuation); the construct encodes for puromycin resistance gene and is inducible by doxycyclin. **(B)** Schematic representation of the experimental strategy used to identify miR-28 targets in Ramos BL cells.

RNAseq analysis revealed that miR-28 expression in BL cells induced changes in the expression of 1202 transcripts ($p < 0.05$), 568 of which were downregulated (Fig. 32A) (see complete list of changed genes in annex 2).

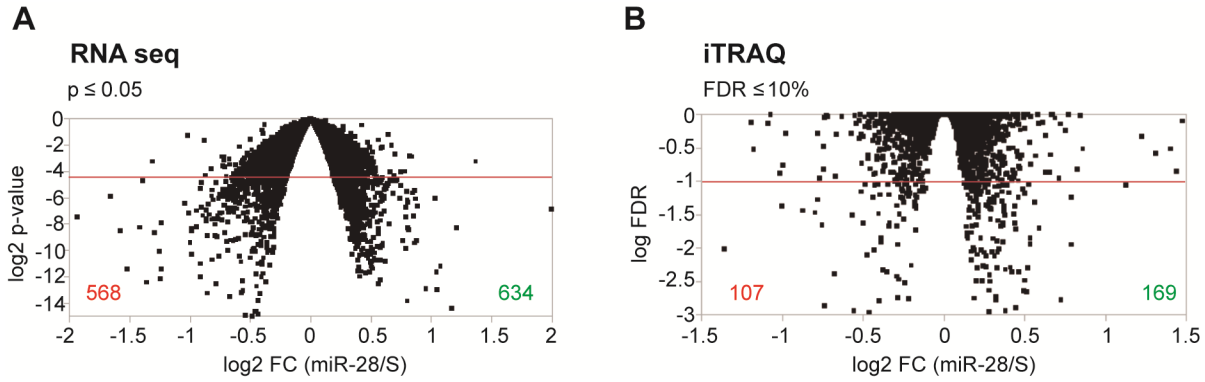

Figure 32. Volcano plots showing global differences in the transcriptome and proteome induced by miR-28 expression in BL cells. Volcano representation of 6 replicate RNAseq data and 4 replicate iTRAQ data used to identify changes in Ramos BL cells upon miR-28 re-expression. Points under the cut-off line (red) are significantly altered upon miR-28 expression. **(A)** RNAseq expression data represented as $\log_2$ fold change (FC) (miR-28/Scramble, X axis) versus statistical significance (log2 p value, Y axis) in transduced Ramos BL cells. 1202 genes were identified as differentially expressed (568 down, shown in red, and 634 up, in green) in miR-28 expressing cells with a $p \leq 0.05$. **(B)** Protein expression data represented as $\log_2$ FC (miR-28/Scramble, X axis) versus False Discovery Rate (FDR) (Y axis). 276 proteins were identified as differentially in miR-28 expressing cells with FDR ≤ 10%, of which 107 (in red) were downregulated and 169 up (in green).

We found that transcripts downregulated by miR-28 were significantly enriched in *in silico* miR-28 predicted targets by Gene Set Enrichment analysis (GSEA) (Fig. 33A), which suggests that a high proportion of the downregulated genes identified by RNAseq are direct miR-28 targets. Downregulation induced by miR-28 expression identified in the RNAseq analysis was verified by qRT-PCR analysis for a number of transcripts, including CD44, CCDC50, CELSR3, VAV3, FOSB and JAK3 (Fig. 33B).

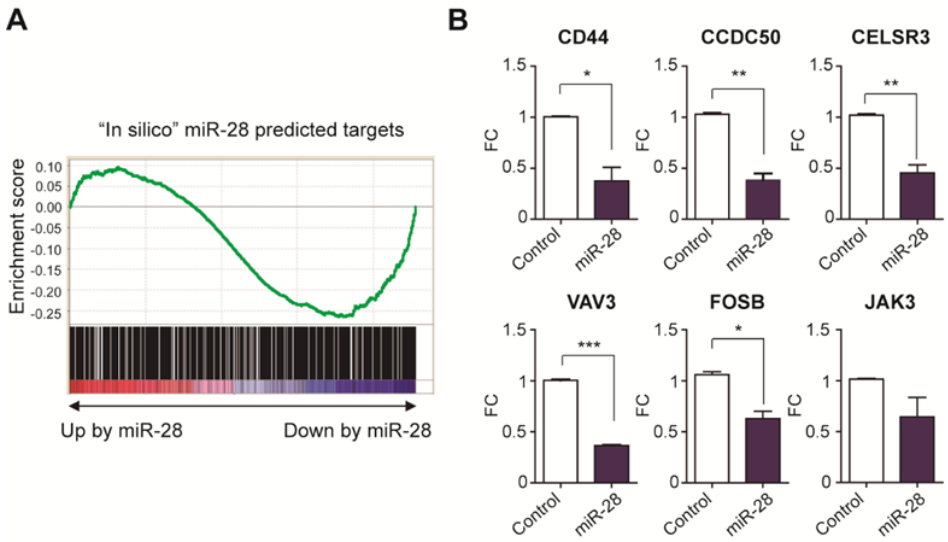

Figure 33 (continuation). Transcripts downregulated by miR-28 expression in BL cells are enriched in miR-28 predicted targets. **(A)** Gene Set Enrichment analysis of miR-28 targets as predicted by at least four independent prediction software against the differentially expressed genes identified in the RNAseq analysis. **(B)** Relative expression of six representative genes significantly downregulated in the RNAseq analysis measured by q-RT-PCR . Data from 2 independent experiments is shown (*p < 0.05, unpaired t test).

iTRAQ quantification of protein level changes induced by miR-28 expression in BL cells identified 276 differentially expressed proteins (10% FDR) (see annex 3 to have the complete list of changed proteins), 107 of which were downregulated (Fig. 32, right panel). We subjected the miR-28 regulated transcripts and proteins to Gene Ontology cellular function pathway identification analysis. Importantly, we found that both the transcriptome and proteome changes induced by miR-28 grouped in the same cellular functions pathways (Fig. 34. The most represented Gene Ontology cellular functions affected by miR-28 expression at the mRNA and protein levels were cell cycle, chromatin assembly, DNA replication and cell cycle.

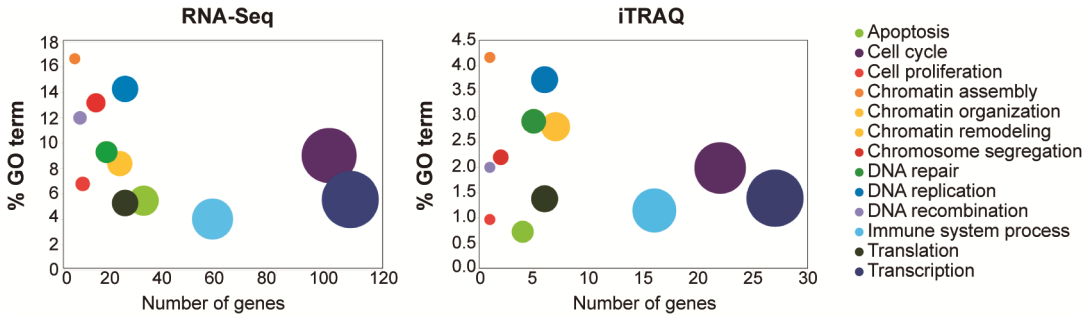

Figure 34. Transcriptome and proteome analysis identify similar cellular functions regulated by miR-28 in BL B cells. Bubble plot representation of the functional annotation of transcripts (left) and proteins (right) changed by miR-28. Categories correspond to the Gene Ontology Consortium of biological function database. Total number of genes/proteins inside each category are plotted on X axis; Y axis represents the proportion of each GO category found to be changed at the transcript (left) or protein (right) level; bubble area is proportional to the number of elements in each category relative to the total number of genes (left) or proteins (right) depicted.

Next, we subjected quantitative proteome data to Systems Biology Triangle analysis, a novel functional class scoring algorithm that identifies alterations in functional categories produced by coordinated protein responses in high-throughput quantitative proteomics experiments (Garcia-Marques et al submitted). We found that miR-28 expression in Ramos BL cells induced the coordinated downregulation of different cellular pathways on cell cycle progression; including cell cycle G1/S checkpoint regulation, G2/M phase transition, cyclins and cyclins dependent kinase activity and mitosis of tumor cell lines. In addition, the analysis revealed that miR-28 expression resulted in a coordinated upregulation of proteins from the p53 tumor suppressor pathway (Fig. 35).

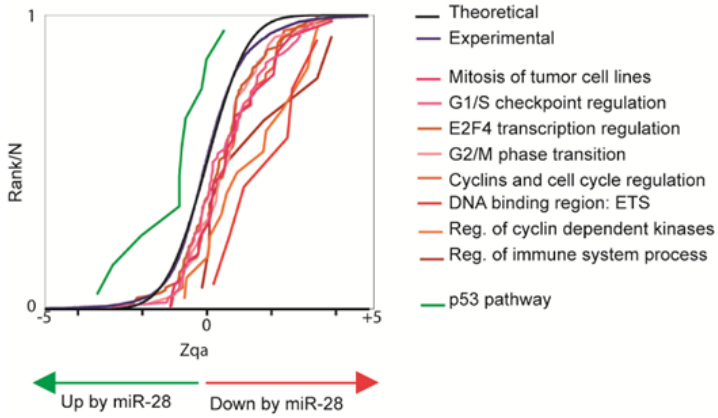

Figure 35. miR-28 expression induces the coordinated downregulation of cell cycle proteins and the upregulation of p53 tumor suppressor pathway proteins. Distribution curves of the standardized variable of proteins (Zqa values, X axis), plotted separately in the different functionally changing categories.

To gain more insight into the gene networks that could be significantly altered by miR-28 in BL B cells, we performed Ingenuity pathway analysis on the proteins differentially expressed in BL cells transduced with miR-28 and found that miR-28 regulates the BCR signaling pathway. This gene network contained four main hubs, BCR, PI3K, AKT and ERK1/2 that play pivotal functions in B cell biology and regulate the induction of cell cycle and apoptosis regulatory molecules such as CDC6, CDC25C, tnfsf11 and ILF3 (Fig. 36). These results suggest that reintroducing miR-28 in lymphoma cells affects the signaling network that emanates from the BCR and whose hyperactivation is recurrently linked to B cell lymphomagenesis (Rickert 2013) (Davis, Ngo et al. 2010, Young, Shaffer et al. 2015).

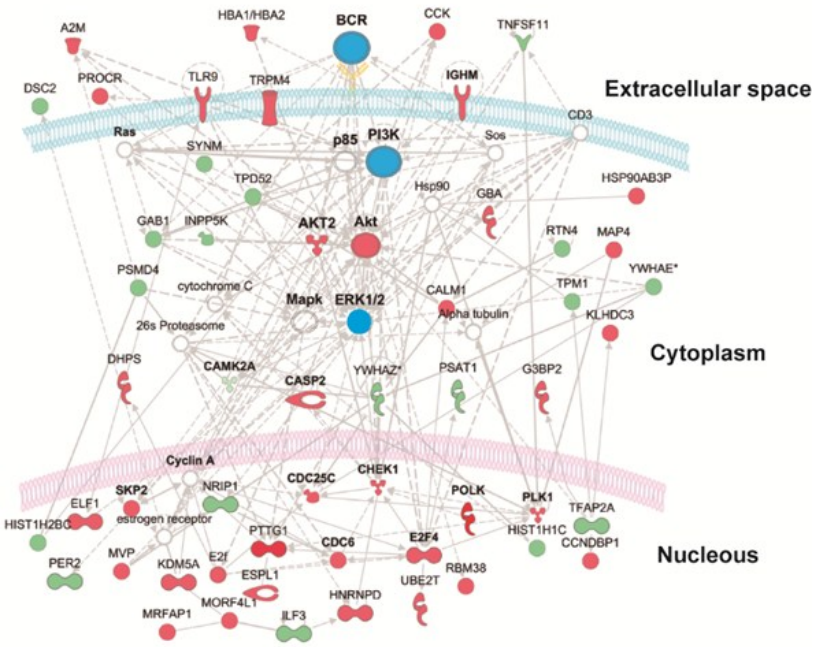

Figure 36. miR-28 regulates BCR signaling pathway. Ingenuity Pathway Analysis of proteins differentially expressed as a result of miR-28 expression in BL cells shows enrichment in BCR signaling pathway ($p = 10^{-46}$). Upregulated proteins are depicted in green, downregulated in red and nodes in blue.

2.4.2- Impact of miR-28 expression in the BCR signaling pathway of BL cells

As our proteome analysis revealed that miR-28 expression regulates the expression of BCR signaling related proteins, we next analyzed the functional impact of miR-28 expression in the key kinases downstream BCR signaling. Western Blott (WB) analysis of the phosphorylated and active forms of AKT (p-AKT) and ERK (p-ERK) showed that miR-28 expression in B cells dampens BCR signaling. We found a tendency to have reduced p-ERK levels upon miR-28 expression (32.5% in miR-28 RFP$^+$ compared to scrambled RFP$^+$ Ramos BL cells, p = 0.1) (Fig. 37A). Similarly, p-AKT phosphorylation in serine 472 was reduced by 34% in miR-28 RFP$^+$ cells compared with control scrambled RFP$^+$ cells (p = 0.022). In addition, flow cytometry analysis of AKT phosphorylation in response to BCR stimulation with anti-IgM revealed that miR-28 expressing cells had a reduction of a 23% in p-AKT levels when compared with controls (Fig. 37B) (p = 0.042). Overall, these data show that miR-28 expression dampens BCR signaling in BL cells.

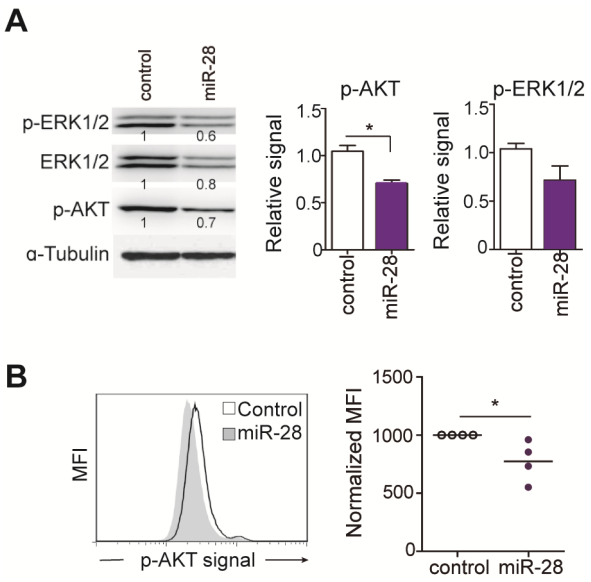

Figure 37. miR-28 expression dampens BCR signaling in BL cells. In vitro cultured miR-28 or control transduced Ramos BL cells 48h after induction with doxycycline. **(A)** Immunoblot analysis of p-ERK1/2, ERK1/2 and p-AKT in extracts from Ramos cells transduced with miR-28 or a scrambled control. Numbers underneath the bands show protein levels after normalization to the α-tubulin loading control signal (p-AKT and p-ERK1/2). Bar graphs show data from two independent experiments. **(B)** AKT phosphorylation measured by flow cytometry after anti-IgM stimulation of Ramos-miR-28 RFP$^+$ or Scramble RFP$^+$ cells. Representative examples of flow cytometry plots are shown in the left. Quantification from 4 independent experiments is shown on the right. MFI, mean fluorescence intensity. *p < 0.05, unpaired t test.

Human malignant B cells are dependent on "tonic" BCR signaling for proliferation and survival (Shaffer, Young et al. 2012). Following a stringent candidate selection proteomics approach, we have found that miR-28 expression impacts on BCR signaling network and indeed impairs BCR signaling in human B cell lymphoma. We wondered if other components of molecular pathways that play key roles in the generation and/or maintenance of human mature B cell malignancies could have been overlooked in our proteome analysis but were nonetheless altered by miR-28 expression. To assess this issue we followed a hypothesis-driven approach and directly analyzed the expression of genes frequently deregulated in GC-derived malignancies (extracted from (Shaffer, Young et al. 2012)) in

our RNAseq data sets. We found that the expression of 3 genes (NFKB2, IKKB and BCL2) that have recurrent gain-of–function genetic aberrations in GC-derived malignancies was downregulated by miR-28 expression in Ramos BL cells. NF-κB2 and IKKB are components of the NF-κB pathway, the most common gene pathway found to be altered in lymphoid malignancies and whose constitutive activation results in the inhibition of cell death pathways. BCL2 gene encodes for Bcl-2, an integral outer mitochondrial membrane protein that blocks the apoptotic cell death in lymphocytes and whose expression is induced through NF-κB and other signaling pathways downstream of the BCR. Bcl-2 gain of function due to genetic alterations is a molecular feature of a number of mature B cell malignancies, including CLL, FL, the GC subtype of DLBCL and MCL. The downregulation of NFKB2, IKKB and BCL2 transcripts induced by miR-28 expression in Ramos BL cells was confirmed by quantitative RT-PCR (Fig. 38).

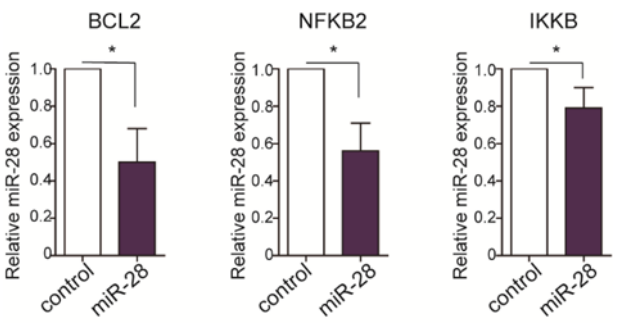

Figure 38. miR-28 negatively regulates transcript expression of the Bcl-2 pro-survival gene and of NF-κB2 and IKKB. Q-RT-PCR of Bcl-2 (left graph), NF-κB2 (middle) and IKKB (right graph) in Ramos BL cells transduced with miR-28 or a scrambled control lentivirus and maintained in the presence of doxycycline for two days *in vitro*. Data are representative from 3 independent experiments. *, $p < 0.05$, unpaired t test.

Overall, these results show that miR-28 expression downregulates the expression of a gene network downstream of BCR signaling that plays key roles in B lymphocyte proliferation and survival, and whose expression is frequently upregulated in GC-derived malignancies.

2.4.3- miR-28 expression diminishes B cell proliferation

Given that miR-28 dampens BCR signaling and targets genes involved in the regulation of cell cycle and survival, we next analyzed whether miR-28 expression has an impact on the proliferation of B cells. First, we analyzed the effect of miR-28 expression in the proliferation of non-transformed B cells by retroviral transduction of naive mouse splenic B cells that had been labeled with violet cell tracer to monitor cell division. Interestingly, we found that mouse primary B cells overexpressing miR-28 had a lower proliferation index (PI) and an increased proportion of cells with low divisions (0-2) that control B cells (Fig. 39).

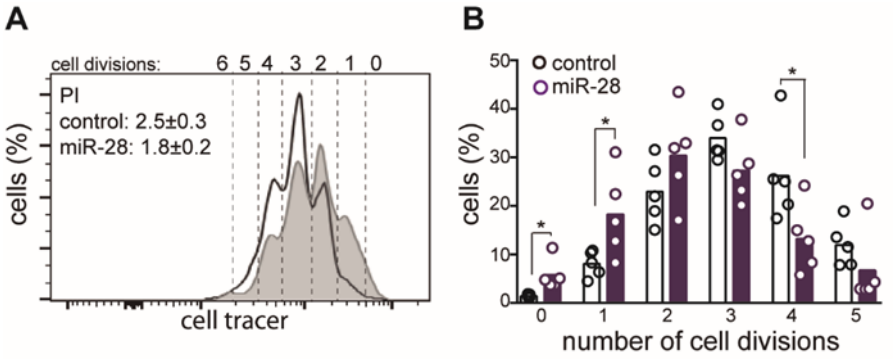

Figure 39. miR-28 impairs proliferation of primary B cells. Splenic B cells were labeled with violet cell tracer, transduced with miR-28 or an empty control retroviral vector and cultured *in vitro* with LPS+IL4. Cell divisions were monitored by FACS analysis. **(A)** Representative histograms 2 days after retroviral transduction (open line, control; shaded histogram, miR-28). PI, proliferation index. **(B)** Quantification of the proportion of cells that have undergone 0 to 5 divisions. *, $p < 0.05$, unpaired t test.

Next, we analyzed the impact of miR-28 expression on cell cycle and proliferation of transformed human BL cells. Propidium Iodide (PI) cell cycle analysis and BrdU incorporation assays in Ramos miR-28 or control transduced RFP^+ cells revealed that miR-28 expressing cells had a significant decrease in the proportions of proliferating cells, both in terms of reduced proportion of cells in cycling S+G2/M phases ($p = 0.02$) and a reduced proportion of BrdU incorporating cells ($p = 0.0078$) (Fig. 40). These results show that miR-28 expression reduces B cell proliferation both in primary mouse B cells and in transformed human B cell lymphoma.

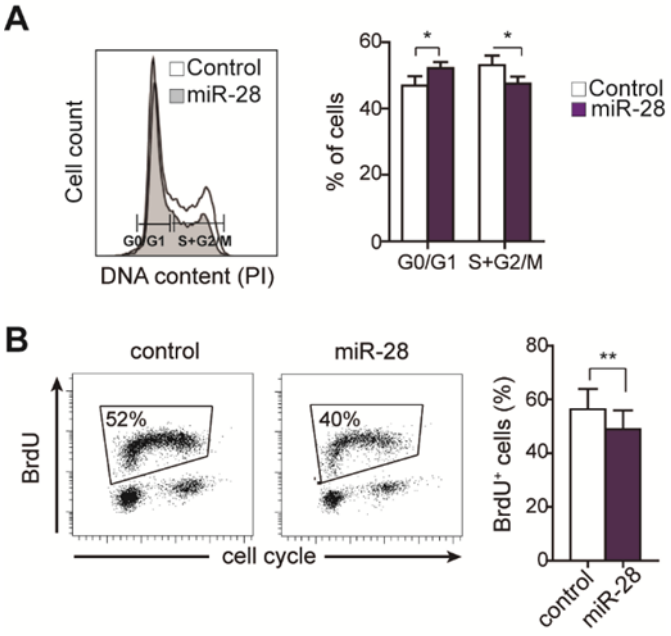

Figure 40. miR-28 impairs cell cycle progression. *In vitro* cultured miR-28 or control transduced Ramos BL cells 48h after induction with doxycycline were assessed for cell cycle progression. **(A)** Propidium iodide cell cycle analysis and **(B)** BrdU incorporation assays analyzed 30 minutes after pulse. Representative plots are depicted. Data from 4 independent experiments are shown. *, $p < 0.05$, unpaired t test.

2.4.4- miR-28 promotes apoptosis of BL cells

Next, we assessed whether the expression of miR-28 impacts cell death by apoptosis in BL cells. We found that miR-28 expression in Ramos BL cells promotes a significant increase in both the proportions of active caspase 3^+ cells (a 3.16-fold increase compared to the control; p = 0,037) and annexin V^+ $7AAD^-$ early apoptotic cells (2.1-fold increase in control versus miR-28 RFP^+ cells; p = 0.015) (Fig. 41). Thus, these results demonstrate that miR-28 expression promotes cell death by apoptosis in human BL cells.

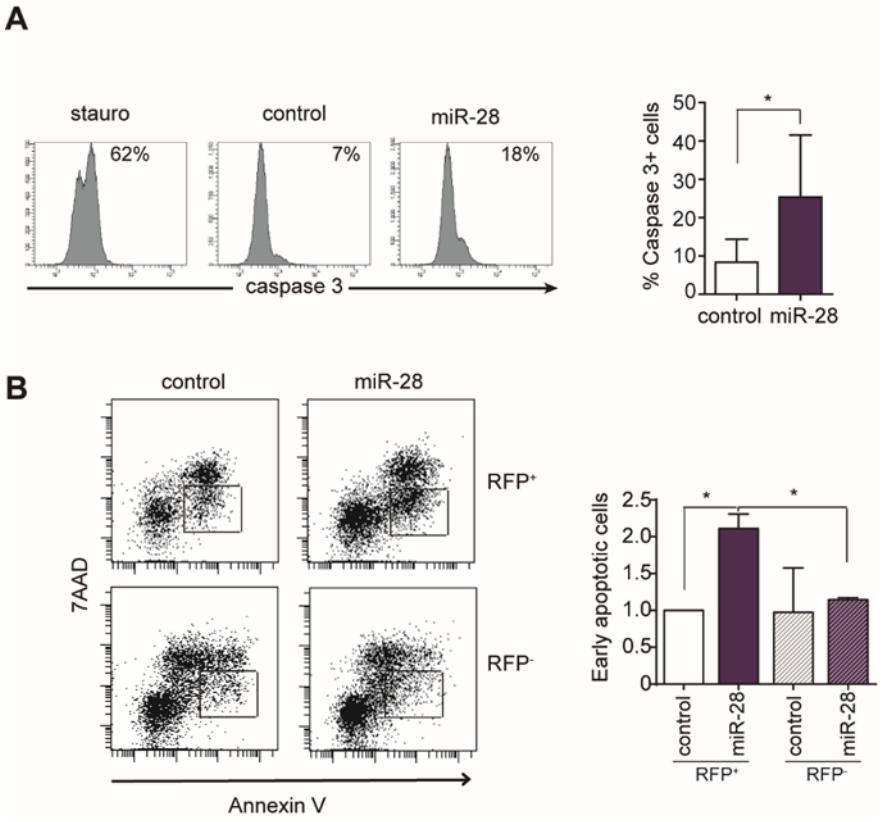

Figure 41. miR-28 expression promotes apoptosis in Ramos BL cells. (A) Active caspase 3 (data from 6 independent experiments) and **(B)** 7AAD and Annexin V stainings (data from 2 independent experiments) in *in vitro* cultured miR-28 or control transduced Ramos BL cells 48h after induction with doxycycline. Representative plots are shown on the left and the respective quantifications on the right. *, $p < 0.05$, unpaired t test.

2.5 - miR-28 is a tumor suppressor in human GC derived neoplasms

2.5.1- miR-28 expression impairs BL and DLBCL cell growth *in vitro*

As we have found that miR-28 impairs proliferation and survival of B cells and is frequently lost in human GC derived neoplasias we decided to assess whether miR-28 has tumor suppressor activity. First, we analyzed the effect of miR-28 replacement in the cell growth potential of different human BL and DLBCL lymphomas *in vitro*. We transduced the Ramos and Raji BL and the MD901 ABC-DLBCL

cell lines, with an inducible lentiviral pTRIPZ construct encoding miR-28 or a scramble control. Lymphoma growth was monitored by counting live cells during 5-6 days in *in vitro* cultures in the presence of doxycycline. We found that mir-28 significantly decreased the growth of all B cell lymphoma cell lines. MD901 ABC-DLBCL cell number was reduced by 40% and Raji and Ramos BL cell numbers were reduced by 45% and 77%, respectively, after 5-6 days of culture (Fig. 42A). Importantly, we found that the growth inhibitory effect of miR-28 expression was B cell specific, as the cell numbers of Jurkat tumoral T cells and NIH/3T3 fibroblasts were not affected by miR-28 expression (Fig. 42B). These results suggest that miR-28 acts as a tumor suppressor for GC derived B cell lymphomas.

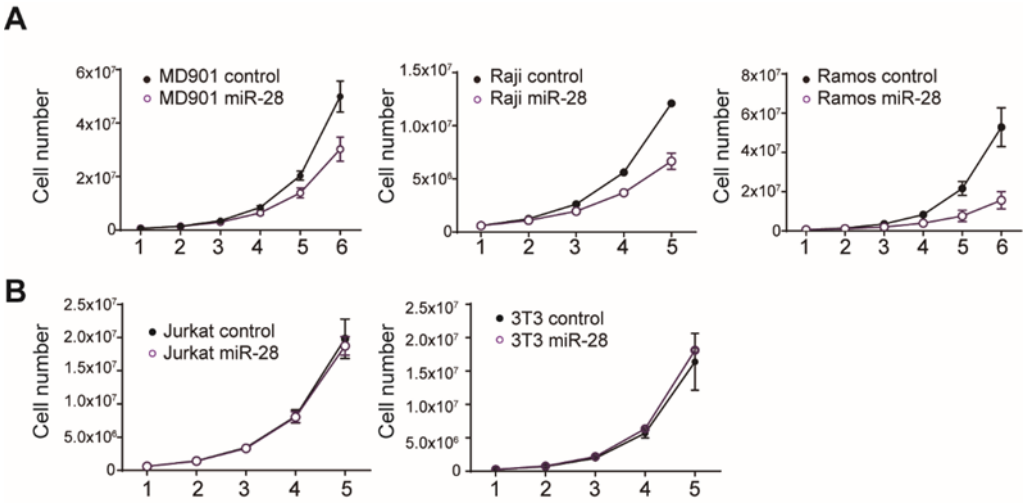

Figure 42. miR-28 is a tumor suppressor for GC derived B cell lymphomas. (A) GC derived human lymphoma cell lines MD901 (DLBCL), Raji (BL) and Ramos (BL), and **(B)**, non B cell lines Jurkat T cell line and 3T3 fibroblasts, were lentivirally transduced with pTRIPZ vectors containing the miR-28 precursor sequence (purple circles) or a scrambled sequence as negative control (black circles). After transduction cells were selected with antibiotic, induced with doxycycline for two days and RFP^+ cells were isolated by preparative flow cytometry. Cells were cultured in complete medium and cell number was calculated everyday by live cell counting. Data of at least two independent experiments are shown.

2.5.2- miR-28 expression prevents BL and DLBCL growth *in vivo*

To analyze whether miR-28 impairs B cell lymphoma growth *in vivo*, we generated xenograft models of BL and ABC-DLBCL where miR-28 expression can be induced by doxycycline administration. First, Ramos BL cells were transduced with miR-28 or scramble pTRIPZ lentiviral vectors, selected with puromycin, induced with doxycyclin, and 100% pure RFP^+ cells were injected subcutaneously into NOD Scid Gamma (NSG), immunodeficient mice. miR-28 expressing cells were injected in the left flank and the control RFP^+ lymphoma cells were injected in the right flank of the mice (Fig. 43A). To ensure continuous expression of the constructs, doxycycline was added in the drinking water of the host mice one week prior to cell injection and maintained throughout the experiment (Fig. 43A). Tumor volume was assessed every two days. Notably, we found that miR-28 expression slowed the

growth of Ramos (Fig. 43B) and increased the survival of mice, defined as the fraction of mice with a tumor burden smaller than 20 mm in any of the three dimensions (Fig. 43C). Indeed, tumor weight at end-point was dramatically reduced when miR-28 was re-expressed in Ramos cells, as compared to control transduced cells (Fig. 44). miR-28 replacement in Raji BL and MD901 ABC-DLBCL cells also resulted in a delay in tumor growth (Fig. 45), indicating that antitumoral activity of miR-28 is not restricted to a single BL cell line or to a single B cell lymphoma type.

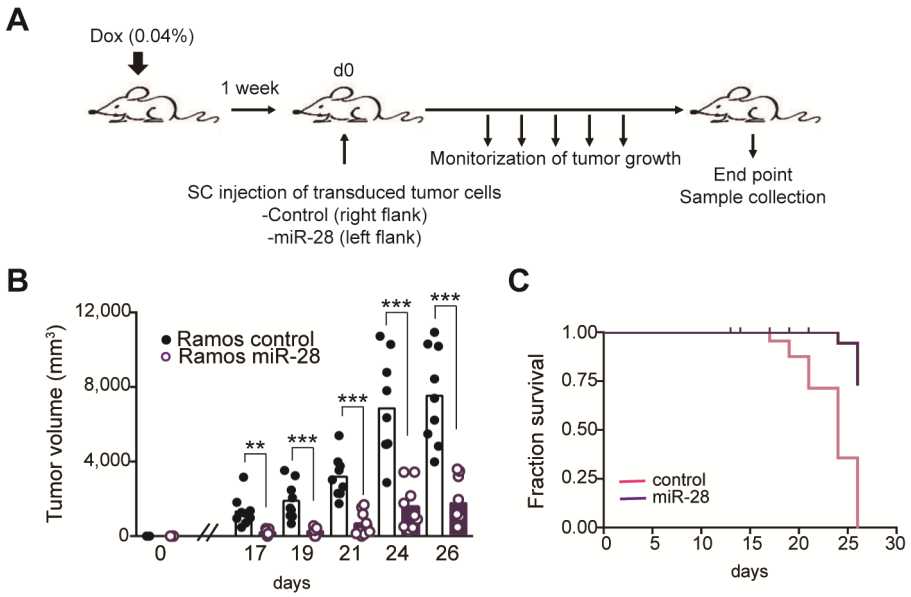

Figure 43. miR-28 impairs Ramos BL growth *in vivo* and extends the survival of transplanted mice. (A) Schematic representation of the experimental approach. 10^7 lentivirally transduced Ramos miR-28 RFP^+ (purple circles) and control RFP^+ (black circles) cells were injected subcutaneously at each flank of NOD scid gamma (NSG) mice. Doxycycline was administered in the drinking water a week before injection and throughout the experiment. Tumor growth was monitored every two days with a caliper and volume was calculated as $(width)^2 \times length/2$. Each dot is a tumor. **(B)** Tumor growth over time. Tumor volume was measured at the indicated times ***$p < 0.001$, each dot is a tumor. **(C)** Kaplan-Meyer survival plot of transplanted mice. End-point was performed when tumors reached ≥ 20 mm in any of the 3 dimensions. Data from two independent experiments are shown. P value calculated with Paired t test.

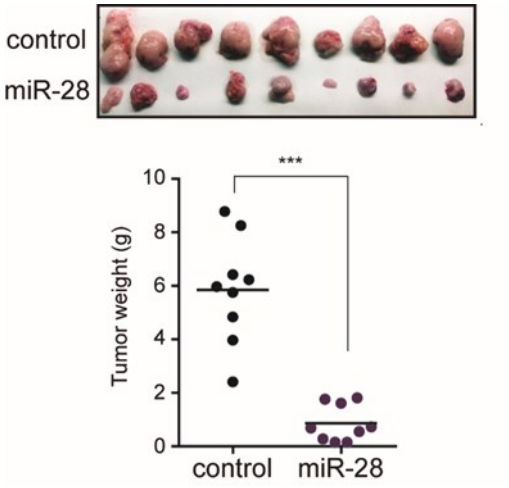

Figure 44. miR-28 reduces tumor weight of BL xenografts. 10^7 lentivirally transduced Ramos miR-28 RFP^+ (closed purple circles) and control RFP^+ (open circles) cells were injected subcutaneously at each flank of NSG mice. Doxycycline was administered in the drinking water a week before injection and throughout the experiment. Upper panel, representative images of Ramos xenograft tumors transduced with control (upper row) or miR-28 (lower row) lentiviruses. Tumor weight (lower panel) was determined 26 days after injection, ***$p < 0.001$, paired t test.

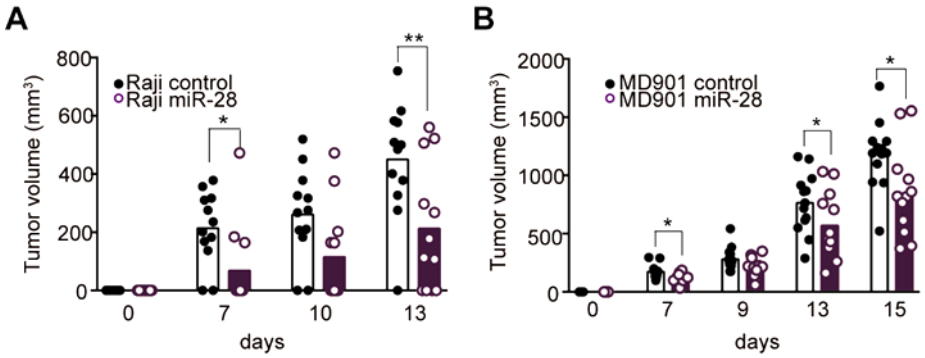

Figure 45. miR-28 delays ABC-DLBCL and BL growth *in vivo*. (A) MD901 ABC-DLBCL cells and **(B)** Raji BL cells were lentivirally transduced with miR-28 (closed purple circles) or control (open circles) and 10^7 control or miR-28 cells were injected subcutaneously at each flank of NSG mice. Doxycycline was administered in the drinking water a week before injection and throughout the experiment. Tumors were measured with a caliper at the indicated times and volume was calculated $(width)^2$x length/2. *, $p < 0.05$, paired t test, each dot is a tumor.

Immunohistochemical analysis of the tumors revealed that miR-28 expressing Ramos BL tumors had reduced proportions of Ki67 proliferating cells and of Bcl-2^+ cells. In contrast, an increase in the proportion of apoptotic caspase 3^+ cells was observed in miR-28 expressing BL cells (Fig. 46). These results show that miR-28 is a tumor suppressor in BL and ABC-DLBCL GC-derived lymphomas and that its expression is sufficient to impair lymphoma establishment *in vivo*.

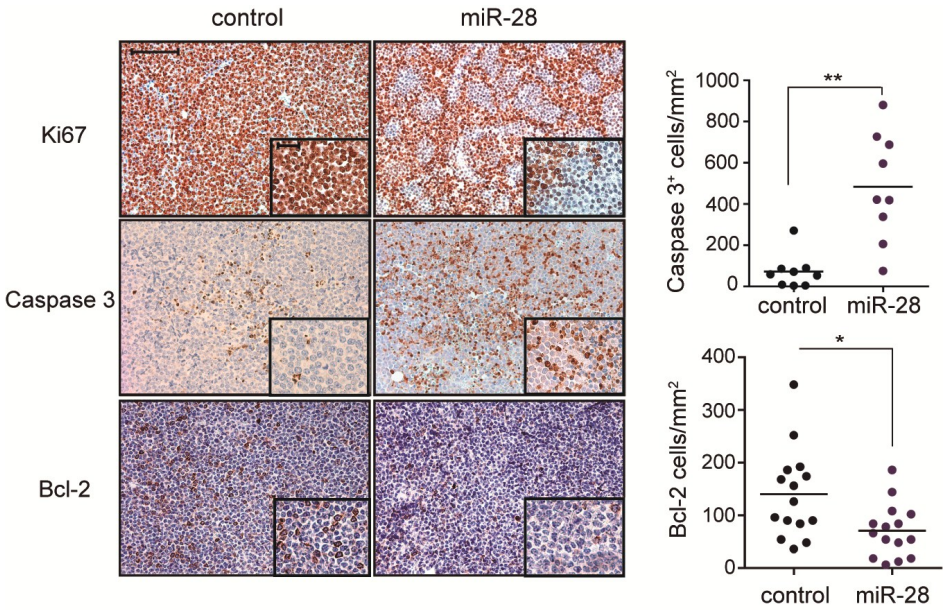

Figure 46. miR-28 expression reduces proliferation and Bcl-2 expression and increases apoptosis in BL xenografts. 10^7 lentivirally transduced Ramos miR-28 RFP^+ (closed purple circles) and control RFP^+ (open circles) cells were injected subcutaneously at each flank of NSG mice. Doxycycline was administered in the drinking water a week before injection and throughout the experiment. 26 days after injection mice were sacrificed and tumors were stained with the proliferation marker Ki67, with anti-Caspase-3 for apoptosis detection and with the pro-survival factor Bcl-2. Left, representative micrographs of control and miR-28 -transduced xenografts. Right, quantification of Caspase-3 and Bcl-2 staining. Bars show average values, p = 0.017**, Paired t test. Scale bar is 100 µm and 25 µm (in the inset).

2.6. Therapeutics of GC derived lymphomas by miR-28 replacement

2.6.1- Treatment of established BL xenografts by lentiviral miR-28 replacement

We have found that prophylactic expression of miR-28 is sufficient to impair the growth of B cell lymphoma in xenograft models; thus we next wanted to address whether miR-28 could be useful as a therapeutic agent, to interfere with the growth of already established lymphomas. First, we performed lentiviral miR-28 replacement in Ramos human BL xenografts. We transduced Ramos cells with miR-28 or scramble lentiviral vectors, selected transduced cells in the presence of puromycin and injected the cells subcutaneously into NSG mice prior to induction of the constructs with doxycycline treatment. Tumors were allowed to grow till they reached a volume of 200 mm^3 and doxycycline was then administered to the mouse in the drinking water and tumor growth monitored for several weeks (Fig. 47A). We found that Ramos BL tumors replaced with miR-28 expression had a significantly slower growth rate compared to control tumors (Fig. 47B and 47C). Tumor mass was reduced by 47%-58% in miR-28 expressing lymphoma cells at all time points analyzed (*p ≤ 0.05). These results show that lentiviral delivery of miR-28 is therapeutically useful for the treatment of established BL tumors.

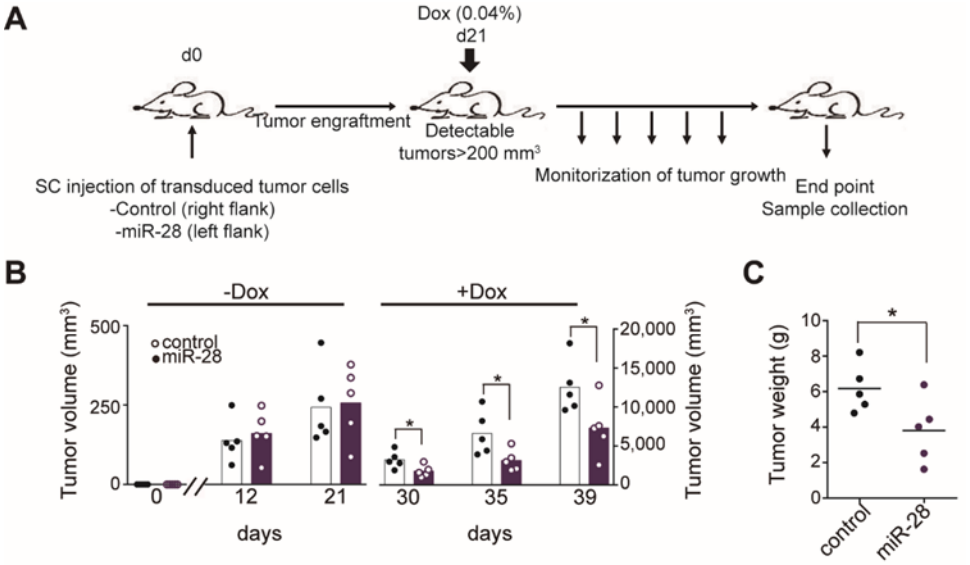

Figure 47. miR-28 impairs the growth of established human BL. (A) Schematic representation of the experiment. Ramos cells were transduced with lentivirus containing miR-28 or scrambled sequences and injected subcutaneously in NOD scid gamma mice. miR-28 expression was induced by doxycycline administration in drinking water after xenografts were 200 mm^3. **(B)** Graphs represent volume of individual tumors and average values at the indicated times before (-Dox) and after (+Dox) doxycycline administration. Note that Y axes on the left and right graphs are set at different scales. **(C)** miR-28 expression reduces tumor weight. Graph shows the tumor weights of Ramos xenografts (as described in (A) at day 39. Statistical significance was calculated with unpaired T test *, $p < 0.05$ (each dot is a tumor).

2.6.2- Treatment of established BL xenografts by synthetic miR-28 replacement

To avoid viral delivery to replace miR-28 expression, we assayed the therapeutic activity of synthetic miR-28 mimics in a series of experiments in BL xenograft models. miRNA mimics are ana-

logs of the physiological miRNAs that have been chemically modified to enhance their stability (Sibley, Seow et al. 2010) (Yin, Kanasty et al. 2014). Wild type Ramos BL cells were injected subcutaneously in NSG mice, tumors were allowed to reach a volume of 200 mm^3 and mice were then treated with miR-28 mimic by intratumoral injection (Fig. 48A). Two different concentrations of miR-28 mimic (0.1 nmoles and 0.5 nmoles) were injected intratumorally 3 times within a week. We found that treatment with both concentrations of miR-28 mimic delayed the growth of established BL tumors, which showed reduced volumes at all analyzed time points (Fig. 48B). This effect was highly statistically significant at end-point analysis of tumor weight (Fig. 48C).

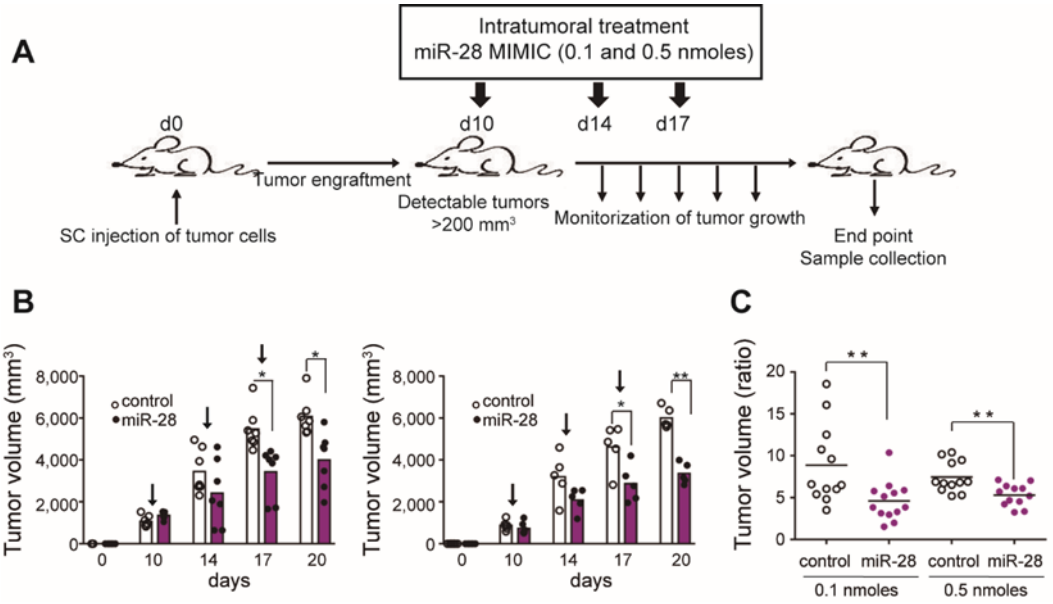

Figure 48. Synthetic miR-28 intratumoral administration reduces the growth of established BL tumors. (A) Schematic representation of the experiment. Wild type Ramos cells were injected subcutaneously into NSG mice, tumors were allowed to establish and synthetic miR-28 (miR-28 mimic) or scrambled control oligonucleotides (mimic) was administered intratumorally. **(B)** Graphs show tumor volumes at the indicated times before and after treatment (indicated with arrows) with 0.1 nmoles mimic (left) or 0.5 nmoles mimic (right). **(C)** Volume-at-endpoint/volume-before-treatment ratio is represented for the indicated conditions. Statistical significance was calculated with student's unpaired t test. Data from two independent experiments are shown.

We next assayed the efficacy of miR-28 mimic intravenous administration to treat human BL in xenograft models. Ramos BL cells were injected subcutaneously in NSG mice and once the tumors had reached a volume of 200 mm^3 mice were treated with miR-28 or scramble (control) mimic oligonucleotides (7 nmoles) by two intravenous injections separated 3 days (Fig. 49). Four days after the first intravenous mimic injection the slower growth of miR-28 treated mice was already notable (Fig. 49B). To determine if intravenous miR-28 mimic administration entails organic toxicity we performed histopathological and biochemical analysis of miR-28 and control-treated NGS mice. Histopathological analysis of kidney, liver, heart and spleen showed no evidence of macroscopic or microscopic to-

xicity (not shown). Likewise, we found no evidence of hematologic, renal or hepatic toxicity, as determined by complete blood counts, blood chemistry, liver function tests and thyroid hormone testing (Table 9). These data indicate that treatment of BL by intravenous administration of synthetic miR-28 mimic is not associated to a significant toxic activity.

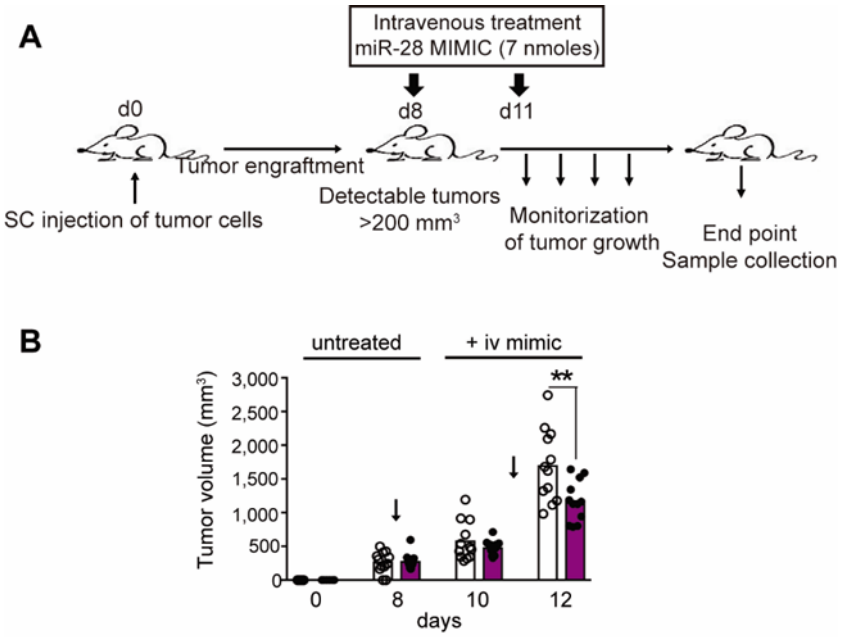

Figure 49. Intravenous injection of synthetic miR-28 (miR-28 mimic) reduces the growth of BL xenografts. **(A)** Schematic representation of the experiment. Ramos BL xenografts were established by injecting subcutaneously the BL cells in NOD scid gamma mice and treated by intravenous administration of miR-28 or scrambled (control) mimic oligonucleotides (7 nmoles). **(B)** Graph shows tumor volumes at the indicated times. Statistical significance was calculated with student's unpaired T test, **p < 0.005.

Table 9. Biochemical analysis of BL xenografted NGS mice intratumorally treated with miR-28 or control mimic.

	PBS	0,5 nmoles control mimic	0,5 nmoles miR28 mimic	Units
Blood Urea Nitrogen	21,5 ± 0,70	23,5 ± 3,5	21 ± 2,82	md/dL
Triglycerides	64 ± 26,87	63,5 ± 3,5	97 ± 26,87	md/dL
Total Protein	6,3 ± 0	6,8 ± 0,4	6 ± 0,99	md/dL
ALT/GPT	102 ± 24,04	98 ± 21,20	96 ± 32,52	U/L
AST/GOT	398 ± 301,22	271 ± 82,0	259 ± 352,14	U/L
GGT	12,5 ± 3,53	15,5 ± 9,2	7 ± 7,07	U/L
Total Cholesterol	125 ± 7,21	105,1 ± 10,3	60,65 ± 32,17	mg/dL
Alkaline phosphatase	94,5 ± 47,37	68,5 ± 81,3	82 ± 16,97	U/L
Glucose	134,5 ± 16,26	147,5 ± 23,3	91 ± 0	mg/dL
Albumin	1,25 ± 0,07	1,25 ± 0,20	1,2 ± 0	g/dL

2.6.3- Primary BL treatment by miR-28 replacement with synthetic miR-28 mimic

To extend our study of miR-28 therapeutic potential to primary lymphomas we made use of the lambda/MYC (λ-MYC) transgenic mouse model (Kovalchuk, Qi et al. 2000), in which the Myc proto-oncogene is constitutively expressed under the regulatory elements of the immunoglobulin λ light chain gene and recapitulates in the mouse much of the pathogenesis of human BL. First, we analyzed

miR-28 expression in naïve B cells, normal GC B cells and tumoral B cells from λ-MYC mice, and observed that expectedly, miR-28 is upregulated in normal GC B cells. Importantly, and in agreement with the human lymphoma data, miR-28 is lost in transformed B cells, thus validating the use of the λ–MYC model for our analysis (Fig. 50).

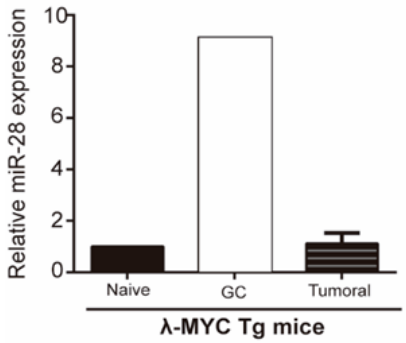

Figure 50. miR-28 expression is downregulated in B cell lymphomas developed in λ-MYC transgenic mice. Quantitative RT-PCR analysis showing miR-28 expression in naïve B cells and GC B cells sorted from Peyer's patches of young λ-MYC mice and in B cell tumors from older λ-MYC mice.

To assess the therapeutic potential of miR-28 replacement therapy in primary BL *in vivo* we used λ-MYC mice as donors of primary BL lymphomas, which we employed to generate local and systemic BL models in NSG host mice. In the local tumor model we performed subcutaneous injection of λ-MYC BL cells and 0.5 nmoles of miR-28 mimic was administrated intratumorally 3 times within a week (Fig. 51A). We observed from 3 days after the first mimic injection of primary BL (from d10, Fig . 51B) that miR-28 treated tumors showed a clear growth reduction and were significantly smaller than those in mice treated with control miRNA mimics at the end of the treatment (Fig. 51C).

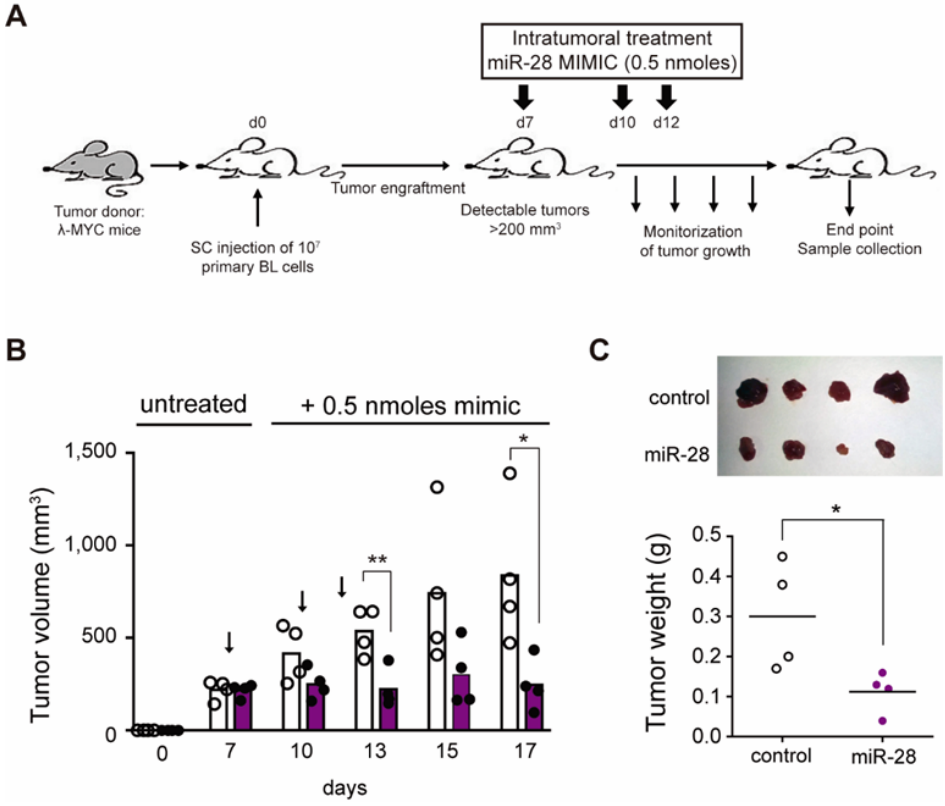

Figure 51 (continuation); Synthetic miR-28 intratumoral administration reduces the volume of murine primary BLs. (A) Schematic representation of the experiment. Subcutaneous mouse lymphomas were established by injection of 10^7 cells from enlarged spleen and/or lymph nodes of sick λ-MYC transgenic mice. Once tumors were detectable (> 200mm^3), miR-28 or control mimics were administered intratumorally at 0,5 nmoles in 50 µl at the indicated days. **(B)** Tumor volume over time. The arrows indicate mimic injection days. **(C)** Representative tumor photos and quantification of the tumor mass. Statistical significance was calculated with student's unpaired T test, *p < 0.05.

In the systemic primary BL model, we performed intravenous injection of BL cells from enlarged spleens or lymph nodes from sick λ-MYC mice into NSG recipient mice and miR-28 mimics or scramble control were administrated intravenously 7 nmoles of miR-28 mimic or control mimic at day 10 and 14 after tumor injection (Fig. 52A). Recipient mice were sacrificed 17 days after the injection of the primary BL cells and the effect of miR-28 on BL growth was assessed. We found that the spleens of the mice treated with miR-28 mimics were notably smaller than those treated with control mimic (Fig. 52B) and contained a reduced proportion of BL B cells (Fig. 52C). Immunohistochemistry analysis of the spleens revealed that mice treated with miR-28 mimic had increased proportions of caspase 3$^+$ apoptotic cells.

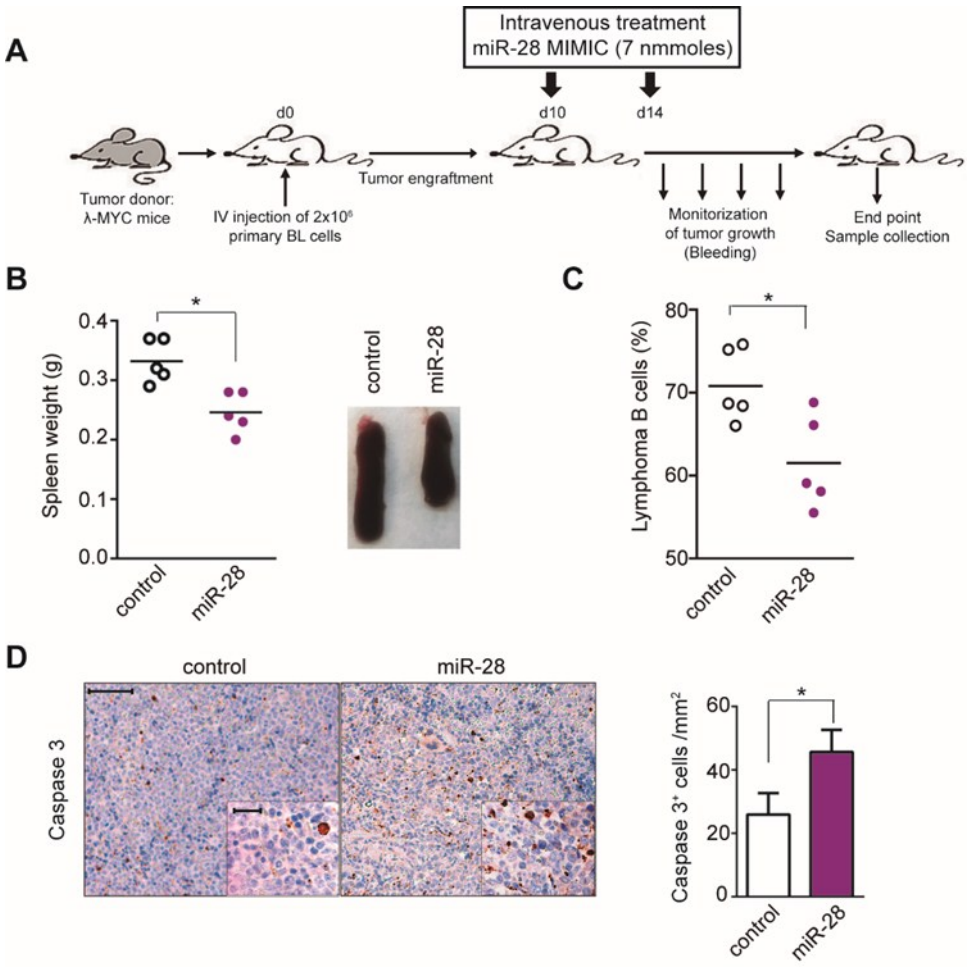

Figure 52. Intravenous delivery of miR-28 mimic reduces the volume of mouse primary lymphomas.

Figure 52 (continuation); (A) Schematic representation of the experiment. $2x10^6$ tumor cells from enlarged spleen and/or lymph nodes of λ-MYC transgenic mice were injected intravenously into NSG recipient mice and treated with intravenous injection of miR-28 mimic or scrambled control 10 days and 14 days after tumor injection. **(B)** Spleen weight quantification and representative spleen images obtained from mice after treatment. **(C)** Percentage of lymphoma B cells in the blood of transplanted mice treated with control or miR-28 mimics. Open circles, scrambled control-treated, closed purple circles, miR-28-treated. Student t test (5 mice per group). **(D)** Left, representative images of caspase 3 staining at 10X and 40X magnification (inset). Right, quantification of caspase 3 positive cells. Scale bar is 100 μm and 25 μm for the insets. *$p < 0.05$, unpaired t test.

In summary, we have used a number of different *in vivo* lymphoma models (including human BL and DLBCL xenografts and primary BL allografts) and different methods to achieve miR-28 expression in lymphoma cells (including lentiviral transduction, intratumoral and intravenous synthetic miR-28 administration) to assess the therapeutic potential of miR-28 in GC-derived lymphomas. Our results show that miR-28 replacement therapy is effective for the treatment of GC-derived neoplasms and provide a promising and novel approach for the treatment of human B cell NHLs.

DISCUSSION

In this thesis work we have focused on understanding the role of miR-217 and miR-28 as regulators of the biology of GC B cells, and on their putative contribution to mature B cell lymphomagenesis. Interestingly, we have found that miR-217 and miR-28 have antagonistic functions; while miR-217 is a positive regulator of the GC reaction and promotes B lymphomagenesis, miR-28 is a negative regulator of the GC reaction with tumor suppressor activity in mature B cell lymphomas (Fig. 53). In addition, we have explored whether miR-28 re-expression in lymphomas can be a useful strategy to develop new therapeutic approaches.

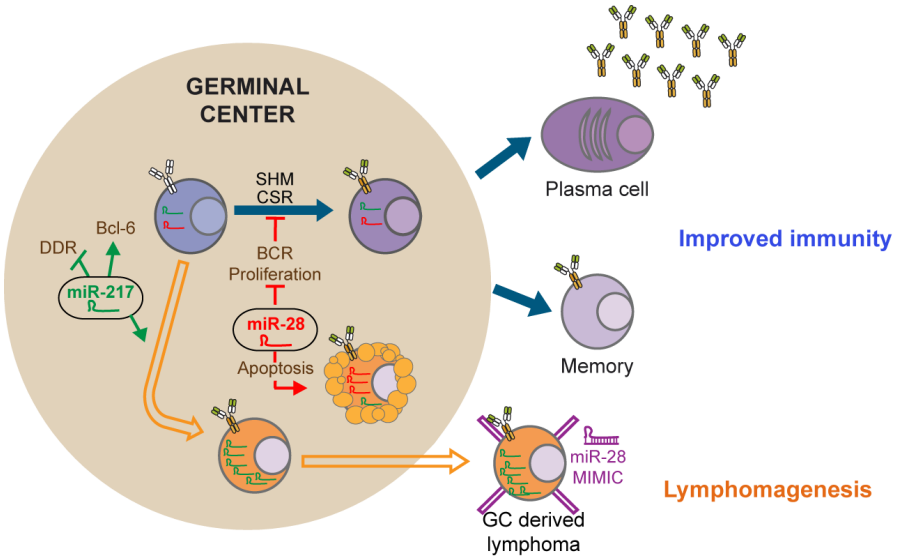

Figure 53. Working model for miR-217 and miR-28 control of the GC reaction and B cell lymphomagenesis. Both miR-217 and miR-28 are expressed in GC B cells and are needed to ensure a proper immune response against T cell dependent antigens. miR-217 is a positive regulator that boosts the GC response by dampening DDR and stabilizing Bcl-6. Importantly, miR-217 is an oncomiR whose overexpression causes mature B cell lymphomas. miR-28 is a negative regulator of GC that reduces B cell proliferation and BCR signaling, and promotes apoptosis in both murine and human B cells. The relevance of our findings is highlighted by the fact that the expression of both miR-217 and miR-28 are deregulated in human GC derived malignancies; miR-217 is overexpressed in certain types of aggressive B cell lymphomas, while miR-28 expression is absent in a wide range of B cell neoplasms. Moreover, we have successfully explored the therapeutic benefit that miR-28 replacement (by a synthetic miR-28 mimic as it is depicted in the model, or by other techniques) in lymphoma cells could have to treat this kind of aggressive cancer type, opening new treatment possibilities against mature B cell lymphomas.

1. miR-217 is a positive modulator of the GC reaction

We have identified miR-217 as a positive regulator of the GC reaction. miR-217 is specifically upregulated as a result of B-cell stimulation in the context of the GC reaction during the immune response, and the gain and loss of function approaches developed in the study directly establish the functional relevance of miR-217 in vivo. We generated mature B cell specific miR-217 overexpressing mouse models. miR-217 overexpression boosted the number of GC B cells and promoted the SHM and CSR reactions, and conversely, inhibition of endogenous miR-217 limited these events. Inter-

estingly, miR-217 gain of function did not promote any measurable alterations in B-cell differentiation, suggesting that the function of miR-217 in the B-cell lineage is restricted to the context of GCs and antibody diversification.

2. Molecular mechanisms of miR-217 activity

On the basis of sequence complementarity, individual miRNAs can be predicted to target hundreds or thousands of mRNAs, a finding that very early led to the development of in silico prediction tools to facilitate the task of miRNA-target identification. However, these prediction analyses of miRNA targets suffer from a high rate of false positives, due to the incomplete sequence complementarity between miRNAs and their targets and the large heterogeneity of 3' UTRs, as revealed by next generation sequencing technology (Yatsenko, Marrone et al. 2014) (Mihailovich, Bremang et al. 2015). In addition, a substantial fraction of these predicted interactions may depend on cell type and context (Bartel 2009) (Ebert and Sharp 2012) (Pelaez and Carthew 2012) and on the binding of additional cofactors (Lujambio and Lowe 2012). Furthermore, an even smaller subset of target interactions is expected to affect tumor development and progression in vivo. These limitations make it critical to combine in silico predictions with experimental data. In our case, we performed genome wide analysis of the B cells transcriptomes upon perturbation of miR-217 levels in GC B cells and merged the results with those obtained with a compound algorithm for miRNA target prediction.

Our analysis performed in GC B cells from miR-217^{KI} and littermate controls showed that miR-217 regulates the expression of a gene network involved in DDR and repair, including Rad50, Nbs1, Wrn, Lig4, and XRCC2, as well as a set of genes of the cohesin complex, all of which are downregulated by miR-217. GC B cells are intrinsically prone to genome instability: (1) they are programmed to undergo AID-mediated gene remodeling; (2) the intense proliferation of GC B cells subjects them to replicative stress (Victora and Nussenzweig 2012); and (3) the GC reaction depends on Bcl-6, a master transcriptional repressor that dampens the DDR in GC B cells and whose deregulation generates B-cell lymphomas (Pasqualucci, Bhagat et al. 2008) (Cattoretti, Pasqualucci et al. 2005). Our data show that miR-217 downregulates a network of genes that sense and repair genotoxic events on DNA, which in turn can increase the tolerance of GC B cells to DNA damage, very much like Bcl-6. Notably, we found that miR-217 protects Bcl-6 from genotoxic stress-induced degradation (Phan, Saito et al. 2007), suggesting that both molecules are part of the same network that renders GC cells permissive to genomic instability and prone to malignant transformation.

3. miR-217 is an oncogene in B cells

Consistent with the idea that miR-217 diminishes DDR and stabilizes Bcl-6 in B cells we found that miR-217 overexpression promotes B-cell lymphomagenesis. Interestingly, mice that overexpress miR-217 resemble Bcl-6-overexpressing Iμ-HABCL6 mice in that both show increased GC formation and develop long latency mature B-cell lymphomas (Cattoretti, Pasqualucci et al. 2005). We also found that Ink4a/Arf but not p53 loss sensitizes B cells to miR-217-promoted lymphomagenesis. Although it is possible that a protective role of p53 is masked by the early appearance of T-cell lymphomas in $p53^{-/-}$ mice, our data suggest that Ink4a rather than the Arf-p53 oncogenic stress pathway plays the predominant role in protecting GC B cells against the transforming activity of miR-217. This result is in agreement with the finding that Ink4a protein is frequently lost through gene methylation or deletion in aggressive B-cell lymphomas, whereas ARF silencing is a rarer event (Baur, Shaw et al. 1999).

Deregulation of miRNA expression in human B-cell lymphomas has been extensively documented (Eis, Tam et al. 2005, Lawrie, Soneji et al. 2007) (Xiao, Calado et al. 2007) (Calin, Dumitru et al. 2002) reviewed in the introduction, Table 1). In some instances, the functional relevance of miRNA deregulation has been tested in genetically modified mouse models ((Medina, Nolde et al. 2010) (Costinean, Zanesi et al. 2006) (Enomoto, Kitaura et al. 2011) (Santanam, Zanesi et al. 2010) reviewed in the introduction, Table 2). This gives formal proof of the lymphomagenic potential of the miRNA. Prior to our work, evidence for miRNAs involved in GC or post-GC lymphomagenesis was absent. During this years a significant amount of papers have appeared regarding the lymphomagenic potential of miR-17-92, which is far restricted to the combined action of the whole miR-17-92 miRNA cluster to give rise to DLBCL in a frequency of 10% (while around 30% of the ill mice had leukemias) (Sandhu, Fassan et al. 2013). Other mouse models of miRNA deregulation that give rise to mature B cell lymphomas combine the overexpression of some members of the miR-17-92 cluster with the expression of Myc oncogene (He, Thomson et al. 2005). In our work we have found that miR-217 overexpression in B cells promotes lymphomas of GC or post-GC origin, what supposes the 92% of the generated lymphomas, most likely by impinging on the regulation of the DDR and Bcl-6. Accordingly, we found increased levels of miR-217 in BL and DLBCL, two of the most aggressive lymphomas arising from GCs. Overall, our results identify miR-217 as a novel molecular link between the GC response and B-cell transformation, provide an in vivo model of mature B-cell lymphomagenesis and point to miR-217 inhibition as a potential new therapeutic strategy for the treatment of two aggressive subtypes of human mature B cell lymphomas.

4. miR-28 is a GC miRNA

We initially selected miR-28 as a potentially relevant miRNA for GC reaction from a very extensive miRNA-Seq study that characterized the miRNA profile in human and mouse lymphopoiesis (Kuchen, Resch et al. 2010) and where miR-28 was found as being highly expressed in GC B cells from immunized mice. We confirmed these results and additionally found that miR-28 expression is transient –it is shut down when the B cells exit the GC- and that its expression is progressively increased with the progression of the GC reaction.

Interestingly, miR-28 was not identified in our original expression profiling performed in *in vitro* activated B cells that served for miR-217 identification (de Yebenes, Belver et al. 2008). Likewise, miRNA-seq analysis of B cells activated *in vitro* failed to detect a significant increase of miR-28 levels ((Kuchen, Resch et al. 2010) and our unpublished results). This apparent contradiction very likely reflects that *in vitro* conditions for B cell stimulation, although experimentally useful, are not completely faithful in mimicking the transcriptional program induced in an *in vivo* immune response, including the expression of miR-28. Although we have not approached the regulation of miR-28 expression, it is plausible that costimulatory molecules that mediate B-T cell crosstalk *in vivo* could be triggering regulatory elements involved in its transcriptional activation.

5. miR-28 is a negative regulator of GCs

We next analyzed the role of miR-28 in mature B cell activation and the GC reaction. Using *in vitro* miR-28 gain of function assays we found that miR-28 expression negatively regulates CSR; which implies that even though miR-28 is not naturally induced in these conditions, some or all of its targets must be expressed in vitro that exert the miRNA's functional effect. Conversely, loss of function miR-28 vivo assays show increased CSR, GC and PC B cell generation. Our results reveal that miR-28, a GC specific miRNA, is a negative regulator of the GC reaction in B cells may seem counterintuitive. We hypothesize that miR-28 expression could be required to limit or finish GC reactions in vivo, and that this negative regulation would represent a brake for B cell transformation. In agreement with this idea, we detect that miR-28 expression is a late event during the progression of the GC, and that the loss of miR-28 expression is a frequent event in mature B cell neoplasms, as discussed below.

6. miR-28 is lost in GC-derived neoplasms

A notable feature of miR-28 expression is its strong downregulation in an extensive variety of human mature GC-derived B cell neoplasms; including CLL leukemia and various B cell NHL subtypes, such as FL and the aggressive DLBCL and BL. This observation is in agreement with the finding reported during the development of this work by K. Basso and co-workers, which showed reduced miR-28 expression in various human GC-derived lymphomas (Schneider, Setty et al. 2014). We found that miR-28 expression is lost both in primary tumor biopsies as well as in a variety of immortalized cell lines derived from BL and DLBCL human B cell lymphomas. In addition, we found that miR-28 expression is downregulated in tumoral B cells from λ-Myc transgenic mouse. Interestingly, miR-28 dowregulation in this BL mouse model occurs only in transformed BL cells, as miR-28 downregulation is not observed in non tumoral λ-Myc TG^+ GC B cells. The specific loss of miR-28 expression in GC-derived B cell neoplasms suggests that miR-28 could be a tumor suppressor for GC B cells.

Although the mechanisms that account for the loss of miR-28 expression in GC-derived neoplasms have not been addressed specifically, there are some evidences that point to genomic deletions and transcription factor deregulation as plausible mechanisms. miR-28 is an intronic miRNA, encoded in the Lipoma Preferred Partner (LPP) gene on chromosome 3q27, and very close to the Bcl-6 gene. Genomic deletions affecting the LPP locus have been reported in FL (Schwaenen, Viardot et al. 2009). Moreover, a genomic region that is likely involved in regulating miR-28 and LPP expression has been identified as a susceptibility locus associated with increased risks of B cell NHL, such as DLBCL, in the Chinese population (Tan, Foo et al. 2013). In addition, K. Basso and co-workers have found that Myc expression negatively regulates the expression of LPP and miR-28 (Schneider, Setty et al. 2014). As Myc gain of expression is a common event in a proportion of GC-derived lymphomas, mainly BL and ABC-DLBCL, it would expectably contribute to miR-28 downregulation. Nevertheless, we have found here that in λ-MYC mice the loss of miR-28 expression is an event that associates with B cell transformation, suggesting that increased Myc expression alone is not sufficient to result in impaired miR-28 expression in vivo.

7. Molecular mechanisms of miR-28 activity

To identify the genes regulated by miR-28 expression in B cells we have combined genome wide transcriptomic analysis by RNA-Seq with quantitative proteomic profiling analysis by iTRAQ. As gene expression regulation by miRNAs can involve either diminishing mRNA stability or inhibiting mRNA translation, transcriptome profiling alone would fail to detect genes regulated by translational inhibition (Selbach, Schwanhausser et al. 2008) (Mihailovich, Bremang et al. 2015). On the other hand, gi-

ven the relatively subtle changes in gene expression promoted by miRNAs, proteome analysis would very likely miss a number of targets for lack of enough sensitivity. Therefore we decided that the combination of these two techniques was the preferable choice for miRNA target identification. Notably, we have found a high overlap in the cellular function of the genes regulated by miR-28 both at the transcriptome and at the proteome level. Our results show that miR-28 expression in BL B cells regulates genes involved in immune system regulation, cell cycle and proliferation, DNA replication, recombination and repair, and cell death by apoptosis. Importantly, we have functionally verified that miR-28 expression impacts proliferation and apoptosis in both human and mouse B cells, as we find that miR-28 expressing B cells have reduced proliferation and increased cell death in vitro and in vivo.

Causal network analysis of proteome profiling has shown that miR-28 significantly alters the expression of genes involved in the BCR signaling network, the key signaling pathway that regulates B cell proliferation and cell death. We have found that tonic and anti-IgM mediated BCR signaling is dampened in miR-28 expressing B cells, as we find reduced phosphorylation of key mediators of the BCR signaling, such as AKT and ERK, reduced expression of NF-ĸB2 and IKKB mediators and of the anti-apoptotic effector Bcl-2. Therefore, our data support the notion that miR-28 modulates the strength of BCR signaling promoting a deficient or slower proliferative activity together with impaired survival, which in turn would account for the defect in CSR (Rush, Liu et al. 2005) (Celeste, Petersen et al. 2002) . However, we cannot rule out that other targets, unrelated to BCR signaling could also contribute to the functional effect of miR-28.

Importantly, BCR signaling has also been shown to play a central role the survival of neoplasic B cells. Indeed several B cell lymphomas, such as BL (Schmitz, Ceribelli et al. 2014) (Rickert 2013) and DLBCL (Young, Shaffer et al. 2015) (Davis, Ngo et al. 2010) rely on BCR signaling to sustain lymphoma growth. Accordingly, different current therapeutic strategies for mature B cell lymphoma treatment are based in the inhibition of key intermediates of the BCR signaling network such as NF-ĸB and IKKB (Baldwin 2001) (Ceribelli, Kelly et al. 2014).

Overall our expression profiling shows that miR-28 regulates a number of key physiological processes in GC B cells, including BCR signaling, proliferation and apoptosis, that are required to fine tune and limit the extent of GC responses. In addition, these results suggest that miR-28 could have tumor suppressive activity for GC derived B cell tumors.

8. miR-28 tumor suppressive activity in GC B cells

Two important evidences obtained during the development of the project suggested that miR-28 could have tumor-suppressor activity in GC derived tumors: (1) the finding that miR-28 promotes cell

death, reduces proliferation and dampens BCR signaling in immortalized BL cells suggest that miR-28 expression could impair B cell lymphoma growth; and (2) the loss of miR-28 expression in a large number of GC-derived human B cell neoplasms, as well in mouse BL cells, suggests that miR-28 could be a tumor suppressor for B cell tumors.

Although formal proof that miR-28 is a tumor suppressor miRNA for GC B cells would require the development of loss of function mouse models in which the absence of miR-28 expression in GC cells leads to B cell lymphomagenesis, the results obtained in this work unequivocally demonstrate that miR-28 expression has tumor suppressor activity in GC-derived BL and DLBCL lymphomas.

We have tested the tumor suppressor potential of miR-28 by replacing miR-28 expression in GC-derived lymphomas where its expression had been lost –presumably during the transformation process. We found that miR-28 re-expression promotes a dramatic block in tumor growth in vitro and in xenograft models. miR-28 re-expression diminishes proliferation and promotes apoptosis of lymphoma cells in vivo, as revealed by decreased Ki67 and increased active caspase 3 expression in BL xenografts. It is very likely that different genes found to be regulated by miR-28 in BL cells, including elements of the BCR signaling pathway such as AKT, ERK, IKKB, NF-κB2 and Bcl-2 account for miR-28 tumor suppressor activity, as they have been shown to be involved in the establishment or maintenance of different GC-derived lymphomas. For example, constitutive activation of BCR pathway has been reported in BL and in DLBCL, correlating with a poor clinical outcome (Kloo, Nagel et al. 2011) (Sander, Calado et al. 2012) (Schmitz, Young et al. 2012). ABC-DLBCL, which is one of the lymphomas with a poorer prognosis and a high incidence of relapses, has gain of function mutations that enhance the PI3K signaling and NF-κB signaling (Davis, Ngo et al. 2010) (Kloo, Nagel et al. 2011) (Young, Shaffer et al. 2015). In addition, the anti-apoptotic effector Bcl-2 has been shown to be a clinically relevant target for the treatment of a significant number of GC-derived B cell neoplasms (reviewed in (Braun, de Carne Trecesson et al. 2013) (Musilova and Mraz 2015) (Lin, Mao et al. 2015)). Importantly, we found decreased Bcl-2 expression in BL xenografts overexpressing miR-28, indicating that one of the mechanism that contributes to miR-28 induced apoptosis of lymphoma cells *in vivo* is the downregulation of the anti-apoptotic effector molecule Bcl-2.

Here we have been able to show lymphoma growth block by miR-28 both when using viral vehicles and with miRNA mimics, which are thought to be the safest way to reintroduce a miRNA in a therapeutic setting. In addition, we found that both intratumoral and intravenous administration of miR-28 mimic were effective to reduce BL growth in vivo. Interestingly, the growth inhibiting effect of miR-28 expression seems to be B cell specific, as other types of transformed cells such as Jurkat T cells or NIH 3T3 fibroblasts were not affected in their growth by miR-28 overexpression. In addition, we found no evi-

dence of hematologic, renal or hepatic toxicity associated to in vivo mi-28 mimic administration, suggesting that this approach could be a feasible therapeutic strategy for mature B cell lymphoma treatment. Although therapeutic development requires a number of exhaustive analysis to thoroughly prove the safety of the treatment, our data, together with the point that this therapeutic strategy aims at replacing the normal levels of miR-28 that were once lost by the tumor cells rather than at a broad elimination of B cells, suggest that the toxicity of miR-28 will be considerably lower than current strategies for the treatment of B cell neoplasms.

In this regard, it is important to note that BL and DLBCL are often refractory to conventional chemotherapy, usually based on R-CHOP administration (Lenz, Wright et al. 2008) (Flodr, Latalova et al. 2014). In recent years the functional impact of miRNAs in cancer development have made them very attractive candidates for therapeutic strategies (Review in (Braicu, Calin et al. 2013) (Bader, Brown et al. 2010)). miRNA-based therapeutics can provide a higher level of target specificity compared to other chemotherapy agents, thanks to the intrinsic sequence-dependent targeting of microRNAs. In addition, the potential to simultaneously regulate multiple pathways and processes altered in cancer may make miRNA-based therapy less susceptible to developing drug resistance. Indeed, a number of microRNA inhibitors are already in clinical trials, and one clinical trial is also approved for the use of miR-34 mimic for the treatment of hepatocarcinoma. A next stage towards a clinical application of miR-28 replacement therapy would involve to compare miR-28 replacement and conventional R-CHOP treatment in terms of efficacy and toxicity, as well as to assess whether the combination of both therapeutics can improve the efficacy of the individual treatments. In addition, the finding that miR-28 expression is lost also in other B cell neoplasms, such as FL and CLL, makes it likely that miR-28 based therapeutic approaches could be useful to treat a wider range B cell neoplasms.

9. Final considerations

Overall, our work has identified miR-217 and miR-28 as crucial modulators of the GC response and whose deregulation is mechanistically linked to the generation of GC-derived B cell neoplasms. In addition, our work provides the generation of new tools that can be useful for the development of innovative therapeutic strategies for the treatment of B cell NHL; a novel mouse model of GC derived lymphomagenesis based on B cell specific miR-217 overexpression and the experimental basis for the development of miR-28 replacement therapies.

CONCLUSIONS

CONCLUSIONS

1. miR-217 is a positive regulator of the GC reaction that promotes CSR, SHM and the generation of GC B cells.

2. miR-217 regulates a DNA damage response and repair gene network and stabilizes Bcl-6 in GC B cells.

3. miR-217 is an oncogene in mature B cells and is overexpressed in aggressive human B-cell lymphomas.

4. The generation of mature B cell specific miR-217 overexpressing mice provides an *in vivo* model of GC-derived B cell lymphomagenesis.

5. miR-28 is a negative regulator of the GC reaction that inhibits CSR and the generation of GC B cells.

6. miR-28 is lost in various human GC derived malignancies, including BL, DLBCL, FL and CLL.

7. miR-28 expression dampens BCR signaling, inhibits proliferation and induces cell death in human and mouse B cells.

8. miR-28 re-expression in lymphoma cells inhibits tumor growth, which indicates that it has tumor suppressor activity and opens the possibility of a new therapeutic strategy for the treatment of mature B cell neoplasms.

9. miR-217 and miR-28 molecularly link the GC reaction and B cell lymphomagenesis.

CONCLUSIONES

1. miR-217 es un regulador positivo de la reacción de centro germinal, cuya expresión promueve la reacción de cambio de isotipo, la hipermutación somática y la generación de células B de CG.

2. miR-217 atenúa la expresión de una red de genes implicados en la respuesta al daño y la reparación del ADN, y estabiliza la expresión de Bcl-6 en células B de CG.

3. miR-217 es un oncogén en linfocitos B maduros y su expresión se encuentra incrementada en linfomas B agresivos humanos.

4. La generación de un modelo murino de sobre-expresión de miR-217 específico de linfocitos B maduros provee de un modelo *in vivo* de linfomas B derivados de CG.

5. miR-28 es un regulador negativo de la reacción de centro germinal que inhibe la reacción de cambio de isotipo y la generación de células B de CG.

6. La expresión de miR-28 se pierde en varias neoplasias humanas derivadas de CG, incluyendo BL, DLBCL, FL, y CLL.

7. La expresión de miR-28 disminuye la señalización a través de BCR, inhibe la proliferación e induce la muerte celular en células B murinas y humanas.

8. La re-expresión de miR-28 en células de linfoma inhibe el crecimiento tumoral, lo que indica que miR-28 tiene actividad supresora de tumores y abre la posibilidad de una nueva estrategia terapéutica para tratar neoplasias B maduras.

9. miR-217 y miR-28 vinculan a nivel molecular la reacción de CG y los procesos linfomagénicos de los linfocitos B.

BIBLIOGRAPHY

Babar, I. A., C. J. Cheng, C. J. Booth, X. Liang, J. B. Weidhaas, W. M. Saltzman and F. J. Slack (2012). "Nanoparticle-based therapy in an in vivo microRNA-155 (miR-155)-dependent mouse model of lymphoma." Proc Natl Acad Sci U S A **109**(26): E1695-1704.

Bader, A. G., D. Brown and M. Winkler (2010). "The promise of microRNA replacement therapy." Cancer Res **70**(18): 7027-7030.

Baldwin, A. S. (2001). "Control of oncogenesis and cancer therapy resistance by the transcription factor NF-kappaB." J Clin Invest **107**(3): 241-246.

Bartel, D. P. (2009). "MicroRNAs: target recognition and regulatory functions." Cell **136**(2): 215-233.
Basso, K. and R. Dalla-Favera (2010). "BCL6: master regulator of the germinal center reaction and key oncogene in B cell lymphomagenesis." Adv Immunol **105**: 193-210.

Basso, K. and R. Dalla-Favera (2012). "Roles of BCL6 in normal and transformed germinal center B cells." Immunol Rev **247**(1): 172-183.

Basso, K. and R. Dalla-Favera (2015). "Germinal centres and B cell lymphomagenesis." Nat Rev Immunol **15**(3): 172-184.

Basso, K., P. Sumazin, P. Morozov, C. Schneider, R. L. Maute, Y. Kitagawa, J. Mandelbaum, J. Haddad, C. Z. Chen, A. Califano and R. Dalla-Favera (2009). "Identification of the human mature B cell miRNome." Immunity **30**(5): 744-752.

Baur, A. S., P. Shaw, N. Burri, F. Delacretaz, F. T. Bosman and P. Chaubert (1999). "Frequent methylation silencing of p15(INK4b) (MTS2) and p16(INK4a) (MTS1) in B-cell and T-cell lymphomas." Blood **94** (5): 1773-1781.

Belver, L., V. G. de Yébenes and A. R. Ramiro (2010). "MicroRNAs prevent the generation of autoreactive antibodies." Immunity **33**(5): 713-722.

Blum, K. A. (2015). "B-cell receptor pathway modulators in NHL." Hematology Am Soc Hematol Educ Program **2015**(1): 82-91.

Bonzon-Kulichenko, E., F. Garcia-Marques, M. Trevisan-Herraz and J. Vazquez (2015). "Revisiting peptide identification by high-accuracy mass spectrometry: problems associated with the use of narrow mass precursor windows." J Proteome Res **14**(2): 700-710.

Bothmer, A., P. C. Rommel, A. Gazumyan, F. Polato, C. R. Reczek, M. F. Muellenbeck, S. Schaetzlein, W. Edelmann, P. L. Chen, R. M. Brosh, Jr., R. Casellas, T. Ludwig, R. Baer, A. Nussenzweig, M. C. Nussenzweig and D. F. Robbiani (2013). "Mechanism of DNA resection during intrachromosomal recombination and immunoglobulin class switching." J Exp Med **210**(1): 115-123.

Braicu, C., G. A. Calin and I. Berindan-Neagoe (2013). "MicroRNAs and cancer therapy - from bystanders to major players." Curr Med Chem **20**(29): 3561-3573.

Braun, F., S. de Carne Trecesson, J. Bertin-Ciftci and P. Juin (2013). "Protect and serve: Bcl-2 proteins as guardians and rulers of cancer cell survival." Cell Cycle **12**(18): 2937-2947.

BIBLIOGRAPHY

Calado, D. P., Y. Sasaki, S. A. Godinho, A. Pellerin, K. Köchert, B. P. Sleckman, I. M. de Alborán, M. Janz, S. Rodig and K. Rajewsky (2012). "The cell-cycle regulator c-Myc is essential for the formation and maintenance of germinal centers." Nat Immunol **13**(11): 1092-1100.

Calado, D. P., B. Zhang, L. Srinivasan, Y. Sasaki, J. Seagal, C. Unitt, S. Rodig, J. Kutok, A. Tarakhovsky, M. Schmidt-Supprian and K. Rajewsky (2010). "Constitutive canonical NF-κB activation cooperates with disruption of BLIMP1 in the pathogenesis of activated B cell-like diffuse large cell lymphoma." Cancer Cell **18**(6): 580-589.

Calin, G. A. and C. M. Croce (2006). "MicroRNA signatures in human cancers." Nat Rev Cancer **6**(11): 857-866.

Calin, G. A., C. D. Dumitru, M. Shimizu, R. Bichi, S. Zupo, E. Noch, H. Aldler, S. Rattan, M. Keating, K. Rai, L. Rassenti, T. Kipps, M. Negrini, F. Bullrich and C. M. Croce (2002). "Frequent deletions and down-regulation of micro- RNA genes miR15 and miR16 at 13q14 in chronic lymphocytic leukemia." Proc Natl Acad Sci U S A **99**(24): 15524-15529.

Calvano, S. E., W. Xiao, D. R. Richards, R. M. Felciano, H. V. Baker, R. J. Cho, R. O. Chen, B. H. Brownstein, J. P. Cobb, S. K. Tschoeke, C. Miller-Graziano, L. L. Moldawer, M. N. Mindrinos, R. W. Davis, R. G. Tompkins, S. F. Lowry, Inflamm and P. Host Response to Injury Large Scale Collab. Res (2005). "A network-based analysis of systemic inflammation in humans." Nature **437**(7061): 1032-1037.

Cardona, M., J. A. Lopez, A. Serafin, A. Rongvaux, J. Inserte, D. Garcia-Dorado, R. Flavell, M. Llovera, X. Canas, J. Vazquez and D. Sanchis (2015). "Executioner Caspase-3 and 7 Deficiency Reduces Myocyte Number in the Developing Mouse Heart." PLoS One **10**(6): e0131411.

Cattoretti, G., L. Pasqualucci, G. Ballon, W. Tam, S. V. Nandula, Q. Shen, T. Mo, V. V. Murty and R. Dalla-Favera (2005). "Deregulated BCL6 expression recapitulates the pathogenesis of human diffuse large B cell lymphomas in mice." Cancer Cell **7**(5): 445-455.

Celeste, A., S. Petersen, P. J. Romanienko, O. Fernandez-Capetillo, H. T. Chen, O. A. Sedelnikova, B. Reina-San-Martin, V. Coppola, E. Meffre, M. J. Difilippantonio, C. Redon, D. R. Pilch, A. Olaru, M. Eckhaus, R. D. Camerini-Otero, L. Tessarollo, F. Livak, K. Manova, W. M. Bonner, M. C. Nussenzweig and A. Nussenzweig (2002). "Genomic instability in mice lacking histone H2AX." Science **296**(5569): 922-927.

Ceribelli, M., P. N. Kelly, A. L. Shaffer, G. W. Wright, W. Xiao, Y. Yang, L. A. Mathews Griner, R. Guha, P. Shinn, J. M. Keller, D. Liu, P. R. Patel, M. Ferrer, S. Joshi, S. Nerle, P. Sandy, E. Normant, C. J. Thomas and L. M. Staudt (2014). "Blockade of oncogenic IkappaB kinase activity in diffuse large B-cell lymphoma by bromodomain and extraterminal domain protein inhibitors." Proc Natl Acad Sci U S A **111**(31): 11365-11370.

Costinean, S., N. Zanesi, Y. Pekarsky, E. Tili, S. Volinia, N. Heerema and C. M. Croce (2006). "Pre-B cell proliferation and lymphoblastic leukemia/high-grade lymphoma in E(mu)-miR155 transgenic mice." Proc Natl Acad Sci U S A **103**(18): 7024-7029.

Criscuolo, A. and S. Brisse (2014). "AlienTrimmer removes adapter oligonucleotides with high sensitivity in short-insert paired-end reads. Commentary on Turner (2014) Assessment of insert sizes and adapter content in FASTQ data from NexteraXT libraries." Front Genet **5**: 130.

Chaudhuri, A. A., A. Y. So, A. Mehta, A. Minisandram, N. Sinha, V. D. Jonsson, D. S. Rao, R. M. O'Connell and D. Baltimore (2012). "Oncomir miR-125b regulates hematopoiesis by targeting the gene Lin28A." Proc Natl Acad Sci U S A **109**(11): 4233-4238.

Chaudhuri, J., C. Khuong and F. W. Alt (2004). "Replication protein A interacts with AID to promote deamination of somatic hypermutation targets." Nature **430**(7003): 992-998.

Cheng, C. J., R. Bahal, I. A. Babar, Z. Pincus, F. Barrera, C. Liu, A. Svoronos, D. T. Braddock, P. M. Glazer, D. M. Engelman, W. M. Saltzman and F. J. Slack (2015). "MicroRNA silencing for cancer therapy targeted to the tumour microenvironment." Nature **518**(7537): 107-110.

Daige, C. L., J. F. Wiggins, L. Priddy, T. Nelligan-Davis, J. Zhao and D. Brown (2014). "Systemic delivery of a miR34a mimic as a potential therapeutic for liver cancer." Mol Cancer Ther **13**(10): 2352-2360.
Dang, C. V. (2012). "MYC on the path to cancer." Cell **149**(1): 22-35.

Davis, R. E., V. N. Ngo, G. Lenz, P. Tolar, R. M. Young, P. B. Romesser, H. Kohlhammer, L. Lamy, H. Zhao, Y. Yang, W. Xu, A. L. Shaffer, G. Wright, W. Xiao, J. Powell, J. K. Jiang, C. J. Thomas, A. Rosenwald, G. Ott, H. K. Muller-Hermelink, R. D. Gascoyne, J. M. Connors, N. A. Johnson, L. M. Rimsza, E. Campo, E. S. Jaffe, W. H. Wilson, J. Delabie, E. B. Smeland, R. I. Fisher, R. M. Braziel, R. R. Tubbs, J. R. Cook, D. D. Weisenburger, W. C. Chan, S. K. Pierce and L. M. Staudt (2010). "Chronic active B-cell-receptor signalling in diffuse large B-cell lymphoma." Nature **463**(7277): 88-92.

Davis, S., S. Propp, S. M. Freier, L. E. Jones, M. J. Serra, G. Kinberger, B. Bhat, E. E. Swayze, C. F. Bennett and C. Esau (2009). "Potent inhibition of microRNA in vivo without degradation." Nucleic Acids Res **37**(1): 70-77.

De Silva, N. S. and U. Klein (2015). "Dynamics of B cells in germinal centres." Nat Rev Immunol **15**(3): 137-148.

de Yebenes, V. G., N. Bartolome-Izquierdo and A. R. Ramiro (2013). "Regulation of B-cell development and function by microRNAs." Immunological reviews **253**(1): 25-39.

de Yebenes, V. G., L. Belver, D. G. Pisano, S. Gonzalez, A. Villasante, C. Croce, L. He and A. R. Ramiro (2008). "miR-181b negatively regulates activation-induced cytidine deaminase in B cells." The Journal of experimental medicine **205**(10): 2199-2206.

de Yebenes, V. G. and A. R. Ramiro (2006). "Activation-induced deaminase: light and dark sides." Trends in molecular medicine **12**(9): 432-439.

Di Lisio, L., M. Sánchez-Beato, G. Gómez-López, M. E. Rodríguez, S. Montes-Moreno, M. Mollejo, J. Menárguez, M. A. Martínez, F. J. Alves, D. G. Pisano, M. A. Piris and N. Martínez (2012). "MicroRNA signatures in B-cell lymphomas." Blood Cancer J **2**(2): e57.

Di Noia, J. M. and M. S. Neuberger (2007). "Molecular mechanisms of antibody somatic hypermutation." Annu Rev Biochem **76**: 1-22.

Dominguez-Sola, D., G. D. Victora, C. Y. Ying, R. T. Phan, M. Saito, M. C. Nussenzweig and R. Dalla-Favera (2012). "The proto-oncogene MYC is required for selection in the germinal center and cyclic reentry." Nat Immunol **13**(11): 1083-1091.

BIBLIOGRAPHY

Dorsett, Y., K. M. McBride, M. Jankovic, A. Gazumyan, T. H. Thai, D. F. Robbiani, M. Di Virgilio, B. Reina San-Martin, G. Heidkamp, T. A. Schwickert, T. Eisenreich, K. Rajewsky and M. C. Nussenzweig (2008). "MicroRNA-155 suppresses activation-induced cytidine deaminase-mediated Myc-Igh translocation." Immunity **28**(5): 630-638.

Ebert, M. S., J. R. Neilson and P. A. Sharp (2007). "MicroRNA sponges: competitive inhibitors of small RNAs in mammalian cells." Nat Methods **4**(9): 721-726.

Ebert, M. S. and P. A. Sharp (2012). "Roles for microRNAs in conferring robustness to biological processes." Cell **149**(3): 515-524.

Eis, P. S., W. Tam, L. Sun, A. Chadburn, Z. Li, M. F. Gomez, E. Lund and J. E. Dahlberg (2005). "Accumulation of miR-155 and BIC RNA in human B cell lymphomas." Proc Natl Acad Sci U S A **102**(10): 3627-3632.

Elmen, J., M. Lindow, S. Schutz, M. Lawrence, A. Petri, S. Obad, M. Lindholm, M. Hedtjarn, H. F. Hansen, U. Berger, S. Gullans, P. Kearney, P. Sarnow, E. M. Straarup and S. Kauppinen (2008). "LNA-mediated microRNA silencing in non-human primates." Nature **452**(7189): 896-899.

Engel, A. and G. M. Barton (2010). "Unfolding new roles for XBP1 in immunity." Nat Immunol **11**(5): 365-367.

Enomoto, Y., J. Kitaura, K. Hatakeyama, J. Watanuki, T. Akasaka, N. Kato, M. Shimanuki, K. Nishimura, M. Takahashi, M. Taniwaki, C. Haferlach, R. Siebert, M. J. Dyer, N. Asou, H. Aburatani, H. Nakakuma, T. Kitamura and T. Sonoki (2011). "Emu/miR-125b transgenic mice develop lethal B-cell malignancies." Leukemia **25**(12): 1849-1856.

Erikson, J., A. ar-Rushdi, H. L. Drwinga, P. C. Nowell and C. M. Croce (1983). "Transcriptional activation of the translocated c-myc oncogene in burkitt lymphoma." Proc Natl Acad Sci U S A **80**(3): 820-824.

Esau, C. C. (2008). "Inhibition of microRNA with antisense oligonucleotides." Methods **44**(1): 55-60.
Ficenec, D., M. Osborne, J. Pradines, D. Richards, R. Felciano, R. J. Cho, R. O. Chen, T. Liefeld, J. Owen, A. Ruttenberg, C. Reich, J. Horvath and T. Clark (2003). "Computational knowledge integration in biopharmaceutical research." Brief Bioinform **4**(3): 260-278.

Flodr, P., P. Latalova, M. Tichy, Z. Kubova, T. Papajik, M. Svachova, K. Vrzalikova, L. Radova, M. Jarosova and P. Murray (2014). "Diffuse large B-cell lymphoma: the history, current view and new perspectives." Neoplasma **61**(5): 491-504.

Gentleman, R. C., V. J. Carey, D. M. Bates, B. Bolstad, M. Dettling, S. Dudoit, B. Ellis, L. Gautier, Y. Ge, J. Gentry, K. Hornik, T. Hothorn, W. Huber, S. Iacus, R. Irizarry, F. Leisch, C. Li, M. Maechler, A. J. Rossini, G. Sawitzki, C. Smith, G. Smyth, L. Tierney, J. Y. Yang and J. Zhang (2004). "Bioconductor: open software development for computational biology and bioinformatics." Genome Biol **5**(10): R80.

Gentleman, S. M., P. D. Leclercq, L. Moyes, D. I. Graham, C. Smith, W. S. Griffin and J. A. Nicoll (2004). "Long-term intracerebral inflammatory response after traumatic brain injury." Forensic Sci Int **146**(2-3): 97-104.

Gentner, B., G. Schira, A. Giustacchini, M. Amendola, B. D. Brown, M. Ponzoni and L. Naldini (2009). "Stable knockdown of microRNA in vivo by lentiviral vectors." Nat Methods **6**(1): 63-66.

Greeve, J., A. Philipsen, K. Krause, W. Klapper, K. Heidorn, B. E. Castle, J. Janda, K. B. Marcu and R. Parwaresch (2003). "Expression of activation-induced cytidine deaminase in human B-cell non-Hodgkin lymphomas." Blood **101**(9): 3574-3580.

Grosswendt, S., A. Filipchyk, M. Manzano, F. Klironomos, M. Schilling, M. Herzog, E. Gottwein and N. Rajewsky (2014). "Unambiguous identification of miRNA:target site interactions by different types of ligation reactions." Mol Cell **54**(6): 1042-1054.

Gururajan, M., C. L. Haga, S. Das, C. M. Leu, D. Hodson, S. Josson, M. Turner and M. D. Cooper (2010). "MicroRNA 125b inhibition of B cell differentiation in germinal centers." Int Immunol **22**(7): 583-592.

He, L., J. M. Thomson, M. T. Hemann, E. Hernando-Monge, D. Mu, S. Goodson, S. Powers, C. Cordon-Cardo, S. W. Lowe, G. J. Hannon and S. M. Hammond (2005). "A microRNA polycistron as a potential human oncogene." Nature **435**(7043): 828-833.

Heise, N., N. S. De Silva, K. Silva, A. Carette, G. Simonetti, M. Pasparakis and U. Klein (2014). "Germinal center B cell maintenance and differentiation are controlled by distinct NF-kappaB transcription factor subunits." J Exp Med **211**(10): 2103-2118.

Huang da, W., B. T. Sherman and R. A. Lempicki (2009). "Systematic and integrative analysis of large gene lists using DAVID bioinformatics resources." Nat Protoc **4**(1): 44-57.

Isern, J., B. Martin-Antonio, R. Ghazanfari, A. M. Martin, J. A. Lopez, R. del Toro, A. Sanchez-Aguilera, L. Arranz, D. Martin-Perez, M. Suarez-Lledo, P. Marin, M. Van Pel, W. E. Fibbe, J. Vazquez, S. Scheding, A. Urbano-Ispizua and S. Mendez-Ferrer (2013). "Self-renewing human bone marrow mesenspheres promote hematopoietic stem cell expansion." Cell Rep **3**(5): 1714-1724.

Kenter, A. L. (2012). "AID targeting is dependent on RNA polymerase II pausing." Semin Immunol **24** (4): 281-286.

Kim, D., G. Pertea, C. Trapnell, H. Pimentel, R. Kelley and S. L. Salzberg (2013). "TopHat2: accurate alignment of transcriptomes in the presence of insertions, deletions and gene fusions." Genome Biol **14**(4): R36.

Kitano, M., S. Moriyama, Y. Ando, M. Hikida, Y. Mori, T. Kurosaki and T. Okada (2011). "Bcl6 protein expression shapes pre-germinal center B cell dynamics and follicular helper T cell heterogeneity." Immunity **34**(6): 961-972.

Klein, U., S. Casola, G. Cattoretti, Q. Shen, M. Lia, T. Mo, T. Ludwig, K. Rajewsky and R. Dalla-Favera (2006). "Transcription factor IRF4 controls plasma cell differentiation and class-switch recombination." Nat Immunol **7**(7): 773-782.

Klein, U., S. Casola, G. Cattoretti, Q. Shen, M. Lia, T. Mo, T. Ludwig, K. Rajewsky and R. Dalla-Favera (2006). "Transcription factor IRF4 controls plasma cell differentiation and class-switch recombination." Nature immunology **7**(7): 773-782.

Klein, U., G. Klein, B. Ehlin-Henriksson, K. Rajewsky and R. Kuppers (1995). "Burkitt's lymphoma is a malignancy of mature B cells expressing somatically mutated V region genes." Molecular medicine **1** (5): 495-505.

Kloo, B., D. Nagel, M. Pfeifer, M. Grau, M. Düwel, M. Vincendeau, B. Dörken, P. Lenz, G. Lenz and D. Krappmann (2011). "Critical role of PI3K signaling for NF-kappaB-dependent survival in a subset of activated B-cell-like diffuse large B-cell lymphoma cells." Proc Natl Acad Sci U S A **108**(1): 272-277.

Koralov, S. B., S. A. Muljo, G. R. Galler, A. Krek, T. Chakraborty, C. Kanellopoulou, K. Jensen, B. S. Cobb, M. Merkenschlager, N. Rajewsky and K. Rajewsky (2008). "Dicer ablation affects antibody diversity and cell survival in the B lymphocyte lineage." Cell **132**(5): 860-874.

Kota, J., R. R. Chivukula, K. A. O'Donnell, E. A. Wentzel, C. L. Montgomery, H. W. Hwang, T. C. Chang, P. Vivekanandan, M. Torbenson, K. R. Clark, J. R. Mendell and J. T. Mendell (2009). "Therapeutic microRNA delivery suppresses tumorigenesis in a murine liver cancer model." Cell **137**(6): 1005-1017.

Kovalchuk, A. L., C. F. Qi, T. A. Torrey, L. Taddesse-Heath, L. Feigenbaum, S. S. Park, A. Gerbitz, G. Klobeck, K. Hoertnagel, A. Polack, G. W. Bornkamm, S. Janz and H. C. Morse (2000). "Burkitt lymphoma in the mouse." J Exp Med **192**(8): 1183-1190.

Krueger, F., S. R. Andrews and C. S. Osborne (2011). "Large scale loss of data in low-diversity illumina sequencing libraries can be recovered by deferred cluster calling." PLoS One **6**(1): e16607.

Krützfeldt, J., N. Rajewsky, R. Braich, K. G. Rajeev, T. Tuschl, M. Manoharan and M. Stoffel (2005). "Silencing of microRNAs in vivo with 'antagomirs'." Nature **438**(7068): 685-689.

Kuchen, S., W. Resch, A. Yamane, N. Kuo, Z. Li, T. Chakraborty, L. Wei, A. Laurence, T. Yasuda, S. Peng, J. Hu-Li, K. Lu, W. Dubois, Y. Kitamura, N. Charles, H. W. Sun, S. Muljo, P. L. Schwartzberg, W. E. Paul, J. O'Shea, K. Rajewsky and R. Casellas (2010). "Regulation of microRNA expression and abundance during lymphopoiesis." Immunity **32**(6): 828-839.

Küppers, R. (2005). "Mechanisms of B-cell lymphoma pathogenesis." Nat Rev Cancer **5**(4): 251-262.
Lam, L. T., R. E. Davis, J. Pierce, M. Hepperle, Y. Xu, M. Hottelet, Y. Nong, D. Wen, J. Adams, L. Dang and L. M. Staudt (2005). "Small molecule inhibitors of IkappaB kinase are selectively toxic for subgroups of diffuse large B-cell lymphoma defined by gene expression profiling." Clin Cancer Res **11**(1): 28-40.

Landgraf, P., M. Rusu, R. Sheridan, A. Sewer, N. Iovino, A. Aravin, S. Pfeffer, A. Rice, A. O. Kamphorst, M. Landthaler, C. Lin, N. D. Socci, L. Hermida, V. Fulci, S. Chiaretti, R. Foà, J. Schliwka, U. Fuchs, A. Novosel, R. U. Müller, B. Schermer, U. Bissels, J. Inman, Q. Phan, M. Chien, D. B. Weir, R. Choksi, G. De Vita, D. Frezzetti, H. I. Trompeter, V. Hornung, G. Teng, G. Hartmann, M. Palkovits, R. Di Lauro, P. Wernet, G. Macino, C. E. Rogler, J. W. Nagle, J. Ju, F. N. Papavasiliou, T. Benzing, P. Lichter, W. Tam, M. J. Brownstein, A. Bosio, A. Borkhardt, J. J. Russo, C. Sander, M. Zavolan and T. Tuschl (2007). "A mammalian microRNA expression atlas based on small RNA library sequencing." Cell **129**(7): 1401-1414.

Lawrie, C. H., S. Soneji, T. Marafioti, C. D. Cooper, S. Palazzo, J. C. Paterson, H. Cattan, T. Enver, R. Mager, J. Boultwood, J. S. Wainscoat and C. S. Hatton (2007). "MicroRNA expression distinguishes between germinal center B cell-like and activated B cell-like subtypes of diffuse large B cell lymphoma." Int J Cancer **121**(5): 1156-1161.

Lenz, G., R. E. Davis, V. N. Ngo, L. Lam, T. C. George, G. W. Wright, S. S. Dave, H. Zhao, W. Xu, A. Rosenwald, G. Ott, H. K. Muller-Hermelink, R. D. Gascoyne, J. M. Connors, L. M. Rimsza, E. Campo, E. S. Jaffe, J. Delabie, E. B. Smeland, R. I. Fisher, W. C. Chan and L. M. Staudt (2008). "Oncogenic CARD11 mutations in human diffuse large B cell lymphoma." Science **319**(5870): 1676-1679.

Lenz, G., G. W. Wright, N. C. Emre, H. Kohlhammer, S. S. Dave, R. E. Davis, S. Carty, L. T. Lam, A. L. Shaffer, W. Xiao, J. Powell, A. Rosenwald, G. Ott, H. K. Muller-Hermelink, R. D. Gascoyne, J. M. Connors, E. Campo, E. S. Jaffe, J. Delabie, E. B. Smeland, L. M. Rimsza, R. I. Fisher, D. D. Weisenburger, W. C. Chan and L. M. Staudt (2008). "Molecular subtypes of diffuse large B-cell lymphoma arise by distinct genetic pathways." Proc Natl Acad Sci U S A **105**(36): 13520-13525.

Li, B. and C. N. Dewey (2011). "RSEM: accurate transcript quantification from RNA-Seq data with or without a reference genome." BMC Bioinformatics **12**: 323.

Lin, Q., Y. Mao, Y. Song and D. Huang (2015). "MicroRNA34a induces apoptosis in PC12 cells by reducing Bcell lymphoma 2 and sirtuin1 expression." Mol Med Rep **12**(4): 5709-5714.

Lu, J., G. Getz, E. A. Miska, E. Alvarez-Saavedra, J. Lamb, D. Peck, A. Sweet-Cordero, B. L. Ebert, R. H. Mak, A. A. Ferrando, J. R. Downing, T. Jacks, H. R. Horvitz and T. R. Golub (2005). "MicroRNA expression profiles classify human cancers." Nature **435**(7043): 834-838.

Lujambio, A. and S. W. Lowe (2012). "The microcosmos of cancer." Nature **482**(7385): 347-355.

Mandelbaum, J., G. Bhagat, H. Tang, T. Mo, M. Brahmachary, Q. Shen, A. Chadburn, K. Rajewsky, A. Tarakhovsky, L. Pasqualucci and R. Dalla-Favera (2010). "BLIMP1 is a tumor suppressor gene frequently disrupted in activated B cell-like diffuse large B cell lymphoma." Cancer Cell **18**(6): 568-579.

Marshall, A. J., H. Niiro, T. J. Yun and E. A. Clark (2000). "Regulation of B-cell activation and differentiation by the phosphatidylinositol 3-kinase and phospholipase Cgamma pathway." Immunol Rev **176**: 30 -46.
Martinez-Bartolome, S., P. Navarro, F. Martin-Maroto, D. Lopez-Ferrer, A. Ramos-Fernandez, M. Villar, J. P. Garcia-Ruiz and J. Vazquez (2008). "Properties of average score distributions of SEQUEST: the probability ratio method." Mol Cell Proteomics **7**(6): 1135-1145.

Medina, P. P., M. Nolde and F. J. Slack (2010). "OncomiR addiction in an in vivo model of microRNA-21 -induced pre-B-cell lymphoma." Nature **467**(7311): 86-90.

Merkenschlager, M. and D. T. Odom (2013). "CTCF and cohesin: linking gene regulatory elements with their targets." Cell **152**(6): 1285-1297.

Mihailovich, M., M. Bremang, V. Spadotto, D. Musiani, E. Vitale, G. Varano, F. Zambelli, F. M. Mancuso, D. A. Cairns, G. Pavesi, S. Casola and T. Bonaldi (2015). "miR-17-92 fine-tunes MYC expression and function to ensure optimal B cell lymphoma growth." Nat Commun **6**: 8725.

Momen-Heravi, F., S. Bala, T. Bukong and G. Szabo (2014). "Exosome-mediated delivery of functionally active miRNA-155 inhibitor to macrophages." Nanomedicine **10**(7): 1517-1527.
Muniategui, A., R. Nogales-Cadenas, M. Vazquez, X. L. Aranguren, X. Agirre, A. Luttun, F. Prosper, A. Pascual-Montano and A. Rubio (2012). "Quantification of miRNA-mRNA interactions." PLoS One **7**(2): e30766.

Musilova, K. and M. Mraz (2015). "MicroRNAs in B-cell lymphomas: how a complex biology gets more complex." Leukemia **29**(5): 1004-1017.

Nambu, Y., M. Sugai, H. Gonda, C. G. Lee, T. Katakai, Y. Agata, Y. Yokota and A. Shimizu (2003). "Transcription-coupled events associating with immunoglobulin switch region chromatin." Science **302**(5653): 2137-2140.

Navarro, P., M. Trevisan-Herraz, E. Bonzon-Kulichenko, E. Nunez, P. Martinez-Acedo, D. Perez-Hernandez, I. Jorge, R. Mesa, E. Calvo, M. Carrascal, M. L. Hernaez, F. Garcia, J. A. Barcena, K. Ashman, J. Abian, C. Gil, J. M. Redondo and J. Vazquez (2014). "General statistical framework for quantitative proteomics by stable isotope labeling." J Proteome Res **13**(3): 1234-1247.

Navarro, P. and J. Vazquez (2009). "A refined method to calculate false discovery rates for peptide identification using decoy databases." J Proteome Res **8**(4): 1792-1796.

Niiro, H. and E. A. Clark (2002). "Regulation of B-cell fate by antigen-receptor signals." Nat Rev Immunol **2**(12): 945-956.

Nyabi, O., M. Naessens, K. Haigh, A. Gembarska, S. Goossens, M. Maetens, S. De Clercq, B. Drogat, L. Haenebalcke, S. Bartunkova, I. De Vos, B. De Craene, M. Karimi, G. Berx, A. Nagy, P. Hilson, J. C. Marine and J. J. Haigh (2009). "Efficient mouse transgenesis using Gateway-compatible ROSA26 locus targeting vectors and F1 hybrid ES cells." Nucleic Acids Res **37**(7): e55.

Pasqualucci, L., G. Bhagat, M. Jankovic, M. Compagno, P. Smith, M. Muramatsu, T. Honjo, H. C. Morse, 3rd, M. C. Nussenzweig and R. Dalla-Favera (2008). "AID is required for germinal center-derived lymphomagenesis." Nat Genet **40**(1): 108-112.

Pasqualucci, L., M. Compagno, J. Houldsworth, S. Monti, A. Grunn, S. V. Nandula, J. C. Aster, V. V. Murty, M. A. Shipp and R. Dalla-Favera (2006). "Inactivation of the PRDM1/BLIMP1 gene in diffuse large B cell lymphoma." J Exp Med **203**(2): 311-317.

Pavri, R., A. Gazumyan, M. Jankovic, M. Di Virgilio, I. Klein, C. Ansarah-Sobrinho, W. Resch, A. Yamane, B. Reina San-Martin, V. Barreto, T. J. Nieland, D. E. Root, R. Casellas and M. C. Nussenzweig (2010). "Activation-induced cytidine deaminase targets DNA at sites of RNA polymerase II stalling by interaction with Spt5." Cell **143**(1): 122-133.

Pelaez, N. and R. W. Carthew (2012). "Biological robustness and the role of microRNAs: a network perspective." Curr Top Dev Biol **99**: 237-255.

Peled, J. U., F. L. Kuang, M. D. Iglesias-Ussel, S. Roa, S. L. Kalis, M. F. Goodman and M. D. Scharff (2008). "The biochemistry of somatic hypermutation." Annu Rev Immunol **26**: 481-511.

Perez-Duran, P., L. Belver, V. G. de Yebenes, P. Delgado, D. G. Pisano and A. R. Ramiro (2012). "UNG shapes the specificity of AID-induced somatic hypermutation." The Journal of experimental medicine **209**(7): 1379-1389.

Phan, R. T. and R. Dalla-Favera (2004). "The BCL6 proto-oncogene suppresses p53 expression in germinal-centre B cells." Nature **432**(7017): 635-639.

Phan, R. T., M. Saito, Y. Kitagawa, A. R. Means and R. Dalla-Favera (2007). "Genotoxic stress regulates expression of the proto-oncogene Bcl6 in germinal center B cells." Nat Immunol **8**(10): 1132-1139.
Rajewsky, K. (1996). "Clonal selection and learning in the antibody system." Nature **381**(6585): 751-758.

Ramiro, A., B. Reina San-Martin, K. McBride, M. Jankovic, V. Barreto, A. Nussenzweig and M. C. Nussenzweig (2007). "The role of activation-induced deaminase in antibody diversification and chromosome translocations." Adv Immunol **94**: 75-107.

Ramiro, A. R., M. Jankovic, T. Eisenreich, S. Difilippantonio, S. Chen-Kiang, M. Muramatsu, T. Honjo, A. Nussenzweig and M. C. Nussenzweig (2004). "AID is required for c-myc/IgH chromosome translocations in vivo." Cell **118**(4): 431-438.

Ranuncolo, S. M., J. M. Polo, J. Dierov, M. Singer, T. Kuo, J. Greally, R. Green, M. Carroll and A. Melnick (2007). "Bcl-6 mediates the germinal center B cell phenotype and lymphomagenesis through transcriptional repression of the DNA-damage sensor ATR." Nat Immunol **8**(7): 705-714.

Rao, D. S., R. M. O'Connell, A. A. Chaudhuri, Y. Garcia-Flores, T. L. Geiger and D. Baltimore (2010). "MicroRNA-34a perturbs B lymphocyte development by repressing the forkhead box transcription factor Foxp1." Immunity **33**(1): 48-59.

Remeseiro, S. and A. Losada (2013). "Cohesin, a chromatin engagement ring." Curr Opin Cell Biol **25**(1): 63-71.

Rickert, R. C. (2013). "New insights into pre-BCR and BCR signalling with relevance to B cell malignancies." Nat Rev Immunol **13**(8): 578-591.

Rickert, R. C., J. Roes and K. Rajewsky (1997). "B lymphocyte-specific, Cre-mediated mutagenesis in mice." Nucleic Acids Res **25**(6): 1317-1318.

Robbiani, D. F., A. Bothmer, E. Callen, B. Reina-San-Martin, Y. Dorsett, S. Difilippantonio, D. J. Bolland, H. T. Chen, A. E. Corcoran, A. Nussenzweig and M. C. Nussenzweig (2008). "AID is required for the chromosomal breaks in c-myc that lead to c-myc/IgH translocations." Cell **135**(6): 1028-1038.

Robbiani, D. F., K. Colon, M. Affer, M. Chesi and P. L. Bergsagel (2005). "Maintained rules of development in a mouse B-cell tumor." Leukemia **19**(7): 1278-1280.

Robbiani, D. F. and M. C. Nussenzweig (2013). "Chromosome translocation, B cell lymphoma, and activation-induced cytidine deaminase." Annu Rev Pathol **8**: 79-103.

Robinson, M. D., D. J. McCarthy and G. K. Smyth (2010). "edgeR: a Bioconductor package for differential expression analysis of digital gene expression data." Bioinformatics **26**(1): 139-140.

Robinson, M. D. and G. K. Smyth (2008). "Small-sample estimation of negative binomial dispersion, with applications to SAGE data." Biostatistics **9**(2): 321-332.

Rockwood, L. D., T. A. Torrey, J. S. Kim, A. E. Coleman, A. L. Kovalchuk, S. Xiang, T. Ried, H. C. Morse and S. Janz (2002). "Genomic instability in mouse Burkitt lymphoma is dominated by illegitimate genetic recombinations, not point mutations." Oncogene **21**(47): 7235-7240.

Rodriguez, A., E. Vigorito, S. Clare, M. V. Warren, P. Couttet, D. R. Soond, S. van Dongen, R. J. Grocock, P. P. Das, E. A. Miska, D. Vetrie, K. Okkenhaug, A. J. Enright, G. Dougan, M. Turner and A. Bradley (2007). "Requirement of bic/microRNA-155 for normal immune function." Science **316**(5824): 608-611.

Ruepp, A., B. Brauner, I. Dunger-Kaltenbach, G. Frishman, C. Montrone, M. Stransky, B. Waegele, T. Schmidt, O. N. Doudieu, V. Stumpflen and H. W. Mewes (2008). "CORUM: the comprehensive resource of mammalian protein complexes." Nucleic Acids Res **36**(Database issue): D646-650.

Rush, J. S., M. Liu, V. H. Odegard, S. Unniraman and D. G. Schatz (2005). "Expression of activation-induced cytidine deaminase is regulated by cell division, providing a mechanistic basis for division-linked class switch recombination." Proc Natl Acad Sci U S A **102**(37): 13242-13247.

Saito, M., J. Gao, K. Basso, Y. Kitagawa, P. M. Smith, G. Bhagat, A. Pernis, L. Pasqualucci and R. Dalla-Favera (2007). "A signaling pathway mediating downregulation of BCL6 in germinal center B cells is blocked by BCL6 gene alterations in B cell lymphoma." Cancer Cell **12**(3): 280-292.

Sander, S., D. P. Calado, L. Srinivasan, K. Köchert, B. Zhang, M. Rosolowski, S. J. Rodig, K. Holzmann, S. Stilgenbauer, R. Siebert, L. Bullinger and K. Rajewsky (2012). "Synergy between PI3K signaling and MYC in Burkitt lymphomagenesis." Cancer Cell **22**(2): 167-179.

Sandhu, S. K., M. Fassan, S. Volinia, F. Lovat, V. Balatti, Y. Pekarsky and C. M. Croce (2013). "B-cell malignancies in microRNA Emu-miR-17~92 transgenic mice." Proc Natl Acad Sci U S A **110**(45): 18208-18213.

Santanam, U., N. Zanesi, A. Efanov, S. Costinean, A. Palamarchuk, J. P. Hagan, S. Volinia, H. Alder, L. Rassenti, T. Kipps, C. M. Croce and Y. Pekarsky (2010). "Chronic lymphocytic leukemia modeled in mouse by targeted miR-29 expression." Proc Natl Acad Sci U S A **107**(27): 12210-12215.

Sciammas, R., A. L. Shaffer, J. H. Schatz, H. Zhao, L. M. Staudt and H. Singh (2006). "Graded expression of interferon regulatory factor-4 coordinates isotype switching with plasma cell differentiation." Immunity **25**(2): 225-236.

Schmitz, R., M. Ceribelli, S. Pittaluga, G. Wright and L. M. Staudt (2014). "Oncogenic mechanisms in Burkitt lymphoma." Cold Spring Harb Perspect Med **4**(2).

Schmitz, R., R. M. Young, M. Ceribelli, S. Jhavar, W. Xiao, M. Zhang, G. Wright, A. L. Shaffer, D. J. Hodson, E. Buras, X. Liu, J. Powell, Y. Yang, W. Xu, H. Zhao, H. Kohlhammer, A. Rosenwald, P. Kluin, H. K. Müller-Hermelink, G. Ott, R. D. Gascoyne, J. M. Connors, L. M. Rimsza, E. Campo, E. S. Jaffe, J. Delabie, E. B. Smeland, M. D. Ogwang, S. J. Reynolds, R. I. Fisher, R. M. Braziel, R. R. Tubbs, J. R. Cook, D. D. Weisenburger, W. C. Chan, S. Pittaluga, W. Wilson, T. A. Waldmann, M. Rowe, S. M. Mbulaiteye, A. B. Rickinson and L. M. Staudt (2012). "Burkitt lymphoma pathogenesis and therapeutic targets from structural and functional genomics." Nature **490**(7418): 116-120.

Schneider, C., M. Setty, A. B. Holmes, R. L. Maute, C. S. Leslie, L. Mussolin, A. Rosolen, R. Dalla-Favera and K. Basso (2014). "MicroRNA 28 controls cell proliferation and is down-regulated in B-cell lymphomas." Proc Natl Acad Sci U S A **111**(22): 8185-8190.

Schwaenen, C., A. Viardot, H. Berger, T. F. Barth, S. Bentink, H. Dohner, M. Enz, A. C. Feller, M. L. Hansmann, M. Hummel, H. A. Kestler, W. Klapper, M. Kreuz, D. Lenze, M. Loeffler, P. Moller, H. K. Muller-Hermelink, G. Ott, M. Rosolowski, A. Rosenwald, S. Ruf, R. Siebert, R. Spang, H. Stein, L. Truemper, P. Lichter, M. Bentz, S. Wessendorf and K. Molecular Mechanisms in Malignant Lymphomas Network Project of the Deutsche (2009). "Microarray-based genomic profiling reveals novel genomic aberrations in follicular lymphoma which associate with patient survival and gene expression status." Genes Chromosomes Cancer **48**(1): 39-54.

Selbach, M., B. Schwanhausser, N. Thierfelder, Z. Fang, R. Khanin and N. Rajewsky (2008). "Widespread changes in protein synthesis induced by microRNAs." Nature **455**(7209): 58-63.

Selbach, M., B. Schwanhäusser, N. Thierfelder, Z. Fang, R. Khanin and N. Rajewsky (2008). "Widespread changes in protein synthesis induced by microRNAs." Nature **455**(7209): 58-63.

Shaffer, A. L., K. I. Lin, T. C. Kuo, X. Yu, E. M. Hurt, A. Rosenwald, J. M. Giltnane, L. Yang, H. Zhao, K. Calame and L. M. Staudt (2002). "Blimp-1 orchestrates plasma cell differentiation by extinguishing the mature B cell gene expression program." Immunity **17**(1): 51-62.

Shaffer, A. L., M. Shapiro-Shelef, N. N. Iwakoshi, A. H. Lee, S. B. Qian, H. Zhao, X. Yu, L. Yang, B. K. Tan, A. Rosenwald, E. M. Hurt, E. Petroulakis, N. Sonenberg, J. W. Yewdell, K. Calame, L. H. Glimcher and L. M. Staudt (2004). "XBP1, downstream of Blimp-1, expands the secretory apparatus and other organelles, and increases protein synthesis in plasma cell differentiation." Immunity **21**(1): 81-93.

Shaffer, A. L., R. M. Young and L. M. Staudt (2012). "Pathogenesis of human B cell lymphomas." Annu Rev Immunol **30**: 565-610.

Shapiro-Shelef, M., K. I. Lin, L. J. McHeyzer-Williams, J. Liao, M. G. McHeyzer-Williams and K. Calame (2003). "Blimp-1 is required for the formation of immunoglobulin secreting plasma cells and pre-plasma memory B cells." Immunity **19**(4): 607-620.

Shapiro-Shelef, M., K. I. Lin, D. Savitsky, J. Liao and K. Calame (2005). "Blimp-1 is required for maintenance of long-lived plasma cells in the bone marrow." J Exp Med **202**(11): 1471-1476.

Sibley, C. R., Y. Seow and M. J. Wood (2010). "Novel RNA-based strategies for therapeutic gene silencing." Mol Ther **18**(3): 466-476.

Søkilde, R., I. Newie, H. Persson, Å. Borg and C. Rovira (2015). "Passenger strand loading in overexpression experiments using microRNA mimics." RNA Biol: 0.

Staudt, L. M. (2010). "Oncogenic activation of NF-kappaB." Cold Spring Harb Perspect Biol **2**(6): a000109.

Staudt, L. M. and W. H. Wilson (2002). "Focus on lymphomas." Cancer Cell **2**(5): 363-366.
Stavnezer, J., J. E. Guikema and C. E. Schrader (2008). "Mechanism and regulation of class switch recombination." Annu Rev Immunol **26**: 261-292.

Stracker, T. H. and J. H. Petrini (2011). "The MRE11 complex: starting from the ends." Nat Rev Mol Cell Biol **12**(2): 90-103.

Tam, W. (2001). "Identification and characterization of human BIC, a gene on chromosome 21 that encodes a noncoding RNA." Gene **274**(1-2): 157-167.

Tan, D. E., J. N. Foo, J. X. Bei, J. Chang, R. Peng, X. Zheng, L. Wei, Y. Huang, W. Y. Lim, J. Li, Q. Cui, S. H. Chew, R. P. Ebstein, P. Kuperan, S. T. Lim, M. Tao, S. H. Tan, A. Wong, G. C. Wong, S. Y. Tan, S. B. Ng, Y. X. Zeng, C. C. Khor, D. Lin, A. L. Seow, W. H. Jia and J. Liu (2013). "Genome-wide association study of B cell non-Hodgkin lymphoma identifies 3q27 as a susceptibility locus in the Chinese population." Nat Genet **45**(7): 804-807.

Thai, T. H., D. P. Calado, S. Casola, K. M. Ansel, C. Xiao, Y. Xue, A. Murphy, D. Frendewey, D. Valenzuela, J. L. Kutok, M. Schmidt-Supprian, N. Rajewsky, G. Yancopoulos, A. Rao and K. Rajewsky (2007). "Regulation of the germinal center response by microRNA-155." Science **316**(5824): 604-608.

Todd, D. J., L. J. McHeyzer-Williams, C. Kowal, A. H. Lee, B. T. Volpe, B. Diamond, M. G. McHeyzer-Williams and L. H. Glimcher (2009). "XBP1 governs late events in plasma cell differentiation and is not required for antigen-specific memory B cell development." J Exp Med **206**(10): 2151-2159.

Turner, C. A., Jr., D. H. Mack and M. M. Davis (1994). "Blimp-1, a novel zinc finger-containing protein that can drive the maturation of B lymphocytes into immunoglobulin-secreting cells." Cell **77**(2): 297-306.

Victora, G. D. and M. C. Nussenzweig (2012). "Germinal centers." Annu Rev Immunol **30**: 429-457.
Vigorito, E., K. L. Perks, C. Abreu-Goodger, S. Bunting, Z. Xiang, S. Kohlhaas, P. P. Das, E. A. Miska, A. Rodriguez, A. Bradley, K. G. Smith, C. Rada, A. J. Enright, K. M. Toellner, I. C. Maclennan and M. Turner (2007). "microRNA-155 regulates the generation of immunoglobulin class-switched plasma cells." Immunity **27**(6): 847-859.

Volinia, S., G. A. Calin, C. G. Liu, S. Ambs, A. Cimmino, F. Petrocca, R. Visone, M. Iorio, C. Roldo, M. Ferracin, R. L. Prueitt, N. Yanaihara, G. Lanza, A. Scarpa, A. Vecchione, M. Negrini, C. C. Harris and C. M. Croce (2006). "A microRNA expression signature of human solid tumors defines cancer gene targets." Proc Natl Acad Sci U S A **103**(7): 2257-2261.

Vuong, B. Q. and J. Chaudhuri (2012). "Combinatorial mechanisms regulating AID-dependent DNA deamination: interacting proteins and post-translational modifications." Semin Immunol **24**(4): 264-272.

Werner, M., E. Hobeika and H. Jumaa (2010). "Role of PI3K in the generation and survival of B cells." Immunol Rev **237**(1): 55-71.

Wilson, W. H., R. M. Young, R. Schmitz, Y. Yang, S. Pittaluga, G. Wright, C. J. Lih, P. M. Williams, A. L. Shaffer, J. Gerecitano, S. de Vos, A. Goy, V. P. Kenkre, P. M. Barr, K. A. Blum, A. Shustov, R. Advani, N. H. Fowler, J. M. Vose, R. L. Elstrom, T. M. Habermann, J. C. Barrientos, J. McGreivy, M. Fardis, B. Y. Chang, F. Clow, B. Munneke, D. Moussa, D. M. Beaupre and L. M. Staudt (2015). "Targeting B cell receptor signaling with ibrutinib in diffuse large B cell lymphoma." Nat Med.

Woyach, J. A., A. J. Johnson and J. C. Byrd (2012). "The B-cell receptor signaling pathway as a therapeutic target in CLL." Blood **120**(6): 1175-1184.

Xiao, C., D. P. Calado, G. Galler, T. H. Thai, H. C. Patterson, J. Wang, N. Rajewsky, T. P. Bender and K. Rajewsky (2007). "MiR-150 controls B cell differentiation by targeting the transcription factor c-Myb." Cell **131**(1): 146-159.

Xiao, C., L. Srinivasan, D. P. Calado, H. C. Patterson, B. Zhang, J. Wang, J. M. Henderson, J. L. Kutok and K. Rajewsky (2008). "Lymphoproliferative disease and autoimmunity in mice with increased miR-17-92 expression in lymphocytes." Nat Immunol **9**(4): 405-414.

Xu, S., K. Guo, Q. Zeng, J. Huo and K. P. Lam (2012). "The RNase III enzyme Dicer is essential for germinal center B-cell formation." Blood **119**(3): 767-776.

Yatsenko, A. S., A. K. Marrone and H. R. Shcherbata (2014). "miRNA-based buffering of the cobblestone -lissencephaly-associated extracellular matrix receptor dystroglycan via its alternative 3'-UTR." Nat Commun **5**: 4906.

Yin, H., R. L. Kanasty, A. A. Eltoukhy, A. J. Vegas, J. R. Dorkin and D. G. Anderson (2014). "Non-viral vectors for gene-based therapy." Nat Rev Genet **15**(8): 541-555.
Young, R. M., A. L. Shaffer, J. D. Phelan and L. M. Staudt (2015). "B-cell receptor signaling in diffuse large B-cell lymphoma." Semin Hematol **52**(2): 77-85.

ANNEX

Annex 1.Table of the differentially expressed genes in miR-217^{TG} GC B cells vs Control GC B cells

Gene	Fold_Change	P_Value
ankrd55	-6,82	0,01
acacb	6,51	0,02
utp20	-6,10	0,00
ccdc33	6,29	0,03
trcg1	-5,74	0,03
tsnaxip1	-5,33	0,01
kcne3	7,28	0,00
stx19	-7,30	0,00
prkx	-6,66	0,00
dusp28	-3,05	0,05
cldn23	-7,46	0,00
lrrc7	4,46	0,02
map3k2	3,30	0,03
slc34a2	-4,19	0,01
xkr9	-7,77	0,00
setmar	4,24	0,01
cd5	3,58	0,02
tspan1	-6,44	0,02
gm15760	-5,57	0,01
4933439k11rik	-5,83	0,03
glyctk	3,37	0,04
ush2a	-6,01	0,03
olfr352	7,99	0,00
clcn1	7,28	0,00
d630037f22rik	-4,03	0,02
gm5420	-6,09	0,03
slc2a5	-6,01	0,02
lrrc36	-7,61	0,00
fbxo48	-5,10	0,01
nbn	-3,44	0,03
ccdc57	-6,67	0,01
olfr1507	7,07	0,01
rnd3	5,72	0,04
oplah	8,47	0,00
gm10336	-5,93	0,03
csrnp3	-6,72	0,01
hiatl1	-3,46	0,04
ifrd1	-5,00	0,01
dsg4	6,70	0,02
ugt1a9	-7,00	0,01
obfc2a	-6,36	0,00
zfp661	6,21	0,02

tbc1d24	3,27	0,05
zfp407	-4,03	0,03
fam199x	-3,37	0,04
cbs	-6,31	0,03
kif1c	-4,60	0,02
arsg	7,54	0,00
plb1	-6,44	0,01
gtf2a1l	-5,74	0,04
thnsl2	-6,62	0,02
car9	8,68	0,00
kcnh1	-8,37	0,00
elac1	6,92	0,01
c330046g13rik	-5,52	0,04
myo1h	-6,31	0,03
ankrd28	8,48	0,00
adam4	-7,40	0,00
zbtb41	-9,06	0,00
prickle3	-4,64	0,01
mtap7d2	-5,52	0,04
suox	-8,56	0,00
ogfrl1	-3,65	0,02
1700034p13rik	-6,31	0,03
tinag	-5,74	0,05
vprbp	-3,60	0,05
rnf125	-8,21	0,00
clvs2	5,46	0,05
cyp4f17	-6,09	0,03
tmem63b	-4,41	0,03
ascl3	6,29	0,03
fam101a	-7,97	0,00
setd2	-4,00	0,01
odz1	-6,17	0,02
mcfd2	-6,84	0,00
d9ertd402e	-4,86	0,02
cyr61	7,36	0,01
thsd7b	-6,38	0,02
fmo6	-5,93	0,03
cwh43	-6,50	0,01
klkb1	6,58	0,02
sult1c2	6,51	0,02
elk4	3,86	0,02
cdo1	-6,17	0,02
gm10635	-6,38	0,02
smtnl2	7,64	0,00
six1	-6,72	0,01
prdm5	-6,44	0,02

wnt10a	-7,81	0,00
csf2rb	-7,86	0,00
otud4	-3,80	0,03
spast	-3,60	0,04
zfp91	-3,86	0,03
nr2c2	-4,87	0,01
cwc22	-3,14	0,05
plxna3	7,12	0,00
alkbh8	-5,22	0,00
ptpn4	8,04	0,00
iglon5	6,44	0,02
lilrb4	7,84	0,00
ano7	4,45	0,01
zfp459	-5,93	0,04
nkrf	-7,16	0,01
au015228	6,44	0,01
zfp113	-4,87	0,01
lhx2	-5,63	0,04
rhou	-3,97	0,02
tmprss2	-6,91	0,01
cxcr7	4,31	0,02
oaz3	-5,63	0,04
gad1	-7,16	0,01
mut	-7,43	0,00
clec2e	-6,17	0,03
tex15	4,88	0,01
clcn2	-6,17	0,02
epb4.9	-5,52	0,04
oprl1	4,20	0,03
ythdc2	-3,93	0,02
gtf2e1	-4,56	0,01
9430031j16rik	6,91	0,00
zbtb2	-3,10	0,05
slc4a5	-6,17	0,03
efemp1	5,80	0,01
bbs9	-5,76	0,00
fcgrt	-3,97	0,04
marveld1	6,03	0,03
cyp2c70	-5,63	0,04
thrb	6,11	0,00
tert	-6,31	0,02
gm14057	-6,17	0,02
gzf1	-4,74	0,01
bcap29	-3,80	0,03
cd28	-7,99	0,00
tmem158	-6,44	0,02

rhbdf1	4,28	0,02
nkd2	-6,56	0,02
tmem35	-7,52	0,00
e330009j07rik	-6,96	0,01
mfsd2a	-7,49	0,00
ect2	-5,91	0,00
fancm	-3,75	0,02
cyp2c39	6,87	0,01
ptpn21	-8,06	0,00
2700090o03rik	-6,31	0,03
gcap14	-5,33	0,01
cebpa	7,70	0,00
zfp758	-7,55	0,00
pou4f1	-8,58	0,00
mctp2	-8,51	0,00
cyb5rl	-6,17	0,02
klhl31	-6,62	0,01
a630089n07rik	4,55	0,02
atp6v0a4	-5,52	0,04
tgfa	-7,95	0,00
trmt61a	-4,53	0,01
akap14	5,72	0,03
1700120g07rik	7,02	0,01
aspa	5,20	0,00
zfp810	-6,56	0,02
kif16b	-3,71	0,04
clic3	-5,83	0,03
pcnx	-4,54	0,01
aa545190	-6,01	0,02
rab39	-5,21	0,01
rarb	8,30	0,00
g630090e17rik	-6,38	0,01
zc3hav1l	-7,12	0,01
sox2ot	-7,27	0,00
bc016423	-3,93	0,04
apoh	4,58	0,04
aqp1	5,72	0,03
fer1l4	6,13	0,02
itga6	-3,65	0,05
2810422o20rik	3,73	0,03
gm6583	7,24	0,01
prkch	4,68	0,02
zpld1	6,03	0,03
maged2	-4,32	0,02
ptpn5	7,70	0,00
rbfox2	9,09	0,00

plekhf1	-5,83	0,04
2410089e03rik	-3,22	0,05
gm20581	7,76	0,00
1700080o16rik	-7,08	0,01
mmp7	-6,17	0,03
scn1a	-6,38	0,02
wdr78	-6,67	0,01
pak1	-3,94	0,03
purg	-7,23	0,00
tbc1d8b	-5,64	0,01
myom1	-7,58	0,00
b630019k06rik	3,37	0,03
ttyh1	-5,93	0,04
4930431a04rik	-6,87	0,01
1700061f12rik	6,64	0,02
bhmt	5,83	0,05
serpina11	6,13	0,02
ubox5	-3,57	0,04
ldhal6b	7,24	0,00
gm10024	6,29	0,03
mrs2	3,87	0,02
exd2	-5,88	0,00
ces4a	-5,83	0,03
donson	-3,97	0,02
rnf13	-3,40	0,03
xlr4a	-6,56	0,01
trim30e-ps1	-6,50	0,01
1810033b17rik	6,13	0,03
4930429d17rik	-6,62	0,02
d930032p07rik	-6,09	0,02
fndc1	-6,87	0,01
uggt2	-7,43	0,00
gm6907	-4,32	0,02
ankrd61	-5,93	0,04
ggt6	-5,74	0,04
ninj2	7,78	0,00
ttc30b	-7,61	0,00
specc1	-6,62	0,02
kndc1	-4,47	0,01
zfp790	-4,18	0,01
zfp536	-7,08	0,01
rgs22	-5,93	0,03
lif	-5,93	0,04
gm16157	-6,17	0,02
psd3	-7,20	0,01
fgf10	-7,12	0,00

ifit1	-7,43	0,01
cd99l2	-7,55	0,00
c330011f03	7,54	0,00
rpl3	-4,21	0,01
macrod2	-7,23	0,01
stard13	6,29	0,03
ube2cbp	-8,63	0,00
2810029c07rik	-6,56	0,02
hepacam2	-7,00	0,01
cyp2u1	-7,20	0,00
xrn1	-4,68	0,02
zfp874a	-6,67	0,01
ntrk3	-7,86	0,00
rnf103	-4,36	0,03
stat4	-7,74	0,00
amigo1	-5,63	0,05
ptpn22	-7,77	0,00
heg1	-5,84	0,00
tomm20l	6,03	0,04
ppm1l	4,61	0,02
rnf182	-6,44	0,01
2500004c02rik	-5,10	0,01
colq	7,40	0,00
c920006o11rik	-7,12	0,01
pou4f2	-8,02	0,00
nphs1	-6,62	0,01
mpp6	-3,96	0,02
lrrc66	-7,66	0,00
serpinb11	5,83	0,05
tmem163	-7,58	0,00
camk2g	-3,52	0,05
atp7a	-4,11	0,03
cdc42ep2	-7,12	0,00
ai646023	7,60	0,00
myo19	-5,33	0,01
abca14	6,92	0,01
gm10565	7,51	0,00
atp2b2	-4,14	0,03
pask	-5,06	0,00
4930583h14rik	6,82	0,01
rp1l1	-6,82	0,01
cyp2c44	6,92	0,01
hspa4l	-5,45	0,01
cylc2	6,29	0,03
b3galt5	5,83	0,05
mtap9	-7,72	0,00

mep1b	-5,16	0,01
chac2	-5,20	0,01
gdap2	-3,28	0,04
fam161a	-6,91	0,01
agap3	-7,20	0,00
tpmt	-7,40	0,00
4931408c20rik	5,94	0,04
zfp763	7,28	0,01
scoc	-7,49	0,00
itga10	6,03	0,03
snord99	-6,82	0,01
4831426i19rik	-4,32	0,03
zfp389	-6,38	0,01
kctd18	-4,91	0,01
gm2447	-3,60	0,03
olfr1273-ps	8,09	0,00
4930405d11rik	-5,83	0,03
klf15	-5,63	0,04
2610035d17rik	-9,04	0,00
wdfy3	-6,01	0,03
itsn1	-7,43	0,00
vps13d	-6,20	0,00
c8g	7,92	0,00
aoc2	7,57	0,00
pcmtd2	-5,83	0,00
sh2d1a	-3,71	0,03
sucnr1	-7,40	0,00
tecpr1	-6,55	0,00
adrbk2	6,15	0,00
tmprss4	-5,63	0,04
smurf1	-4,39	0,01
plekhn1	-6,01	0,04
lpar1	6,95	0,00
foxj1	-5,74	0,04
ugt2b5	-7,27	0,01
klrg1	-6,72	0,01
ctbp2	-6,77	0,01
rundc3a	-6,50	0,01
lrrc39	6,92	0,01
rimbp2	-5,93	0,03
tmem136	-6,91	0,01
zfp266	-5,08	0,00
mir217	7,73	0,00
tmem81	-6,01	0,03
ahr	7,36	0,00
oas1a	-5,83	0,03

tfcp2l1	-7,16	0,01
pacsin3	-5,63	0,05
snora74a	6,03	0,02
prg2	-8,15	0,00
akr1c19	-6,31	0,02
tbxas1	-6,17	0,02
zfp791	-7,49	0,00
plekha1	-5,97	0,00
eef2k	4,15	0,03
kdm1b	-8,75	0,00
dyrk3	-4,21	0,04
il1rap	6,39	0,00
rnft2	4,52	0,02
rnf38	-3,24	0,04
tmem41b	-3,54	0,04
unc5cl	-3,60	0,03
khdrbs3	4,36	0,02
gfra2	6,44	0,02
celsr3	-6,24	0,03
lcorl	2,87	0,05
4933413j09rik	-7,08	0,01
zfp808	-6,31	0,03
serpinb1c	-6,62	0,02
dclre1a	-5,24	0,01
glce	-7,00	0,01
egf	-6,67	0,01
tmigd1	-5,83	0,03
ammecr1	3,29	0,03
tnfrsf1a	4,40	0,03
4930509e16rik	-7,72	0,00
add2	-5,63	0,05
st6galnac2	5,84	0,01
xpnpep2	-8,08	0,00
tmc1	3,75	0,05
mir1949	6,29	0,03
syt4	-6,31	0,02
serpine3	6,70	0,02
ptgfrn	-6,96	0,01
rnf183	4,62	0,01
evc	-4,90	0,01
gckr	-5,63	0,04
mpp7	-6,50	0,01
fam163a	-5,74	0,03
2810021j22rik	-4,67	0,01
zfp959	-5,54	0,01
map4k5	-3,88	0,04

rab17	-6,01	0,04
ptx3	-6,31	0,02
phtf2	-3,59	0,02
slc10a1	-5,52	0,04
rttn	-4,79	0,01
bc037034	4,34	0,03
1700054n08rik	3,48	0,03
olfr1120	-6,24	0,02
cldn4	-6,38	0,01
gm5077	-5,63	0,05
odz4	-3,51	0,05
4930444m15rik	7,60	0,00
il1rapl2	-5,52	0,04
dnajc6	-5,74	0,05
dclk3	-6,01	0,02
acss2	-5,52	0,04
slc39a3	-3,13	0,04
ofd1	-5,36	0,01
hkdc1	-8,58	0,00
1700025k24rik	7,07	0,00
gm10638	5,94	0,04
galm	8,86	0,00
rfwd2	-4,21	0,04
gm15401	-6,96	0,01
six4	-4,69	0,01
frmd4b	8,90	0,00
cd1d1	-4,21	0,03
slc9a6	-4,35	0,02
9830132p13	-6,77	0,01
sv2c	-6,01	0,02
chrna3	-6,67	0,01
4930444a02rik	-3,20	0,04
zfp963	-4,26	0,04
trim12a	-8,58	0,00
ralgapb	-3,91	0,02
col1a2	3,67	0,02
cul4a	-4,69	0,01
zfp51	-5,37	0,00
s100a4	6,29	0,03
adam15	-4,71	0,02
stard6	5,83	0,05
slmap	-6,28	0,00
jhdm1d	-4,11	0,02
auts2	-6,91	0,01
zap70	-4,18	0,02
neurod1	-6,01	0,04

rasl11b	-6,82	0,01
tcea2	-4,37	0,03
kank1	-6,09	0,02
zfp788	-4,79	0,01
pak3	-7,04	0,01
tecpr2	-6,24	0,00
4833422c13rik	6,03	0,04
mcts2	3,96	0,02
uty	-6,89	0,00
mcf2l	6,51	0,02
col12a1	-6,67	0,01
fignl2	-7,00	0,01
lyzl4	7,02	0,01
nipal1	6,88	0,00
f830045p16rik	7,02	0,01
rbbp9	-7,20	0,01
rpap2	-3,68	0,03
clcn5	-7,43	0,00
padi2	-3,47	0,04
ptgis	6,82	0,01
csf1r	2,94	0,05
slc11a1	-8,14	0,00
olfr66	8,02	0,00
ccdc126	8,38	0,00
gm5177	7,32	0,01
exoc1	-3,82	0,02
fbxw24	-5,52	0,04
mex3c	-5,77	0,00
gng4	5,75	0,01
acad8	-7,16	0,01
clmn	-7,58	0,00
h6pd	-7,43	0,00
anln	-9,14	0,00
zfp120	-7,84	0,00
anxa9	-5,63	0,04
cyp3a13	-9,13	0,00
kcnf1	5,46	0,05
6330403a02rik	-3,32	0,05
fam171b	8,95	0,00
fgf12	-7,93	0,00
tmem176a	-4,99	0,01
cacna1d	-4,56	0,02
ai593442	-5,83	0,03
vcpip1	-5,62	0,00
tacc2	4,63	0,03
il22ra2	-7,99	0,00

hrk	4,41	0,02
hmgcs2	8,81	0,00
uts2d	-6,44	0,02
mios	-3,63	0,03
bahd1	-3,64	0,04
slc25a29	4,20	0,02
ly6k	-7,61	0,00
usp20	-7,81	0,00
bc026585	-7,23	0,00
lzts2	-7,08	0,01
opn1sw	-6,09	0,02
etv1	7,51	0,00
lynx1	-6,24	0,02
actn1	-4,04	0,03
4930570g19rik	-5,63	0,04
4930558g05rik	-5,63	0,04
zfp354c	-5,63	0,04
slc10a2	6,37	0,02
olfr456	-5,93	0,03
gm6320	-5,63	0,04
mfsd6	-4,26	0,03
tnfrsf11a	4,52	0,01
zfp940	-5,03	0,01
qpct	-7,20	0,01
usp44	-6,72	0,01
loc100504608	5,83	0,05
atp2b4	-5,63	0,05
efcab4b	-6,77	0,01
4933411g11rik	4,09	0,02
scube2	5,83	0,05
spic	6,70	0,02
olfr1188	-6,50	0,01
slc6a13	-6,24	0,02
st8sia4	-6,01	0,00
trim33	-4,14	0,02
mmp16	-6,01	0,04
aqp4	-7,34	0,01
5730577i03rik	3,99	0,05
csnk1g3	-7,52	0,00
b3gnt1	-3,37	0,04
slamf8	3,81	0,03
ndst3	-6,09	0,02
siah1b	-3,52	0,04
tram2	-6,38	0,01
drd1a	5,85	0,00
atp8b1	-6,62	0,01

scg5	-6,01	0,03
ky	-5,03	0,01
gatm	-4,28	0,01
dok2	-3,56	0,04
diap3	-4,19	0,02
polq	-6,01	0,03
zfp52	-8,71	0,00
olfr878	3,77	0,03
klf17	7,12	0,01
vwce	-6,24	0,03
1700074p13rik	8,11	0,00
slc9a3r2	6,29	0,02
alk	4,68	0,03
slc30a9	4,74	0,01
zfp85-rs1	-6,91	0,01
egfl7	-7,55	0,00
gpx7	7,73	0,00
gramd2	-6,77	0,01
4933413g19rik	6,29	0,03
5430427o19rik	-5,53	0,00
spata19	-5,63	0,04
lpar3	6,70	0,01
mgat3	8,07	0,00
map3k7	-5,39	0,00
ptbp2	-7,37	0,01
cyp2d22	-5,93	0,03
cct6b	-5,74	0,03
d330045a20rik	-5,83	0,03
magi3	-6,37	0,00
senp8	-9,06	0,00
elmod2	-7,74	0,00
tppp3	-6,01	0,02
zdhhc13	-4,26	0,02
bbs10	-8,63	0,00
pias2	-3,44	0,03
rdh16	6,70	0,01
gstm2	-5,63	0,05
cypt3	-6,72	0,01
1300017j02rik	6,13	0,03
cbln2	-6,87	0,01
prss55	6,03	0,02
ankar	-6,31	0,02
fbln7	-6,09	0,03
armc4	-6,01	0,03
rasal1	-5,04	0,01
liph	-6,82	0,01

pgc	-5,74	0,03
oas2	-6,31	0,02
capn5	-4,71	0,01
slc15a1	-3,47	0,05
samd3	7,70	0,00
jam3	-6,77	0,01
plekha3	-3,97	0,02
dnmt3a	-3,88	0,02
sos1	-4,26	0,02
gm1322	-7,88	0,00
serpinc1	7,02	0,01
hyal1	-7,23	0,00
2610018g03rik	-8,26	0,00
olfr1444	-6,72	0,01
atp11c	-8,28	0,00
gm505	-6,17	0,02
jrk	-4,17	0,02
cenpo	-3,16	0,05
shq1	-5,97	0,00
bc030307	6,13	0,03
ikbke	-7,04	0,01
dgkh	-7,40	0,01
cngb3	3,74	0,05
armcx5	-4,32	0,01
pus3	-9,48	0,00
dnaja4	4,02	0,02
als2cr11	-5,74	0,05
phkb	-4,71	0,02
adra1a	-6,01	0,02
kif17	8,22	0,00
gm5127	6,40	0,00
pter	-7,81	0,00
mlh3	-6,25	0,00
pank3	-4,93	0,01
cd36	-6,50	0,00
0610007p08rik	-3,57	0,04
tmem151b	-7,23	0,00
kcna1	-6,17	0,02
rdh5	-6,31	0,02
ces1g	6,58	0,02
hsd3b3	-7,16	0,01
0610040j01rik	-5,09	0,01
eif2c4	-4,43	0,03
zfp941	6,98	0,01
abca17	7,07	0,01
cln8	-6,44	0,01

lcor	6,65	0,00
il18r1	-6,96	0,01
gm10767	6,92	0,01
a230046k03rik	-5,89	0,00
zfp119b	-8,04	0,00
epha10	-7,20	0,00
nr6a1	-3,27	0,03
2210019i11rik	7,24	0,01
tmem67	-8,49	0,00
cntn3	-6,96	0,01
4930542c21rik	-5,83	0,04
cyp7a1	-6,96	0,01
lpcat2	5,09	0,01
golt1a	-4,63	0,02
bend4	7,47	0,01
slamf9	-7,12	0,01
smpd3	-3,63	0,04
zfp420	-6,96	0,01
olfr262	-7,37	0,00
dmbt1	-5,93	0,04
sag	6,08	0,00
ttc37	5,01	0,01
arhgap28	5,49	0,01
a630033h20rik	-6,56	0,01
ints6	-3,18	0,04
ppp1r3c	8,43	0,00
enc1	-6,01	0,04
erap1	-3,59	0,04
ypel1	6,51	0,02
rph3al	-5,83	0,03
eea1	-5,17	0,01
rapgefl1	-7,23	0,00
tas2r125	-7,00	0,01
hyls1	-8,53	0,00
col5a2	6,21	0,02
spin2	-6,56	0,02
ebf4	-6,01	0,02
efhd1	-6,38	0,01
af529169	-6,56	0,01
fam45a	-4,95	0,01
fermt2	5,94	0,04
itgb4	-6,72	0,01
gpr52	5,83	0,05
fam59a	-7,16	0,00
fjx1	7,21	0,00
tmem139	-7,23	0,01

hsd17b6	-5,74	0,05
zfp715	-5,00	0,01
megf10	-6,50	0,02
tmem161b	-5,22	0,00
gstm3	-7,95	0,00
lrp3	7,28	0,01
phex	-7,72	0,00
penk	6,58	0,01
odf2l	-8,15	0,00
slc13a2	-7,00	0,01
scamp5	-6,72	0,01
loxl3	-3,97	0,03
cyp2s1	7,40	0,01
adam21	-7,69	0,00
oas3	-6,96	0,01
e130311k13rik	4,52	0,01
samd4	-5,83	0,04
4833422f24rik	7,94	0,00
trim62	-6,17	0,03
gm16861	-7,23	0,01
creld1	-6,05	0,00
zfp866	5,18	0,00
cacna1f	-6,31	0,03
trip6	-4,15	0,05
8430410k20rik	-4,63	0,03
aa388235	-5,63	0,04
bc027231	-5,26	0,01
srpx2	-6,01	0,02
rad50	-3,53	0,05
rhoj	-7,30	0,00
gltpd2	4,78	0,03
lrrc46	7,40	0,01
cidec	-6,77	0,01
pcm1	-6,17	0,00
hrasls	-6,96	0,01
tmem143	-3,21	0,05
oasl2	7,12	0,00
zfp146	7,44	0,00
pde3b	-3,08	0,05
mastl	-5,52	0,00
krt71	-5,83	0,03
armcx6	2,98	0,04
av051173	-6,17	0,03
rnase12	-6,67	0,01
zfp345	5,94	0,04
trib3	6,70	0,01

rnf186	6,57	0,00
slc22a15	-5,31	0,01
col6a2	5,83	0,03
cntd1	-5,74	0,05
hephl1	-6,67	0,02
tdrd7	-5,52	0,05
adora1	-4,21	0,03
axl	5,94	0,03
e130008d07rik	-5,74	0,05
f13b	-5,83	0,03
wdr35	-4,29	0,02
kcna2	4,81	0,02
mageb3	6,92	0,01
usp46	-8,56	0,00
xirp1	6,58	0,02
scml4	-4,03	0,05
1700063d05rik	5,83	0,05
tubb4a	-5,74	0,04
slc25a35	-5,03	0,01
spg11	-6,21	0,00
efna1	-7,34	0,00
zfp280b	-3,91	0,02
unc5c	5,83	0,05
slc6a15	-6,38	0,02
st8sia6	-5,31	0,01
lig4	-6,96	0,00
cstad	-7,04	0,01
tmprss11d	-5,83	0,04
lrrn3	-8,06	0,00
cd302	6,64	0,01
fmn2	6,29	0,02
fancb	-9,10	0,00
f8	-7,16	0,01
nckap5	-6,01	0,03
myo5a	-3,29	0,04
2210009g21rik	-7,55	0,00
atp8b3	-5,63	0,04
rtkn2	4,73	0,02
gab3	-5,63	0,04
dsc3	-7,04	0,01
dok4	7,64	0,00
ttll3	-7,00	0,01
fnbp1l	-5,52	0,01
bc030336	-3,41	0,05
tiam2	-6,44	0,02
cd209a	7,28	0,01

col5a3	-5,93	0,03
g630016d24rik	-6,01	0,02
luzp2	5,57	0,00
zfp445	-3,62	0,05
zfp318	-5,13	0,01
serpinb9	6,34	0,00
phf1	-5,65	0,00
cml5	-5,52	0,04
apol9a	-6,17	0,02
d830013o20rik	-5,52	0,04
kpna2	-8,06	0,00
per2	-7,20	0,00
dbndd2	-4,45	0,02
c230035i16rik	7,57	0,00
tgs1	-4,50	0,01
uba3	-6,59	0,00
magee1	-6,67	0,00
plxnb3	-6,72	0,01
slfn1	-6,91	0,01
trip10	-4,86	0,01
fstl1	8,65	0,00
nhsl1	-7,30	0,00
pomt2	-7,93	0,00
zscan12	-6,31	0,03
engase	-7,08	0,01
gucy1a2	8,11	0,00
sun3	7,78	0,00
dpep3	5,94	0,04
fgf15	8,28	0,00
gm20408	-6,24	0,02
cdh12	3,46	0,04
c530008m17rik	-6,50	0,02
5033406o09rik	3,92	0,01
rlbp1	-4,26	0,04
mir5104	5,60	0,04
mlf1	-8,87	0,00
ttc23	-8,12	0,00
pcdhb21	-6,09	0,02
ahcyl2	-4,65	0,01
kcnn3	-4,32	0,03
lrrc47	-4,59	0,03
npdc1	7,64	0,00
ccdc68	6,51	0,01
col4a4	-7,99	0,00
fsd1l	-8,70	0,00
dcaf12l1	-6,24	0,03

1700081h04rik	-5,74	0,03
zfp473	-5,63	0,01
b230217c12rik	-4,28	0,01
bnc2	7,51	0,00
1700001l05rik	-7,30	0,01
gm5129	6,51	0,01
ncrna00086	4,16	0,03
2200002j24rik	-6,91	0,01
mpzl3	7,51	0,00
zfp418	7,51	0,00
c2	-6,24	0,03
osbpl5	-3,67	0,04
eml5	-8,99	0,00
ppap2b	-7,12	0,01
paqr4	-7,37	0,01
fam196a	-6,38	0,01
ercc6	-6,61	0,00
ccrl2	-3,86	0,05
ric3	-6,44	0,02
ccdc157	3,86	0,03
utp14b	-4,35	0,02
l1cam	-7,43	0,00
gen1	-7,30	0,01
fam69b	-5,63	0,04
zfp943	-8,97	0,00
arl4d	-7,16	0,00
rbp7	-6,72	0,01
xirp2	-6,24	0,02
srxn1	-3,97	0,04
1700025g04rik	-4,07	0,02
slc25a36	-8,40	0,00
adh6a	-7,99	0,00
nckipsd	-4,72	0,01
popdc3	6,70	0,02
kcnab1	6,21	0,02
atp13a4	-6,31	0,02
kdm4d	6,75	0,00
zfp280c	6,29	0,02
1700009j07rik	-6,44	0,01
5430411k18rik	4,07	0,02
ceacam13	6,51	0,02
gtf2ird2	-3,89	0,03
9130011e15rik	-8,76	0,00
lrrn4	-6,09	0,02
prrx1	-5,52	0,04
cntn5	-6,91	0,01

slc18a2	-7,40	0,01
gm9897	-5,20	0,01
lair1	8,94	0,00
adnp2	-4,34	0,02
2010106e10rik	-6,91	0,01
igll1	6,21	0,03
1700022p22rik	5,94	0,03
d3ertd254e	4,82	0,01
ttll4	-3,69	0,03
rlf	-8,48	0,00
gm10248	-8,58	0,00
2410004p03rik	7,44	0,00
hfm1	5,94	0,04
zfp820	-5,74	0,05
hspb6	-3,34	0,03
sipa1l3	-7,46	0,00
fhl2	-5,63	0,04
hibch	-4,60	0,01
ttc21b	-3,91	0,03
chst1	-6,17	0,03
9330182l06rik	-4,37	0,03
parp12	6,37	0,02
lass6	-6,08	0,00
kynu	-8,69	0,00
golga7b	6,21	0,03
klhl8	-6,24	0,02
stap2	-7,72	0,00
mmaa	4,63	0,02
chrm1	6,37	0,02
sst	-5,52	0,04
mefv	5,83	0,05
apol9b	-4,41	0,03
smok2a	4,78	0,03
bc006965	-6,09	0,02
itgb6	-7,77	0,00
sirpa	-3,78	0,03
kbtbd8	-4,35	0,03
tbx6	-6,87	0,01
susd2	-7,49	0,00
sync	-5,74	0,05
fndc7	7,28	0,01
spon1	6,64	0,01
pgbd1	7,20	0,00
ly6g5b	6,40	0,00
hnf4a	-7,49	0,00
gbp7	-5,40	0,00

4930455b14rik	-6,17	0,02
olfr957	5,83	0,03
i830012o16rik	-6,09	0,02
kl	-5,93	0,03
4632428n05rik	-3,98	0,03
6720489n17rik	-6,18	0,00
ngef	8,09	0,00
cdh13	9,07	0,00
cend1	-6,62	0,01
etd	5,94	0,04
fam20c	-6,77	0,01
tnnt3	3,03	0,05
klhl14	-4,35	0,02
naip5	-6,87	0,01
cntnap5a	-5,63	0,04
zfat	-9,02	0,00
kif13b	-6,87	0,01
rasef	5,83	0,03
zfyve16	-8,40	0,00
osr2	-7,74	0,00
col4a5	5,60	0,05
veph1	-5,74	0,05
ifi203	3,23	0,03
suv39h2	6,76	0,01
dcaf12l2	-6,17	0,02
ldlrap1	-7,81	0,00
zfp474	-6,09	0,02
fam169a	5,46	0,01
nrn1	-7,12	0,00
hbb-bh1	-10,62	0,00
haus6	-4,44	0,02
krt18	-3,96	0,02
ptchd1	-4,63	0,03
wbscr17	-6,56	0,01
ednrb	-8,37	0,00
eno3	3,86	0,01
zfp518a	-3,90	0,03
dll1	8,74	0,00
ubash3a	9,14	0,00
2010107g23rik	4,78	0,02
llgl2	-6,96	0,01
paqr5	-6,72	0,01
creb3l1	5,72	0,03
heatr3	-3,86	0,03
2310068j16rik	4,68	0,03
gpr37l1	-5,52	0,04

siglec1	6,29	0,02
vmn1r228	7,50	0,00
ugt1a1	-5,74	0,05
pgm2l1	-6,82	0,01
angel1	-9,11	0,00
tmem184a	-6,56	0,01
aard	7,36	0,01
zfp697	-5,74	0,04
sowahc	-7,30	0,01
bmp4	7,51	0,00
grin2a	7,47	0,01
atp13a5	-5,93	0,04
d630032n06rik	-4,75	0,02
rps18	-5,96	0,00
ceacam14	7,78	0,00
gm4636	-4,65	0,01
aqp8	-7,46	0,00
slc22a21	-6,09	0,02
gjd4	7,40	0,01
fam23a	-5,83	0,04
ppp1r9a	5,94	0,04
ifih1	8,88	0,00
pcdh12	-6,01	0,04
cdc14a	-3,82	0,04
atp8b5	6,03	0,04
cdk12	-3,70	0,03
4732491k20rik	6,21	0,02
fam122b	-8,19	0,00
d630039a03rik	-6,31	0,03
dppa2	-5,74	0,03
olfr1201	8,09	0,00
zfp248	-9,23	0,00
cdkl1	-3,86	0,02
gpd1	-8,38	0,00
fam70a	-4,46	0,03
polr3b	-3,89	0,03
1190007f08rik	-5,52	0,04
olfr862	-6,38	0,01
gdpd1	-4,74	0,01
sdc1	-5,63	0,04
fyco1	-4,50	0,02
vmn1r184	-7,23	0,01
kif5c	-7,77	0,00
smok2b	-6,91	0,01
zfp101	-5,63	0,01
prl7a2	-5,83	0,04

ddx10	-6,84	0,00
gpr55	-5,52	0,04
ppt2	-7,97	0,00
pyroxd1	-8,37	0,00
2610020h08rik	-8,87	0,00
slc44a5	-5,83	0,03
vasn	3,99	0,03
cldn12	4,90	0,01
zdhhc17	-5,75	0,00
ai428936	6,51	0,02
gdap10	-6,38	0,01
c130060k24rik	5,83	0,05
smarca2	-5,59	0,00
dlgap1	8,30	0,00
cep76	-6,31	0,02
slfn3	-5,74	0,03
zfp60	-4,61	0,01
ace2	-6,50	0,01
lrrc25	-5,63	0,04
plk1s1	-8,82	0,00
capn9	-5,74	0,03
phf13	-7,23	0,01
gbp8	5,35	0,00
catsper3	-5,52	0,04
msh3	-8,98	0,00
olfr958	-6,62	0,01
pde1a	-5,93	0,03
sh2d2a	-5,67	0,00
pign	-4,12	0,03
zfp451	-3,60	0,04
acadsb	-6,24	0,02
1700048o20rik	3,32	0,03
zbtb26	-8,49	0,00
sec14l2	-7,16	0,00
ttpa	-7,30	0,00
tbc1d13	-3,14	0,04
gm13031	5,72	0,03
art2a-ps	6,82	0,01
eif5b	-3,78	0,03
tmem87a	-3,53	0,04
ddo	7,44	0,00
pdp1	-7,84	0,00
tprg	-5,93	0,03
spink6	6,21	0,03
ccdc135	-5,63	0,04
pbx1	-5,80	0,00

bc052040	-6,22	0,00
app	3,63	0,04
fam132b	3,55	0,05
ifi204	-6,31	0,02
slc16a13	6,58	0,01
rhpn2	-7,95	0,00
rnase1	-6,31	0,02
slc2a13	6,03	0,03
zkscan1	3,51	0,02
piwil1	-7,23	0,00
wdr93	-7,00	0,01
asb2	3,00	0,05
yod1	-9,02	0,00
tdo2	5,89	0,01
avpi1	7,36	0,00
chst14	-6,77	0,01
epb4.1l3	-8,66	0,00
zfp873	5,04	0,00
phf21b	-6,01	0,03
wdr38	-5,93	0,03
mageh1	-7,64	0,00
rdh9	8,90	0,00
1700016c15rik	7,24	0,01
robo3	7,28	0,01
gpr113	5,72	0,03
9230112d13rik	-6,31	0,02
gm7538	6,92	0,01
5830416i19rik	-6,01	0,03
zfp945	-7,55	0,00
atp12a	6,51	0,02
ehf	-6,82	0,01
capsl	6,44	0,01
sorbs1	-3,42	0,04
ugt3a1	6,37	0,02
4930578m01rik	-5,74	0,04
xylb	-3,30	0,04
maml2	-6,06	0,00
tmtc4	-6,09	0,03
hhat	7,24	0,01
adipoq	-6,01	0,03
ar	-5,83	0,04
onecut2	-6,16	0,00
zbed6	-6,01	0,04
p2ry10	-3,77	0,04
notum	6,70	0,02
krt23	6,58	0,02

efcab5	-6,09	0,03
gatsl2	-6,56	0,02
nom1	-4,46	0,01
fam164a	-8,14	0,00
pex26	-5,83	0,04
acot4	-6,96	0,01
ctbs	7,44	0,00
larp1b	-6,96	0,01
calr3	-6,09	0,03
ccr1	-7,58	0,00
gprc5c	8,04	0,00
e130309f12rik	7,60	0,00
nr0b2	-6,50	0,01
sep-04	6,87	0,01
gopc	-4,41	0,01
bloc1s3	4,51	0,01
enox2	3,62	0,03
cdkl2	-7,69	0,00
2310014l17rik	-6,82	0,01
mcoln3	-7,04	0,01
epb4.1l4a	-6,38	0,02
clrn3	-8,49	0,00
pds5b	-3,19	0,04
gdpd2	-6,17	0,02
gm949	-5,93	0,04
pnliprp1	6,13	0,03
tmem198	-5,74	0,05
nhedc1	6,29	0,03
zfp647	-6,50	0,02
sh2d5	4,92	0,01
4930511m11rik	-5,63	0,04
a730090n16rik	-6,31	0,02
2210407c18rik	-3,74	0,04
sbk2	-6,38	0,01
dusp18	9,20	0,00
chrnb3	-6,31	0,02
caprin2	-6,45	0,00
fsip1	5,83	0,05
cldn13	-6,31	0,02
1600029o15rik	-3,97	0,04
gsdmc2	-6,09	0,02
zfp846	5,51	0,00
olfr1353	-6,72	0,01
4632415k11rik	-4,23	0,02
uba6	-6,24	0,00
zfp719	-4,55	0,01

bcl6b	-8,53	0,00
srl	5,68	0,01
ubd	3,60	0,02
2900056m20rik	-4,14	0,02
1700003e16rik	-5,83	0,03
hmgn2	-4,04	0,01
sh3gl3	7,54	0,00
opcml	8,84	0,00
st3gal1	-3,76	0,03
khnyn	-3,20	0,05
gm5108	5,72	0,03
gja8	-6,72	0,01
nmnat1	-4,86	0,02
6330409n04rik	8,72	0,00
mtap	-8,06	0,00
ttc26	4,43	0,01
ltbr	5,60	0,01
bag3	-8,65	0,00
gm13032	-5,93	0,03
josd1	-3,63	0,03
tsga10	-6,09	0,03
fbxl16	7,70	0,00
ptprf	5,89	0,01
lclat1	-7,00	0,00
pus10	-6,97	0,00
uevld	-8,26	0,00
rfx2	7,94	0,00
cyp4b1	7,20	0,01
nol8	-4,44	0,01
prl7d1	-5,74	0,05
tm7sf3	-3,23	0,05
kcng1	-6,17	0,02
cmpk2	-6,82	0,01
mid2	-6,44	0,02
trim15	-7,77	0,00
sema3b	-7,37	0,00
vwa3a	6,82	0,01
omd	5,04	0,02
xpo4	-6,17	0,03
c1rl	6,03	0,04
il28ra	-7,61	0,00
gjb2	7,97	0,00
gm129	-6,91	0,01
tchp	-7,55	0,00
bean1	-6,82	0,01
4933433g15rik	-6,17	0,02

p2ry1	7,44	0,01
ret	-3,44	0,05
uprt	-7,97	0,00
nts	-8,65	0,00
dock3	-6,62	0,01
tcam1	5,83	0,03
nexn	7,20	0,01
naa15	-6,25	0,00
d830005e20rik	-7,72	0,00
gchfr	-5,63	0,04
efna5	-4,21	0,03
emilin2	5,60	0,04
myl9	6,82	0,01
onecut3	6,15	0,00
ddhd1	-7,27	0,01
4930512b01rik	-5,83	0,04
hmox1	-4,43	0,02
bc022687	-6,82	0,01
oxsm	-4,59	0,02
vmn2r82	-5,93	0,03
acsl4	-4,72	0,01
dsel	-6,01	0,02
man2c1	-3,22	0,04
ankrd22	-5,52	0,04
spam1	5,83	0,04
ly6a	-5,35	0,00
d230030e09rik	-5,63	0,04
fam184a	6,37	0,02
bmi1	-4,21	0,01
gabpa	-6,50	0,00
sep-05	-6,72	0,01
tada2a	-4,83	0,01
rbm41	-6,56	0,00
tnfrsf12a	-4,15	0,03
epb4.1l4b	4,59	0,01
atl1	-5,74	0,05
zfp449	-7,30	0,01
a730036i17rik	-5,83	0,04
gm16516	-7,00	0,01
mapk8	-4,24	0,02
hemt1	-6,01	0,02
il10	3,65	0,03
1200009i06rik	-8,33	0,00
hmmr	-3,93	0,03
ceacam20	-3,29	0,05
4930458l03rik	-6,44	0,01

wdr67	-6,29	0,00
ube2q2	-6,77	0,01
ovol1	-4,51	0,02
4933430n04rik	4,83	0,03
gm2518	-4,15	0,04
bmpr1a	-8,10	0,00
nos1ap	-6,09	0,02
zfp182	-7,97	0,00
gm12886	-6,01	0,02
d130017n08rik	4,52	0,04
4930422g04rik	-4,70	0,01
spock2	-6,62	0,02
2610034b18rik	-4,68	0,02
aldh1a2	7,60	0,00
spag17	-5,83	0,04
abp1	5,20	0,00
acvr1b	-3,47	0,03
zim3	6,03	0,04
zfp799	-5,93	0,04
mcc	-6,17	0,03
fkbp5	-3,66	0,03
ccdc113	6,13	0,03
dhrs13	-3,64	0,05
fgfr3	8,24	0,00
akap17b	-7,34	0,00
pxt1	-6,67	0,01
sec14l4	-6,38	0,01
esrp2	-5,93	0,03
vgf	-5,52	0,04
tmod2	8,22	0,00
selm	-5,74	0,05
cdr2	4,14	0,01
il1r1	-5,63	0,04
rgs1	-8,33	0,00
zdhhc5	-3,38	0,04
klf3	-3,74	0,03
msln	-5,74	0,04
kcnq1ot1	-3,47	0,03
wdr16	6,76	0,01
slc26a2	-8,17	0,00
coil	-3,76	0,03
siglece	-4,55	0,02
zfp385b	6,29	0,03
e230019m04rik	-7,08	0,01
zscan20	-7,49	0,00
il12b	4,89	0,01

aadacl2	-6,09	0,03
meis1	7,51	0,00
cc2d2a	4,78	0,02
bco2	-5,52	0,05
olfr1056	-6,17	0,02
5830417i10rik	-5,83	0,03
tm7sf4	8,43	0,00
gm11545	-5,63	0,04
epb4.1l5	-3,07	0,05
serpind1	-6,09	0,03
cdh20	-6,17	0,02
naalad2	7,24	0,01
tmem55a	-5,36	0,01
braf	-6,89	0,00
sidt1	-6,09	0,02
myo3b	6,87	0,01
4732490b19rik	4,75	0,01
scfd2	-3,44	0,04
ehbp1	-7,23	0,01
klhl21	7,47	0,01
gm16023	-6,44	0,02
rapsn	5,60	0,04
sardh	-6,31	0,02
pglyrp2	4,23	0,03
ccdc76	-7,69	0,00
cyyr1	6,76	0,01
sgk1	3,40	0,03
cnnm2	-6,72	0,01
gm11696	-4,45	0,01
setbp1	-4,20	0,01
arsb	-6,09	0,03
kif21a	-5,93	0,04
zkscan16	8,36	0,00
mospd1	3,60	0,03
4931417g12rik	-7,12	0,01
car4	-5,63	0,04
dram1	-7,12	0,01
4930506m07rik	-7,93	0,00
fam164c	-6,38	0,01
il1b	-7,52	0,00
lyplal1	-6,44	0,01
mbd6	-3,89	0,02
zfp59	-6,24	0,03
napb	-6,62	0,01
mis12	-4,49	0,01
wdr44	-5,64	0,00

1700008j07rik	-6,01	0,02
4930528f23rik	7,78	0,00
gm1568	-5,89	0,00
tmem53	5,23	0,01
harbi1	-5,67	0,01
rab3d	5,34	0,00
narg2	-4,32	0,02
rgl1	-4,21	0,04
alpk2	-6,31	0,02
osbpl1a	-6,01	0,03
lilra5	9,23	0,00
vsig8	5,60	0,04
aox3	-5,74	0,04
parp16	-5,12	0,01
ppil4	-3,86	0,03
yap1	-6,01	0,03
sox12	-7,04	0,01
gdpd4	-5,52	0,04
4931430n09rik	-6,91	0,01
clca1	-7,08	0,01
clec7a	-7,84	0,00
gsdmc4	6,87	0,01
gm11602	-4,86	0,02
mtap2	-7,08	0,01
smarca5	-4,30	0,01
lingo2	5,83	0,03
tmem180	-7,69	0,00
sgms2	-4,03	0,04
mycs	6,76	0,01
rpgrip1	4,78	0,03
fgfbp3	7,73	0,00
astl	7,64	0,00
ush1c	-6,56	0,01
vmn1r45	8,41	0,00
rtp2	7,81	0,00
dync2li1	6,92	0,01
ak7	-6,67	0,01
tmem125	-7,66	0,00
sorcs3	-6,01	0,02
kctd11	-7,91	0,00
pcnxl2	-5,93	0,03
fcer1a	6,29	0,03
9530027j09rik	-6,09	0,03
mras	5,94	0,04
bc030870	-6,87	0,01
fam167a	4,84	0,02

prf1	8,36	0,00
gm15708	-6,34	0,00
lysmd2	6,76	0,01
golga3	-3,62	0,04
myh3	7,02	0,01
wdr17	-6,17	0,02
steap1	6,29	0,03
pkd1	-4,22	0,01
nuak1	-6,09	0,02
aim1	-4,28	0,02
xylt2	-7,04	0,01
als2cl	-6,01	0,02
pafah2	-8,10	0,00
usp28	-3,13	0,05
oosp1	-6,24	0,03
1700028k03rik	-5,74	0,04
nfib	-6,01	0,03
wdr96	4,14	0,03
iqck	-6,82	0,01
igsf11	6,29	0,03
ntn4	6,29	0,03
fbp1	-3,94	0,04
ap4e1	-5,15	0,01
asb5	3,52	0,04
gm20098	6,13	0,03
4930527f14rik	5,83	0,05
thy1	-5,96	0,00
sema3d	-5,63	0,04
arl11	7,36	0,00
zbtb33	-6,56	0,00
2610316d01rik	-6,24	0,03
hcn1	-6,17	0,03
lrrtm4	-6,01	0,04
zfp948	7,84	0,00
d630045j12rik	8,13	0,00
ptch1	-5,83	0,04
gm3414	-4,03	0,04
actr3b	-4,21	0,04
il18bp	3,15	0,04
vmn2r112	6,29	0,03
mipol1	-4,83	0,02
tmem225	8,02	0,00
zeb1	-5,98	0,00
acp2	-8,19	0,00
9330151l19rik	-6,24	0,03
gm17762	8,02	0,00

vmn2r84	5,94	0,04
slc7a15	-7,52	0,00
kdelc1	-5,63	0,04
pard3	-5,74	0,03
dach1	6,51	0,02
kcnb2	7,28	0,01
tmem54	-6,31	0,02
tmem30b	-6,31	0,03
dlg4	-6,67	0,02
map3k10	4,58	0,04
ctps2	-3,35	0,05
oog3	7,07	0,01
cdkl5	6,76	0,01
resp18	-6,31	0,02
dbpht2	6,98	0,01
prss39	6,92	0,01
ccnb1ip1	-3,39	0,04
casc4	-7,81	0,00
tmem38a	6,04	0,00
rasl10a	-6,17	0,03
trim45	8,20	0,00
ctnna1	-3,46	0,02
camsap2	-4,04	0,03
cpeb1	4,00	0,04
4930529f22rik	-5,52	0,04
ttc8	-5,09	0,01
ang4	-5,63	0,04
gfpt1	-6,35	0,00
gm12216	-4,15	0,03
hc	-6,38	0,02
plekhg6	-6,77	0,01
zscan18	-6,01	0,04
itga1	8,30	0,00
pmel	-5,93	0,03
lrrc29	-5,77	0,00
dpp4	-5,48	0,00
nrbp2	-6,77	0,01
abcb9	7,07	0,01
kif18a	-9,86	0,00
kctd4	-6,38	0,01
a230073k19rik	5,70	0,00
fkbp7	-7,00	0,01
mphosph8	-4,06	0,02
aa986860	-7,30	0,01
bod1	-6,67	0,01
adora2b	-4,15	0,03

slc30a1	-6,44	0,02
cdhr2	-5,71	0,00
sprr2j-ps	-5,93	0,03
ulk2	-5,17	0,01
olfr127	7,44	0,01
rpl29	-4,51	0,02
ccdc30	-7,16	0,01
b130006d01rik	-6,17	0,03
cdk6	-4,79	0,02
lxn	-9,76	0,00
golga4	-5,48	0,01
myh4	7,02	0,01
cxcr3	-7,77	0,00
stag3	-8,14	0,00
slc26a4	6,58	0,02
rapgef5	-6,91	0,01
steap2	5,30	0,01
rep15	-6,31	0,02
pkd2	-6,56	0,02
hist2h3c1	-7,08	0,01
pla1a	3,93	0,02
strn	-5,10	0,01
olfr894	-5,83	0,04
slc2a2	-7,79	0,00
gucy1b2	8,57	0,00
slc25a18	-6,17	0,02
ccdc162	-6,09	0,03
abcc3	6,13	0,02
plcg1	-7,81	0,00
gm10509	-6,82	0,01
gramd1c	-5,23	0,01
jmy	7,20	0,01
mr1	7,60	0,00
mmgt1	-5,43	0,01
3110047p20rik	-6,31	0,02
olfr131	7,16	0,01
a530088e08rik	-4,93	0,02
mtmr1	-3,98	0,03
zfp955a	5,73	0,00
parvb	7,28	0,00
mcph1	-3,48	0,03
zfp37	-6,96	0,01
dock6	-3,82	0,04
ccdc78	4,40	0,01
zfp157	-3,29	0,04
rnf32	-7,66	0,00

gnb3	-6,01	0,04
gxylt2	5,46	0,05
fam120c	-4,67	0,01
zeb2	-6,67	0,01
gm9159	6,21	0,03
gas2l1	6,44	0,02
vash1	6,76	0,01
ihh	-6,72	0,01
a330040f15rik	6,29	0,02
nln	-5,81	0,00
b230323a14rik	-5,93	0,03
efcab9	-6,17	0,03
4930478p22rik	-5,63	0,04
prss16	5,54	0,01
rims1	6,37	0,02
hoxa3	-8,10	0,00
zfp428	-6,56	0,02
tmem178	5,46	0,05
dus4l	-4,15	0,02
alg10b	-3,50	0,05
pde6g	-6,17	0,02
a430033k04rik	-3,85	0,04
dlg5	-4,52	0,01
olfr1206	8,11	0,00
fpgt	-9,27	0,00
1700095a21rik	-5,52	0,04
lamc1	-4,49	0,02
ano10	-3,53	0,02
kcnj2	-5,93	0,03
mn1	-6,67	0,01
bc037704	-5,31	0,01
hhip	-6,17	0,03
lipt1	-8,06	0,00
trim46	-6,72	0,01
megf9	8,78	0,00
nlrp6	-7,20	0,01
mypn	5,94	0,04
4930430f08rik	-6,38	0,02
alg6	-4,00	0,02
c030016d13rik	5,46	0,05
tmem120b	4,45	0,01
kalrn	-3,87	0,02
1500009c09rik	-6,82	0,01
apod	-6,09	0,02
gpr83	-6,77	0,01
1700125g22rik	4,08	0,05

gfpt2	-7,34	0,01
ttc23l	6,03	0,04
ppp1r2-ps7	9,04	0,00
extl1	-7,04	0,01
hnf4g	-5,63	0,04
ccdc116	-7,04	0,01
wrn	-8,44	0,00
mphosph9	-5,37	0,00
fa2h	-6,38	0,02
dnajc25	-6,09	0,02
6430573f11rik	6,70	0,02
1810014b01rik	-4,32	0,01
zfp110	-3,13	0,04
akr1b7	4,52	0,01
fam187b	-4,59	0,02
lphn1	-7,49	0,00
6030422m02rik	-6,50	0,02
treml4	7,84	0,00
mib2	6,58	0,02
lrig1	-5,26	0,01
tsga14	-3,21	0,04
siglech	6,29	0,02
dgkq	-6,91	0,01
nxn	-4,46	0,03
apaf1	-5,49	0,00
plekhh1	7,32	0,01
cttnbp2nl	5,83	0,03
atg14	-4,26	0,02
6430531b16rik	-6,17	0,02
elavl2	-5,54	0,00
zfp14	-7,49	0,00
ptpn14	-7,52	0,00
scn3a	6,69	0,00
rbak	5,68	0,00
ddx43	3,59	0,04
asb7	-7,37	0,00
lin7a	-8,32	0,00
1700109h08rik	-5,74	0,05
olfr1258	-6,31	0,03
acad12	-3,65	0,04
cep135	-5,59	0,01
igsf9	-4,90	0,01
cd80	-6,09	0,02
akr1c14	-6,77	0,01
rcan1	-7,64	0,00
anxa3	-5,20	0,01

2010002m12rik	-7,12	0,01
a130049a11rik	-6,50	0,01
zfp955b	-5,31	0,01
gli3	6,82	0,01
sdr42e1	-7,61	0,00
scn11a	3,68	0,04
faah	-5,05	0,01
gm16897	-7,20	0,00
pygl	-5,83	0,03
oit1	-7,00	0,01
osgin1	-3,74	0,03
dnajb7	-5,83	0,03
atg4c	-7,95	0,00
slco1a4	-5,74	0,03
smc2	-3,78	0,03
car7	-6,91	0,01
slc25a23	-6,96	0,01
rims2	4,98	0,01
2310047b19rik	3,92	0,03
neu3	-8,15	0,00
kdm3a	-6,12	0,00
4930448c13rik	6,58	0,02
rpusd2	-3,94	0,03
fert2	-6,20	0,00
d030045p18rik	-5,93	0,03
gm6377	-8,65	0,00
nudcd1	-4,85	0,00
e230029c05rik	-5,93	0,03
poc1b	-4,67	0,01
arrb1	-4,43	0,01
ift88	-7,40	0,01
slc27a5	-6,44	0,01
mtus1	-6,62	0,01
c87977	8,07	0,00
efnb3	-6,96	0,01
vmn1r24	-6,72	0,01
pex5	-6,52	0,00
4930487h11rik	-6,38	0,01
myo15	-6,38	0,01
st14	-3,00	0,05
pla2g4c	-5,63	0,04
ocln	-7,88	0,00
sema6d	-5,74	0,05
clca4	-6,31	0,02
rab36	-4,02	0,03
tmcc1	-3,52	0,05

tbk1	-3,76	0,04
pgr15l	-6,62	0,01
gpr84	4,73	0,03
itga3	4,03	0,05
fcho2	-4,20	0,03
gabrb2	-7,00	0,01
extl2	-5,31	0,01
1700067k01rik	-6,24	0,03
hsd17b13	7,54	0,00
cdc42bpa	-6,56	0,01
rab4a	-6,09	0,02
9330159f19rik	-6,67	0,02
cdkn2b	-6,62	0,01
polk	-7,66	0,00
agt	-6,01	0,02
sfxn4	-3,89	0,02
gm9833	-6,09	0,03
1300015d01rik	7,51	0,00
slc22a8	-5,93	0,04
xrcc2	-8,33	0,00
cdx1	4,55	0,02
rps6kc1	-3,73	0,04
b3gat2	7,67	0,00
mbnl1	-3,32	0,04
ulk4	-4,86	0,02
abca1	-4,77	0,01
pcgf3	-8,35	0,00
zfp783	-8,48	0,00
tlcd1	-7,40	0,01
lphn2	3,54	0,02
gml	6,37	0,01
rgs5	-5,52	0,04
rnf144a	3,40	0,04
cldn22	7,32	0,01
lipo1	-7,61	0,00
adcy8	-3,84	0,05
slc26a6	-3,62	0,03
nradd	-4,21	0,04
cfi	5,72	0,03
rbm18	-5,76	0,00
mmrn2	6,64	0,02
3200001d21rik	7,40	0,00
frmd7	4,20	0,02
kremen2	7,32	0,01
adam34	7,02	0,01
cyp2t4	3,67	0,02

gm16548	-5,83	0,03
fbxo47	-6,50	0,01
lrrc16a	6,98	0,01
fam135a	-6,37	0,00
ccbl2	-5,63	0,04
slc4a3	4,40	0,03
bbs7	-7,23	0,01
tyrp1	-6,17	0,02
arhgap5	-7,72	0,00
gpr174	-4,60	0,02
fbln1	-3,27	0,04
1110017d15rik	6,37	0,02
chm	-7,77	0,00
id1	-7,12	0,01
hrh1	-8,02	0,00
hs2st1	5,72	0,04
klhl25	-7,20	0,01
clgn	-5,63	0,04
mblac1	3,00	0,05
darc	-6,31	0,02
zfyve1	-3,78	0,03
timp2	5,83	0,03
gm5069	-5,93	0,03
osgin2	-5,01	0,01
yy2	-9,79	0,00
c5ar1	-7,43	0,01
a3galt2	3,25	0,05
shisa2	-6,09	0,02
rhoc	-3,48	0,03
gas2l3	-9,05	0,00
trpm5	-8,51	0,00
papd7	-5,69	0,00
thnsl1	-3,73	0,04
smc3	-4,14	0,02
car8	8,88	0,00
h2-t3	-4,49	0,01
4933408b17rik	6,37	0,02
figla	5,94	0,04
sntb1	6,13	0,03
2210417k05rik	-6,62	0,02
catsperg1	6,13	0,03
dbn1	-3,81	0,03
2010109a12rik	-6,01	0,02
plcb2	-6,67	0,01
tnfrsf26	-2,95	0,04
sema4a	-6,17	0,03

antxr2	5,24	0,00
lgr6	4,52	0,04
nrip1	-4,35	0,01
map3k13	6,45	0,00
gm12250	-3,60	0,03
pcdh9	-5,74	0,03
slc27a6	6,44	0,02
gm16576	-6,87	0,01
tctex1d1	5,94	0,04
olfm4	6,52	0,00
txlng	-6,17	0,03
ascl2	-5,63	0,04
spn	-6,77	0,01
taf1	-6,31	0,00
uaca	7,70	0,00
grin3b	-7,20	0,01
il15	-7,27	0,00
mapkbp1	6,44	0,02
bcl9	-7,40	0,01
thsd7a	-6,96	0,01
fn3krp	-7,27	0,00
4930430d24rik	6,76	0,01
bc051142	-7,08	0,01
srr	-5,83	0,04
mmp11	3,85	0,02
tbc1d2	-4,37	0,02
rg9mtd1	-7,48	0,00
agphd1	-7,00	0,01
socs5	3,20	0,03
aldh1a7	-6,67	0,02
laptm4b	-3,92	0,05
cdc42bpb	-6,24	0,03
atoh1	6,03	0,04
olfr1212	-6,38	0,02
arhgap22	-5,74	0,04
lman2l	-5,76	0,00
gm16998	6,37	0,01
cyp2c65	-5,12	0,01
casd1	-4,40	0,02
mrvi1	-5,93	0,03
zfp458	-8,40	0,00
gm10785	-5,15	0,01

Annex 2. Genes changed upon miR-28 expression in BL cells versus Scrambled control BL cells

Gene ID	hgnc_symbol	logFC	P.Value
ENSG00000207651	MIR28	10,211	1,95E-39
ENSG00000129128	SPCS3	-0,877	2,38E-17
ENSG00000116044	NFE2L2	-0,567	2,45E-09
ENSG00000132846	ZBED3	-0,604	1,32E-06
ENSG00000136111	TBC1D4	0,693	1,35E-06
ENSG00000172995	ARPP21	1,405	2,47E-06
ENSG00000198888	MT-ND1	-0,611	3,38E-06
ENSG00000123472	ATPAF1	-0,474	1,38E-05
ENSG00000198886	MT-ND4	-0,524	1,66E-05
ENSG00000198763	MT-ND2	-0,520	2,19E-05
ENSG00000114026	OGG1	0,547	2,61E-05
ENSG00000198727	MT-CYB	-0,483	3,10E-05
ENSG00000212907	MT-ND4L	-0,487	3,16E-05
ENSG00000225630	MTND2P28	-0,542	3,27E-05
ENSG00000248527	MTATP6P1	-0,437	3,43E-05
ENSG00000110934	BIN2	-0,459	4,01E-05
ENSG00000228253	MT-ATP8	-0,453	4,11E-05
ENSG00000124813	RUNX2	1,168	4,60E-05
ENSG00000175567	UCP2	0,800	6,90E-05
ENSG00000198899	MT-ATP6	-0,435	7,00E-05
ENSG00000169136	ATF5	-0,672	8,79E-05
ENSG00000134109	EDEM1	-0,421	9,98E-05
ENSG00000105639	JAK3	-0,859	1,04E-04
ENSG00000237973	MIR6723	-0,578	1,08E-04
ENSG00000026103	FAS	-0,562	1,20E-04
ENSG00000163947	ARHGEF3	1,048	1,23E-04
ENSG00000211898	IGHD	0,954	1,30E-04
ENSG00000198712	MT-CO2	-0,450	1,50E-04
ENSG00000198208	RPS6KL1	-0,785	1,67E-04
ENSG00000119042	SATB2	0,563	1,69E-04
ENSG00000226849		-1,360	1,85E-04
ENSG00000166822	TMEM170A	-0,374	1,88E-04
ENSG00000131471	AOC3	-0,568	1,99E-04
ENSG00000048052	HDAC9	0,578	2,08E-04
ENSG00000176771	NCKAP5	-1,245	2,23E-04
ENSG00000198938	MT-CO3	-0,408	2,45E-04
ENSG00000120896	SORBS3	-0,915	2,48E-04
ENSG00000237296	SMG1P1	0,408	2,52E-04
ENSG00000120889	TNFRSF10B	-0,452	2,85E-04
ENSG00000125834	STK35	-0,393	2,92E-04
ENSG00000187699	C2orf88	0,457	3,03E-04
ENSG00000146072	TNFRSF21	1,042	3,11E-04

ENSG00000271699		0,486	3,13E-04
ENSG00000054654	SYNE2	0,415	3,23E-04
ENSG00000142798	HSPG2	0,386	3,32E-04
ENSG00000236152	MRPS36P1	-1,526	3,71E-04
ENSG00000267426		-1,242	3,71E-04
ENSG00000117461	PIK3R3	0,512	3,81E-04
ENSG00000127666	TICAM1	0,396	4,09E-04
ENSG00000117091	CD48	0,504	4,23E-04
ENSG00000232573	RPL3P4	1,075	4,32E-04
ENSG00000106348	IMPDH1	-0,342	4,46E-04
ENSG00000029364	SLC39A9	-0,404	4,84E-04
ENSG00000198804	MT-CO1	-0,440	4,89E-04
ENSG00000205307	SAP25	-0,916	4,92E-04
ENSG00000161011	SQSTM1	-0,417	5,09E-04
ENSG00000131153	GINS2	0,497	5,23E-04
ENSG00000160796	NBEAL2	-0,407	5,29E-04
ENSG00000197063	MAFG	-0,578	5,43E-04
ENSG00000182836	PLCXD3	0,619	5,61E-04
ENSG00000211772	TRBC2	0,508	5,62E-04
ENSG00000138778	CENPE	0,392	5,85E-04
ENSG00000141441	GAREM	0,537	5,88E-04
ENSG00000133739	LRRCC1	0,577	5,97E-04
ENSG00000185215	TNFAIP2	-0,821	6,07E-04
ENSG00000111247	RAD51AP1	0,475	6,39E-04
ENSG00000123453	SARDH	0,525	6,39E-04
ENSG00000145907	G3BP1	-0,392	6,68E-04
ENSG00000210082	MT-RNR2	-0,499	6,69E-04
ENSG00000235174	RPL39P3	-3,205	6,93E-04
ENSG00000267368	UPK3BL	-0,762	7,12E-04
ENSG00000256043	CTSO	-0,592	7,37E-04
ENSG00000165304	MELK	0,402	7,49E-04
ENSG00000163312	HELQ	0,463	7,52E-04
ENSG00000160326	SLC2A6	0,431	7,90E-04
ENSG00000116514	RNF19B	0,340	8,00E-04
ENSG00000128886	ELL3	0,500	8,04E-04
ENSG00000210112	MT-TM	-0,988	8,07E-04
ENSG00000157734	SNX22	0,532	8,65E-04
ENSG00000182718	ANXA2	-0,359	8,80E-04
ENSG00000198858	R3HDM4	-0,315	8,86E-04
ENSG00000001167	NFYA	-0,460	9,21E-04
ENSG00000165092	ALDH1A1	-1,258	9,33E-04
ENSG00000008300	CELSR3	-0,484	9,41E-04
ENSG00000110427	KIAA1549L	0,473	9,66E-04
ENSG00000157764	BRAF	-0,340	9,72E-04
ENSG00000188277	C15orf62	-0,690	1,00E-03

ENSG00000071794	HLTF	0,418	1,01E-03
ENSG00000104936	FOSB	-0,482	1,02E-03
ENSG00000186472	PCLO	0,514	1,04E-03
ENSG00000258947		0,435	1,07E-03
ENSG00000113070	HBEGF	0,785	1,09E-03
ENSG00000186716	BCR	0,371	1,09E-03
ENSG00000177409	SAMD9L	-0,472	1,11E-03
ENSG00000147234	FRMPD3	0,500	1,15E-03
ENSG00000072778	ACADVL	-0,361	1,15E-03
ENSG00000180834	MAP6D1	0,579	1,16E-03
ENSG00000134602	RBM4B	-0,310	1,17E-03
ENSG00000168078	PBK	0,395	1,18E-03
ENSG00000107938	EDRF1	0,554	1,23E-03
ENSG00000152332	UHMK1	-0,414	1,25E-03
ENSG00000108798	ABI3	0,591	1,29E-03
ENSG00000109805	NCAPG	0,382	1,37E-03
ENSG00000106479	ZNF862	-0,441	1,37E-03
ENSG00000164849	GPR146	0,598	1,39E-03
ENSG00000103647	CORO2B	0,862	1,45E-03
ENSG00000272410		-1,000	1,47E-03
ENSG00000186951	PPARA	-0,365	1,48E-03
ENSG00000150054	MPP7	0,398	1,52E-03
ENSG00000169100	SLC25A6	0,472	1,53E-03
ENSG00000167995	BEST1	-0,699	1,56E-03
ENSG00000136286	MYO1G	0,499	1,57E-03
ENSG00000198106	SNX29P2	0,366	1,60E-03
ENSG00000059145	UNKL	-0,411	1,60E-03
ENSG00000165905	GYLTL1B	0,877	1,62E-03
ENSG00000105613	MAST1	0,764	1,62E-03
ENSG00000152492	CCDC50	-0,644	1,68E-03
ENSG00000129048	ACKR4	0,460	1,70E-03
ENSG00000224420	ADM5	-0,666	1,70E-03
ENSG00000033170	FUT8	0,393	1,72E-03
ENSG00000108515	ENO3	-0,621	1,72E-03
ENSG00000198624	CCDC69	0,337	1,75E-03
ENSG00000184661	CDCA2	0,430	1,77E-03
ENSG00000090975	PITPNM2	0,364	1,78E-03
ENSG00000122224	LY9	-0,599	1,82E-03
ENSG00000074266	EED	0,326	1,87E-03
ENSG00000072571	HMMR	0,405	1,91E-03
ENSG00000092470	WDR76	0,522	1,93E-03
ENSG00000174428	GTF2IRD2B	-0,387	1,97E-03
ENSG00000198840	MT-ND3	-0,332	2,02E-03
ENSG00000213199	ASIC3	-0,775	2,04E-03
ENSG00000197746	PSAP	-0,303	2,06E-03

ENSG00000263528	IKBKE	0,409	2,12E-03
ENSG00000263136		0,450	2,13E-03
ENSG00000204681	GABBR1	-0,793	2,13E-03
ENSG00000183604	SMG1P5	0,363	2,15E-03
ENSG00000166326	TRIM44	-0,454	2,15E-03
ENSG00000209082	MT-TL1	-0,856	2,15E-03
ENSG00000024526	DEPDC1	0,342	2,17E-03
ENSG00000140848	CPNE2	0,380	2,20E-03
ENSG00000197747	S100A10	-0,494	2,21E-03
ENSG00000225373	WASH5P	-0,446	2,21E-03
ENSG00000198695	MT-ND6	-0,422	2,23E-03
ENSG00000126787	DLGAP5	0,389	2,24E-03
ENSG00000128274	A4GALT	0,349	2,25E-03
ENSG00000091592	NLRP1	-0,544	2,26E-03
ENSG00000100162	CENPM	0,438	2,29E-03
ENSG00000104972	PODNL1	0,559	2,34E-03
ENSG00000065308	TRAM2	-0,303	2,38E-03
ENSG00000243207	PPAN-P2RY11	-1,298	2,45E-03
ENSG00000107742	SPOCK2	-0,485	2,46E-03
ENSG00000196422	PPP1R26	-0,713	2,47E-03
ENSG00000147905	ZCCHC7	0,342	2,50E-03
ENSG00000121152	NCAPH	0,367	2,60E-03
ENSG00000114841	DNAH1	-0,990	2,73E-03
ENSG00000161939	RNASEK-C17orf49	-1,582	2,78E-03
ENSG00000198786	MT-ND5	-0,408	2,93E-03
ENSG00000228590		0,813	2,95E-03
ENSG00000163382	APOA1BP	0,372	2,95E-03
ENSG00000228716	DHFR	0,389	2,95E-03
ENSG00000157933	SKI	-0,428	2,98E-03
ENSG00000005844	ITGAL	0,396	3,00E-03
ENSG00000196517	SLC6A9	-0,310	3,05E-03
ENSG00000197385	ZNF860	0,563	3,05E-03
ENSG00000142347	MYO1F	-0,991	3,06E-03
ENSG00000108375	RNF43	0,311	3,08E-03
ENSG00000077150	NFKB2	-0,338	3,13E-03
ENSG00000118193	KIF14	0,340	3,15E-03
ENSG00000112308	C6orf62	-0,338	3,15E-03
ENSG00000148341	SH3GLB2	0,386	3,16E-03
ENSG00000136213	CHST12	0,803	3,18E-03
ENSG00000108984	MAP2K6	1,208	3,18E-03
ENSG00000114554	PLXNA1	-0,398	3,24E-03
ENSG00000128335	APOL2	-0,478	3,28E-03
ENSG00000114529	C3orf52	0,437	3,29E-03
ENSG00000160685	ZBTB7B	-0,358	3,29E-03
ENSG00000187210	GCNT1	0,367	3,31E-03

ENSG00000249319		-1,415	3,31E-03
ENSG00000269728		0,404	3,32E-03
ENSG00000144645	OSBPL10	0,374	3,40E-03
ENSG00000196189	SEMA4A	0,346	3,41E-03
ENSG00000130779	CLIP1	-0,370	3,41E-03
ENSG00000113448	DPYSL3	-0,949	3,42E-03
ENSG00000103249	CLCN7	-0,369	3,50E-03
ENSG00000197530	MIB2	-0,390	3,56E-03
ENSG00000213402	PTPRCAP	0,417	3,60E-03
ENSG00000061337	LZTS1	0,491	3,62E-03
ENSG00000187621	TCL6	0,447	3,68E-03
ENSG00000072310	SREBF1	-0,323	3,78E-03
ENSG00000149115	TNKS1BP1	-0,351	3,80E-03
ENSG00000168961	LGALS9	-0,793	3,86E-03
ENSG00000132359	RAP1GAP2	0,425	3,87E-03
ENSG00000182010	RTKN2	0,392	3,88E-03
ENSG00000139200	PIANP	0,652	3,91E-03
ENSG00000226958	RNA28S5	-0,406	3,96E-03
ENSG00000163618	CADPS	0,388	3,99E-03
ENSG00000160298	C21orf58	0,472	4,00E-03
ENSG00000166135	HIF1AN	-0,321	4,05E-03
ENSG00000100365	NCF4	0,416	4,05E-03
ENSG00000126003	PLAGL2	-0,320	4,12E-03
ENSG00000264558		-1,237	4,13E-03
ENSG00000068489	PRR11	0,405	4,17E-03
ENSG00000254413	CHKB-CPT1B	-0,501	4,27E-03
ENSG00000182087	TMEM259	-0,345	4,30E-03
ENSG00000079313	REXO1	-0,305	4,31E-03
ENSG00000188486	H2AFX	0,343	4,37E-03
ENSG00000095397	DFNB31	-0,691	4,41E-03
ENSG00000149970	CNKSR2	0,551	4,42E-03
ENSG00000130589	HELZ2	-0,426	4,44E-03
ENSG00000156471	PTDSS1	0,376	4,45E-03
ENSG00000134215	VAV3	-0,487	4,45E-03
ENSG00000134057	CCNB1	0,338	4,49E-03
ENSG00000182986	ZNF320	-0,551	4,52E-03
ENSG00000226029		-0,864	4,59E-03
ENSG00000166803	KIAA0101	0,489	4,67E-03
ENSG00000131778	CHD1L	0,382	4,73E-03
ENSG00000239219		0,579	4,74E-03
ENSG00000051341	POLQ	0,346	4,84E-03
ENSG00000114450	GNB4	0,362	4,86E-03
ENSG00000204946	ZNF783	-0,522	4,88E-03
ENSG00000149054	ZNF215	0,404	4,88E-03
ENSG00000250506	CDK3	-0,740	4,92E-03

ENSG00000154229	PRKCA	0,323	5,02E-03
ENSG00000111445	RFC5	0,371	5,04E-03
ENSG00000211896	IGHG1	-0,820	5,04E-03
ENSG00000131462	TUBG1	0,391	5,07E-03
ENSG00000123360	PDE1B	-0,765	5,09E-03
ENSG00000062282	DGAT2	-0,533	5,21E-03
ENSG00000180867	PDIA3P1	-0,868	5,21E-03
ENSG00000198520	C1orf228	-0,805	5,23E-03
ENSG00000115677	HDLBP	-0,276	5,26E-03
ENSG00000225889		-0,463	5,27E-03
ENSG00000102760	RGCC	0,468	5,29E-03
ENSG00000083454	P2RX5	0,335	5,29E-03
ENSG00000169220	RGS14	0,420	5,32E-03
ENSG00000164916	FOXK1	-0,379	5,33E-03
ENSG00000184226	PCDH9	0,332	5,39E-03
ENSG00000182095	TNRC18	-0,362	5,40E-03
ENSG00000140534	TICRR	0,400	5,40E-03
ENSG00000139636	LMBR1L	-0,376	5,44E-03
ENSG00000215252	GOLGA8B	-0,389	5,45E-03
ENSG00000114346	ECT2	0,298	5,46E-03
ENSG00000179532	DNHD1	-0,391	5,47E-03
ENSG00000145979	TBC1D7	0,431	5,51E-03
ENSG00000242539		0,364	5,54E-03
ENSG00000238164		-0,537	5,57E-03
ENSG00000189057	FAM111B	0,333	5,59E-03
ENSG00000117724	CENPF	0,302	5,63E-03
ENSG00000142765	SYTL1	-0,408	5,63E-03
ENSG00000177542	SLC25A22	-0,312	5,64E-03
ENSG00000197256	KANK2	0,337	5,65E-03
ENSG00000262526		-1,939	5,72E-03
ENSG00000188985	DHFRP1	0,463	5,78E-03
ENSG00000149499	EML3	-0,313	5,79E-03
ENSG00000262728		0,789	5,81E-03
ENSG00000104413	ESRP1	-0,598	5,84E-03
ENSG00000028277	POU2F2	0,343	5,84E-03
ENSG00000276043	UHRF1	0,370	5,85E-03
ENSG00000011275	RNF216	-0,351	5,87E-03
ENSG00000163006	CCDC138	0,322	5,88E-03
ENSG00000042062	FAM65C	0,852	5,91E-03
ENSG00000148834	GSTO1	0,394	5,96E-03
ENSG00000104081	BMF	-0,341	6,03E-03
ENSG00000137135	ARHGEF39	0,515	6,04E-03
ENSG00000148773	MKI67	0,292	6,05E-03
ENSG00000111674	ENO2	-0,773	6,07E-03
ENSG00000164815	ORC5	0,294	6,08E-03

ENSG00000111665	CDCA3	0,362	6,09E-03
ENSG00000173991	TCAP	-0,895	6,16E-03
ENSG00000049541	RFC2	0,389	6,17E-03
ENSG00000242265	PEG10	0,368	6,20E-03
ENSG00000151725	CENPU	0,465	6,21E-03
ENSG00000088986	DYNLL1	-0,333	6,23E-03
ENSG00000160408	ST6GALNAC6	-0,380	6,25E-03
ENSG00000259772		0,468	6,32E-03
ENSG00000205542	TMSB4X	-0,285	6,32E-03
ENSG00000068137	PLEKHH3	0,485	6,38E-03
ENSG00000048471	SNX29	0,339	6,38E-03
ENSG00000112715	VEGFA	-0,310	6,39E-03
ENSG00000082641	NFE2L1	-0,289	6,43E-03
ENSG00000183137	CEP57L1	0,394	6,45E-03
ENSG00000274292		-0,839	6,48E-03
ENSG00000141956	PRDM15	0,361	6,48E-03
ENSG00000129173	E2F8	0,358	6,60E-03
ENSG00000079462	PAFAH1B3	0,584	6,61E-03
ENSG00000174371	EXO1	0,390	6,61E-03
ENSG00000111452	GPR133	0,420	6,64E-03
ENSG00000112293	GPLD1	0,335	6,65E-03
ENSG00000185963	BICD2	0,305	6,72E-03
ENSG00000112312	GMNN	0,330	6,73E-03
ENSG00000147535	PPAPDC1B	-0,368	6,77E-03
ENSG00000142583	SLC2A5	0,380	6,87E-03
ENSG00000244342	LINC00698	-1,011	6,96E-03
ENSG00000215769	MIR6080	-0,559	6,97E-03
ENSG00000127838	PNKD	0,362	6,99E-03
ENSG00000167900	TK1	0,444	7,03E-03
ENSG00000182158	CREB3L2	0,412	7,04E-03
ENSG00000100479	POLE2	0,520	7,05E-03
ENSG00000080839	RBL1	0,322	7,05E-03
ENSG00000196586	MYO6	-0,751	7,16E-03
ENSG00000164050	PLXNB1	-0,739	7,21E-03
ENSG00000137404	NRM	0,537	7,24E-03
ENSG00000140941	MAP1LC3B	-0,367	7,25E-03
ENSG00000014138	POLA2	0,486	7,30E-03
ENSG00000211897	IGHG3	-0,682	7,30E-03
ENSG00000142102	ATHL1	-0,636	7,33E-03
ENSG00000188070	C11orf95	-0,313	7,50E-03
ENSG00000244165	P2RY11	-0,522	7,51E-03
ENSG00000197774	EME2	-0,380	7,53E-03
ENSG00000092036	HAUS4	0,484	7,56E-03
ENSG00000152409	JMY	-0,371	7,60E-03
ENSG00000131480	AOC2	-0,649	7,67E-03

ENSG00000042980	ADAM28	-0,652	7,68E-03
ENSG00000182013	PNMAL1	0,318	7,72E-03
ENSG00000234769	WASH4P	-0,387	7,78E-03
ENSG00000205544	TMEM256	0,462	7,79E-03
ENSG00000106537	TSPAN13	0,607	7,80E-03
ENSG00000093009	CDC45	0,399	7,88E-03
ENSG00000035720	STAP1	0,299	7,91E-03
ENSG00000080986	NDC80	0,321	7,92E-03
ENSG00000157557	ETS2	-0,301	7,96E-03
ENSG00000196338	NLGN3	-0,950	8,00E-03
ENSG00000135740	SLC9A5	-0,869	8,06E-03
ENSG00000175782	SLC35E3	0,369	8,07E-03
ENSG00000078804	TP53INP2	-0,443	8,21E-03
ENSG00000146263	MMS22L	0,380	8,29E-03
ENSG00000142197	DOPEY2	0,358	8,32E-03
ENSG00000136492	BRIP1	0,389	8,36E-03
ENSG00000113387	SUB1	-0,284	8,37E-03
ENSG00000124243	BCAS4	0,291	8,39E-03
ENSG00000269968		0,415	8,53E-03
ENSG00000270898	TMIGD2	1,996	8,57E-03
ENSG00000177646	ACAD9	0,456	8,60E-03
ENSG00000153936	HS2ST1	0,351	8,72E-03
ENSG00000231925	TAPBP	-0,288	8,73E-03
ENSG00000125245	GPR18	0,524	8,78E-03
ENSG00000261604		-0,617	8,85E-03
ENSG00000121621	KIF18A	0,306	8,87E-03
ENSG00000137078	SIT1	0,323	8,88E-03
ENSG00000157470	FAM81A	0,414	9,01E-03
ENSG00000225828	FAM229A	-0,628	9,08E-03
ENSG00000183044	ABAT	-0,311	9,08E-03
ENSG00000185022	MAFF	-0,663	9,19E-03
ENSG00000250067	YJEFN3	-0,691	9,20E-03
ENSG00000135093	USP30	0,403	9,22E-03
ENSG00000081320	STK17B	0,427	9,23E-03
ENSG00000103066	PLA2G15	0,320	9,24E-03
ENSG00000101144	BMP7	0,302	9,27E-03
ENSG00000109674	NEIL3	0,370	9,35E-03
ENSG00000145386	CCNA2	0,314	9,37E-03
ENSG00000153815	CMIP	0,248	9,41E-03
ENSG00000231443		-0,909	9,42E-03
ENSG00000112658	SRF	-0,298	9,44E-03
ENSG00000070371	CLTCL1	0,785	9,46E-03
ENSG00000123219	CENPK	0,345	9,46E-03
ENSG00000197961	ZNF121	-0,360	9,48E-03
ENSG00000138160	KIF11	0,288	9,49E-03

ENSG00000121413	ZSCAN18	-0,427	9,51E-03
ENSG00000213413	PVRIG	0,443	9,65E-03
ENSG00000258727		-0,546	9,79E-03
ENSG00000169607	CKAP2L	0,292	9,80E-03
ENSG00000139684	ESD	0,278	9,81E-03
ENSG00000104903	LYL1	0,374	9,87E-03
ENSG00000105486	LIG1	0,316	9,88E-03
ENSG00000123352	SPATS2	0,284	9,90E-03
ENSG00000163536	SERPINI1	0,403	9,93E-03
ENSG00000132326	PER2	-0,368	9,94E-03
ENSG00000237594		0,886	9,95E-03
ENSG00000137310	TCF19	0,359	1,00E-02
ENSG00000104805	NUCB1	0,337	1,00E-02
ENSG00000020577	SAMD4A	-0,453	1,01E-02
ENSG00000138834	MAPK8IP3	-0,388	1,01E-02
ENSG00000221978	CCNL2	-0,336	1,01E-02
ENSG00000119711	ALDH6A1	-0,295	1,01E-02
ENSG00000196199	MPHOSPH8	-0,294	1,02E-02
ENSG00000163322	FAM175A	0,404	1,02E-02
ENSG00000128944	KNSTRN	0,352	1,03E-02
ENSG00000198826	ARHGAP11A	0,292	1,03E-02
ENSG00000176871	WSB2	-0,436	1,04E-02
ENSG00000139291	TMEM19	0,379	1,05E-02
ENSG00000196664	TLR7	0,439	1,05E-02
ENSG00000260916	OCM	-0,271	1,05E-02
ENSG00000183741	CBX6	-0,500	1,05E-02
ENSG00000135473	PAN2	-0,358	1,06E-02
ENSG00000111602	TIMELESS	0,351	1,06E-02
ENSG00000007312	CD79B	0,320	1,06E-02
ENSG00000183048	SLC25A10	0,555	1,06E-02
ENSG00000137393	RNF144B	0,501	1,06E-02
ENSG00000136141	LRCH1	0,318	1,06E-02
ENSG00000163808	KIF15	0,343	1,06E-02
ENSG00000161912	ADCY10P1	-0,711	1,06E-02
ENSG00000145687	SSBP2	0,309	1,06E-02
ENSG00000267680	ZNF224	-0,368	1,07E-02
ENSG00000187796	CARD9	-0,723	1,08E-02
ENSG00000111640	GAPDH	0,345	1,08E-02
ENSG00000099899	TRMT2A	0,351	1,08E-02
ENSG00000079691	LRRC16A	0,317	1,08E-02
ENSG00000165832	TRUB1	-0,253	1,09E-02
ENSG00000079257	LXN	0,536	1,09E-02
ENSG00000169016	E2F6	-0,318	1,09E-02
ENSG00000158402	CDC25C	0,431	1,09E-02
ENSG00000082805	ERC1	0,279	1,09E-02

ENSG00000072135	PTPN18	0,336	1,10E-02
ENSG00000203668	CHML	0,348	1,10E-02
ENSG00000126562	CERS5	-0,852	1,11E-02
ENSG00000188827	SLX4	0,283	1,11E-02
ENSG00000168970	JMJD7-PLA2G4B	-0,459	1,13E-02
ENSG00000123485	HJURP	0,276	1,13E-02
ENSG00000211459	MT-RNR1	-0,354	1,14E-02
ENSG00000069956	MAPK6	-0,267	1,15E-02
ENSG00000101444	AHCY	0,372	1,16E-02
ENSG00000171320	ESCO2	0,314	1,17E-02
ENSG00000196990	FAM163B	0,397	1,18E-02
ENSG00000127603	MACF1	0,283	1,18E-02
ENSG00000168246	UBTD2	-0,282	1,18E-02
ENSG00000203667	COX20	-0,271	1,18E-02
ENSG00000102384	CENPI	0,353	1,19E-02
ENSG00000026508	CD44	-1,043	1,19E-02
ENSG00000259529		-0,589	1,19E-02
ENSG00000148343	FAM73B	-0,287	1,20E-02
ENSG00000140525	FANCI	0,314	1,20E-02
ENSG00000181817	LSM10	0,290	1,20E-02
ENSG00000198885	ITPRIPL1	0,388	1,20E-02
ENSG00000117399	CDC20	0,339	1,22E-02
ENSG00000196367	TRRAP	0,242	1,23E-02
ENSG00000124257	NEURL2	0,804	1,23E-02
ENSG00000187954	CYHR1	-0,296	1,24E-02
ENSG00000272335		-0,618	1,24E-02
ENSG00000213722	DDAH2	-0,625	1,26E-02
ENSG00000166004	KIAA1731	0,263	1,26E-02
ENSG00000047644	WWC3	0,325	1,27E-02
ENSG00000171617	ENC1	0,578	1,27E-02
ENSG00000135441	BLOC1S1	0,346	1,27E-02
ENSG00000139734	DIAPH3	0,309	1,28E-02
ENSG00000077454	LRCH4	-0,299	1,28E-02
ENSG00000183624	HMCES	0,322	1,28E-02
ENSG00000171298	GAA	-0,405	1,28E-02
ENSG00000122188	LAX1	0,326	1,29E-02
ENSG00000126067	PSMB2	-0,256	1,29E-02
ENSG00000168502	MTCL1	0,324	1,29E-02
ENSG00000184271	POU6F1	-0,526	1,29E-02
ENSG00000235621	LINC00494	-0,525	1,30E-02
ENSG00000145476	CYP4V2	-0,390	1,30E-02
ENSG00000163535	SGOL2	0,292	1,30E-02
ENSG00000236144		-0,275	1,30E-02
ENSG00000147168	IL2RG	-0,321	1,31E-02
ENSG00000184207	PGP	0,306	1,31E-02

ENSG00000145779	TNFAIP8	0,300	1,31E-02
ENSG00000173950	XXYLT1	0,344	1,32E-02
ENSG00000096746	HNRNPH3	-0,337	1,32E-02
ENSG00000148154	UGCG	-0,293	1,32E-02
ENSG00000170365	SMAD1	0,361	1,33E-02
ENSG00000163093	BBS5	-0,644	1,35E-02
ENSG00000144331	ZNF385B	0,401	1,35E-02
ENSG00000174123	TLR10	0,307	1,36E-02
ENSG00000000938	FGR	0,442	1,36E-02
ENSG00000253733	LZTS1-AS1	0,799	1,37E-02
ENSG00000161888	SPC24	0,393	1,37E-02
ENSG00000132680	KIAA0907	-0,295	1,37E-02
ENSG00000155629	PIK3AP1	0,253	1,38E-02
ENSG00000111981	ULBP1	-0,298	1,38E-02
ENSG00000178685	PARP10	-0,294	1,38E-02
ENSG00000185101	ANO9	-0,374	1,38E-02
ENSG00000106415	GLCCI1	0,371	1,38E-02
ENSG00000123473	STIL	0,282	1,38E-02
ENSG00000168404	MLKL	0,598	1,38E-02
ENSG00000205189	ZBTB10	-0,301	1,39E-02
ENSG00000006576	PHTF2	0,300	1,39E-02
ENSG00000068831	RASGRP2	-0,264	1,39E-02
ENSG00000101224	CDC25B	0,263	1,41E-02
ENSG00000078487	ZCWPW1	-0,441	1,41E-02
ENSG00000133678	TMEM254	-0,689	1,41E-02
ENSG00000272899		-0,811	1,41E-02
ENSG00000157514	TSC22D3	-0,298	1,42E-02
ENSG00000085999	RAD54L	0,479	1,42E-02
ENSG00000253729	PRKDC	0,251	1,43E-02
ENSG00000223745		-0,344	1,43E-02
ENSG00000103021	CCDC113	-0,573	1,44E-02
ENSG00000092068	SLC7A8	-0,437	1,44E-02
ENSG00000147434	CHRNA6	-0,383	1,44E-02
ENSG00000102096	PIM2	-0,306	1,48E-02
ENSG00000174130	TLR6	-0,433	1,48E-02
ENSG00000166292	TMEM100	0,868	1,49E-02
ENSG00000100403	ZC3H7B	-0,262	1,50E-02
ENSG00000164463	CREBRF	-0,403	1,50E-02
ENSG00000164002	EXO5	0,614	1,50E-02
ENSG00000254815		-0,627	1,50E-02
ENSG00000156042	TTC18	-0,658	1,51E-02
ENSG00000267194		1,033	1,51E-02
ENSG00000168528	SERINC2	0,456	1,52E-02
ENSG00000172869	DMXL1	0,248	1,52E-02
ENSG00000228171		0,737	1,52E-02

ENSG00000100219	XBP1	0,326	1,52E-02
ENSG00000111424	VDR	0,588	1,53E-02
ENSG00000100368	CSF2RB	0,391	1,53E-02
ENSG00000175348	TMEM9B	-0,260	1,53E-02
ENSG00000148700	ADD3	0,289	1,53E-02
ENSG00000213213	CCDC183	-0,765	1,54E-02
ENSG00000101255	TRIB3	-0,302	1,54E-02
ENSG00000100320	RBFOX2	0,241	1,56E-02
ENSG00000186480	INSIG1	-0,273	1,56E-02
ENSG00000144749	LRIG1	0,289	1,56E-02
ENSG00000153551	CMTM7	0,460	1,56E-02
ENSG00000154556	SORBS2	0,249	1,57E-02
ENSG00000261087		-0,623	1,58E-02
ENSG00000178162	FAR2P2	0,261	1,58E-02
ENSG00000224578	HNRNPA1P48	0,420	1,58E-02
ENSG00000125170	DOK4	-0,571	1,58E-02
ENSG00000005059	CCDC109B	0,274	1,59E-02
ENSG00000258168		0,331	1,59E-02
ENSG00000092140	G2E3	0,261	1,59E-02
ENSG00000085719	CPNE3	0,240	1,59E-02
ENSG00000097046	CDC7	0,282	1,60E-02
ENSG00000165476	REEP3	-0,370	1,60E-02
ENSG00000106404	CLDN15	-0,369	1,60E-02
ENSG00000089685	BIRC5	0,270	1,60E-02
ENSG00000180096	SEPT1	-0,295	1,61E-02
ENSG00000138376	BARD1	0,294	1,61E-02
ENSG00000115355	CCDC88A	0,260	1,61E-02
ENSG00000134508	CABLES1	-0,251	1,61E-02
ENSG00000185811	IKZF1	0,329	1,61E-02
ENSG00000104517	UBR5	0,252	1,62E-02
ENSG00000256618	MTRNR2L1	-0,571	1,62E-02
ENSG00000167513	CDT1	0,418	1,62E-02
ENSG00000139193	CD27	0,532	1,63E-02
ENSG00000260032	LINC00657	-0,298	1,63E-02
ENSG00000120093	HOXB3	-0,552	1,63E-02
ENSG00000164713	BRI3	-0,283	1,64E-02
ENSG00000172340	SUCLG2	0,340	1,64E-02
ENSG00000175643	RMI2	0,346	1,65E-02
ENSG00000101199	ARFGAP1	-0,256	1,65E-02
ENSG00000132003	ZSWIM4	-0,314	1,65E-02
ENSG00000095002	MSH2	0,315	1,65E-02
ENSG00000220201	ZGLP1	-0,609	1,65E-02
ENSG00000259522		-0,700	1,66E-02
ENSG00000167925	GHDC	-0,245	1,66E-02
ENSG00000137807	KIF23	0,288	1,67E-02

ENSG00000104889	RNASEH2A	0,338	1,67E-02
ENSG00000186638	KIF24	0,308	1,67E-02
ENSG00000112234	FBXL4	0,267	1,67E-02
ENSG00000138757	G3BP2	-0,239	1,67E-02
ENSG00000257594	GALNT4	-1,659	1,68E-02
ENSG00000133612	AGAP3	0,429	1,68E-02
ENSG00000243335	KCTD7	0,289	1,68E-02
ENSG00000173281	PPP1R3B	-0,309	1,68E-02
ENSG00000196118	C16orf93	0,360	1,69E-02
ENSG00000048028	USP28	0,255	1,69E-02
ENSG00000164611	PTTG1	0,280	1,70E-02
ENSG00000153066	TXNDC11	0,400	1,70E-02
ENSG00000138796	HADH	0,331	1,70E-02
ENSG00000130413	STK33	0,611	1,71E-02
ENSG00000214655	ZSWIM8	-0,328	1,71E-02
ENSG00000258674		-0,745	1,72E-02
ENSG00000146918	NCAPG2	0,265	1,72E-02
ENSG00000140854	KATNB1	0,297	1,72E-02
ENSG00000260853		-0,719	1,73E-02
ENSG00000108528	SLC25A11	0,352	1,73E-02
ENSG00000103966	EHD4	0,260	1,74E-02
ENSG00000166851	PLK1	0,321	1,74E-02
ENSG00000249003	CLUHP4	-0,822	1,74E-02
ENSG00000005243	COPZ2	-0,648	1,74E-02
ENSG00000164850	GPER1	0,310	1,75E-02
ENSG00000109063	MYH3	-0,696	1,75E-02
ENSG00000127415	IDUA	-0,441	1,76E-02
ENSG00000182054	IDH2	0,447	1,76E-02
ENSG00000155008	APOOL	-0,309	1,76E-02
ENSG00000198771	RCSD1	0,263	1,76E-02
ENSG00000137070	IL11RA	-0,609	1,76E-02
ENSG00000170476	MZB1	0,271	1,77E-02
ENSG00000160058	BSDC1	-0,304	1,78E-02
ENSG00000159496	RGL4	-0,671	1,79E-02
ENSG00000102738	MRPS31	-0,277	1,79E-02
ENSG00000137766	UNC13C	0,291	1,79E-02
ENSG00000185359	HGS	-0,293	1,80E-02
ENSG00000198554	WDHD1	0,318	1,80E-02
ENSG00000144354	CDCA7	0,588	1,81E-02
ENSG00000123329	ARHGAP9	-0,288	1,81E-02
ENSG00000008710	PKD1	-0,279	1,81E-02
ENSG00000167766	ZNF83	-0,284	1,81E-02
ENSG00000182934	SRPR	-0,266	1,82E-02
ENSG00000159588	CCDC17	-0,546	1,82E-02
ENSG00000267924		-0,407	1,82E-02

ENSG00000048991	R3HDM1	0,266	1,82E-02
ENSG00000126804	ZBTB1	-0,263	1,82E-02
ENSG00000025708	TYMP	-0,467	1,83E-02
ENSG00000124496	TRERF1	0,390	1,83E-02
ENSG00000151148	UBE3B	-0,281	1,83E-02
ENSG00000234771		-0,460	1,84E-02
ENSG00000137411	VARS2	-0,333	1,84E-02
ENSG00000101194	SLC17A9	-0,238	1,85E-02
ENSG00000108785	HSD17B1P1	-0,754	1,86E-02
ENSG00000094804	CDC6	0,284	1,86E-02
ENSG00000242802	AP5Z1	-0,284	1,87E-02
ENSG00000121671	CRY2	-0,277	1,87E-02
ENSG00000112081	SRSF3	0,249	1,88E-02
ENSG00000124920	MYRF	-0,694	1,89E-02
ENSG00000147010	SH3KBP1	0,320	1,89E-02
ENSG00000152455	SUV39H2	0,289	1,90E-02
ENSG00000274272		-0,465	1,90E-02
ENSG00000130810	PPAN	-0,348	1,90E-02
ENSG00000104852	SNRNP70	-0,321	1,90E-02
ENSG00000185760	KCNQ5	0,313	1,90E-02
ENSG00000127423	AUNIP	0,384	1,91E-02
ENSG00000139370	SLC15A4	0,277	1,92E-02
ENSG00000171204	TMEM126B	0,249	1,92E-02
ENSG00000048140	TSPAN17	-0,244	1,92E-02
ENSG00000158805	ZNF276	-0,334	1,93E-02
ENSG00000197724	PHF2	-0,255	1,93E-02
ENSG00000042286	AIFM2	-0,385	1,93E-02
ENSG00000124429	POF1B	-0,519	1,93E-02
ENSG00000166128	RAB8B	-0,239	1,94E-02
ENSG00000215301	DDX3X	-0,317	1,94E-02
ENSG00000124208	TMEM189-UBE2V1	-2,939	1,96E-02
ENSG00000144043	TEX261	-0,227	1,96E-02
ENSG00000106991	ENG	-0,638	1,96E-02
ENSG00000197498	RPF2	-0,278	1,97E-02
ENSG00000156831	NSMCE2	0,313	1,97E-02
ENSG00000013810	TACC3	0,256	1,98E-02
ENSG00000023839	ABCC2	-0,714	1,98E-02
ENSG00000055609	KMT2C	0,239	1,98E-02
ENSG00000116062	MSH6	0,296	1,99E-02
ENSG00000100307	CBX7	-0,282	1,99E-02
ENSG00000158711	ELK4	-0,313	1,99E-02
ENSG00000032444	PNPLA6	-0,287	2,00E-02
ENSG00000174151	CYB561D1	-0,345	2,00E-02
ENSG00000198169	ZNF251	-0,275	2,00E-02
ENSG00000240024	LINC00888	0,401	2,00E-02

ENSG00000164989	CCDC171	0,305	2,01E-02
ENSG00000175873		0,685	2,01E-02
ENSG00000171202	TMEM126A	0,268	2,02E-02
ENSG00000231424		0,548	2,02E-02
ENSG00000205978	NYNRIN	0,843	2,02E-02
ENSG00000260083	MIR4519	-0,525	2,02E-02
ENSG00000174500	GCSAM	0,397	2,04E-02
ENSG00000224597	PTCHD3P1	0,577	2,04E-02
ENSG00000076248	UNG	0,331	2,04E-02
ENSG00000035499	DEPDC1B	0,292	2,05E-02
ENSG00000253200		-0,535	2,05E-02
ENSG00000150991	UBC	-0,286	2,07E-02
ENSG00000162739	SLAMF6	0,279	2,09E-02
ENSG00000242125	SNHG3	-0,314	2,09E-02
ENSG00000157483	MYO1E	0,317	2,09E-02
ENSG00000196092	PAX5	0,251	2,10E-02
ENSG00000159753	RLTPR	-0,249	2,10E-02
ENSG00000173727		0,366	2,11E-02
ENSG00000271119		-0,693	2,11E-02
ENSG00000142556	ZNF614	-0,312	2,12E-02
ENSG00000163141	BNIPL	-0,728	2,12E-02
ENSG00000255339		-0,531	2,12E-02
ENSG00000173366		0,320	2,12E-02
ENSG00000108256	NUFIP2	-0,329	2,14E-02
ENSG00000249679		0,422	2,14E-02
ENSG00000144711	IQSEC1	0,249	2,14E-02
ENSG00000137496	IL18BP	-0,528	2,15E-02
ENSG00000162063	CCNF	0,266	2,15E-02
ENSG00000165169	DYNLT3	-0,283	2,16E-02
ENSG00000162062	C16orf59	0,319	2,17E-02
ENSG00000167700	MFSD3	0,407	2,17E-02
ENSG00000145425	RPS3A	0,256	2,17E-02
ENSG00000167747	C19orf48	0,428	2,18E-02
ENSG00000186104	CYP2R1	0,442	2,18E-02
ENSG00000023697	DERA	0,330	2,18E-02
ENSG00000158882	TOMM40L	0,306	2,19E-02
ENSG00000269982		-0,652	2,19E-02
ENSG00000145088	EAF2	0,302	2,20E-02
ENSG00000140105	WARS	-0,259	2,21E-02
ENSG00000146143	PRIM2	0,271	2,21E-02
ENSG00000255641		0,795	2,22E-02
ENSG00000085840	ORC1	0,409	2,22E-02
ENSG00000196363	WDR5	-0,244	2,22E-02
ENSG00000127564	PKMYT1	0,329	2,24E-02
ENSG00000126005	MMP24-AS1	0,365	2,24E-02

ENSG00000196967	ZNF585A	-0,284	2,24E-02
ENSG00000107796	ACTA2	-0,609	2,24E-02
ENSG00000240038	AMY2B	-0,546	2,25E-02
ENSG00000134574	DDB2	0,423	2,26E-02
ENSG00000130005	GAMT	0,441	2,26E-02
ENSG00000011426	ANLN	0,263	2,26E-02
ENSG00000075826	SEC31B	-0,375	2,28E-02
ENSG00000214562	NUTM2D	-0,677	2,28E-02
ENSG00000160201	U2AF1	-0,249	2,28E-02
ENSG00000109079	TNFAIP1	-0,266	2,28E-02
ENSG00000143314	MRPL24	-0,277	2,28E-02
ENSG00000164045	CDC25A	0,252	2,29E-02
ENSG00000119969	HELLS	0,244	2,29E-02
ENSG00000028137	TNFRSF1B	0,860	2,29E-02
ENSG00000119509	INVS	0,258	2,29E-02
ENSG00000175048	ZDHHC14	0,293	2,30E-02
ENSG00000131470	PSMC3IP	0,324	2,30E-02
ENSG00000261556	SMG1P7	-0,437	2,30E-02
ENSG00000260917		-0,346	2,31E-02
ENSG00000085465	OVGP1	-0,634	2,32E-02
ENSG00000099377	HSD3B7	-0,670	2,32E-02
ENSG00000101246	ARFRP1	0,358	2,33E-02
ENSG00000131127	ZNF141	-0,623	2,34E-02
ENSG00000130164	LDLR	-0,297	2,35E-02
ENSG00000090861	AARS	-0,240	2,35E-02
ENSG00000007923	DNAJC11	-0,274	2,35E-02
ENSG00000123933	MXD4	0,281	2,35E-02
ENSG00000071575	TRIB2	-0,222	2,36E-02
ENSG00000254087	LYN	0,255	2,36E-02
ENSG00000068400	GRIPAP1	-0,281	2,36E-02
ENSG00000251357		-0,818	2,36E-02
ENSG00000143387	CTSK	-0,671	2,37E-02
ENSG00000165025	SYK	0,288	2,39E-02
ENSG00000210135	MT-TN	-0,456	2,40E-02
ENSG00000143850	PLEKHA6	-0,594	2,41E-02
ENSG00000121440	PDZRN3	0,607	2,42E-02
ENSG00000053371	AKR7A2	0,377	2,43E-02
ENSG00000095539	SEMA4G	-0,707	2,43E-02
ENSG00000116761	CTH	-0,261	2,44E-02
ENSG00000277449		-0,358	2,45E-02
ENSG00000129187	DCTD	-0,221	2,46E-02
ENSG00000174437	ATP2A2	-0,252	2,46E-02
ENSG00000269751		-0,361	2,46E-02
ENSG00000010361	FUZ	0,347	2,47E-02
ENSG00000004897	CDC27	0,224	2,47E-02

ENSG00000153044	CENPH	0,371	2,48E-02
ENSG00000183814	LIN9	0,279	2,48E-02
ENSG00000224645		-0,726	2,49E-02
ENSG00000113328	CCNG1	0,261	2,50E-02
ENSG00000089280	FUS	-0,246	2,51E-02
ENSG00000273841	AK6	-0,575	2,51E-02
ENSG00000198839	ZNF277	0,296	2,51E-02
ENSG00000141391	SLMO1	0,335	2,51E-02
ENSG00000168016	TRANK1	0,228	2,51E-02
ENSG00000173276	ZBTB21	-0,292	2,53E-02
ENSG00000127663	KDM4B	-0,250	2,54E-02
ENSG00000104375	STK3	0,428	2,55E-02
ENSG00000256269	HMBS	0,290	2,55E-02
ENSG00000245857		0,623	2,55E-02
ENSG00000151553	FAM160B1	-0,271	2,56E-02
ENSG00000250575		-0,914	2,56E-02
ENSG00000168071	CCDC88B	-0,302	2,56E-02
ENSG00000171132	PRKCE	0,270	2,56E-02
ENSG00000182484	WASH6P	-0,279	2,56E-02
ENSG00000134330	IAH1	0,280	2,57E-02
ENSG00000176208	ATAD5	0,254	2,58E-02
ENSG00000131389	SLC6A6	0,225	2,58E-02
ENSG00000224051	GLTPD1	0,272	2,58E-02
ENSG00000104361	NIPAL2	-0,251	2,59E-02
ENSG00000198382	UVRAG	0,268	2,59E-02
ENSG00000141965	FEM1A	-0,371	2,59E-02
ENSG00000048462	TNFRSF17	0,517	2,59E-02
ENSG00000124831	LRRFIP1	0,256	2,60E-02
ENSG00000104312	RIPK2	0,281	2,60E-02
ENSG00000102057	KCND1	-0,637	2,60E-02
ENSG00000172264	MACROD2	0,431	2,61E-02
ENSG00000146830	GIGYF1	-0,268	2,61E-02
ENSG00000111012	CYP27B1	-0,480	2,62E-02
ENSG00000136379	ABHD17C	-0,674	2,62E-02
ENSG00000142188	TMEM50B	-0,288	2,63E-02
ENSG00000100503	NIN	0,220	2,63E-02
ENSG00000257433		-0,642	2,64E-02
ENSG00000115163	CENPA	0,311	2,65E-02
ENSG00000107829	FBXW4	-0,240	2,66E-02
ENSG00000113739	STC2	-0,252	2,67E-02
ENSG00000076555	ACACB	0,475	2,67E-02
ENSG00000073464	CLCN4	0,303	2,68E-02
ENSG00000152061	RABGAP1L	0,245	2,69E-02
ENSG00000134138	MEIS2	0,294	2,69E-02
ENSG00000188917	TRMT2B	-0,276	2,70E-02

ENSG00000198056	PRIM1	0,366	2,70E-02
ENSG00000162004	CCDC78	-0,383	2,70E-02
ENSG00000143126	CELSR2	-0,392	2,71E-02
ENSG00000166024	R3HCC1L	0,256	2,73E-02
ENSG00000255389		-0,536	2,74E-02
ENSG00000067533	RRP15	-0,288	2,75E-02
ENSG00000213599	SLX1A-SULT1A3	-0,352	2,75E-02
ENSG00000228315	GUSBP11	-0,371	2,76E-02
ENSG00000166401	SERPINB8	-0,529	2,77E-02
ENSG00000139433	GLTP	-0,242	2,77E-02
ENSG00000136280	CCM2	0,299	2,77E-02
ENSG00000172493	AFF1	0,266	2,78E-02
ENSG00000271303	SRXN1	-0,248	2,78E-02
ENSG00000105397	TYK2	-0,233	2,79E-02
ENSG00000178999	AURKB	0,267	2,81E-02
ENSG00000130511	SSBP4	0,279	2,82E-02
ENSG00000276710	CSPG4P8	-0,436	2,82E-02
ENSG00000152253	SPC25	0,327	2,82E-02
ENSG00000088280	ASAP3	-0,370	2,83E-02
ENSG00000196372	ASB13	0,323	2,84E-02
ENSG00000123374	CDK2	0,233	2,84E-02
ENSG00000014641	MDH1	0,274	2,84E-02
ENSG00000138430	OLA1	0,287	2,85E-02
ENSG00000160753	RUSC1	0,314	2,85E-02
ENSG00000118482	PHF3	0,246	2,85E-02
ENSG00000142046	TMEM91	-0,671	2,85E-02
ENSG00000132361	CLUH	-0,268	2,85E-02
ENSG00000170734	POLH	0,219	2,86E-02
ENSG00000115956	PLEK	-0,241	2,88E-02
ENSG00000131401	NAPSB	0,294	2,88E-02
ENSG00000120053	GOT1	-0,239	2,88E-02
ENSG00000196843	ARID5A	-0,346	2,88E-02
ENSG00000138180	CEP55	0,247	2,89E-02
ENSG00000101412	E2F1	0,256	2,90E-02
ENSG00000005022	SLC25A5	0,260	2,90E-02
ENSG00000171067	C11orf24	0,253	2,90E-02
ENSG00000214425	LRRC37A4P	0,243	2,91E-02
ENSG00000104381	GDAP1	0,345	2,92E-02
ENSG00000161010	C5orf45	-0,278	2,92E-02
ENSG00000215717	TMEM167B	-0,230	2,92E-02
ENSG00000008128	CDK11A	-0,313	2,92E-02
ENSG00000156970	BUB1B	0,220	2,93E-02
ENSG00000175197	DDIT3	-0,249	2,93E-02
ENSG00000260852	FBXL19-AS1	-0,449	2,93E-02
ENSG00000166197	NOLC1	-0,245	2,94E-02

ENSG00000112232	KHDRBS2	0,749	2,94E-02
ENSG00000255182		-0,593	2,94E-02
ENSG00000165457	FOLR2	0,447	2,96E-02
ENSG00000213339	QTRT1	-0,328	2,98E-02
ENSG00000154237	LRRK1	0,223	2,99E-02
ENSG00000065615	CYB5R4	0,246	3,00E-02
ENSG00000213983	AP1G2	-0,282	3,00E-02
ENSG00000172167	MTBP	0,278	3,00E-02
ENSG00000253778		0,633	3,02E-02
ENSG00000049323	LTBP1	0,256	3,02E-02
ENSG00000151503	NCAPD3	0,235	3,02E-02
ENSG00000133392	MYH11	-0,540	3,03E-02
ENSG00000152240	HAUS1	0,298	3,03E-02
ENSG00000083799	FAM134C	-0,241	3,03E-02
ENSG00000138346	DNA2	0,249	3,04E-02
ENSG00000197442	MAP3K5	0,311	3,04E-02
ENSG00000184524	CEND1	0,248	3,05E-02
ENSG00000072736	NFATC3	0,218	3,05E-02
ENSG00000132424	PNISR	-0,285	3,05E-02
ENSG00000157227	MMP14	-0,606	3,05E-02
ENSG00000258388	PPT2-EGFL8	-0,597	3,06E-02
ENSG00000172349	IL16	0,224	3,06E-02
ENSG00000186469	GNG2	0,296	3,07E-02
ENSG00000111885	MAN1A1	-0,236	3,07E-02
ENSG00000198890	PRMT6	0,264	3,08E-02
ENSG00000180353	HCLS1	-0,250	3,08E-02
ENSG00000146416	AIG1	0,617	3,08E-02
ENSG00000173715	C11orf80	0,299	3,08E-02
ENSG00000092853	CLSPN	0,299	3,08E-02
ENSG00000233822	HIST1H2BN	-0,578	3,08E-02
ENSG00000122483	CCDC18	0,242	3,09E-02
ENSG00000162231	NXF1	-0,296	3,09E-02
ENSG00000008952	SEC62	0,238	3,10E-02
ENSG00000084092	NOA1	0,314	3,10E-02
ENSG00000269693		-0,470	3,10E-02
ENSG00000131747	TOP2A	0,251	3,11E-02
ENSG00000065328	MCM10	0,264	3,11E-02
ENSG00000227671	MIR3916	-0,265	3,11E-02
ENSG00000224565		0,461	3,12E-02
ENSG00000171425	ZNF581	0,288	3,12E-02
ENSG00000184678	HIST2H2BE	-0,591	3,13E-02
ENSG00000166432	ZMAT1	-0,384	3,14E-02
ENSG00000151006	PRSS53	-0,567	3,14E-02
ENSG00000176890	TYMS	0,289	3,15E-02
ENSG00000136122	BORA	0,279	3,15E-02

ENSG00000109685	WHSC1	0,229	3,15E-02
ENSG00000173812	EIF1	-0,232	3,16E-02
ENSG00000182446	NPLOC4	-0,247	3,16E-02
ENSG00000168003	SLC3A2	-0,230	3,16E-02
ENSG00000275591	XKR5	0,557	3,16E-02
ENSG00000177548	RABEP2	0,286	3,17E-02
ENSG00000149743	TRPT1	0,334	3,17E-02
ENSG00000187741	FANCA	0,209	3,18E-02
ENSG00000214595	EML6	-0,313	3,18E-02
ENSG00000064547	LPAR2	-0,444	3,19E-02
ENSG00000198496	NBR2	-0,329	3,20E-02
ENSG00000164306	PRIMPOL	0,387	3,21E-02
ENSG00000259583		0,427	3,21E-02
ENSG00000106077	ABHD11	0,465	3,21E-02
ENSG00000135205	CCDC146	-0,556	3,23E-02
ENSG00000089558	KCNH4	-0,553	3,23E-02
ENSG00000132510	KDM6B	-0,298	3,24E-02
ENSG00000113552	GNPDA1	-0,236	3,24E-02
ENSG00000170142	UBE2E1	0,251	3,24E-02
ENSG00000172766	NAA16	0,240	3,24E-02
ENSG00000198589	LRBA	0,205	3,24E-02
ENSG00000163975	MFI2	0,400	3,25E-02
ENSG00000178966	RMI1	0,255	3,25E-02
ENSG00000272620	AFAP1-AS1	-0,617	3,25E-02
ENSG00000227517		0,647	3,25E-02
ENSG00000173706	HEG1	-0,480	3,27E-02
ENSG00000161013	MGAT4B	-0,214	3,27E-02
ENSG00000173334	TRIB1	0,451	3,27E-02
ENSG00000057935	MTA3	0,230	3,29E-02
ENSG00000211751	TRBV25-1	0,520	3,29E-02
ENSG00000155367	PPM1J	0,634	3,30E-02
ENSG00000214783	POLR2J4	-0,515	3,30E-02
ENSG00000154822	PLCL2	0,265	3,30E-02
ENSG00000136159	NUDT15	0,250	3,30E-02
ENSG00000197062	ZSCAN26	0,466	3,30E-02
ENSG00000184677	ZBTB40	-0,296	3,30E-02
ENSG00000261434		0,446	3,31E-02
ENSG00000171097	CCBL1	0,352	3,32E-02
ENSG00000274561		-0,633	3,32E-02
ENSG00000071051	NCK2	0,267	3,33E-02
ENSG00000147130	ZMYM3	0,215	3,33E-02
ENSG00000084112	SSH1	0,225	3,33E-02
ENSG00000265241	RBM8A	-0,246	3,34E-02
ENSG00000137842	TMEM62	0,346	3,35E-02
ENSG00000197329	PELI1	0,302	3,35E-02

ENSG00000204305	AGER	-0,458	3,35E-02
ENSG00000230266	XXYLT1-AS2	0,539	3,36E-02
ENSG00000140750	ARHGAP17	0,326	3,37E-02
ENSG00000111206	FOXM1	0,243	3,38E-02
ENSG00000166963	MAP1A	0,485	3,39E-02
ENSG00000119866	BCL11A	0,304	3,40E-02
ENSG00000133265	HSPBP1	-0,259	3,40E-02
ENSG00000073921	PICALM	0,216	3,41E-02
ENSG00000153029	MR1	-0,248	3,42E-02
ENSG00000261611		-0,910	3,42E-02
ENSG00000077152	UBE2T	0,247	3,43E-02
ENSG00000160094	ZNF362	-0,786	3,44E-02
ENSG00000145012	LPP	-0,332	3,44E-02
ENSG00000141736	ERBB2	-0,442	3,44E-02
ENSG00000205413	SAMD9	-0,289	3,47E-02
ENSG00000273154		-0,320	3,47E-02
ENSG00000090104	RGS1	-0,248	3,47E-02
ENSG00000087995	METTL2A	0,234	3,47E-02
ENSG00000096060	FKBP5	0,244	3,49E-02
ENSG00000175792	RUVBL1	0,251	3,49E-02
ENSG00000052749	RRP12	-0,291	3,50E-02
ENSG00000180712		-0,346	3,50E-02
ENSG00000140443	IGF1R	-0,271	3,51E-02
ENSG00000151623	NR3C2	0,580	3,51E-02
ENSG00000198947	DMD	-0,322	3,52E-02
ENSG00000128203	ASPHD2	-0,240	3,52E-02
ENSG00000156976	EIF4A2	-0,235	3,52E-02
ENSG00000103404	USP31	-0,402	3,52E-02
ENSG00000100241	SBF1	-0,297	3,52E-02
ENSG00000187486	KCNJ11	0,515	3,53E-02
ENSG00000198176	TFDP1	0,266	3,54E-02
ENSG00000198538	ZNF28	-0,248	3,54E-02
ENSG00000143033	MTF2	0,240	3,55E-02
ENSG00000096070	BRPF3	-0,255	3,56E-02
ENSG00000169442	CD52	0,243	3,56E-02
ENSG00000169499	PLEKHA2	0,221	3,57E-02
ENSG00000084652	TXLNA	-0,238	3,59E-02
ENSG00000071054	MAP4K4	0,222	3,60E-02
ENSG00000169668	BCRP2	0,459	3,61E-02
ENSG00000255857	PXN-AS1	0,479	3,62E-02
ENSG00000263264		0,300	3,63E-02
ENSG00000196365	LONP1	-0,230	3,64E-02
ENSG00000166548	TK2	-0,268	3,64E-02
ENSG00000109881	CCDC34	0,288	3,65E-02
ENSG00000157110	RBPMS	-0,592	3,65E-02

ENSG00000229474	PATL2	-0,546	3,66E-02
ENSG00000185386	MAPK11	-0,449	3,68E-02
ENSG00000170871	KIAA0232	-0,260	3,68E-02
ENSG00000163931	TKT	0,289	3,68E-02
ENSG00000172748	ZNF596	-0,494	3,69E-02
ENSG00000204248	COL11A2	-0,702	3,70E-02
ENSG00000134242	PTPN22	0,216	3,70E-02
ENSG00000180035	ZNF48	0,257	3,70E-02
ENSG00000160285	LSS	-0,304	3,72E-02
ENSG00000167325	RRM1	0,251	3,72E-02
ENSG00000005469	CROT	-0,295	3,73E-02
ENSG00000102172	SMS	0,295	3,73E-02
ENSG00000211640	IGLV6-57	0,355	3,73E-02
ENSG00000177728	KIAA0195	-0,230	3,75E-02
ENSG00000064225	ST3GAL6	0,508	3,75E-02
ENSG00000162073	PAQR4	0,385	3,75E-02
ENSG00000167972	ABCA3	-0,483	3,76E-02
ENSG00000197093	GAL3ST4	-0,534	3,76E-02
ENSG00000168906	MAT2A	-0,243	3,76E-02
ENSG00000277972	CISD3	0,313	3,77E-02
ENSG00000117650	NEK2	0,251	3,78E-02
ENSG00000052802	MSMO1	-0,279	3,79E-02
ENSG00000259040	BLOC1S5-TXNDC5	0,326	3,79E-02
ENSG00000169762	TAPT1	0,247	3,80E-02
ENSG00000157637	SLC38A10	-0,238	3,80E-02
ENSG00000143811	PYCR2	-0,206	3,81E-02
ENSG00000273230		-0,614	3,81E-02
ENSG00000124357	NAGK	-0,241	3,81E-02
ENSG00000182985	CADM1	0,257	3,81E-02
ENSG00000104980	TIMM44	-0,213	3,81E-02
ENSG00000149636	DSN1	0,206	3,82E-02
ENSG00000004838	ZMYND10	-0,566	3,82E-02
ENSG00000099331	MYO9B	0,203	3,83E-02
ENSG00000163534	FCRL1	0,211	3,86E-02
ENSG00000116698	SMG7	0,216	3,86E-02
ENSG00000101104	PABPC1L	-0,279	3,86E-02
ENSG00000152192	POU4F1	0,669	3,86E-02
ENSG00000148835	TAF5	0,275	3,87E-02
ENSG00000198964	SGMS1	0,229	3,88E-02
ENSG00000254870	ATP6V1G2-DDX39B	-1,394	3,88E-02
ENSG00000249437	NAIP	0,358	3,89E-02
ENSG00000152487	ARL5B-AS1	-0,651	3,89E-02
ENSG00000147471	PROSC	-0,233	3,89E-02
ENSG00000130254	SAFB2	-0,249	3,90E-02
ENSG00000258130		0,706	3,90E-02

ENSG00000112511	PHF1	-0,227	3,90E-02
ENSG00000151079		0,472	3,91E-02
ENSG00000105204	DYRK1B	0,409	3,91E-02
ENSG00000160584	SIK3	0,197	3,92E-02
ENSG00000131069	ACSS2	0,241	3,93E-02
ENSG00000116685	KIAA2013	0,242	3,93E-02
ENSG00000165097	KDM1B	0,216	3,94E-02
ENSG00000114107	CEP70	0,283	3,94E-02
ENSG00000169826	CSGALNACT2	0,214	3,96E-02
ENSG00000099821	POLRMT	-0,240	3,96E-02
ENSG00000226479	TMEM185B	-0,405	3,98E-02
ENSG00000077044	DGKD	0,259	3,99E-02
ENSG00000119333	WDR34	0,293	3,99E-02
ENSG00000165966	PDZRN4	0,716	4,00E-02
ENSG00000186710	CCDC42B	0,585	4,00E-02
ENSG00000113273	ARSB	-0,275	4,00E-02
ENSG00000165684	SNAPC4	-0,281	4,01E-02
ENSG00000262001	DLGAP1-AS2	-0,585	4,01E-02
ENSG00000136982	DSCC1	0,280	4,01E-02
ENSG00000088899		-0,345	4,01E-02
ENSG00000272994		-0,416	4,01E-02
ENSG00000127946	HIP1	0,219	4,03E-02
ENSG00000258839	MC1R	-0,367	4,03E-02
ENSG00000125520	SLC2A4RG	0,343	4,03E-02
ENSG00000105723	GSK3A	-0,207	4,03E-02
ENSG00000112290	WASF1	0,261	4,04E-02
ENSG00000105647	PIK3R2	0,449	4,04E-02
ENSG00000169718	DUS1L	-0,236	4,05E-02
ENSG00000081692	JMJD4	0,447	4,08E-02
ENSG00000181544	FANCB	0,329	4,08E-02
ENSG00000171604	CXXC5	0,354	4,08E-02
ENSG00000164615	CAMLG	0,282	4,08E-02
ENSG00000150347	ARID5B	0,239	4,09E-02
ENSG00000164751	PEX2	-0,207	4,09E-02
ENSG00000188846	RPL14	0,297	4,10E-02
ENSG00000078674	PCM1	0,223	4,10E-02
ENSG00000112118	MCM3	0,230	4,11E-02
ENSG00000136205	TNS3	0,544	4,11E-02
ENSG00000078808	SDF4	-0,208	4,12E-02
ENSG00000112576	CCND3	0,267	4,12E-02
ENSG00000171700	RGS19	0,268	4,12E-02
ENSG00000108786	HSD17B1	-0,426	4,12E-02
ENSG00000110395	CBL	0,200	4,12E-02
ENSG00000164362	TERT	0,535	4,12E-02
ENSG00000148660	CAMK2G	0,330	4,14E-02

ENSG00000153406	NMRAL1	0,313	4,14E-02
ENSG00000171206	TRIM8	0,212	4,15E-02
ENSG00000087586	AURKA	0,250	4,15E-02
ENSG00000128536	CDHR3	0,659	4,15E-02
ENSG00000105136	ZNF419	-0,408	4,16E-02
ENSG00000133316	WDR74	-0,221	4,16E-02
ENSG00000270015		-0,388	4,16E-02
ENSG00000088305	DNMT3B	0,280	4,17E-02
ENSG00000228830		-0,376	4,19E-02
ENSG00000168421	RHOH	0,234	4,20E-02
ENSG00000264343	SMG8	-0,369	4,20E-02
ENSG00000131067	GGT7	-0,284	4,21E-02
ENSG00000173320	GDAP1	0,297	4,21E-02
ENSG00000184014	DENND5A	0,261	4,22E-02
ENSG00000165271	NOL6	-0,291	4,22E-02
ENSG00000143369	ECM1	-0,626	4,24E-02
ENSG00000134986	NREP	0,235	4,24E-02
ENSG00000163938	GNL3	-0,236	4,24E-02
ENSG00000172216	CEBPB	-0,247	4,25E-02
ENSG00000100983	GSS	0,242	4,25E-02
ENSG00000113013	HSPA9	-0,216	4,26E-02
ENSG00000170325	PRDM10	0,222	4,26E-02
ENSG00000158987	RAPGEF6	0,206	4,27E-02
ENSG00000111254	AKAP3	-0,574	4,27E-02
ENSG00000223496	EXOSC6	-0,275	4,28E-02
ENSG00000054967	RELT	0,300	4,28E-02
ENSG00000166860	ZBTB39	-0,255	4,28E-02
ENSG00000149196	C11orf73	0,222	4,29E-02
ENSG00000176390	CRLF3	0,212	4,29E-02
ENSG00000166153	DEPDC4	0,561	4,29E-02
ENSG00000175189	INHBC	-0,397	4,32E-02
ENSG00000097021	ACOT7	0,393	4,32E-02
ENSG00000088836	SLC4A11	-0,291	4,33E-02
ENSG00000152495	CAMK4	0,236	4,33E-02
ENSG00000136450	SRSF1	-0,242	4,34E-02
ENSG00000121931	LRIF1	-0,209	4,34E-02
ENSG00000150672	DLG2	0,295	4,35E-02
ENSG00000116497	S100PBP	0,220	4,35E-02
ENSG00000102981	PARD6A	0,365	4,35E-02
ENSG00000011243	AKAP8L	-0,197	4,35E-02
ENSG00000111481	COPZ1	-0,226	4,35E-02
ENSG00000077514	POLD3	0,251	4,36E-02
ENSG00000139626	ITGB7	0,241	4,36E-02
ENSG00000111641	NOP2	-0,276	4,36E-02
ENSG00000013364	MVP	-0,376	4,36E-02

ENSG00000106397	PLOD3	-0,242	4,37E-02
ENSG00000112984	KIF20A	0,263	4,38E-02
ENSG00000149187	CELF1	-0,243	4,38E-02
ENSG00000250615		-0,570	4,38E-02
ENSG00000271605	MILR1	0,286	4,39E-02
ENSG00000230975		0,365	4,39E-02
ENSG00000198648	STK39	0,219	4,39E-02
ENSG00000105085	MED26	0,249	4,40E-02
ENSG00000160216	AGPAT3	-0,213	4,40E-02
ENSG00000110108	TMEM109	0,225	4,41E-02
ENSG00000152457	DCLRE1C	0,266	4,41E-02
ENSG00000122359	ANXA11	0,218	4,42E-02
ENSG00000163072	NOSTRIN	0,546	4,43E-02
ENSG00000122778	KIAA1549	-0,510	4,43E-02
ENSG00000159761	C16orf86	0,593	4,43E-02
ENSG00000136877	FPGS	0,236	4,44E-02
ENSG00000266340		-0,304	4,44E-02
ENSG00000140030	GPR65	-0,303	4,44E-02
ENSG00000112182	BACH2	0,217	4,45E-02
ENSG00000109736	MFSD10	-0,218	4,47E-02
ENSG00000135077	HAVCR2	-0,608	4,47E-02
ENSG00000186871	ERCC6L	0,229	4,47E-02
ENSG00000157680	DGKI	0,195	4,48E-02
ENSG00000006607	FARP2	0,236	4,48E-02
ENSG00000215440	NPEPL1	-0,574	4,49E-02
ENSG00000131351	HAUS8	0,251	4,49E-02
ENSG00000180776	ZDHHC20	0,201	4,49E-02
ENSG00000132824	SERINC3	-0,209	4,49E-02
ENSG00000139531	SUOX	-0,434	4,50E-02
ENSG00000155330	C16orf87	0,219	4,51E-02
ENSG00000143252	SDHC	-0,227	4,51E-02
ENSG00000169403	PTAFR	0,222	4,52E-02
ENSG00000203875	SNHG5	0,207	4,53E-02
ENSG00000048540	LMO3	0,300	4,53E-02
ENSG00000177380	PPFIA3	-0,238	4,54E-02
ENSG00000119862	LGALSL	0,355	4,55E-02
ENSG00000072210	ALDH3A2	-0,413	4,56E-02
ENSG00000159363	ATP13A2	-0,253	4,56E-02
ENSG00000140320	BAHD1	-0,214	4,57E-02
ENSG00000171703	TCEA2	-0,265	4,58E-02
ENSG00000106560	GIMAP2	-0,516	4,58E-02
ENSG00000035115	SH3YL1	-0,353	4,58E-02
ENSG00000278233	RNA5-8S5	-0,570	4,58E-02
ENSG00000278189	RNA5-8S5	-0,570	4,58E-02
ENSG00000277739	RNA5-8S5	-0,570	4,58E-02

ENSG00000276700	RNA5-8S5	-0,570	4,59E-02
ENSG00000113163	COL4A3BP	-0,219	4,59E-02
ENSG00000275757	RNA5-8S5	-0,570	4,59E-02
ENSG00000118965	WDR35	-0,654	4,59E-02
ENSG00000275215	RNA5-8S5	-0,570	4,59E-02
ENSG00000171843	MLLT3	0,287	4,59E-02
ENSG00000094631	HDAC6	-0,236	4,59E-02
ENSG00000274917	RNA5-8S5	-0,570	4,60E-02
ENSG00000273730	RNA5-8S5	-0,571	4,60E-02
ENSG00000090238	YPEL3	-0,240	4,62E-02
ENSG00000186866	POFUT2	-0,238	4,63E-02
ENSG00000239213	NCK1-AS1	0,348	4,64E-02
ENSG00000135925	WNT10A	0,353	4,64E-02
ENSG00000118308	LRMP	0,258	4,65E-02
ENSG00000172301	COPRS	0,255	4,66E-02
ENSG00000136754	ABI1	0,237	4,68E-02
ENSG00000089916	GPATCH2L	-0,248	4,68E-02
ENSG00000196968	FUT11	0,307	4,68E-02
ENSG00000185028	LRRC14B	0,349	4,68E-02
ENSG00000260280	SLX1B-SULT1A4	-0,444	4,69E-02
ENSG00000224470	ATXN1L	-0,257	4,69E-02
ENSG00000107902	LHPP	0,389	4,69E-02
ENSG00000163655	GMPS	0,255	4,71E-02
ENSG00000100429	HDAC10	-0,256	4,71E-02
ENSG00000132970	WASF3	0,324	4,72E-02
ENSG00000183426	NPIPA1	-0,236	4,72E-02
ENSG00000264112		-0,447	4,73E-02
ENSG00000124193	SRSF6	-0,246	4,73E-02
ENSG00000214021	TTLL3	-0,291	4,73E-02
ENSG00000165732	DDX21	-0,220	4,74E-02
ENSG00000170456	DENND5B	0,283	4,75E-02
ENSG00000174996	KLC2	-0,217	4,75E-02
ENSG00000205885	C1RL-AS1	-0,388	4,76E-02
ENSG00000166575	TMEM135	0,202	4,77E-02
ENSG00000233695	GAS6-AS1	-0,345	4,77E-02
ENSG00000182247	UBE2E2	0,267	4,79E-02
ENSG00000273398		-0,468	4,79E-02
ENSG00000006625	GGCT	0,298	4,79E-02
ENSG00000185432	METTL7A	0,254	4,79E-02
ENSG00000173848	NET1	0,211	4,79E-02
ENSG00000137804	NUSAP1	0,203	4,80E-02
ENSG00000166582	CENPV	0,253	4,80E-02
ENSG00000183010	PYCR1	-0,217	4,80E-02
ENSG00000102098	SCML2	0,194	4,81E-02
ENSG00000146828	SLC12A9	-0,233	4,81E-02

ENSG00000265298		-0,585	4,82E-02
ENSG00000263327	TAPT1-AS1	0,401	4,82E-02
ENSG00000085511	MAP3K4	0,252	4,84E-02
ENSG00000196576	PLXNB2	0,194	4,84E-02
ENSG00000182379	NXPH4	0,264	4,84E-02
ENSG00000163513	TGFBR2	0,238	4,85E-02
ENSG00000141384	TAF4B	0,214	4,85E-02
ENSG00000100104	SRRD	0,228	4,86E-02
ENSG00000167984	NLRC3	0,187	4,87E-02
ENSG00000110080	ST3GAL4	0,419	4,87E-02
ENSG00000164300	SERINC5	-0,192	4,87E-02
ENSG00000185480	PARPBP	0,224	4,88E-02
ENSG00000139182	CLSTN3	-0,237	4,88E-02
ENSG00000250251	PKD1P6	-0,239	4,89E-02
ENSG00000102401	ARMCX3	-0,227	4,89E-02
ENSG00000165494	PCF11	-0,235	4,89E-02
ENSG00000049089	COL9A2	-0,299	4,90E-02
ENSG00000065457	ADAT1	0,245	4,90E-02
ENSG00000232613		0,542	4,90E-02
ENSG00000196074	SYCP2	-0,701	4,90E-02
ENSG00000105298	CACTIN	-0,222	4,90E-02
ENSG00000189007	ADAT2	-0,266	4,91E-02
ENSG00000141030	COPS3	0,222	4,91E-02
ENSG00000058056	USP13	0,209	4,92E-02
ENSG00000114790	ARHGEF26	0,691	4,92E-02
ENSG00000011478	QPCTL	0,235	4,93E-02
ENSG00000100297	MCM5	0,236	4,94E-02
ENSG00000205746		-0,274	4,94E-02
ENSG00000175895	PLEKHF2	0,202	4,95E-02
ENSG00000115128	SF3B6	-0,213	4,96E-02
ENSG00000006534	ALDH3B1	-0,498	4,96E-02
ENSG00000103335	PIEZO1	-0,212	4,97E-02
ENSG00000216775		-0,296	4,97E-02
ENSG00000104738	MCM4	0,260	4,98E-02
ENSG00000010818	HIVEP2	0,183	4,99E-02

Annex 3. Table of the differentially expressed proteins (FDR<10%) in miR-28 overexpressing BL cells versus Control BL cells

Gene Name	Ensembl Gene ID	FDR
A1BG	ENSG00000121410	0,0127
A2M	ENSG00000175899	0,0425
ABAT	ENSG00000183044	0,0341
ABCC5	ENSG00000114770	0,0000
ABHD16A	ENSG00000235676	0,0000
ABHD16A	ENSG00000204427	0,0000
ABHD16A	ENSG00000236063	0,0000
ABHD16A	ENSG00000206403	0,0000
ABHD16A	ENSG00000224552	0,0000
ABHD16A	ENSG00000231488	0,0000
ABHD16A	ENSG00000230475	0,0000
ACSBG1	ENSG00000103740	0,0632
ACTG1	ENSG00000184009	0,0330
AKT2	ENSG00000105221	0,0320
ALB	ENSG00000163631	0,0023
ALKBH6	ENSG00000239382	0,0324
ANAPC11	ENSG00000141552	0,0089
ANKRD39	ENSG00000213337	0,0022
APOM	ENSG00000235754	0,0114
APOM	ENSG00000227567	0,0114
APOM	ENSG00000204444	0,0114
APOM	ENSG00000206409	0,0114
APOM	ENSG00000231974	0,0114
APOM	ENSG00000226215	0,0114
APOM	ENSG00000224290	0,0114
ARHGAP19	ENSG00000213390	0,0086
ARL6IP4	ENSG00000182196	0,0896
ATP6AP2	ENSG00000182220	0,0096
BBS9	ENSG00000122507	0,0000
BCL11A	ENSG00000119866	0,0499
BCL6B	ENSG00000161940	0,0076
BCL7C	ENSG00000099385	0,0000
BRAT1	ENSG00000106009	0,0423
BTBD1	ENSG00000064726	0,0076
BTF3	ENSG00000145741	0,0097
C16orf13	ENSG00000130731	0,0001
C19orf25	ENSG00000119559	0,0006
C1orf140	ENSG00000234754	0,0000
C5orf30	ENSG00000181751	0,0436
CALM1	ENSG00000198668	0,0636
CAMK2A	ENSG00000070808	0,0810
CASP2	ENSG00000106144	0,0067
CCDC106	ENSG00000173581	0,0273

CCDC81	ENSG00000149201	0,0042
CCDC88B	ENSG00000168071	0,0113
CCK	ENSG00000187094	0,0495
CCNDBP1	ENSG00000166946	0,0017
CCNYL1	ENSG00000163249	0,0325
CCRN4L	ENSG00000151014	0,0000
CD74	ENSG00000019582	0,0982
CDC20	ENSG00000117399	0,0008
CDC25C	ENSG00000158402	0,0396
CDC6	ENSG00000094804	0,0223
CENPB	ENSG00000125817	0,0113
CENPP	ENSG00000188312	0,0484
CHEK1	ENSG00000149554	0,0415
CHIC2	ENSG00000109220	0,0583
CHMP6	ENSG00000176108	0,0708
CHURC1	ENSG00000258289	0,0013
CKAP2L	ENSG00000169607	0,0040
CLUH	ENSG00000132361	0,0000
CNTD2	ENSG00000105219	0,0000
CNTN3	ENSG00000113805	0,0000
COPZ2	ENSG00000005243	0,0000
COX17	ENSG00000138495	0,0426
CSNK1A1	ENSG00000113712	0,0000
CXorf57	ENSG00000147231	0,0048
CYBA	ENSG00000051523	0,0000
CYP51A1	ENSG00000001630	0,0143
DAZAP2	ENSG00000183283	0,0000
DBI	ENSG00000155368	0,0034
DCD	ENSG00000161634	0,0005
DCLRE1B	ENSG00000118655	0,0354
DENND2D	ENSG00000162777	0,0578
DENND4B	ENSG00000198837	0,0972
DERL1	ENSG00000136986	0,0733
DHPS	ENSG00000095059	0,0940
DHRS7	ENSG00000100612	0,0905
DIP2A	ENSG00000160305	0,0140
DSC2	ENSG00000134755	0,0094
DSCC1	ENSG00000136982	0,0217
E2F4	ENSG00000205250	0,0425
EDRF1	ENSG00000107938	0,0914
EFCAB13	ENSG00000178852	0,0000
ELF1	ENSG00000120690	0,0149
ELL3	ENSG00000128886	0,0686
ERVFRD-1	ENSG00000244476	0,0002
ESD	ENSG00000139684	0,0788
ESPL1	ENSG00000135476	0,0033

FBXO30	ENSG00000118496	0,0917
FCHSD2	ENSG00000137478	0,0317
FLYWCH1	ENSG00000059122	0,0495
FPGS	ENSG00000136877	0,0094
FYTTD1	ENSG00000122068	0,0000
G3BP2	ENSG00000138757	0,0708
GAB1	ENSG00000109458	0,0393
GBA	ENSG00000262446	0,0095
GEMIN8	ENSG00000046647	0,0577
GLB1L3	ENSG00000166105	0,0012
GNL3L	ENSG00000130119	0,0100
GPATCH1	ENSG00000076650	0,0044
GPHN	ENSG00000171723	0,0883
GRIP2	ENSG00000144596	0,0000
GSDMA	ENSG00000167914	0,0745
GTSF1	ENSG00000170627	0,0223
HBA1	ENSG00000206172	0,0000
HDGFRP2	ENSG00000167674	0,0772
HERPUD1	ENSG00000051108	0,0089
HIST1H1A	ENSG00000124610	0,0000
HIST1H1C	ENSG00000187837	0,0000
HIST1H1E	ENSG00000168298	0,0004
HIST1H2AD	ENSG00000196866	0,0533
HIST1H2BC	ENSG00000158373	0,0044
HIST3H3	ENSG00000168148	0,0030
HLCS	ENSG00000159267	0,0224
HMGB2	ENSG00000164104	0,0788
HMGN5	ENSG00000198157	0,0000
HNRNPD	ENSG00000138668	0,0216
HSP90AA5P	ENSG00000205955	0,0886
HSP90AB3P	ENSG00000183199	0,0755
HTR2B	ENSG00000135914	0,0632
IFRG15	ENSG00000169905	0,0240
IGHM	ENSG00000211899	0,0288
IGJ	ENSG00000132465	0,0833
IGLL5	ENSG00000254709	0,0000
IL17RB	ENSG00000056736	0,0093
IL4R	ENSG00000077238	0,0051
ILF3	ENSG00000129351	0,0585
INPP5K	ENSG00000132376	0,0918
IP6K1	ENSG00000176095	0,0699
ITGB7	ENSG00000139626	0,0710
JARID2	ENSG00000008083	0,0000
JPH4	ENSG00000092051	0,0048
KANK1	ENSG00000107104	0,0818
KCNG1	ENSG00000026559	0,0000

KDM5A	ENSG00000073614	0,0709
KLHDC3	ENSG00000124702	0,0002
KLHL38	ENSG00000175946	0,0900
KLHL6	ENSG00000172578	0,0032
KRT1	ENSG00000167768	0,0005
KRT10	ENSG00000186395	0,0000
KRT13	ENSG00000171401	0,0018
KRT17	ENSG00000128422	0,0011
KRT5	ENSG00000186081	0,0005
LARP4	ENSG00000161813	0,0211
LDHA	ENSG00000134333	0,0660
LIMD2	ENSG00000136490	0,0842
LOH12CR2	ENSG00000205791	0,0000
LPGAT1	ENSG00000123684	0,0045
LPHN3	ENSG00000150471	0,0699
LRRC58	ENSG00000163428	0,0495
LXN	ENSG00000079257	0,0494
MANF	ENSG00000145050	0,0995
MAP4	ENSG00000047849	0,0677
MAP9	ENSG00000164114	0,0001
MAX	ENSG00000125952	0,0033
MBD3	ENSG00000071655	0,0142
MDH1	ENSG00000014641	0,0590
METAP2	ENSG00000111142	0,0771
MFN1	ENSG00000171109	0,0018
MICALL1	ENSG00000100139	0,0440
MID1IP1	ENSG00000165175	0,0023
MORF4L1	ENSG00000185787	0,0366
MOV10L1	ENSG00000073146	0,0000
MRFAP1	ENSG00000179010	0,0053
MSMO1	ENSG00000052802	0,0635
MTMR3	ENSG00000100330	0,0001
MTR	ENSG00000116984	0,0505
MUS81	ENSG00000172732	0,0200
MVP	ENSG00000013364	0,0008
NARF	ENSG00000141562	0,0000
NBPF7	ENSG00000215864	0,0000
NDUFA1	ENSG00000125356	0,0660
NNT	ENSG00000112992	0,0000
NRAP	ENSG00000197893	0,0001
NRIP1	ENSG00000180530	0,0217
NTHL1	ENSG00000065057	0,0274
NUDT4	ENSG00000173598	0,0000
NUP93	ENSG00000102900	0,0004
NXF1	ENSG00000162231	0,0000
OCRL	ENSG00000122126	0,0918

OR51V1	ENSG00000176742	0,0002
ORMDL2	ENSG00000123353	0,0880
PACS1	ENSG00000175115	0,0055
PAN2	ENSG00000135473	0,0017
PCDHGA6	ENSG00000253731	0,0904
PCGF2	ENSG00000278644	0,0051
PCGF2	ENSG00000277258	0,0051
PDAP1	ENSG00000106244	0,0561
PER2	ENSG00000132326	0,0425
PIGO	ENSG00000165282	0,0382
PIWIL2	ENSG00000197181	0,0364
PKMYT1	ENSG00000127564	0,0899
PLCD3	ENSG00000161714	0,0000
PLK1	ENSG00000166851	0,0171
PMS1	ENSG00000064933	0,0363
POLK	ENSG00000122008	0,0000
POLM	ENSG00000122678	0,0497
POLR2M	ENSG00000255529	0,0009
POMP	ENSG00000132963	0,0908
PQLC3	ENSG00000162976	0,0217
PRMT10	ENSG00000164169	0,0006
PROCR	ENSG00000101000	0,0657
PRR4	ENSG00000277454	0,0000
PRR4	ENSG00000263247	0,0000
PRR4	ENSG00000111215	0,0000
PSAT1	ENSG00000135069	0,0623
PSD4	ENSG00000125637	0,0754
PSIP1	ENSG00000164985	0,0018
PSMD4	ENSG00000159352	0,0884
PTMA	ENSG00000187514	0,0435
PTPN18	ENSG00000072135	0,0089
PTTG1	ENSG00000164611	0,0000
RANBP17	ENSG00000204764	0,0001
RBM38	ENSG00000132819	0,0434
RNF14	ENSG00000013561	0,0000
RNF149	ENSG00000163162	0,0871
RPAP2	ENSG00000122484	0,0623
RPL35	ENSG00000136942	0,0500
RPP25L	ENSG00000164967	0,0372
RPS27A	ENSG00000143947	0,0038
RSL24D1	ENSG00000137876	0,0311
RTN4	ENSG00000115310	0,0000
RTTN	ENSG00000176225	0,0003
S1PR2	ENSG00000267534	0,0240
SAMD9L	ENSG00000177409	0,0123
SCNN1G	ENSG00000166828	0,0910

SDR16C5	ENSG00000170786	0,0051
SEL1L3	ENSG00000091490	0,0011
SELO	ENSG00000073169	0,0538
SETD5	ENSG00000168137	0,0428
SETMAR	ENSG00000170364	0,0000
SFT2D3	ENSG00000173349	0,0096
SFXN5	ENSG00000144040	0,0000
SHCBP1	ENSG00000171241	0,0563
SIPA1L2	ENSG00000116991	0,0000
SKP2	ENSG00000145604	0,0051
SLC4A7	ENSG00000033867	0,0019
SMTNL2	ENSG00000188176	0,0891
SNX17	ENSG00000115234	0,0010
SOAT1	ENSG00000057252	0,0055
SPAG5	ENSG00000076382	0,0880
SPATA7	ENSG00000042317	0,0002
SPG21	ENSG00000090487	0,0658
SPTY2D1	ENSG00000179119	0,0291
SREBF2	ENSG00000198911	0,0191
SRY	ENSG00000184895	0,0142
SULT2B1	ENSG00000088002	0,0260
SYNM	ENSG00000182253	0,0581
TADA2B	ENSG00000173011	0,0014
TAT	ENSG00000198650	0,0003
TBC1D23	ENSG00000036054	0,0000
TFAP2A	ENSG00000137203	0,0016
TFB2M	ENSG00000162851	0,0806
TIMM17A	ENSG00000134375	0,0171
TKTL1	ENSG00000007350	0,0000
TLR9	ENSG00000239732	0,0950
TMEM123	ENSG00000152558	0,0768
TNFSF11	ENSG00000120659	0,0012
TPD52	ENSG00000076554	0,0423
TPI1	ENSG00000111669	0,0586
TPM1	ENSG00000140416	0,0646
TRABD	ENSG00000170638	0,0994
TRIM9	ENSG00000100505	0,0080
TRPM4	ENSG00000130529	0,0491
TSEN54	ENSG00000182173	0,0000
TTC12	ENSG00000149292	0,0005
TTLL11	ENSG00000175764	0,0122
TUT1	ENSG00000149016	0,0080
TVP23C	ENSG00000175106	0,0000
TXNDC15	ENSG00000113621	0,0580
UBE2S	ENSG00000108106	0,0808
UBE2T	ENSG00000077152	0,0633

URM1	ENSG00000167118	0,0002
USP1	ENSG00000162607	0,0127
USP46	ENSG00000109189	0,0000
VPS53	ENSG00000141252	0,0032
WARS2	ENSG00000116874	0,0241
WDR25	ENSG00000176473	0,0141
WDR54	ENSG00000005448	0,0007
WDR7	ENSG00000091157	0,0429
XXYLT1	ENSG00000173950	0,0905
YWHAE	ENSG00000108953	0,0708
YWHAE	ENSG00000274474	0,0708
YWHAZ	ENSG00000164924	0,0187
YWHAZ	ENSG00000164924	0,0000
ZBED1	ENSG00000214717	0,0239
ZC3H12C	ENSG00000149289	0,0000
ZNF48	ENSG00000180035	0,0899
ZNF532	ENSG00000074657	0,0000

Regular Article

IMMUNOBIOLOGY

miR-217 is an oncogene that enhances the germinal center reaction

Virginia G. de Yébenes,[1] Nahikari Bartolomé-Izquierdo,[1] Rubén Nogales-Cadenas,[2] Pablo Pérez-Durán,[1] Sonia M. Mur,[1] Nerea Martínez,[3] Lorena Di Lisio,[3] Davide F. Robbiani,[4] Alberto Pascual-Montano,[2] Marta Cañamero,[5] Miguel A. Piris,[3] and Almudena R. Ramiro[1]

[1]B Cell Biology Laboratory, Centro Nacional de Investigaciones Cardiovasculares, Madrid, Spain; [2]Functional Bioinformatics Group, National Center for Biotechnology-Consejo Superior de Investigaciones Científicas, Madrid, Spain; [3]Genomica del Cancer, Instituto de Investigación y Formación Marqués de Valdecilla, Santander, Spain; [4]Laboratory of Molecular Immunology, The Rockefeller University, New York, NY; and [5]Comparative Pathology Unit, Spanish National Cancer Research Centre, Madrid, Spain

Key Points

- miR-217 enhances the GC reaction by dampening genotoxic-induced Bcl-6 degradation in GC B cells.
- miR-217 is an oncogene and its overexpression provides a model of miRNA-induced mature B-cell lymphomagenesis.

microRNAs are a class of regulators of gene expression that have been shown critical for a great number of biological processes; however, little is known of their role in germinal center (GC) B cells. Although the GC reaction is crucial to ensure a competent immune response, GC B cells are also the origin of most human lymphomas, presumably due to bystander effects of the immunoglobulin gene remodeling that takes place at these sites. Here we report that miR-217 is specifically upregulated in GC B cells. Gain- and loss-of-function mouse models reveal that miR-217 is a positive modulator of the GC response that increases the generation of class-switched antibodies and the frequency of somatic hypermutation. We find that miR-217 downregulates the expression of a DNA damage response and repair gene network and in turn stabilizes Bcl-6 expression in GC B cells. Importantly, miR-217 overexpression also promotes mature B-cell lymphomagenesis; this is physiologically relevant as we find that miR-217 is overexpressed in aggressive human B-cell lymphomas. Therefore, miR-217 provides a novel molecular link between the normal GC response and B-cell transformation. (*Blood*. 2014; 124(2):229-239)

Introduction

microRNAs (miRNAs) are negative regulators of gene expression that influence virtually all biological processes. A high proportion of human miRNAs are located in cancer-associated genomic regions,[1] and deregulated miRNA expression is a hallmark of most cancer types, including lymphomas.[2-4] Indeed, miRNA profiling is increasingly recognized as a valuable tool for the classification and even prognosis of lymphoma. However, the role of specific miRNAs in the development of B-cell lymphoma has rarely been addressed in vivo;[5] specifically, functional evidence for the involvement of miRNAs in the development of mature B-cell lymphomas is very scarce. This void is particularly important because the vast majority of human B-cell lymphomas originate from mature B cells.

The predominance of mature B-cell lymphomas is most likely due to the unique molecular events taking place in B cells during the immune response. B cells generate a hugely diverse repertoire of antibodies, which enable specific immune responses against virtually any pathogen the organism may encounter. Antibody diversity is achieved in 2 stages. The first takes place during B-cell differentiation through V(D)J recombination. The second stage is unique to mature B cells that have encountered antigen and takes place in germinal centers (GCs), allowing the generation of higher affinity memory B cells and plasma cells.

The GC reaction involves the clonal expansion of antigen-specific B lymphocytes and the generation of B-cell subclones with related antigen specificities, from which those expressing immunoglobulins with improved affinity for the antigen are positively selected.[6] Molecularly, this is triggered by the so-called somatic hypermutation (SHM), which introduces point mutations on the variable region of the Ig molecule—responsible for antigen recognition. In addition, GCs are the home of the class switch recombination (CSR) reaction, a region-specific recombination reaction between 2 switch regions of the immunoglobulin heavy chain (IgH) locus that generates antibodies with different isotypes. SHM and CSR are both initiated by activation-induced deaminase (AID), which deaminates cytosines on the immunoglobulin locus.[7] This initial lesion on DNA is subsequently processed by DNA repair and recombination factors to allow the fixation of a mutation, in the case of SHM, or the generation of a DNA double-strand break and a recombination reaction, in the case of CSR.[8]

The fact that inactivation of AID causes an immunodeficiency in humans[9] highlights the importance of the GC reaction in the immune response. However, the generation of mutations and double-strand breaks associated with the GC reaction entails a risk for the genome

Submitted December 10, 2013; accepted April 23, 2014. Prepublished online as *Blood* First Edition paper, May 21, 2014; DOI 10.1182/blood-2013-12-543611.

The online version of this article contains a data supplement.

There is an Inside *Blood* Commentary on this article in this issue.

The publication costs of this article were defrayed in part by page charge payment. Therefore, and solely to indicate this fact, this article is hereby marked "advertisement" in accordance with 18 USC section 1734.

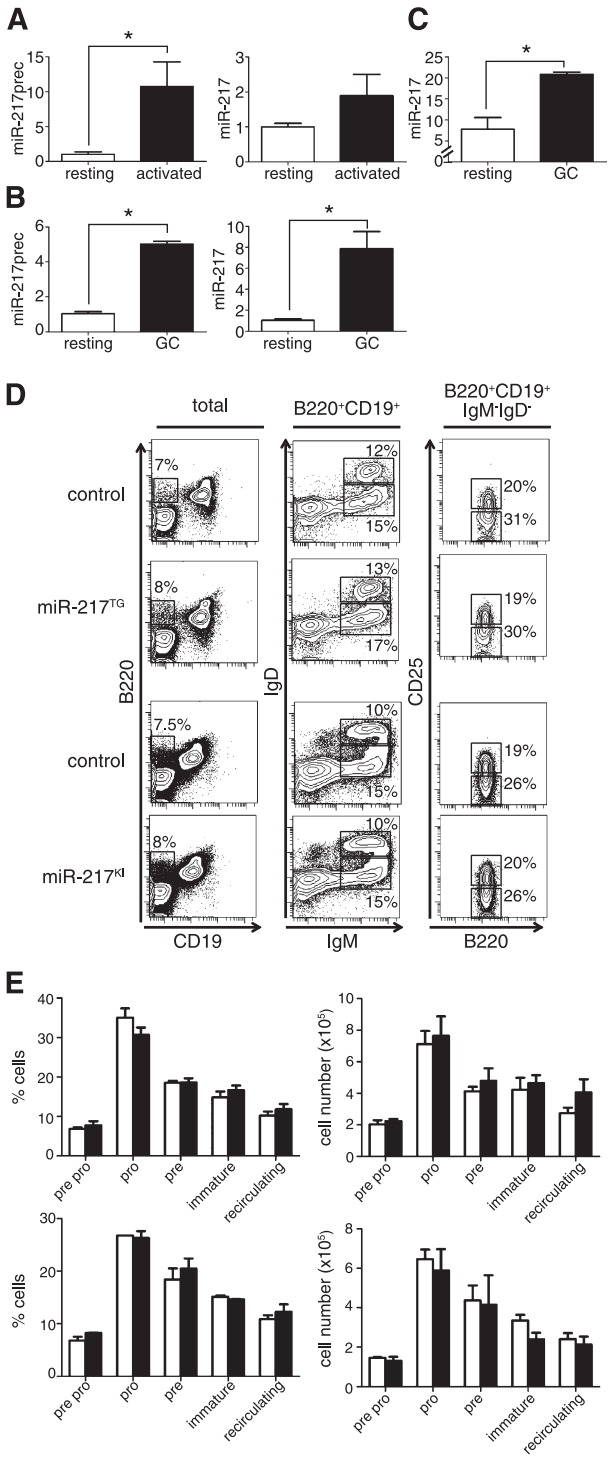

Figure 1. miR-217 expression is upregulated in activated B cells. (A) qRT-PCR analysis of the expression of the (left) miR-217 precursor and (right) mature miR-217 in B cells after 1 (open bars) and 3 days (filled bars) of activation with LPS + IL4. Data from 3 (miR-217 precursor) and 2 (mature miR-217) independent experiments are shown ($P = .05$ for miR-217 precursor and $P = .27$ for miR-217). Each experiment was performed with 2 individual mice. (B) qRT-PCR of the (left) miR-217 precursor and (right) mature miR-217 in resting (open bars) or GC (filled bars) B cells isolated from spleens of wild-type C57BL/6 mice 10 days after immunization with sheep red blood cells. Data are means ± standard deviation from 2 independent experiments with 10 total immunized mice ($P = .0002$ for miR-217 precursor and $P = .01$ for miR-217). Two-tailed Student *t* test: *P* values: $^*P < .05$. (C) Quantification of miR-217 expression in human resting ($CD19^+CD27^-IgD^-$) and GC ($CD19^+CD10^+$) samples as measured by miRNA array hybridization (data were obtained from GSE29493, $P = .003$, 2-tailed Student *t* test). (D) Representative fluorescence-activated cell sorter (FACS) analysis of bone marrow from miR-217^{TG}, miR-217^{KI} and littermate control mice. Plots show the expression of (left) B220/CD19 in total live lymphocytes, (center) IgD/IgM gated in $B220^+CD19^+$ cells, and (right) CD25/B220 gated in $B220^+CD19^+IgM^-IgD^-$ cells. The proportion of cells is indicated in each gated in $B220^+$ cells. (E) Quantification of the proportions and absolute cell numbers of developing bone marrow B-cell subsets in control (open bars), (upper) miR-217^{TG} (filled bars), and (lower) miR-217^{KI} mice (filled bars). The proportions of different B-cell subsets were quantified within the $B220^+$ population.

integrity of mature B lymphocytes, resulting in a permissive environment for lymphomagenesis.[10-12] Indeed, the most prominent hallmark of mature B-cell lymphomas is the presence of recurrent chromosomal translocations that involve the immunoglobulin locus and an oncogene.[13,14] These illegitimate junctions are a direct consequence of AID activity in the GC reaction, because AID deficiency prevents the generation of c-myc-IgH translocations associated with Burkitt lymphoma (BL)[15-17] and reduces the incidence of mature B-cell lymphoma in different mouse models.[15,18] In addition, Bcl-6, a transcriptional repressor indispensable for the GC reaction, seems to provide an environment tolerant to the DNA damage associated with AID-dependent events, which contributes to its oncogenic activity.[19] Remarkably, close to 80% of all human B-cell lymphomas originate from B cells that are GC experienced—generally known as mature B-cell lymphomas[13]—the most aggressive of which are BL and diffuse large B-cell lymphomas (DLBCLs).

Tight regulation of the GC reaction is thus critical with regard both to the efficacy of the immune response and to lymphoma development. miRNAs promote subtle changes in gene expression through imperfect pairing with their target mRNAs.[20,21] Very often a single miRNA can bind hundreds of different target mRNAs, thus acting as a regulator of a gene network rather than individual genes.[20,22] miRNAs have previously been implicated in the regulation of the immune response and tumorigenic processes and mice whose GC B cells are depleted of miRNAs mount inefficient GC responses.[23] However, there is little direct evidence for the role of individual miRNAs in this context, and to date, only miR-155 has been clearly associated with the GC response.[24-26] Here we show that miR-217 is upregulated after in vitro and in vivo stimulation of mature B cells. Using gain and loss of function in vivo models, we found that miR-217 is a positive regulator of the GC reaction and an oncogene in GC B cells.

Methods

miR-217 detection by miRNA microarray hybridization and quantitative reverse transcriptase-polymerase chain reaction

RNA was extracted with Trizol (Invitrogen). Mouse miRNA microarray analysis was performed with paired samples of nonstimulated and stimulated B cells.[27] For quantitative reverse transcriptase-polymerase chain reaction (qRT-PCR) of the miR-217 precursor, total RNA was converted to cDNA using random primers (Roche), reversed transcribed with SuperScript II (Invitrogen), and quantified by SYBR Green assay (Applied Biosystems). Primers are detailed in supplemental Methods available on the *Blood* Web site. Mature miR-217 was quantified from total RNA with miR-217 miRCURY LNA primers (Exiqon). U6 and sno-142 (Exiqon) were used as normalization controls.

T cell-dependent immunizations

Groups of 7 to 9 littermate mice were immunized by footpad injection with 50 μg of 4-hydroxy-3-nitrophenylacetyl (NP) hapten conjugated to chicken γ globulin (NP-CGG; Biosearch Technologies) in complete Freund's adjuvant.

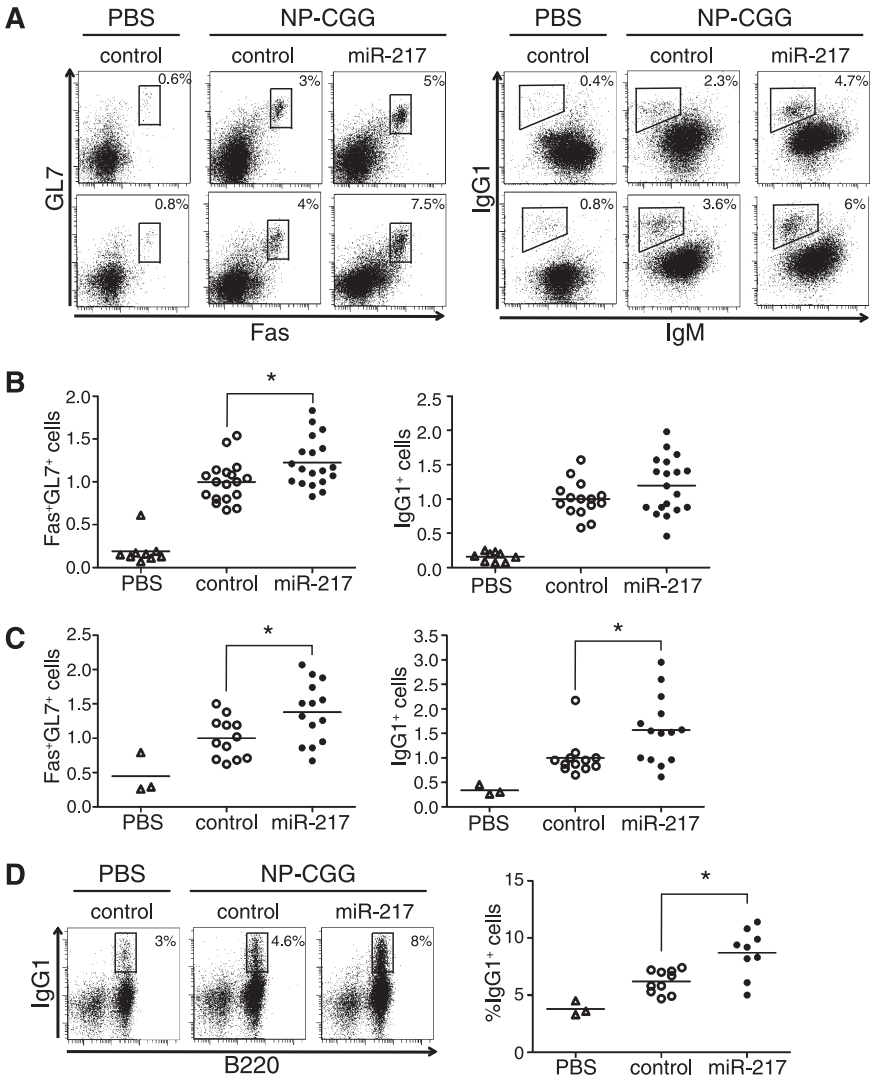

Figure 2. miR-217 expression in B cells enhances the GC response. (A) Representative FACS analysis of B220$^+$ lymphocytes in lymph nodes after primary (upper) or secondary (lower) NP-CGG immunization of miR-217^{TG} mice or littermate controls. (B) miR-217^{TG} mice (closed circles) or littermate controls (open circles) were immunized by subcutaneous injection of NP-CGG in complete Freund's adjuvant, and 14 days after immunization, lymph nodes were analyzed for the presence of GC B cells (Fas$^+$GL7$^+$) and switched B cells (IgG1$^+$). Mice injected with PBS (open triangles) were used as nonimmunized controls. Each symbol represents an individual mouse. Data were normalized to the mean value of control mice in each experiment; results are shown for a total of 4 experiments performed with 4 independent miR-217^{TG} mouse lines (P = .01 for GC B cells and P = .08 for switched B cells). (C) Fourteen days after a primary immunization as in B, mice were reimmunized by subcutaneous injection of NP-CGG and analyzed 7 days later. Symbol code as in B. Data from 2 independent experiments was normalized to the mean response of control mice in each experiment (P = .019 for GC and P = .018 for switched B cells). (D) Spleen memory IgG1$^+$ B cells analyzed by flow cytometry 1 year after NP-CGG immunization of miR-217^{KI} mice. The FACS plots show the frequency of cells in the gate referred to proportion within B220$^+$ cells. Symbol code as in B (P = .003).

Mice were euthanized 14 days after immunization for analysis of primary response or were reimmunized with 50 μg of NP-CGG in incomplete Freund's adjuvant.

Somatic mutation analysis

For analysis of mutations at the Sμ and J_H4 regions, GC B cells were purified by cell sorting of pooled Peyer's patches (4-6 animals per genotype). DNA was extracted, and the Sμ and J_H4 regions were PCR-amplified using specific oligonucleotides (supplemental Methods). Amplification products were purified and sequenced by next-generation sequencing (NGS)[28] or cloned and sequenced by conventional Sanger sequencing.

RNAseq analysis and miRNA target prediction

GC (CD19$^+$Fas$^+$GL7$^+$) B cells from pooled Peyer's patches (4-6 animals per genotype) from control and miR-217^{TG} mice were isolated by cell sorting. Total RNA was extracted with Trizol (Invitrogen) and sequenced by RNAseq. Differential expression analysis was done using the edgeR package from Bioconductor,[29] and genes with $P \leq .05$ were considered for analysis. Pathway analysis of the significantly up- and downregulated genes in miR-217^{TG} vs control GC B cells was performed by ingenuity pathway analysis software (Ingenuity Systems).

Significantly downregulated genes in miR-217^{TG} GC B cells were analyzed for the presence of 835 different miRNAs target sites based on predicted and experimentally validated miRNA-mRNA interactions. Scores for every predictive algorithm were normalized, and the compound score of predictive and experimental databases was calculated.[30] See supplemental Methods for more details.

miR-217 expression in Ramos cells, immunobloting, and cell cycle analysis

Ramos cells were transduced with miR-217 pmiRNA or control vectors[27] and selected by green fluorescent protein (GFP) expression by flow-activated cell sorting (FACS). Cells were treated for 6 hours with etoposide (Sigma-Aldrich) in the presence or absence of caffeine (Sigma-Aldrich), lysed in radioimmunoprecipitation assay buffer, and immunobloted with anti-Bcl-6 (N-3; Santa Cruz Biotechnology) or α-tubulin (Sigma-Aldrich) antibodies or fixed overnight with 70% ethanol and stained with 2.5 μg/mL 4′,6 diamidino-2-phenylindole for flow cytometry cell cycle analysis.

Human samples and animal procedures

The use of human samples was approved by the ethics committee of the Instituto de Salud Carlos III. The study was conducted in accordance with the Declaration of Helsinki.

All animal procedures conformed to European Union Directive 2010/63EU and Recommendation 2007/526/EC regarding the protection of animals used for experimental and other scientific purposes, enforced in Spanish law under Real Decreto 1201/2005.

Results

miR-217 expression is upregulated in activated B cells

To identify miRNAs that play a role during B-cell activation, we profiled miRNA expression in mature B cells during in vitro activation with lipopolysaccharide (LPS) + interleukin (IL)4, which promotes AID expression, SHM in the switch regions, and CSR. Microarray analysis showed that one of the few miRNAs whose expression is upregulated during this process is miR-217[27] (supplemental Figure 1A). Induction of precursor and mature miR-217 during B-cell activation in vitro was confirmed by qRT-PCR (Figure 1A). In addition, we generated GCs in vivo by immunizing mice with sheep red blood cells and conducted qRT-PCR on purified resting and GC B cells. miR-217 precursor and mature miR-217 expression increased by five- and eightfold, respectively, in GC cells (Figure 1B). Similarly, we found that miR-217 expression is increased in GC human B cells compared with resting B cells (Figure 1C). Together, these results show that miR-217 expression is induced during B-cell activation both in mouse and humans.

Generation of B cell-specific miR-217 mouse models

To investigate the role of miR-217 during B-cell activation, we generated 2 independent mouse models of B cell-specific miR-217 overexpression. In the first, 4 independent transgenic mouse lines were generated with a construct encoding the miR-217 precursor and a GFP reporter gene under the control of regulatory elements of the mouse κ light chain (Igκ) gene (miR-217^{TG}). In the second strategy, the miR-217 precursor/GFP construct was preceded by a transcriptional stop cassette flanked by LoxP sites and inserted within the endogenous Rosa26 locus (ROSA26$^{miR217ki/+}$ mice) (supplemental Figure 1B; supplemental Methods); specific expression of miR-217 in B cells was achieved by crossing ROSA26$^{miR217ki/+}$ mice with CD19^{-}Cre$^{ki/+}$ mice (hereafter, miR-217^{KI} mice). ROSA26$^{miR217+/+}$ CD19^{-}Cre$^{ki/+}$ mice were used as controls. B cells from miR-217^{TG} and miR-217^{KI} mice showed full GFP and miR-217 expression in mature splenic B cells (supplemental Figure 1C-D). GFP expression was not detected in non-B-cell lineages, such as T, myeloid, or epithelial cells (data not shown). The proportions and absolute numbers of bone marrow and peripheral B cells in the miR-217^{TG} and miR-217^{KI} models were similar to those in wild-type littermate controls (Figure 1D-E), indicating that the miR-217^{TG} and miR-217^{KI} mouse models allow B cell-specific miR-217 overexpression without perturbing B-cell differentiation.

miR-217 expression enhances the GC reaction

To address the role of miR-217 expression during B-cell activation in GCs, we analyzed the B-cell response to a T cell-dependent antigen in miR-217^{TG} mice. We first immunized miR-217^{TG} mice and wild-type littermate controls with NP-CGG. As an immunization control, mice were injected with phosphate-buffered saline (PBS). The lymph nodes of NP-CGG-immunized wild-type mice contained GC B cells (Fas^{+}GL7^{+}) and B cells that had undergone CSR (IgG1^{+}); but in miR-217^{TG} mice, the response to NP-CGG immunization was greater, with 22% more GC B cells (P = .01) and 20% more IgG1^{+} B cells (P = .08; Figure 2A-B). A similarly enhanced GC response to NP-CGG immunization was found in miR-217^{KI} mice (supplemental Figure 2A). We next analyzed the secondary B-cell immune response in control and miR-217^{TG} mice. The enhancement of the GC reaction in miR-217^{TG} mice was notably greater in secondary

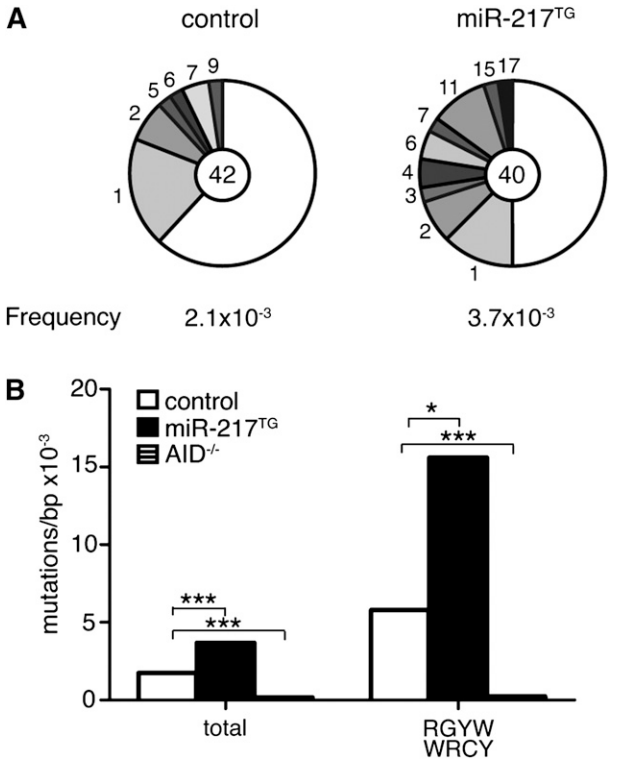

Figure 3. miR-217 expression in B cells enhances SHM. (A-B) Quantification of mutations in the J_H4 intronic sequence of GC (Fas^{+}GL7^{+}) B cells isolated from pooled Peyer's patches of 6 control and 6 miR-217^{TG} mice: (A) Sanger sequencing. Segment sizes in the pie charts are proportional to the number of sequences carrying the number of mutations indicated at the periphery. Mutation frequencies are indicated below each chart, and the total numbers of independent sequences analyzed are indicated in the chart centers. Statistical significance was determined by a 2-tailed Student t test (P = .028). (B) NGS quantification of the total J_H4 mutation frequency and of the mutation frequency at cytosines within the RGYW/WRCY AID hotspots in J_H4 sequences in GC B cells from control (open bars) and miR-217^{TG} mice (filled bars). The mutation frequency in the J_H4 sequence of AID$^{-/-}$ splenic B cells is shown in hatched bars. A total of 300 000 kb/genotype was sequenced. Statistical significance of the mean mutation frequency at each position was determined by a paired Student t test ($P = 1.9 \times 10^{-9}$ for total mutation frequency and P = .002 for mutation frequency at WRCY hotspots).

immunization assays, with 40% more Fas^{+}GL7^{+} B cells and 60% more IgG1^{+}-switched B cells than controls (P = .019 and .018, respectively; Figure 2A,C). In addition, we found that the proportion of CD138^{+} plasma cells is larger in miR-217^{TG} mice than in controls (P = .02; supplemental Figure 2B). To analyze the influence of miR-217 overexpression on the long-lived memory B-cell compartment, we quantified IgG1^{+} B cells in spleens from control and miR-217^{KI} mice 1 year after immunization. The proportion of memory B cells was 40% higher in miR-217^{KI} mice than in controls (P = .003; Figure 2D).

To further characterize the role of miR-217 in the GC reaction, we examined the extent of SHM in miR-217^{TG} mice in vivo. We isolated Fas^{+}GL7^{+} GC B cells from Peyer's patches of control and miR-217^{TG} mice and quantified the mutation frequency in an intronic DNA region downstream of the J_H4 segment of the IgH locus, a region that accumulates mutations but cannot be subject to affinity maturation events. Conventional Sanger sequencing of the J_H4 intronic region showed that miR-217^{TG} B cells have a higher mutation load than wild-type controls (control, 2.1×10^{-3}/bp and miR-217^{TG}, 3.7×10^{-3}/bp, P = .028; Figure 3A). Likewise, GC B cells from miR-217^{KI} mice accumulated more mutations downstream of J_H4 than did wild-type controls (supplemental Figure 2C). Similar results were obtained

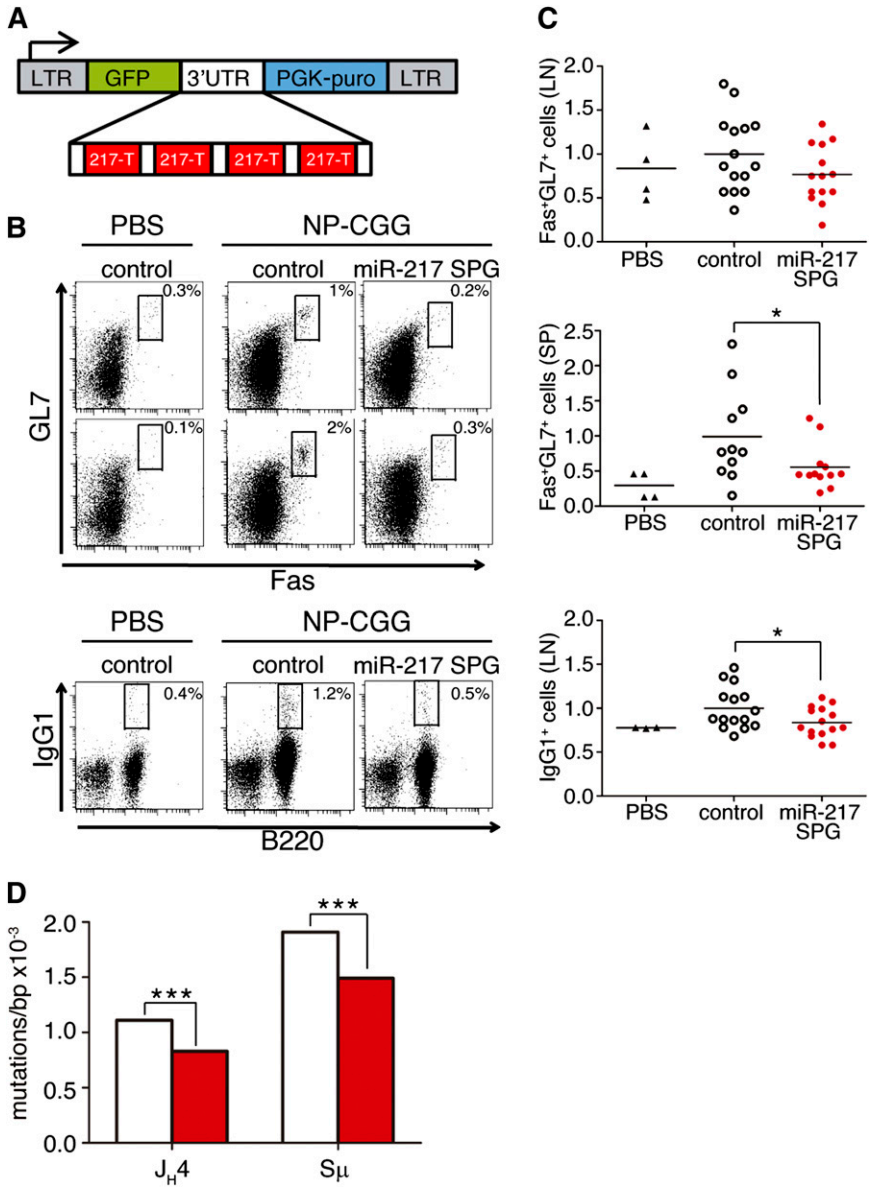

Figure 4. Inhibition of endogenous miR-217 expression in B cells impairs the GC response. (A) miR-217-Sponge (miR-217^{SPG}) retroviral construct. Four miR-217 complementary sites, separated by 4-nt spacers, were placed downstream of GFP in the MGP vector. (B-C) GC response of mouse chimeras reconstituted with control or miR-217^{SPG} retrovirally transduced bone marrow precursors analyzed 14 days after NP-CGG immunization. (B) Representative FACS analysis of B220^{+} GC cells (Fas^{+}GL7^{+}) in (upper) lymph nodes and (lower) spleen and of switched (IgG1^{+}) lymph node cells after NP-CGG immunization. Plots are gated on CD45.1^{+}GFP^{+} cells. (C) Quantification of GC and switched B cells in mouse chimeras reconstituted with control (open circles) or miR-217 ^{SPG} (in red) retrovirally transduced bone marrow precursors. Nonimmunized mice injected with PBS (triangles) were included as immunization controls. Each symbol represents an individual mouse. Data are normalized to the mean response of control mice of 2 independent experiments. Statistical significance was determined by a 2-tailed Student *t* test vs control immunized mice (P = .12 for LN GCs, P = .05 for SP GCs, and P = .04 for switched B-cell generation). (D) NGS quantification of mutations in (left) J_H4 and (right) Sμ sequences in GFP^{+}CD45.1^{+} GC (Fas^{+}GL7^{+}) B cells isolated from pooled Peyer's patches of 8 control (open bars) and 8 miR-217^{SPG} (red bars) mouse chimeras. Data are from 2 (J_H4) and 1 (Sμ) independent experiments. At least 190 000 kb was sequenced per genotype. Statistical significance of the mean total mutation frequency at each position was determined by a paired Student *t* test ($P = 3.7 \times 10^{-5}$ for J_H4 SHM and $P = 4 \times 10^{-4}$ for Sμ SHM).

when we analyzed SHM frequency at the J_H4 intronic region by NGS, which allows large numbers of mutations to be analyzed at very high depth.[28] No mutations were detected in B cells isolated from AID$^{-/-}$ mice, used as a negative control. We detected total mutation frequencies of 1.7×10^{-3}/bp in control animals and 3.7×10^{-3}/bp in miR-217^{TG} mice ($P = 1.9 \times 10^{-9}$), a 2.2-fold difference (Figure 3B). This difference was even higher (2.7-fold) when the analysis was limited to cytosines located in AID mutational hotspots RGYW/WRCY (where R = A/G, Y = C/T, and W = A/T) (5.8×10^{-3}/bp in controls vs 15.6×10^{-3}/bp in miR-217^{TG}; Figure 3B), confirming that miR-217 overexpression in B cells increases the load of SHM in GCs. These results indicate that overexpression of miR-217 in B cells increases the efficiency of GC formation, CSR and SHM, and the generation of terminally differentiated B cells in vivo.

Inhibition of endogenous miR-217 impairs the GC reaction

To address whether endogenous miR-217 expression plays a physiological role in GCs, we generated bone marrow mouse chimeras in which endogenous miR-217 expression was inhibited by the expression of a miR-217 sponge (miR-217^{SPG}) construct (Figure 4A), where sequences complementary to miR-217 were cloned in tandem within the 3′untranslated region of a reporter gene and thus function as competitive inhibitors for the binding of the miRNA to its endogenous binding sites.[31,32] Bone marrow cells from wild-type mice were transduced with miR-217^{SPG} or control retroviruses and transferred into lethally irradiated CD45.1 congenic recipient mice and immunized 4 weeks later with NP-CGG. Chimeric mice injected with PBS were used as immunization negative controls. Spleen and lymph nodes from immunized miR-217^{SPG} mice contained fewer GC and IgG1^{+} switched B cells than immunized control chimeric mice, and indeed, the proportions of these cell subsets in immunized miR-217^{SPG} mice were as low as in PBS-injected, nonimmunized animals (Figure 4B-C). We next analyzed SHM in Peyer's patch GC B cells from miR-217^{SPG} and control chimeric mice by NGS. We found that miR-217^{SPG} GC B cells had a 25% lower mean mutation frequency than control B cells at the J_H4 intronic region ($P = 3.7 \times 10^{-5}$; Figure 4D). Very similar results were obtained when we analyzed the mutation load in a fragment of the μ switch region (Sμ) of IgH ($P = 4 \times 10^{-4}$), where mutations

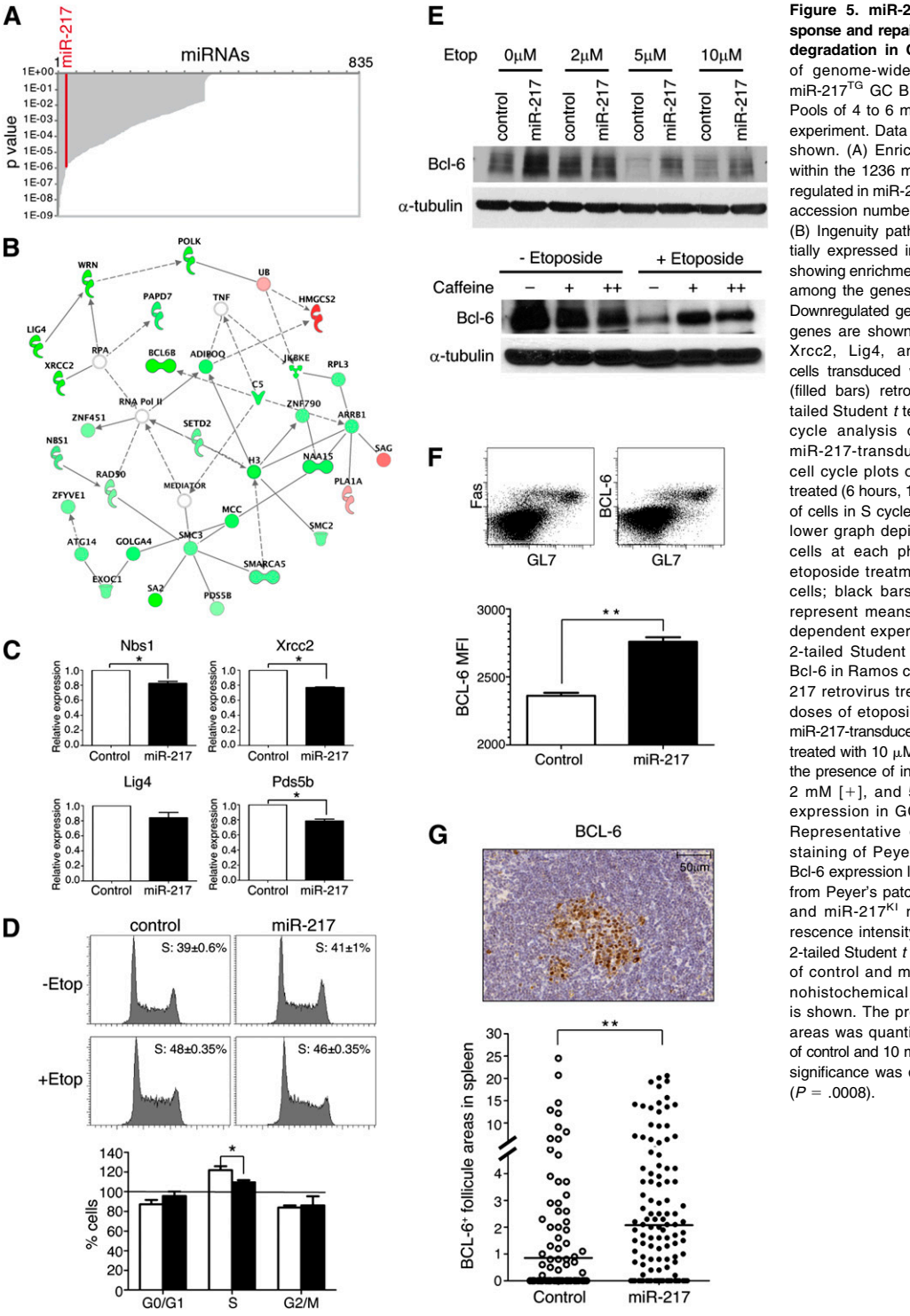

Figure 5. miR-217 regulates a DNA damage response and repair gene network and dampens Bcl-6 degradation in GC B cells. (A-B) RNAseq analysis of genome-wide gene expression in control and miR-217^{TG} GC B cells isolated from Peyer's patches. Pools of 4 to 6 mice per genotype were used in each experiment. Data from 2 independent experiments are shown. (A) Enrichment in miRNA prediction targets within the 1236 mRNAs whose expression was downregulated in miR-217^{TG} vs control GC B cells. The GEO accession number for the RNAseq data is GSE47877. (B) Ingenuity pathway analysis of the genes differentially expressed in control vs miR-217^{TG} GC B cells, showing enrichment for a DDR and repair gene network among the genes regulated by miR-217 ($P = 10^{-31}$). Downregulated genes are shown in green; upregulated genes are shown in red. (C) Quantification of Nbs1, Xrcc2, Lig4, and Pds5b expression in Ramos cells transduced with control (open bars) or miR-217 (filled bars) retrovirus analyzed by qRT-PCR. Two-tailed Student *t* test with *P* values: $^*P < .05$. (D) Cell cycle analysis of etoposide-treated control- and miR-217-transduced Ramos cells. Representative cell cycle plots of untreated (−Etop) or etoposide-treated (6 hours, 10 μM) (+Etop) Ramos cells. Fraction of cells in S cycle ± standard deviation is shown. The lower graph depicts the change in the proportion of cells at each phase of cell cycle in response to etoposide treatment (open bars, control-transduced cells; black bars, miR-217-transduced cells). Bars represent means ± standard deviations from 3 independent experiments ($P = .004$ for S phase cells, 2-tailed Student *t* test). (E) (Upper) Immunoblot of Bcl-6 in Ramos cells transduced with control or miR-217 retrovirus treated for 6 hours with the indicated doses of etoposide. (Lower) Immunoblot of Bcl-6 in miR-217-transduced cells left untreated (−Etoposide) or treated with 10 μM Etposide for 6 hours (+Etoposide) in the presence of increases doses of caffeine (0 mM [−], 2 mM [+], and 5 mM [++]. (F) Analysis of Bcl-6 expression in GC cells by flow cytometry. (Upper) Representative dot plots of Fas, GL7, and Bcl-6 staining of Peyer's patch B cells. Quantification of Bcl-6 expression levels in B220$^+$Fas$^+$GL7$^+$ GC B cells from Peyer's patches of littermate controls (white bar) and miR-217^{KI} mice (black bar) (MFI, mean fluorescence intensity; n = 3 mice/genotype, $P = .0006$, 2-tailed Student *t* test). (G) Bcl-6 expression in spleens of control and miR-217^{TG} mice analyzed by immunohistochemical staining. A representative picture is shown. The proportion of Bcl-6$^+$ stained in follicle areas was quantified in 205 and 201 spleen follicles of control and 10 miR-217^{TG} mice, respectively. Statistical significance was determined by 2-tailed Student *t* test ($P = .0008$).

accumulate concomitantly with CSR (Figure 4D). These results thus show that inhibition of endogenous miR-217 attenuates the GC reaction and decreases the frequency of somatic mutations associated with both the SHM and the CSR reactions.

miR-217 regulates a DNA damage response and repair gene network and stabilizes Bcl-6 expression in GC B cells

To identify the genes regulated by miR-217 in activated B cells, we performed a genome-wide comparison of the gene expression profiles of miR-217^{TG} and wild-type GC B cells by RNAseq. Comparison of GC B cells from Peyer's patches of miR-217^{TG} and wild-type mice identified 1740 differentially expressed genes with $P \leq .05$ (supplemental Table 1), 1236 of which were downregulated. This set of downregulated genes was significantly enriched in predicted miR-217 targets ($P = 9.75 \times 10^{-7}$; Figure 5A), suggesting that a high proportion of the downregulated genes identified in miR-217^{TG} GC B cells are direct miR-217 targets. To identify the gene networks altered by miR-217 expression in GC B cells, we performed a bioinformatics analysis on the genes differentially expressed

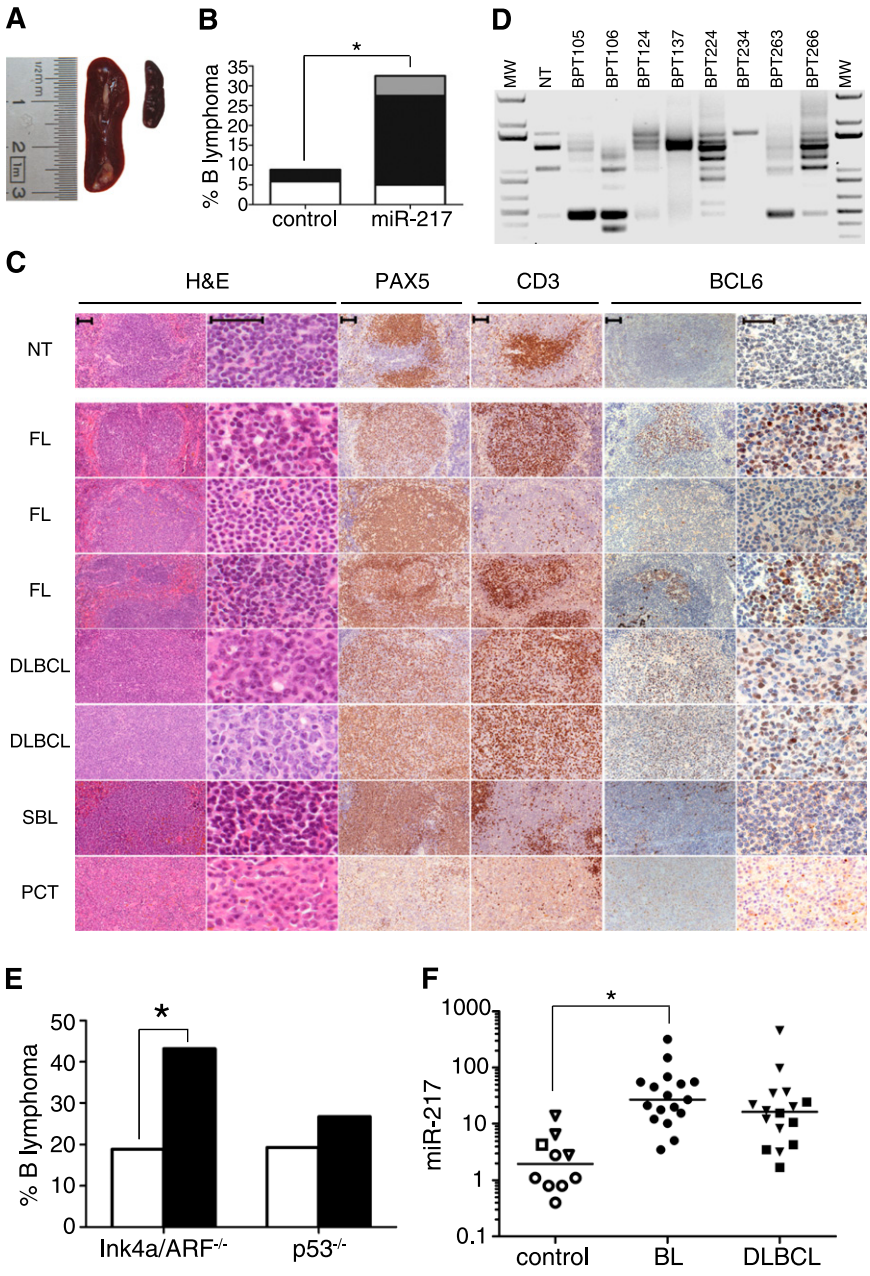

Figure 6. miR-217 expression promotes mature B-cell lymphomas. (A-D) Thirty-four control and 40 miR-217^{KI} mice were monitored over 90 weeks for the appearance of B-cell lymphoma. (A) Representative pictures of (right) a nontumoral control spleen and (left) a miR-217^{KI} spleen with splenomegaly. (B) Quantification of B-cell lymphoma incidence in control mice and miR-217^{KI} mice. The proportions of FL (black), DLBCL (white), or other lymphomas (gray) are shown. Statistical significance was determined by 2-tailed Student *t* test ($P = .028$). (C) Representative hematoxilin and eosin (H&E) and immunohistochemical stainings for Pax5, CD3, and Bcl-6 in spleens from miR-217^{KI} mice with B-cell lymphomas. Scale bar is 50 μm. NT, nontumoral; SBL, small B-cell lymphoma. (D) PCR analysis of V(D)J rearrangements in tumor samples from miR-217^{KI} mice. DNA was isolated from total spleen and amplified using a V-degenerate primer in combination with an antisense primer downstream of J_H4. Sequencing results are shown in Table 2. Mouse IDs are shown. MW, molecular weight marker. (E) Quantification of B-cell lymphoma incidence in control (open bars) and miR-217^{KI} (filled bars) Ink4a/Arf$^{-/-}$ and p53$^{-/-}$ mice. Statistical significance was determined by 2-tailed Student *t* test ($P = .03$ in miR217^{KI} Ink4a/Arf$^{-/-}$ vs control Ink4a/Arf$^{-/-}$ and $P = .33$ in miR217^{KI} p53$^{-/-}$ vs control p53$^{-/-}$). (F) miR-217 relative expression in human control samples (open circles, peripheral blood CD19$^+$ B cells; open squares, tonsils; open triangles, lymph nodes), in BL samples (closed circles) and in DLBCL samples (closed triangles, GC B GCB-DLBCL; closed squares, activated B cell, ABC-DLBCL) as determined by qRT-PCR. Statistical significance was determined by 2-tailed Student *t* test ($P = .05$ for BL).

in miR-217^{TG} vs control GC (Fas$^+$GL7$^+$) B cells. Ingenuity pathway analysis revealed that miR-217 regulates a DNA damage response (DDR) and repair gene network in GC B cells ($P = 10^{-31}$; Figure 5B). Interestingly, this gene network contained 2 main hubs, RNA pol II and replication protein A, which are directly linked to AID activity.[33-37] The miR-217-regulated gene network included a number of genes linked to the DDR (Nbs1 and Rad50 components of the Mre11-Rad50-Nbs1 [MRN] complex),[38] DNA repair and CSR (Wrn, Lig4, and Xrcc2),[11,39,40] and genes of the cohesin complex (SMC2, SMC3, PDS5B, and SA2) involved in chromatid cohesion, as well as in DNA replication, transcription, recombination, and repair[41,42]; all of them were downregulated by miR-217.

Bcl-6 expression is regulated by the DDR through a signaling pathway that promotes Bcl-6 degradation.[43] As we found that miR-217 downregulates the expression of a number of genes involved in DDR and repair in GC B cells, we hypothesized that miR-217 could stabilize Bcl-6 expression in these cells. To test this hypothesis, we transduced Ramos cells, a human BL GC B-cell line, with miR-217-GFP and control retroviral vectors and analyzed Bcl-6 expression on genotoxic stress induction. We first verified that genes linked to the DDR and downregulated by miR-217 expression in mouse GC B cells (Nbs1, Xrcc2, Lig4, and Pds5b) were also downregulated by miR-217 in human Ramos cells (Figure 5C). To determine if miR-217 impacts on the response to genotoxic stress, we analyzed the effect of etoposide treatment on the cell cycle of control- and miR-217-transduced Ramos cells. Expectedly, we found that etoposide-induced DDR promoted an increase in the fraction of cells in the S phase of the cell cycle, consistent with a replicative delay (Figure 5D). However, this S phase increase was milder in miR-217-transduced cells (Figure 5D), which suggested that miR-217 may contribute to bypass the DDR response induced by etoposide. Immunoblot analysis showed that etoposide treatment of control Ramos cells rapidly induced Bcl-6 degradation (Figure 5E), in agreement with previous results.[43] However, Ramos cells overexpressing miR-217 were

Table 1. Characterization of B-cell lymphomas in miR-217^{KI} mice

Mouse ID*	B-cell lymphoma†	Grade‡	Splenomegaly§	Phenotype¶
BPT048	FL			Mature B cell, B220^{+} CD19^{+} sIgM^{+} sIgκ^{+} Fas^{+}GL7^{+}, Pax5^{low} BCL6^{+}; numerous infiltrating T cells
BPT100	FL		Yes	Mature B cells, Pax5^{+} BCL6^{-} and N/A
BPT105	FL			Mature B cell, B220^{+} CD19^{+} sIgM^{-} sIgκ^{+}, Pax5^{+} BCL6^{+}
BPT106	FL			Mature B cell, B220^{+} CD19^{+} sIgM^{-} sIgκ^{+}, Pax5^{low} BCL6^{+}
BPT109	PCT	Aggressive		Mature B cell, Pax5^{-} BCL6^{-} and N/A
BPT124	FL	Aggressive		Mature B cell, B220^{low} CD19^{+} sIgM^{high} sIgκ^{+}, Pax5^{low} BCL6^{-}
BPT137	FL			Mature B cell, B220^{+} CD19^{+} sIgM^{low} sIgκ^{+}, Pax5^{+} BCL6^{-}
BPT148	DLBCL	Aggressive	Yes	Mature B cell, B220^{+} CD19^{+} sIgM^{low} sIgκ^{+}, Pax5^{low} BCL6^{+}; numerous infiltrating T cells
BPT224	DLBCL	Aggressive	Yes	Mature B cell, B220^{+} CD19^{+} sIgM^{low} sIgκ^{low}, Pax5^{low} BCL6^{+}; numerous infiltrating T cells
BPT226	FL	Aggressive	Yes	Mature B cell, B220^{+} CD19^{+} sIgM^{low} sIgκ^{low}, Pax5^{low} BCL6^{+}; numerous infiltrating T cells
BPT234	SBL			Mature B cell, B220^{+} CD19^{+} sIgM^{high} sIgκ^{+}, Pax5^{+} BCL6^{-}
BPT263	FL		Yes	Mature B cell, B220^{high} CD19^{+} sIgM^{+} sIgκ^{+}, Pax5^{+} BCL6^{+}
BPT266	FL	Aggressive		Mature B cell, B220^{+} CD19^{+} sIgM^{low} sIgκ^{+}, Pax5^{low} BCL6^{-}

*Mouse identification number.
†SBL, small B-cell lymphoma.
‡Lymphoma classification grade.
§Splenomegaly: spleens larger than 20 mm length.
¶Phenotype of tumoral cells determined by morphological features, flow cytometry, and immunohistochemica stainings. N/A, not analyzed.

partially protected against genotoxic stress-induced Bcl-6 degradation and showed increased Bcl-6 expression levels (Figure 5E). Caffeine treatment protected miR-217 Ramos cells from etoposide-induced Bcl-6 degradation, indicating that an ataxia telangiectasia mutated/ataxia telangiectasia and Rad3-related–dependent pathway is involved in this process (Figure 5E, lower panels). Analysis of Bcl-6 protein levels in GC B cells from control and miR-217^{KI} mice further confirmed that miR-217 expression promotes the accumulation of Bcl-6 (Figure 5F). Finally, quantification of Bcl-6 expression in spleens from miR-217^{TG} and control mice revealed that miR-217^{TG} mice have larger Bcl-6^{+} follicle areas in spleens ($P = .0008$; Figure 5G). Overall, these data indicate that miR-217 regulates the GC reaction by modulating the expression levels of a gene network involved in DDR and repair and by dampening genotoxic stress-induced Bcl-6 degradation in GC B cells.

Deregulated miR-217 expression promotes mature B-cell lymphomas

GC B cells are highly prone to oncogenic transformation. Our results show that miR-217 is a positive regulator of the GC reaction, presumably by downregulating the expression of DNA repair genes and by stabilizing Bcl-6 expression, which could enhance the susceptibility of these cells to oncogenic events. To test whether miR-217 overexpression in B cells affects the development of mature B-cell lymphomas, we monitored the incidence of B-cell lymphoma in a group of 34 control and 40 miR-217^{KI} mice. Mice were euthanized and analyzed at an end point of 90 weeks or earlier if they showed signs of disease. miR-217^{KI} mice showed early signs of disease more frequently than control mice did (14 miR-217^{KI} and 7 control mice had to be euthanized before 90 weeks; supplemental Figure 3A). miR-217^{KI} mice had larger spleens than control animals, with a fraction showing clear splenomegaly (20% vs 0% spleens larger than 20 mm; Fisher's exact test, $P = .0058$; Figure 6A; Table 1). Histopathological evaluation of the spleens showed that a large proportion (33%) of miR-217^{KI} mice developed B-cell lymphoma ($P = .028$ vs control mice; Figure 6B). Flow cytometry analysis of lymphomas from miR-217^{KI} mice showed frequent alterations in the expression of the B-cell surface molecules B220, IgD, IgM, and Igκ (supplemental Figure 3B; Table 1). We found that lymphomas in miR-217^{KI} mice had features of mature GC or post-GC B-cell origin.[44] Most (70%) were classified as follicular lymphomas (FL), although we also observed other mature B-cell lymphomas, such as DLBCL and B-cell plasmacytomas (PCT) (Figure 6B-C; Table 1). To further characterize the origin of these lymphomas, we performed molecular analysis of their V(D)J rearrangements by PCR amplification and sequencing. We found that a fraction of the lymphomas yielded unique amplification bands (Figure 6D), which were confirmed to correspond with single rearrangements (Table 2), thus providing proof of their clonal origin. In addition, all of the rearrangements subject to this analysis contained mutations (SHM^{+}) in their V genes (Table 2) and an additional fraction showed Bcl-6 expression (Figure 6C; Table 1), confirming their GC/post-GC origin.

To examine the contribution of tumor suppressor pathways to limiting the B-cell lymphomagenesis induced by miR-217, we analyzed the incidence of B-cell lymphoma in miR-217^{KI} mice in the Ink4a/Arf$^{-/-}$ and p53$^{-/-}$ backgrounds. Ink4a/Arf$^{-/-}$ and p53$^{-/-}$ mice often developed histiocytic sarcomas (40%) and T-cell lymphomas (70%), respectively (data not shown).[45-47] In addition, we found that roughly 20% of both control Ink4a/Arf$^{-/-}$ and p53$^{-/-}$ tumor suppressor-deficient mice generated B-cell lymphomas. This incidence was not significantly altered by miR-217 overexpression in the p53$^{-/-}$ background, but in the Ink4a/Arf$^{-/-}$ background, miR-217 overexpression increased B-cell lymphoma incidence to 43% (Figure 6E), although the mean survival of miR-217^{KI} Ink4a/Arf$^{-/-}$ mice was not significantly altered (supplemental Figure 3A). B-cell lymphomas in miR-217^{KI} Ink4a/Arf$^{-/-}$ mice showed histopathological features of mature GC or post-GC B-cell lymphomas (supplemental Figure 3). These results suggest that the Ink4a/Arf, but not the p53, tumor suppressor pathway acts as a surveillance mechanism against the lymphomagenic events induced by miR-217 in mature B cells.

To determine if miR-217 expression levels are altered in mature B-cell human lymphomas, we conducted a qRT-PCR analysis of miR-217 expression in a collection of BL and DLBCL samples. Expression of miR-217 was higher in BL and DLBCL than in control tonsil, lymph node, and peripheral blood B-cell samples (BL vs control, $P = .05$; Figure 6F). In agreement with these findings, analysis of published data of copy number variation in a cohort of DLBCL cases revealed that the genomic region that contains the miR-217 chromosomal location (MCR 1694) is amplified in a fraction of the cases[48] (GSE11318). Together, these data indicate that miR-217 gain of function is associated with human mature B-cell lymphomas.

Table 2. Analysis of VDJ gene rearrangements in clonal B-cell lymphomas of miR-217^{KI} mice

Mouse ID*	V gene†	D gene†	J gene†	V-D-J junction	SHM‡
BPT105	IGHV1-66*01	IGHD2-5*01	IGHJ4*01	GGGGGCTATAGTCAAATGAGGGGG	+
BPT124	IGHV1S16*01	IGHD1-2*01	IGHJ2*01	GAGGGGATTACTACGGCTACC	+
BPT137	IGHV1S127*01	IGHD4-1*02	IGHJ2*01	GACTGGGACGTCGG	+
BPT234	IGHV1-47*01	IGHD2-4*01	IGHJ1*01	ATGATTACGACCACC	+

IGBLAST, immunoglobulin BLAST; IMGT international ImMunoGeneTics information system; NCBI, National Center for Biotechnology Information.
*Mouse identification number.
†Assignment of V, D, and J genes by NCBI/IGBLAST according to the IMGT database.
‡SHM.

Discussion

The results presented in this study identify miR-217 as a positive regulator of the GC reaction and as an oncogene that promotes mature B-cell lymphomagenesis. miR-217 is specifically upregulated as a result of B-cell stimulation in the context of the GC reaction during the immune response, and our gain and loss of function approaches directly establish the functional relevance of miR-217 in vivo. miR-217 overexpression boosted the number of GC B cells and promoted the SHM and CSR reactions, and conversely, inhibition of endogenous miR-217 limited these events. Interestingly, miR-217 gain of function did not promote any measurable alterations in B-cell differentiation, suggesting that the function of miR-217 in the B-cell lineage is restricted to the context of GCs and antibody diversification.

miRNAs modulate the expression of gene networks in a cell context-specific manner.[20,22] Here, RNAseq analysis showed that miR-217 regulates the expression of a gene network involved in DDR and repair, including Rad50, Nbs1, Wrn, Lig4, and XRCC2, as well as a set of genes of the cohesin complex, all of which are downregulated by miR-217. GC B cells are intrinsically prone to genome instability: (1) they are programmed to undergo AID-mediated gene remodeling; (2) the intense proliferation of GC B cells subjects them to replicative stress[6]; and (3) the GC reaction depends on Bcl-6, a master transcriptional repressor that dampens the DDR in GC B cells and whose deregulation generates B-cell lymphomas.[18,49] Our data show that miR-217 downregulates a network of genes that sense and repair genotoxic events on DNA, which in turn can increase the tolerance of GC B cells to DNA damage, very much like Bcl-6. Notably, we found that miR-217 protects Bcl-6 from genotoxic stress-induced degradation,[43] suggesting that both molecules are part of the same network that renders GC cells permissive to genomic instability and prone to malignant transformation.

Consistent with this idea, we found that miR-217 overexpression promotes B-cell lymphomagenesis. Interestingly, mice that overexpress miR-217 resemble Bcl-6-overexpressing Iμ-HABCL6 mice in that both show increased GC formation and develop long latency mature B-cell lymphomas.[49] We also found that Ink4a/Arf but not p53 loss sensitizes B cells to miR-217-promoted lymphomagenesis. Although it is possible that a protective role of p53 is masked by the early appearance of T-cell lymphomas in p53$^{-/-}$ mice, our data suggest that Ink4a rather than the Arf-p53 oncogenic stress pathway plays the predominant role in protecting GC B cells against the transforming activity of miR-217. This result is in agreement with the finding that Ink4a protein is frequently lost through gene methylation or deletion in aggressive B-cell lymphomas, whereas ARF silencing is a rarer event.[50-53]

Deregulation of miRNA expression in human B-cell lymphomas has been extensively documented.[1-4,48] In some instances, the functional relevance of miRNA deregulation has been tested in genetically modified mouse models. This is the case of Eμ-miR-155 transgenic mice, which developed acute lymphoblastic leukemia/high grade lymphoma[54,55] or miR15/miR16 deficiency, which promoted chronic lymphocytic leukemia,[56] among other examples.[57,58] Evidence for miRNAs involved in GC or post-GC lymphomagenesis was thus far restricted to the combined action of the miR-17-92 miRNA cluster.[59] Here we find that miR-217 overexpression in B cells promotes lymphomas of GC or post-GC origin, most likely by impinging on the regulation of the DDR and Bcl-6. Accordingly, we found increased levels of miR-217 in BL and DLBCL, 2 of the most aggressive lymphomas arising from GCs. Our results identify miR-217 as a novel molecular link between the GC response and B-cell transformation and provide an in vivo model of mature B-cell lymphomagenesis.

Acknowledgments

The authors thank all the members of the B Cell Biology Laboratory for helpful discussions, D. S. Rao and D. Baltimore for kindly providing us with the MGP vector, G. Roncador for the anti-Bcl-6 antibody, L. Belver, O. Fernandez-Capetillo, J. Mendez, and M. Serrano for critical reading of the manuscript, O. Dominguez, D. Pisano, F. Sanchez-Cabo, J. M. Ligos for technical advice, and S. Bartlett for English editorial support.

N.B.-I. is a fellow of the research training program funded by the Ministerio de Economía y Competitividad, A.R.R. is supported by the Spanish National Cardiovascular Research Centre, V.G.d.Y. is a Ramón y Cajal Investigator (RYC-2009-04503), and R.N.-C. is supported by the Juan de la Cierva research program. This work was funded by grants from the Ministerio de Economía y Competitividad (SAF2010-21394) and the European Research Council Starting Grant program (BCLYM-207844). A.P.-M. and R.N.-C. were funded by grants from Ministerio de Ciencia e Innovación (BIO2010-17527) and the Government of Madrid (P2010/BMD-2305).

Authorship

Contribution: V.G.d.Y., N.B.-I., P.P.-D., and S.M.M. performed experiments; N.M., L.D.L., and M.A.P. collected and prepared human samples; D.F.R. constructed the original backbone for miR-217 transgene cloning; R.N.-C. and A.P.-M. performed bioinformatics analyses; M.C. did histopathological evaluation; V.G.d.Y., N.B.-I., and A.R.R. analyzed the data; V.G.d.Y. and A.R.R. designed experiments and wrote the manuscript; and A.R.R. supervised the research.

Conflict-of-interest disclosure: The authors declare no competing financial interests.

The current affiliation for P.P.-D. is Department of Pathology, New York University (NYU) Cancer Institute, New York University School of Medicine, New York, NY.

The current affiliation for M.C. is Roche Diagnostics GmbH, Penzberg, Germany.

Correspondence: Almudena R. Ramiro, B Cell Biology Laboratory, Centro Nacional de Investigaciones Cardiovasculares, Melchor Fernández Almagro 3, Madrid 28029, Spain; e-mail: aramiro@cnic.es; or Virginia G. de Yébenes, B Cell Biology Laboratory, Centro Nacional de Investigaciones Cardiovasculares, Melchor Fernández Almagro 3, Madrid 28029, Spain; vgarciay@cnic.es.

References

1. Calin GA, Sevignani C, Dumitru CD, et al. Human microRNA genes are frequently located at fragile sites and genomic regions involved in cancers. *Proc Natl Acad Sci U S A.* 2004;101(9):2999-3004.
2. Lu J, Getz G, Miska EA, et al. MicroRNA expression profiles classify human cancers. *Nature.* 2005;435(7043):834-838.
3. Volinia S, Calin GA, Liu CG, et al. A microRNA expression signature of human solid tumors defines cancer gene targets. *Proc Natl Acad Sci U S A.* 2006;103(7):2257-2261.
4. Di Lisio L, Sánchez-Beato M, Gómez-López G, et al. MicroRNA signatures in B-cell lymphomas. *Blood Cancer J.* 2012;2(2):e57.
5. de Yébenes VG, Bartolomé-Izquierdo N, Ramiro AR. Regulation of B-cell development and function by microRNAs. *Immunol Rev.* 2013;253(1):25-39.
6. Victora GD, Nussenzweig MC. Germinal centers. *Annu Rev Immunol.* 2012;30:429-457.
7. Muramatsu M, Kinoshita K, Fagarasan S, Yamada S, Shinkai Y, Honjo T. Class switch recombination and hypermutation require activation-induced cytidine deaminase (AID), a potential RNA editing enzyme. *Cell.* 2000;102(5):553-563.
8. Di Noia JM, Neuberger MS. Molecular mechanisms of antibody somatic hypermutation. *Annu Rev Biochem.* 2007;76:1-22.
9. Revy P, Muto T, Levy Y, et al. Activation-induced cytidine deaminase (AID) deficiency causes the autosomal recessive form of the Hyper-IgM syndrome (HIGM2). *Cell.* 2000;102(5):565-575.
10. de Yébenes VG, Ramiro AR. Activation-induced deaminase: light and dark sides. *Trends Mol Med.* 2006;12(9):432-439.
11. Robbiani DF, Nussenzweig MC. Chromosome translocation, B cell lymphoma, and activation-induced cytidine deaminase. *Annu Rev Pathol.* 2013;8:79-103.
12. Alt FW, Zhang Y, Meng FL, Guo C, Schwer B. Mechanisms of programmed DNA lesions and genomic instability in the immune system. *Cell.* 2013;152(3):417-429.
13. Küppers R. Mechanisms of B-cell lymphoma pathogenesis. *Nat Rev Cancer.* 2005;5(4):251-262.
14. Nussenzweig A, Nussenzweig MC. Origin of chromosomal translocations in lymphoid cancer. *Cell.* 2010;141(1):27-38.
15. Ramiro AR, Jankovic M, Eisenreich T, et al. AID is required for c-myc/IgH chromosome translocations in vivo. *Cell.* 2004;118(4):431-438.
16. Ramiro AR, Jankovic M, Callen E, et al. Role of genomic instability and p53 in AID-induced c-myc-Igh translocations. *Nature.* 2006;440(7080):105-109.
17. Robbiani DF, Bothmer A, Callen E, et al. AID is required for the chromosomal breaks in c-myc that lead to c-myc/IgH translocations. *Cell.* 2008;135(6):1028-1038.
18. Pasqualucci L, Bhagat G, Jankovic M, et al. AID is required for germinal center-derived lymphomagenesis. *Nat Genet.* 2008;40(1):108-112.
19. Basso K, Dalla-Favera R. Roles of BCL6 in normal and transformed germinal center B cells. *Immunol Rev.* 2012;247(1):172-183.
20. Ebert MS, Sharp PA. Roles for microRNAs in conferring robustness to biological processes. *Cell.* 2012;149(3):515-524.
21. Bartel DP. MicroRNAs: target recognition and regulatory functions. *Cell.* 2009;136(2):215-233.
22. Peláez N, Carthew RW. Biological robustness and the role of microRNAs: a network perspective. *Curr Top Dev Biol.* 2012;99:237-255.
23. Xu S, Guo K, Zeng Q, Huo J, Lam KP. The RNase III enzyme Dicer is essential for germinal center B-cell formation. *Blood.* 2012;119(3):767-776.
24. Rodriguez A, Vigorito E, Clare S, et al. Requirement of bic/microRNA-155 for normal immune function. *Science.* 2007;316(5824):608-611.
25. Vigorito E, Perks KL, Abreu-Goodger C, et al. microRNA-155 regulates the generation of immunoglobulin class-switched plasma cells. *Immunity.* 2007;27(6):847-859.
26. Thai TH, Calado DP, Casola S, et al. Regulation of the germinal center response by microRNA-155. *Science.* 2007;316(5824):604-608.
27. de Yébenes VG, Belver L, Pisano DG, et al. miR-181b negatively regulates activation-induced cytidine deaminase in B cells. *J Exp Med.* 2008;205(10):2199-2206.
28. Pérez-Durán P, Belver L, de Yébenes VG, Delgado P, Pisano DG, Ramiro AR. UNG shapes the specificity of AID-induced somatic hypermutation. *J Exp Med.* 2012;209(7):1379-1389.
29. Gentleman RC, Carey VJ, Bates DM, et al. Bioconductor: open software development for computational biology and bioinformatics. *Genome Biol.* 2004;5(10):R80.
30. Muniategui A, Nogales-Cadenas R, Vázquez M, et al. Quantification of miRNA-mRNA interactions. *PLoS ONE.* 2012;7(2):e30766.
31. Ebert MS, Neilson JR, Sharp PA. MicroRNA sponges: competitive inhibitors of small RNAs in mammalian cells. *Nat Methods.* 2007;4(9):721-726.
32. Rao DS, O'Connell RM, Chaudhuri AA, Garcia-Flores Y, Geiger TL, Baltimore D. MicroRNA-34a perturbs B lymphocyte development by repressing the forkhead box transcription factor Foxp1. *Immunity.* 2010;33(1):48-59.
33. Chaudhuri J, Khuong C, Alt FW. Replication protein A interacts with AID to promote deamination of somatic hypermutation targets. *Nature.* 2004;430(7003):992-998.
34. Kenter AL. AID targeting is dependent on RNA polymerase II pausing. *Semin Immunol.* 2012;24(4):281-286.
35. Nambu Y, Sugai M, Gonda H, et al. Transcription-coupled events associating with immunoglobulin switch region chromatin. *Science.* 2003;302(5653):2137-2140.
36. Pavri R, Gazumyan A, Jankovic M, et al. Activation-induced cytidine deaminase targets DNA at sites of RNA polymerase II stalling by interaction with Spt5. *Cell.* 2010;143(1):122-133.
37. Vuong BQ, Chaudhuri J. Combinatorial mechanisms regulating AID-dependent DNA deamination: interacting proteins and post-translational modifications. *Semin Immunol.* 2012;24(4):264-272.
38. Stracker TH, Petrini JH. The MRE11 complex: starting from the ends. *Nat Rev Mol Cell Biol.* 2011;12(2):90-103.
39. Ramiro A, Reina San-Martin B, McBride K, et al. The role of activation-induced deaminase in antibody diversification and chromosome translocations. *Adv Immunol.* 2007;94:75-107.
40. Bothmer A, Rommel PC, Gazumyan A, et al. Mechanism of DNA resection during intrachromosomal recombination and immunoglobulin class switching. *J Exp Med.* 2013;210(1):115-123.
41. Merkenschlager M, Odom DT. CTCF and cohesin: linking gene regulatory elements with their targets. *Cell.* 2013;152(6):1285-1297.
42. Remeseiro S, Losada A. Cohesin, a chromatin engagement ring. *Curr Opin Cell Biol.* 2013;25(1):63-71.
43. Phan RT, Saito M, Kitagawa Y, Means AR, Dalla-Favera R. Genotoxic stress regulates expression of the proto-oncogene Bcl6 in germinal center B cells. *Nat Immunol.* 2007;8(10):1132-1139.
44. Morse HC III, Anver MR, Fredrickson TN, et al; Hematopathology subcommittee of the Mouse Models of Human Cancers Consortium. Bethesda proposals for classification of lymphoid neoplasms in mice. *Blood.* 2002;100(1):246-258.
45. Donehower LA, Harvey M, Slagle BL, et al. Mice deficient for p53 are developmentally normal but susceptible to spontaneous tumours. *Nature.* 1992;356(6366):215-221.
46. Jacks T, Remington L, Williams BO, et al. Tumor spectrum analysis in p53-mutant mice. *Curr Biol.* 1994;4(1):1-7.
47. Khoo CM, Carrasco DR, Bosenberg MW, Paik JH, Depinho RA. Ink4a/Arf tumor suppressor does not modulate the degenerative conditions or tumor spectrum of the telomerase-deficient mouse. *Proc Natl Acad Sci U S A.* 2007;104(10):3931-3936.
48. Lenz G, Wright GW, Emre NC, et al. Molecular subtypes of diffuse large B-cell lymphoma arise by distinct genetic pathways. *Proc Natl Acad Sci U S A.* 2008;105(36):13520-13525.
49. Cattoretti G, Pasqualucci L, Ballon G, et al. Deregulated BCL6 expression recapitulates the pathogenesis of human diffuse large B cell lymphomas in mice. *Cancer Cell.* 2005;7(5):445-455.
50. Baur AS, Shaw P, Burri N, Delacrétaz F, Bosman FT, Chaubert P. Frequent methylation silencing of p15(INK4b) (MTS2) and p16(INK4a) (MTS1) in B-cell and T-cell lymphomas. *Blood.* 1999;94(5):1773-1781.
51. García JF, Villuendas R, Algara P, et al. Loss of p16 protein expression associated with methylation of the p16INK4A gene is a frequent finding in Hodgkin's disease. *Lab Invest.* 1999;79(12):1453-1459.
52. Villuendas R, Sánchez-Beato M, Martínez JC, et al. Loss of p16/INK4A protein expression in non-Hodgkin's lymphomas is a frequent finding associated with tumor progression. *Am J Pathol.* 1998;153(3):887-897.
53. Drexler HG. Review of alterations of the cyclin-dependent kinase inhibitor INK4 family genes p15, p16, p18 and p19 in human leukemia-lymphoma cells. *Leukemia.* 1998;12(6):845-859.
54. Costinean S, Zanesi N, Pekarsky Y, et al. Pre-B cell proliferation and lymphoblastic leukemia/high-grade lymphoma in E(mu)-miR155

transgenic mice. *Proc Natl Acad Sci U S A.* 2006; 103(18):7024-7029.

55. Costinean S, Sandhu SK, Pedersen IM, et al. Src homology 2 domain-containing inositol-5-phosphatase and CCAAT enhancer-binding protein beta are targeted by miR-155 in B cells of Emicro-MiR-155 transgenic mice. *Blood.* 2009; 114(7):1374-1382.

56. Klein U, Lia M, Crespo M, et al. The DLEU2/miR-15a/16-1 cluster controls B cell proliferation and its deletion leads to chronic lymphocytic leukemia. *Cancer Cell.* 2010;17(1):28-40.

57. Enomoto Y, Kitaura J, Hatakeyama K, et al. Eμ/miR-125b transgenic mice develop lethal B-cell malignancies. *Leukemia.* 2011;25(12): 1849-1856.

58. Medina PP, Nolde M, Slack FJ. OncomiR addiction in an in vivo model of microRNA-21-induced pre-B-cell lymphoma. *Nature.* 2010; 467(7311):86-90.

59. Jin HY, Oda H, Lai M, et al. MicroRNA-17∼92 plays a causative role in lymphomagenesis by coordinating multiple oncogenic pathways. *EMBO J.* 2013;32(17):2377-2391.

2014 124: 229-239
doi:10.1182/blood-2013-12-543611 originally published online May 21, 2014

miR-217 is an oncogene that enhances the germinal center reaction

Virginia G. de Yébenes, Nahikari Bartolomé-Izquierdo, Rubén Nogales-Cadenas, Pablo Pérez-Durán, Sonia M. Mur, Nerea Martínez, Lorena Di Lisio, Davide F. Robbiani, Alberto Pascual-Montano, Marta Cañamero, Miguel A. Piris and Almudena R. Ramiro

Blood (print ISSN 0006-4971, online ISSN 1528-0020), is published weekly by the American Society of Hematology, 2021 L St, NW, Suite 900, Washington DC 20036.

Immunological Reviews

Virginia G de Yébenes
Nahikari Bartolomé-Izquierdo
Almudena R. Ramiro

Regulation of B-cell development and function by microRNAs

Authors' address
Virginia G de Yébenes[1], *Nahikari Bartolomé-Izquierdo*[1], *Almudena R. Ramiro*[1]
[1]B Cell Biology Lab, Centro Nacional de Investigaciones Cardiovasculares, Madrid, Spain.

Correspondence to:
Almudena R. Ramiro
B Cell Biology Lab, Centro Nacional de Investigaciones Cardiovasculares
Melchor Fernández Almagro 3
28029 Madrid, Spain
Tel.: +349 1453 1200
Fax: +349 1453 1245
e-mail: aramiro@cnic.es

Acknowledgements
We are grateful to F. Sánchez-Madrid, C. Cobaleda, and L. Belver for critical reading of the manuscript. We thank S. Bartlett for English editorial support. V. G. Y. is a Ramón y Cajal investigator, N. B. is a fellow of the research training program (FPI) funded by the Spanish Ministry of Economy, and A. R. R. is funded by grants SAF2010-21394 and European Research Council BCLYM-207844. The Centro Nacional de Investigaciones Cardiovasculares (CNIC) is supported by the Spanish Ministry of Economy and the Pro-CNIC Foundation. The authors have no conflicts of interest to declare.

This article is part of a series of reviews covering RNA Regulation of the Immune System appearing in Volume 253 of *Immunological Reviews*.

Immunological Reviews 2013
Vol. 253: 25–39

Immunological Reviews
0105-2896

Summary: MicroRNAs (miRNAs) have emerged as a new class of gene expression regulators whose functions influence a myriad of biological processes, from developmental decisions through immune responses and numerous pathologies, including cancer and autoimmunity. miRNAs are small RNA molecules that drive post-transcriptional negative regulation of gene expression by promoting the degradation or translational block of their target mRNAs. Here, we review some of the data relating to the role of miRNAs in the regulation of the B-cell lineage, with a special focus on results obtained *in vivo*. We start by giving a general overview of miRNA activity, including the issue of target specificity and the experimental approaches more widely used to analyze the function of these molecules. We then go on to discuss the function of miRNAs during B-cell differentiation in the bone marrow and in the periphery as well as during the humoral immune response. Finally, we describe a few examples of the contribution of miRNAs, both as oncogenes and tumor suppressors, to the development of B-cell neoplasias.

Keywords: *microRNA, bone marrow, germinal center, Dicer, Lymphomagenesis*

General concepts on microRNA biology

Two decades ago, the Ambros' and Ruvkun's laboratories (1, 2) identified lin-4 as a small RNA that controls the larval development in the worm *Caenorhabditis elegans* through the negative regulation of lin-14. Strikingly, this RNA exerted its function not through the generation of a protein product but seemingly through pairing with complementary sequences in the 3′ untranslated region (3′ UTR) of lin-14 mRNA. It was not until 2000 that a second small RNA, let-7, was shown to also control developmental transitions in *C. elegans* by the negative regulation of target mRNAs (3). Let-7 homologs were subsequently found in other organisms, including mammals (4), and soon a collection of several dozens of these small RNA molecules were cloned from worms, flies, and mammals and were collectively called microRNAs (miRNAs) (5–7). Today thousands of miRNAs have been identified in nearly 200 species (more than 1000 in humans alone), and they are recognized as a previously unforeseen regulatory layer of gene regulation critical to a plethora of biological processes. In mammals, miRNAs are predicted to control the activity of approximately 50% of all

protein-coding genes (8). Besides miRNAs, other classes of silencing small RNAs have been identified in animals, plants, and fungi, including small interfering RNAs (siRNAs) and piwi-interacting RNAs (piRNAs), which are not discussed here (reviewed in 9).

Several salient features of miRNAs distinguish them from classical regulators of gene expression, such as transcription factors and repressors. First, miRNAs do not encode a protein product, but instead they are biologically active as RNA molecules. Second, miRNAs are exclusively negative regulators of gene expression and act post-transcriptionally, either by promoting degradation of mRNA targets or by blocking their translation. This feature is thought to allow a fast and very precise regulatory response. Finally, miRNA activity on its target mRNAs typically results in a relatively mild (<twofold) reduction in protein levels, which has led to the view that miRNAs act primarily as reinforcers of transcriptional programs conferring robustness to biological processes (10). However, the regulatory activity of miRNAs is in many respects similar to that of transcription factors and transcriptional repressors. Thus, like transcriptional regulators, a single miRNA can potentially regulate many targets to provide coordinated and simultaneous regulation of a network of genes in a particular tissue or at a specific developmental stage. Likewise, although target recognition by transcriptional regulators and miRNAs is based on nucleotide sequence specificity, in both cases, nucleotide sequence alone is insufficient to accurately predict functional targets. These similarities have important implications for the understanding of the physiological activity of miRNAs.

miRNA biogenesis, target specificity, and regulation

miRNAs are 21- to 24-nucleotide long RNA molecules that are processed from longer RNA precursors (pri-miRNAs). Pri-miRNAs are either transcribed as independent genes or are included within intronic sequences of other genes. Pri-miRNAs fold into hairpins that are sequentially cleaved by two RNAseIII endonucleases, called Drosha and Dicer. Drosha cleavage generates a ≈70-nucleotide long pre-miRNA that is exported to the cytoplasm, where Dicer further processes it into a 20–25 bp RNA duplex. One strand of this duplex is the mature miRNA, which is loaded onto the miRNA-induced silencing complex (RISC). The main components of the RISC complex are Argonaute (AGO) proteins, which pair with the mature miRNA and guide it to its targets, and GW182 proteins, which act as downstream effectors for silencing. miRNA-RISC complexes bind to their target mRNAs and either induce their degradation or block their translation [the topic of miRNA biogenesis has been extensively discussed in excellent recent reviews (11–13)].

The regulatory activity of miRNAs on target mRNAs is primarily determined by nucleotide sequence complementarity; however, the small size of miRNAs provides a relatively limited sequence for defining target specificity. In plants, miRNAs often pair with their targets through extensive complementarity. In contrast, in animals quasiperfect alignment between miRNA and target mRNA is much more unusual, and typically, the interaction involves the formation of partial duplexes that contain mismatches and nucleotide wobbles (14). The most important motif in a mature miRNA for determining target specificity resides in the 5′ end, particularly in the stretch from nucleotides 2–7, called the seed. Accordingly, the 5′ end is the most conserved portion of miRNA sequences in metazoans. It has been proposed that imperfect pairing at the 5′ region can be compensated in some cases by interactions through the 3′ end of the miRNA. Expectedly, these features are not stringent enough to faithfully predict miRNA targets on the basis of sequence complementarity alone. Numerous algorithms and predictive tools have been developed to aid in this task, which incorporate both sequence complementarity and evolutionary conservation criteria. These analyses estimate that a single miRNA can be expected to target several hundred mRNAs. However, the divergence between the predictions obtained with different algorithms makes the identification of miRNA functional targets one of the most challenging issues in the field (8, 15).

Gene silencing by miRNAs obviously entails that their expression be tightly regulated. Cellular miRNA levels are regulated by a variety of molecular mechanisms, including transcription, processing, and intercellular transport. Transcription of miRNA genes is regulated in a similar fashion to that of protein-coding genes and is frequently driven by RNApolII. High-throughput approaches have shown that a significant fraction of miRNAs use their own transcription initiation regions, including miRNAs located in intergenic regions and others embedded within introns, and that transcriptional initiation can take place as far as 40 Kb from the pre-miRNA sequences (16, 17). However, there are relatively few detailed transcriptional analyses of individual miRNAs. Notably, myc and MYCN have been shown to regulate miRNAs with oncogenic and tumor suppressor potential, and p53 drives the expression of miRNAs that promote apoptosis and cell-cycle arrest (18–21). In addition, various miRNAs have been shown to regulate their own expression through positive and negative feedback loops (reviewed in

11). Although regulation of miRNA processing is far from being fully understood, it seems clear that the expression and activity of Drosha and Dicer endonucleases are critical and that these are affected by their dsRNA-binding protein partners, DGCR8 and TAR. In turn, the exact position cleaved by Drosha and Dicer can affect not only the sequence identity of the mature miRNA but also its loading onto the RISC complex (reviewed in 11). A mechanism of intercellular regulation by miRNAs has emerged that can constitute a critical additional layer to control their activity. It was first observed in plants and nematodes that RNA silencing signals can spread from the producing cells and travel from cell to cell and over long distances (reviewed in 22). This concept has more recently been expanded to mammals, where miRNAs have been found contained in exosomes, secreted vesicles that can act as intercellular communicators (23, 24). Indeed, exosomal miRNAs regulate the expression of target genes in recipient cells during the immune synapsis, thus providing a transcellular mechanism of gene regulation (24). Notably, exosomes contain a specific repertoire of miRNAs that differs from that found in the cytosol, indicating the existence of a mechanism for selective sorting into these vesicles (23–25). The levels of mature miRNAs in a cell are thus influenced by the rate of transcription of the primary miRNA transcript, the efficiency of the processing of this transcript into mature miRNAs, and the active transport of mature species from neighboring cells.

Approaches to the study of miRNA function

A number of experimental approaches are typically used to gain insights into miRNA function. Perhaps the most global strategy used to dissect the role of miRNAs in specific tissues or at defined developmental stages *in vivo* has been the analysis of mouse models in which the generation of mature miRNAs as a whole is prevented by blocking their biogenesis from precursors. This is the case of Dicer-deficient mice. Germline deletion of Dicer leads to severe developmental defects and embryonic lethality (26), but conditional ablation of this gene has provided extensive information on the requirement of miRNAs for lymphocyte differentiation and function (27, 28). An obvious limitation of this approach is the difficulty of pinpointing the role of a specific miRNA in the observed phenotype by *in vivo* reconstitution with miRNA transgenes, as their maturation would also be blocked in the absence of Dicer. This issue can now be resolved by taking advantage of the identification of miR-451, whose expression levels are refractory to Dicer loss of function (29–31). The backbone of miR-451 can be used to reprogram the biogenesis of heterologous miRNAs, thus rendering them Dicer independent (31). This strategy will help the precise identification of individual miRNAs relevant to the phenotype conferred by Dicer-mediated global miRNA ablation.

One of the most popular approaches used to identify physiologically important miRNAs in biological processes is the systematic study of miRNA expression profiles. Initially these studies were performed by directional cloning and miRNA array analyses, but these strategies are being replaced by next-generation sequencing and high-throughput qRT-PCR [miRNA profiling techniques were recently reviewed (32)]. The underlying assumption of these analyses is that significant miRNA expression in a particular tissue or at a specific differentiation stage very likely reflects functional relevance. This assumption should, however, be taken cautiously, in view of the recent estimate that over 60% of all miRNAs expressed in a particular cell type appear to have no silencing activity (33). In spite of this, it is reasonable to consider differential miRNA expression across sequential developmental or differentiation stages as a good indicator that those particular miRNAs play a role in the biological process under study.

miRNA function can be analyzed by gain- or loss-of-function strategies, both *in vivo* and *in vitro*. Expression libraries have been used to identify miRNAs relevant to B-cell function (34, 35), and a number of transgenic and knockout mouse models have been generated to address the role of miRNAs in lymphocyte lineages (reviewed in 28, 36, 37). In addition, miRNA loss of function can be achieved by the use of miRNA sponges – RNA molecules harboring repeated anti-sense miRNA sequences that can sequester miRNA molecules from their endogenous targets, acting as competitive inhibitors (38). Sponges have been successfully used to block the activity of miRNAs in the hematopoietic system *in vivo* after retroviral transduction and bone marrow transplantation (39, 40).

The ultimate challenge in the study of miRNA function is the identification of physiological targets. Predictive algorithms, such as miRanda, TargetScan, or PicTar, are widely used for this task, although they pose the limitations described above. More recently, cross-linking immunoprecipitation (CLIP) of RISC components has been used in combination with high-throughput sequencing of RNA (HITS-CLIP) to identify miRNAs that physically interact with the silencing machinery and with potential target mRNAs *in vivo* (41, 42). However, this strategy does not provide

definite proof that the identified interactions are functional. Very often, miRNA–mRNA target predictions or interactions have been validated in functional assays where putative target sequences are fused to a reporter gene, such as luciferase, whose expression is assessed in the presence or absence of the candidate miRNA. The limitation of this approach is that the context of the target sequence and the expression levels of both the reporter and the miRNA fail to reflect the natural cellular context in which the silencing takes place. To overcome this issue, mice have been generated in which mutations are introduced into the 3′ UTR of the putative mRNA target to disrupt miRNA binding *in vivo* (43, 44), thus allowing definitive validation of the silencing potential of a particular miRNA–mRNA target interaction. Notably, several studies have succeeded in pinpointing a particular mRNA target as the main contributor to the activity of a miRNA in *in vivo* complementation experiments, some of which will be discussed in detail below. However, it is important to keep in mind that miRNAs resemble transcription factors, in that they can operate as molecular switches through the simultaneous regulation of a large number of targets. Indeed, microarray analysis and quantitative proteomics approaches by stable isotope labeling with amino acids (SILAC) have shown that individual miRNAs can promote the downregulation of hundreds of genes, a large fraction of which are potential direct targets (45–47). Therefore, a thorough search for miRNA targets should combine a prediction analysis (either *in silico* by the use of prediction algorithms or experimentally through HITS-CLIP) with high-throughput studies of the shift in gene expression induced by the miRNA (for instance by RNA-Seq or SILAC).

miRNA-mediated control of early B-cell differentiation

Each individual B cell expresses a B-cell receptor (BCR) for antigen with a unique specificity, so that the total pool of mature B cells is capable of producing antibodies that specifically recognize and respond to virtually any foreign antigen. This involves the generation of a hugely diverse repertoire of BCR specificities. The BCR is composed of two identical immunoglobulin heavy (IgH) chains and two identical immunoglobulin light (IgL) chains. In all vertebrates, the genes encoding antibody variable regions are composed of groups of gene segments called V, D, and J (for the IgH locus) or V and J (for the IgL locus). During B-cell differentiation, a segment from each V (D) and J group is assembled to give rise to a VDJ (or VJ) rearrangement; this combinatorial event is the basis of the primary antibody diversity. Assembly of antibody genes takes place through a process of site-specific recombination called V(D)J recombination and involves the introduction of DNA double-strand breaks (DSBs) at specific recognition signal sequences flanking the V, D, and J elements by recombination activating genes (RAG1 and RAG2), followed by repair. Developing B cells in the bone marrow (or fetal liver) first assemble their IgH locus in two successive steps, D_HJ_H and $V_HD_HJ_H$, at the so-called progenitor B (pro-B) stage. Pro-B cells that achieve a productive IgH rearrangement express an Igμ chain together with the surrogate chains λ5 and VpreB (pre-BCR). pre-BCR expression leads to a phase of vigorous clonal cell expansion of precursor B (pre-B) cells and the subsequent rearrangement of the IgL locus. As a result, a mature BCR is expressed for the first time in immature B cells, which are then ready to leave the bone marrow. Given the stochastic nature of V(D)J recombination, this developmental process is coupled to selective events that guarantee that only cells where a rearrangement has given rise to a functional pre-BCR and BCR receive the appropriate survival signals, whereas the rest undergo apoptosis. In addition, central and peripheral tolerance checkpoints ensure the elimination or inactivation of B cells expressing BCRs with self-reactive specificities (48) (*Fig. 1*).

The first miRNA reported to have a role in B-cell differentiation in the bone marrow was miR-181a (49). In this early study, miR-181a was identified as a miRNA differentially expressed in T and B cells and whose ectopic expression by retroviral transduction and bone marrow reconstitution promoted a substantial increase in the generation of B cells, both *in vitro* and *in vivo* (49). Interestingly, miR-181a was later shown to play an important role in the modulation of the thresholds of TCR signaling in thymocytes (50, 51), providing a nice example of a miRNA playing distinct roles in different cell lineages, presumably by affecting different sets of target genes. miR-181 is a family of miRNAs composed of the closely related miR-181a-d, which are expressed from three polycistronic transcripts (*miR-181a1b1*, *miR-181a2b2*, and *miR-181cd*) where mature miR-181a and miR-181b can be generated from two independent clusters. In agreement with the results obtained in overexpression experiments (49), *miR-181ab1*-deficient mice showed a mild decrease in the number of peripheral and germinal center (GC) B cells (52). Important questions remaining regarding the role of this interesting miRNA cluster in B-cell differentiation include the identity of the precise developmental stage(s) affected in gain- and loss-of-function approaches. It will also be important to assess the role of the *miR-181ab2* cluster in the B-cell lineage and

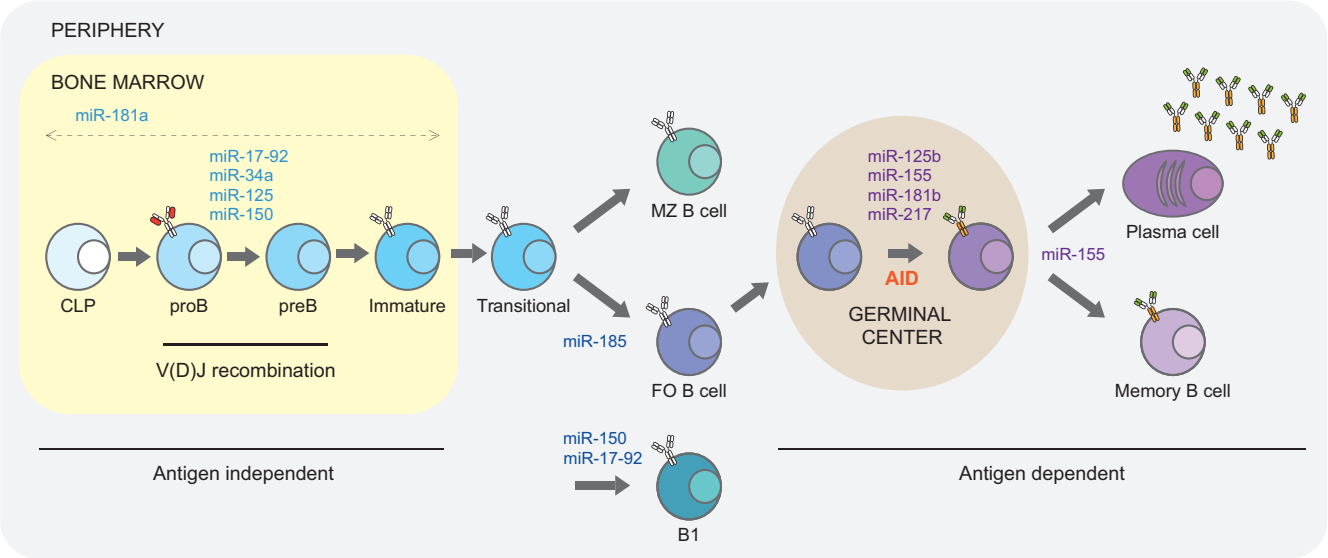

Fig. 1. miRNAs play crucial roles in B-cell development. Scheme depicting the developmental stages of B-cell differentiation in which particular miRNAs have been shown to play a role.

to identify its mRNA targets. In the following section, we discuss the function of miR-181b in GC B cells.

The global importance of miRNA regulatory mechanisms in the B-cell lineage was directly assessed in mice in which Dicer was deleted at the earliest stage of B-cell differentiation (mb1-Cre$^{ki/+}$ Dicer$^{fl/fl}$ mice) (53). miRNAs proved to be crucial, as Dicer-deficient mice displayed a severe block of B-cell differentiation at the pro-B to pre-B transition, at least partly due to massive apoptosis of Dicer-deficient pre-B cells, which resulted in an almost complete absence of B cells in the periphery. Combined bioinformatic analysis of miRNA and mRNA profiles showed that seeds for the miR-17~92 cluster were particularly enriched in the 3′ UTRs of the mRNAs found to be upregulated in Dicer-deficient pro-B cells (53). The miR-17~92 cluster consists of six miRNAs that are processed from the same precursor transcript and was shown early on to have oncogenic potential (54), as discussed below. Indeed, miR-17~92 plays a major role in B-cell differentiation, shown by the fact that germline deletion of this cluster also blocks the pro-B to pre-B checkpoint (55). Two of the top predicted targets of miR-17~92 were the pro-apoptotic gene Bim and the tumor suppressor PTEN, both of which are strongly upregulated in Dicer-deficient animals (53). Accordingly, Bim expression was also upregulated in miR-17~92-deficient mice (55), and both Bim and PTEN were downregulated in mice with ectopic overexpression of this cluster. The Dicer phenotype could be partially rescued by a Bcl2 transgene and by Bim deficiency (53), indicating a critical role of miR-17~92 in the regulation of Bim-induced apoptosis at this developmental stage (*Fig.* 2).

The same pro-B to pre-B transition in B-cell differentiation seems to be also regulated by another miRNA, miR-34a (40). The miR-34 family is transcriptionally regulated by p53 (19, 56, 57), and expression of these miRNAs is altered in various cancers (58), although their germline deletion in the mouse does not seem to influence cancer predisposition

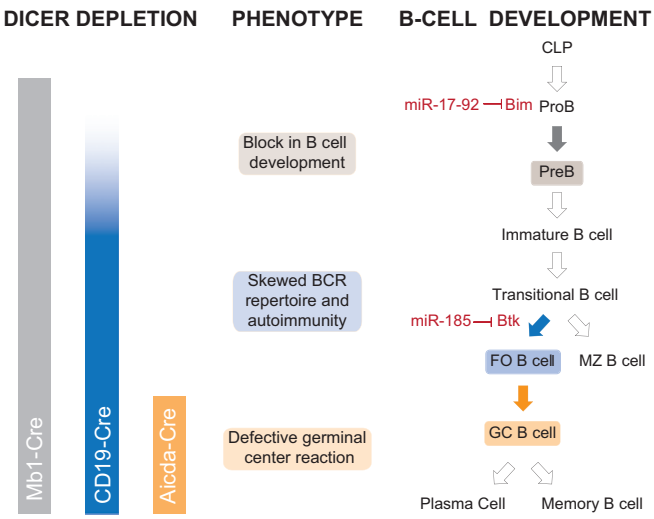

Fig. 2. Stage-specific deletion of Dicer reveals a key role of miRNAs at different B-cell developmental stages. The role of Dicer ablation in the B-cell lineage was assessed by Cre-mediated conditional deletion at three different developmental stages with mb1-Cre (gray), CD19-Cre (blue), and Aicda-Cre (orange) deleter strains. Bars on the left show the kinetics of Dicer deletion. The most prominent functional effect observed in each model is summarized in the middle column. The cartoon on the right depicts the specific developmental blocks with shaded arrows and boxes and the main miRNAs and mRNA targets involved.

(59). Ectopic expression of miR-34a in bone marrow cells followed by reconstitution experiments promoted an increase in the proportion of pro-B cells and a concomitant decrease in pre-B-cell numbers (40). Conversely, knockdown of miR-34a with a sponge construct increased the numbers of mature B cells. Target prediction combined with functional assays showed that Foxp1 is a *bona fide* target of miR-34a (40). Foxp1 is a transcription factor whose loss results in a severe blockade in B-cell development (60). Indeed, a rescue vector containing a 3′ UTR-less Foxp1 together with miR-34a was able to increase the number of pre-B cells, indicating that Foxp1 downregulation is a critical event in the developmental block induced by miR-34a (40). Although the downstream effectors of Foxp1 at this stage are not well characterized, this study identifies a p53-miR-34a-Foxp1 axis that may be critical for pre-B-cell survival.

miR-150 has pleiotropic effects on B-cell differentiation and function through the regulation of c-myb. c-myb is a transcription factor whose inactivation in the B-cell lineage leads to several defects, including a partial block at the pro-B to pre-B transition and a decrease in conventional follicular cells and a subset of B cells, called B1 cells, which are responsible for the production of natural antibodies (61–63). miR-150 expression was detected in mature B and T cells (64, 65) and shown to target c-myb (66). Rajewsky and coworkers (66) performed a comprehensive analysis of miR-150 function in the B-cell lineage through germline deletion and ectopic expression approaches. They found that miR-150 deficiency leads to B1-cell expansion and an enhanced humoral immune response (see below), whereas ectopic expression of miR-150 blocks the pro-B to pre-B transition of bone marrow differentiation, most likely due to an increased rate of cell death (66). A similar developmental block was observed in a parallel study in which miR-150 was overexpressed *in vivo* by retroviral transduction of precursor cells followed by bone marrow transplantation (65). Importantly, although miR-150 overexpression only mildly reduced c-myb levels, this decrease was physiologically relevant, as mice with a heterozygous mutation in c-myb were impaired at the same pro-B to pre-B maturational stage (66). These data provide an example of how miRNAs can play key regulatory roles by keeping protein expression levels within the exquisite narrow range that guarantees optimal functionality.

miRNAs have also been shown to regulate the generation of B cells of fetal origin. The let-7 family of miRNAs acts as regulators of stem-cell differentiation and had also been implicated in tumor suppression (67). Lin28 are small RNA-binding proteins (Lin28a and Lin28b) that regulate the activity of let-7 miRNAs by blocking their biogenesis (68). Lin28 is expressed in ES cells (69) and is a good predictor of cells that become induced pluripotent stem cells (iPSCs) (70). Indeed, ectopic expression of Lin28 (together with Sox2, Oct4, and Nanog) is able to reprogram human somatic cells to iPSCs (70). The immune system emerges in waves during development; the first of which arises during the fetal life and has unique properties, such as the efficient generation of innate-like lymphocytes, including B1 cells and $\gamma\delta$T cells. A recent study showed that ectopic expression of Lin28b in adult bone marrow hematopoietic progenitors can reprogram these cells toward fetal-like hematopoiesis, favoring the development of B1 and marginal zone B cells (as well as $\gamma\delta$T cells) at the expense of B2, or conventional B cells (71). An additional layer of complexity was added to this regulatory network with the finding that Lin28a is negatively regulated by miR-125 (39). In turn, miR-125 overexpression in bone marrow precursors promotes myelopoiesis and compromises B-cell differentiation by impairing the transition to the pre-B stage (39).

Generation of mature B cells involves a complex differentiation program that has long been known to be regulated by a number of transcription factors, including Pax5, PU.1, E2a, and Ebf (72). The data summarized above show that miRNAs are also determining factors in the intricate network that regulates these events. Different miRNAs have been shown to act as positive (miR17-92) or negative (miR34a, miR-150, miR-125) regulators of B-cell generation (*Fig. 1*). Interestingly, alterations to the expression of these miRNAs in the bone marrow appear to principally affect the pro-B to pre-B transition, probably reflecting the importance of an optimal balance between proliferation and cell death at the developmental checkpoint governed by pre-BCR expression. In this regard, it is important to bear in mind that in the case of miR-34a, mir-150, and miR-125, this developmental block was observed in overexpression experiments and that roles for these miRNAs at their endogenous levels at this particular stage are not completely established. This is a difficult issue to tackle, given the multiple effects some of these miRNAs have at different stages of B-cell differentiation and function and in some cases in other lineages as well. Another interesting consideration stemming from these reports concerns general regulatory mechanisms by miRNAs. In the case of miR-34a and miR-150, the two major identified targets are the transcription factors Foxp1 and c-myb, respectively. These findings reveal that although they are primarily

post-transcriptional regulators, miRNAs can be involved in more complex loops of gene expression regulation, for instance by acting upstream of transcriptional regulators, possibly by promoting relatively subtle shifts in their expression levels.

miRNAs in peripheral B-cell development and function

Terminal B-cell differentiation takes place in the spleen and peripheral lymphoid tissues and serves to improve the competence and diversify the effector functions of B lymphocytes. Bone-marrow-derived immature B cells transit in the periphery to their final maturation through a number of transitional stages and give rise to either follicular (FO) or marginal zone (MZ) B cells (*Fig. 1*). These subsets are functionally distinct: FO cells are mainly localized in B-cell follicles and mount classical, T-cell-dependent responses, whereas MZ B cells reside in the marginal zone areas of the spleen and can respond rapidly to blood-borne pathogens (73, 74). This maturational transition is associated with the peripheral B-cell tolerance checkpoint that constrains the generation of lymphocytes expressing autoreactive BCRs (75). The FO versus MZ fate decision is functionally coupled to BCR signaling (74, 76), and it has been suggested that B cells bearing autoreactive BCRs are preferentially driven to an MZ fate (77, 78). When FO B cells encounter an antigen they can engage in the GC reaction, a complex biological process that generates long-lived memory B cells and plasma cells. At the molecular level, this GC program involves two reactions that further diversify the Ig genes, somatic hypermutation (SHM), and class switch recombination (CSR), both of which are initiated by the activity of activation-induced deaminase (AID). SHM introduces nucleotide changes in the V(D)J rearranged variable region of the IgH and IgL chains, allowing the production of B cells with a higher affinity for antigen. CSR is a region-specific recombination reaction that replaces the primary μ constant region with a downstream constant region, giving rise to antibodies with different isotypes and therefore more specialized effector functions (reviewed in 79–82). AID-mediated diversification of the Ig genes entails the generation of DNA mutations or DSB intermediates. However, AID activity can also introduce mutations and generate DSB in other genes. Remarkably, these DSB intermediates have been shown to promote the generation of chromosomal translocations that juxtapose the Ig *loci* to heterologous genomic sites, including oncogenes, which are known to have lymphomagenic potential (83–87). This bystander effect of AID activity establishes a direct connection with the high propensity of germinal center B cells to undergo lymphomagenic transformation. Finally, B cells exit the GC as antibody-secreting plasma cells or long-lived memory B cells (*Fig. 1*).

Work from several groups has helped to characterize the miRNA expression profiles of mature human and mouse B-cell subsets. Two major studies analyzed miRNA expression profiles in B cells by small RNA library sequencing. Tuschl and coworkers (88) sequenced 250 small RNA libraries from different organ systems, including 98 small RNA libraries from the human hematopoietic system. This work provided miRNA cloning frequency data from human total bone marrow, mature B lymphocytes, and hematopoietic tumor biopsy samples, as well as from naive and *in vitro*-stimulated mouse spleen B lymphocytes. An important finding of this analysis is that only a third of the analyzed miRNAs were expressed with a high degree of tissue- or cell-type specificity (88). An independent study focused on identifying the human mature B-cell miRNome and generated small RNA libraries from naive, GC, and memory human B cells and from a Burkitt lymphoma cell line. This study identified 178 miRNAs expressed in normal or transformed B-cell libraries, including 75 previously unreported miRNAs. Interestingly, this work revealed that a large fraction of the most abundant miRNAs is shared by naive and memory B cells. In contrast, GC B cells have a more distinct miRNA profile, suggesting specific functions of these miRNAs in this B-cell type (89). More recently, Cassellas and coworkers (90) combined miRNA-, mRNA-, and ChiP-Seq next-generation sequencing techniques to further characterize the miRNome during lymphopoiesis. In the context of B lymphocytes, they analyzed miRNA expression of essentially all stages of mouse B-cell ontogeny from pro-B cells to terminally differentiated plasma cells, as well as all the mature human B-cell subsets. In addition, their data showed that miRNA expression is tightly regulated by epigenetic, transcriptional, and post-transcriptional mechanisms during mouse lymphopoiesis (90). Together, these studies provide an invaluable resource for singling out miRNAs that might play important roles in B-cell differentiation and function. In this regard, it would be extremely useful to perform a bioinformatics analysis to carefully compare the sensitivity of these analyses and the conservation of miRNA expression in humans and mouse.

Two studies have used conditional Dicer ablation to address the effect of total miRNA depletion in mature B cells. To analyze the impact of miRNA depletion on terminal B-cell differentiation, our group generated a CD19-Cre$^{Ki/+}$Dicer$^{fl/fl}$ mouse model (91). CD19-Cre promotes progressive deletion in the B-cell lineage, which is completed at late stages of

bone marrow differentiation (92). Dicer ablation in CD19-Cre$^{Ki/+}$Dicer$^{fl/fl}$ mice did not significantly alter bone marrow differentiation, but resulted in a decrease in the generation of mature splenic and lymph node B cells. Peripheral B-cell subsets were altered in CD19-Cre$^{Ki/+}$Dicer$^{fl/fl}$ mice, with reduced numbers of conventional FO B cells and a relatively increased proportion of MZ B cells. To examine the miRNAs that might determine the FO versus MZ B-cell fate, we compared miRNA expression profiles in control FO and MZ cells by microarray analysis. Strikingly, all differentially expressed miRNAs were expressed at higher amounts in FO B cells than in MZ B cells, suggesting that miRNAs are more determinant players in FO B-cell differentiation. Bioinformatics analysis was conducted to determine whether genes with a known role in FO- versus MZ-cell generation were among the predicted targets of the differentially expressed miRNAs; this analysis predicted that miR-185, a miRNA overexpressed in FO B cells, would target Btk, a kinase that transduces signals downstream of the BCR. Btk has been shown to be involved in the generation or recruitment of autoreactive B cells to the MZ area (78). We found that overexpression of miR-185 in primary B cells decreased Btk expression and that, conversely, Btk expression was increased in Dicer-deficient B cells. In the absence of Dicer, BCR signaling was enhanced, as measured by the levels of Erk phosphorylation and the rate of CSR in *in vitro*-stimulated B cells. In addition, Btk overexpression in wildtype cells increased, whereas miR-185 expression decreased, CSR efficiency upon BCR stimulation. These results show that miR-185 inhibits BCR signaling through Btk downregulation and suggest that altered BCR signaling is responsible for the biased selection and commitment of CD19-Cre$^{Ki/+}$Dicer$^{fl/fl}$ peripheral B cells. This notion was further reinforced by the finding that CD19-Cre$^{Ki/+}$Dicer$^{fl/fl}$ peripheral cells express a skewed BCR repertoire, suggesting that the establishment of tolerance is incomplete in Dicer-deficient B cells. Dicer deficiency promoted increased titers of autoantibodies in aged females, which led to immune complex depositions in kidney sections, lymphocyte infiltration, and overall damage of glomerulus architecture, characteristic of autoimmune disease (91). In agreement with these findings, Hendriks and coworkers (93) recently reported an autoimmune pathology in transgenic mice overexpressing Btk in B cells. These authors developed two transgenic mouse models for Btk overexpression in the B-cell lineage that achieved a three- to sevenfold increase of Btk levels. Their analysis revealed that Btk-overexpressing B cells are selectively hyperresponsive to BCR signaling and show enhanced Ca^{2+} influx, NF-κB activation, resistance to Fas-mediated apoptosis, and defective elimination of self-reactive B cells. These mice, accordingly, develop a systemic lupus erythematosus (SLE)-like autoimmune disorder, characterized by autoantibody formation, kidney damage, and perivascular lymphocyte infiltration. However, the autoimmune syndrome of these mice is not identical to that found in the CD19-Cre$^{Ki/+}$Dicer$^{fl/fl}$ model, as Btk transgenic mice do not show gender-biased disease. This difference could be due to variations in the levels of Btk overexpression in B cells in the two models, to variations in strain susceptibility to develop autoimmune disease, or to the contribution of other dysregulated genes in the Dicer-deficient model. Moreover, in the collagen-induced arthritis and MRL-Fas(lpr) lupus models, treatment with a selective Btk inhibitor reduces autoantibody production and the development of autoimmune disease (94). Thus, different reports provide evidence that the regulation of Btk expression levels in B cells plays an important role in the development of autoimmune disorders. Together, our results have revealed a crucial role for miRNAs in terminal B-cell differentiation and the establishment of B-cell tolerance (*Fig.* 2).

A second study developed Aicda-Cre$^{Ki/+}$Dicer$^{fl/fl}$ mice to address the impact of global miRNA depletion on the differentiation of antigen-activated B cells in the context of GC responses (95). In this model, Cre recombinase expression is under the physiological control of AID expression, so that Dicer is depleted specifically in antigen-activated B cells. This study showed that the absence of miRNAs severely compromises the GC response and that no memory B and plasma antibody-secreting cells are generated in AicdaCre$^{Ki/+}$Dicer$^{fl/fl}$ mice, establishing that miRNAs are essential for the B-cell response to T-dependent antigens. This is in part due to a defect in the proliferation of Dicer-deficient GC B cells, which expressed high levels of several negative regulators of genes involved in cell proliferation, including eight cyclin-dependent kinase inhibitory (CDKi) genes. Importantly, the authors found that a high proportion of the miRNAs reported to be expressed at high levels in GC B cells (90) were predicted to target all eight CDKi genes examined. The authors also showed that Dicer-deficient GC B cells have an increased apoptosis rate and expressed high levels of the pro-apoptotic molecule Bim (95). This study demonstrates that miRNAs are essential for antigen-dependent immunization responses and exemplify the complexity of the effects that miRNAs can induce in a particular cellular context (*Fig.* 2).

The role of several individual miRNAs expressed in the B-cell lineage has been studied using different genetic gain- and loss-of-function approaches in *in vitro* and *in vivo* models.

One of the most extensively studied miRNAs in mature B cells is miR-155. miR-155 has emerged as a pivotal miRNA in the hematopoietic system and has a significant impact on the biology of multiple immune cells, including B and T lymphocytes, monocytes, dendritic cells, and natural killer cells (96–101), and also plays an oncogenic role in some of these lineages (99, 102–104). miR-155 is expressed in mature B cells and is upregulated in GC B cells as well as in *in vitro*-activated B cells (89, 90, 97, 105). Three independent studies showed that miR-155 is required for the GC response (96, 97, 106). miR-155-germline-deficient mice have an impaired humoral response to immunization, resulting in reduced numbers of GC B cells and reduced amounts of secreted switched antigen-specific antibodies (96, 97). In contrast, mice that conditionally overexpress miR-155 in mature B cells had increased numbers of GC B cells and showed high antigen-specific antibody secretion upon T-cell-dependent immunization (97). Functional characterization of the cell subsets involved in the GC response showed that miR-155 was required for the proper function of DC, T, and B cells (96, 97). *In vitro*, stimulation of miR155$^{-/-}$ B cells resulted in reduced IgG1 production (96) and defective secretion of cytokines (TNF and LT-α) known to be critical for GC formation (97). Confirming these results, analysis of miR155$^{-/-}$ mouse chimeras showed that *in vivo* B cells require miR-155 for the production of switched and high-affinity antibodies in a cell-autonomous manner (106). The gene expression profile of wildtype and miR155$^{-/-}$ B cells revealed that miR-155 regulates many genes in activated B cells (101 genes were significantly increased in miR-155-deficient B cells) (106), a significant proportion of which presumably are direct miR-155 targets (60 of them contain at least one seed match for miR-155 in their 3′ UTR). Two of these putative miR-155 targets have been confirmed. Turner and coworkers (106) showed that the transcription factor PU.1 is a direct target of miR-155 in activated B cells and that its overexpression impairs CSR in *in vitro*-stimulated wildtype B cells. PU.1 had previously been implicated in early B-cell differentiation (72) and in the signaling pathway downstream of the BCR (107). These results therefore add a new role for PU.1 in the B-cell lineage, presumably as a negative regulator of plasma cell differentiation controlled by miR-155. Interestingly, the other characterized target of miR-155 in activated B cells is AID, the enzyme that initiates SHM and CSR. miR-155 is one of the top miRNAs predicted to target AID by algorithms such as TargetScan and miRanda. To assess whether AID is a direct target of miR-155 in B cells, Nussenzweig and coworkers (43) generated a knock-in mouse model in which the conserved miR-155 binding site in the 3′ UTR of the AID gene was mutated (Aicda^{155}). Aicda^{155} B cells showed a modest increase in AID levels (two- to threefold higher than controls), demonstrating that AID is a direct target of miR-155 *in vivo*. Accordingly, Aicda^{155} B cells showed increased CSR and c-myc/IgH translocation frequency in *in vitro* stimulation assays (43). Interestingly, the increase in the c-myc/IgH translocation frequency in Aicda^{155} B cells (four- to sixfold compared with control) was lower than in miR-155$^{-/-}$ B cells (15-fold compared with control) (43), indicating that miR-155 targets additional mRNAs that cooperate to prevent AID-induced translocations in B cells. A similar mouse model was independently generated that harbored an AID BAC transgene with a mutated miR-155-binding site (44). The authors found that this mutation also resulted in higher AID expression levels *in vivo* and higher levels of CSR in *in vitro*-stimulated splenic B cells (44). In addition, the dysregulated expression of AID in these mice increased the mutation rate in an off-target gene for AID activity and was associated with impaired affinity maturation (44). Together, these two studies provide the most physiological approaches used so far for the identification of a *bona fide* miRNA target in the B-cell lineage. At the same time they reveal a functional paradox, in that although miR-155 acts globally as a positive regulator of several aspects of the GC reaction (96, 97, 106), it is at the same time a negative regulator of AID (43, 44), one of the key players in the same reaction (*Fig.* 3). Recent data provide evidence that might help to reconcile these results. Bcl-6, a transcriptional repressor required for the GC reaction, has been found to repress the expression of miR-155 (108). Although apparently counterintuitive, it is possible that miR-

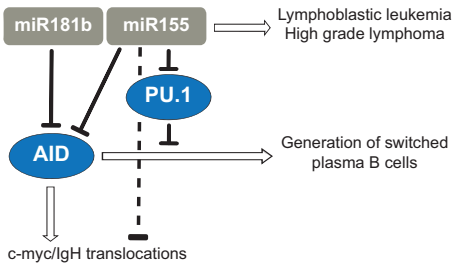

***Fig.* 3. Roles of miR-181b and miR-155 in mature B cells.** miR-181b and miR-155 target AID, an essential enzyme for CSR and SHM in GC B cells that can also promote the generation of oncogenic chromosomal c-myc/IgH translocations. Moreover, miR-155 inhibits the generation of c-myc/IgH translocations by targeting other, not yet identified, genes. miR-155 is also required for the GC response and promotes the generation of class-switched cells by targeting the transcription factor PU.1. In addition, miR-155 overexpression in B cells has been shown to induce B-cell lymphomagenesis.

155 and Bcl-6 are required at different times during the GC reaction. Two functionally and anatomically distinct areas can be distinguished in GCs, called light (LZ) and dark (DZ) zones. The DZ is the main location for B-cell clonal expansion and antigen receptor diversification, whereas the LZ is the site of antigen-driven selection. B cells perform iterative migratory cycles between the two zones to achieve affinity maturation (109). Bcl-6 might act as a positive regulator of AID expression and presumably other GC genes through miR-155 repression in the DZ, and conversely miR-155 expression in the LZ might regulate other aspects of the GC reaction, for instance by inhibiting PU.1. According to this speculation, miR-155 activity would therefore be spatiotemporally compartmentalized to provide various fine regulatory checkpoints during B-cell activation.

AID expression is regulated by yet another miRNA, miR-181b (35). miR-181b was identified in a screen of 150 miRNA clones aimed at identifying miRNAs involved in the regulation of the GC reaction. Ectopic expression of miR-181b during B-cell activation profoundly decreased the CSR rate. miR-181b expression levels are regulated concomitantly with B-cell activation (35, 90). The CSR impairment induced by miR-181b was not caused by altered proliferation, survival, or plasma cell differentiation. To identify putative miR-181b targets, we profiled mRNA expression shifts upon miR-181b overexpression. We found that 20% of the mRNAs expressed in B cells were downregulated in miR-181b expressing cells and that 60% of them contained miR-181b seed sequences in their 3′ UTRs. Interestingly, AID was one of the most downregulated of the mRNAs that contained miR-181b seed sequences. mir-181b overexpression reduced AID protein levels to approximately 50% of the levels found in control B cells. This reduction is physiologically relevant, as AID expression levels in activated B cell are limiting both for the CSR reaction and for the generation of c-myc/IgH chromosome translocations, as revealed in $AID^{+/-}$ mice (110, 111). In turn, the reduction in AID levels promoted by miR-181b parallels decreased efficiency in CSR. We further showed that the putative binding sequences in the AID 3′ UTR can be directly targeted by miR-181b. Interestingly, AID and miR-181b have complementary expression profiles, with AID levels low in resting B cells and increasingly sharply in CSR-stimulated B cells, whereas miR-181b expression is highest in non-stimulated cells and drops upon stimulation. The same complementary expression pattern was found when miR-181b and AID expression levels were analyzed in a collection of Burkitt, mantle cell lymphoma, and diffuse large B-cell lymphoma (DLBCL) human B-cell lines, supporting the idea that high expression of miR-181b prevents the accumulation of high levels of AID transcripts (35). Overall, these studies suggest that AID levels in B cells are controlled by different miRNAs with non-overlapping functions, so that whereas miR-181b would prevent premature AID activity in resting B cells and allow proper AID transcriptional activation upon stimulation, miR-155 would prevent excessive accumulation of AID transcripts in activated B cells (*Fig.* 3).

Other miRNAs have been implicated in the regulation of different aspects of mature B-cell biology, including the GC reaction and plasma B-cell differentiation. miR-125b, a highly expressed miRNA in macrophages that participates in myeloid differentiation and myeloid leukemia (112, 113), is also specifically expressed in a subset of GC B cells (114, 115). miR-125b was shown to directly target BLIMP1 (B-lymphocyte-induced maturation protein-1) and IRF4 (interferon regulatory factor-4), two transcription factors essential for post-GC plasma B-cell differentiation (114–116). Accordingly, overexpression of miR-125b in B cells inhibited plasma B-cell differentiation and Ig secretion *in vitro* (114). This miRNA could therefore enhance B-cell diversification during the GC response by limiting their premature differentiation into plasma cells. Another miRNA implicated in mature B-cell function is miR-150, in addition to its role during B-cell differentiation. miR-150 expression is tightly regulated during B-cell differentiation, being low in developing B cells, peaking in mature B cells, and dropping upon B-cell activation (66). Rajewsky and coworkers (66) reported that $miR150^{-/-}$ mice show increased secretion of antigen-specific Igs in T-cell-dependent responses. Their data suggest that this may be due to enhanced expression of c-Myb in GC B cells. This is supported by the increased expression of the prosurvival protein Bcl2, a direct c-Myb target gene, and the reduction in cell death observed in activated $mir150^{-/-}$ B cells upon IgM cross-linking (66). In addition, we recently identified miR-217 as a novel positive regulator of GC reactions, finding that its expression is upregulated in activated and GC B cells (authors' unpublished observations). To study miR-217 function in mature B cells *in vivo*, we generated B-cell-specific gain- and loss-of-function mouse models. miR-217 overexpression in B cells enhances T-cell-dependent immunization responses, improving the efficiency of GC formation, CSR and SHM, as well as the generation of plasma and terminally differentiated memory B cells. Conversely, when we inhibited endogenous miR-217 expression in B cells the generation of class-switched cells was diminished, and the efficiency of SHM was lower than in control cells. These results show that miR-217 plays a physiological role

in the secondary diversification of Ig genes in the context of the GC reaction (*Fig. 1*).

Several miRNAs have been identified that regulate terminal B-cell differentiation and function, including antigen-dependent and -independent antibody repertoire diversification and the establishment of B-cell tolerance. These regulatory schemes often involve mild changes in gene expression, which, however, result in profound functional alterations. In addition, expression profiling of miRNAs during B-cell activation allows predicting that new players will emerge with critical roles in these events. Dissecting their functional interrelationships will undoubtedly be an exciting challenge.

miRNAs in B-cell lymphomas

Dysregulation of miRNA expression is a common event in cancer, including B-cell lymphomas, and miRNA profiling is increasingly recognized as a valuable tool for cancer classification (117–121). Formal proof of the direct role of miRNAs in B-cell lymphoma development came from the generation of mouse models in which alterations to miRNA expression levels had an impact on B-cell lymphoma incidence. These studies revealed that miRNAs can function both as oncogenes (oncomiRs) and as tumor suppressor genes.

In the first study to demonstrate that miRNAs could promote lymphomagenesis, enforced expression of the miR-17~92 polycistron in hematopoietic stem cells from Eμ-myc transgenic mice accelerated the generation of B-cell lymphomas when these cells were transplanted into lethally irradiated recipient animals (54). In contrast, overexpression of miR-17~92 in wildtype lymphocytes did not induce frank B-cell lymphomas, although these mice died prematurely from lymphoproliferative disease and autoimmunity (122), indicating that the miR-17~92 cluster contributes to but it is not sufficient for lymphomagenesis *in vivo*. Lymphoproliferation and autoimmunity were due partly to repression of the tumor suppressor PTEN and the pro-apoptotic protein Bim, exerted directly by miR-17~92 in lymphocytes (53, 55, 122). When the tumorigenic potential of the individual miRNAs of the miR-17~92 polycistron was assessed in the Eμ-myc B-cell lymphoma model, miR-19 emerged as the key proto-oncogenic component (123, 124). The proto-oncogenic activity of miR-19 was shown, at least in part, to be due to its promotion of cell survival through the repression of the tumor suppressor PTEN and the activation of the AKT mTOR pathway (123, 124).

In contrast to miR-17~92, overexpression of miR-155 in developing B cells is sufficient for neoplasia development (104). miR-155 expression is increased in various lymphoid malignancies, including chronic lymphocytic leukemia (CLL) and DLBCL (102, 124). The oncogenic potential of miR-155 was assessed in B-cell-specific Eμ/V_H miR-155 transgenic mice, which develop transplantable acute lymphoblastic leukemia (ALL)/high-grade lymphoma in which SHIP and C/EBPβ downregulation by miR-155 could be functionally relevant (104, 126, 127). miR-155 might promote B-cell lymphomagenesis by targeting additional proteins, including HGAL, an inhibitor of lymphocyte cell motility (128), and SMAD5, whose downregulation renders lymphoma cells resistant to the growth-inhibitory effects of TGFβ pathway (129). Other targets that might contribute to the proto-oncogenic potential of miR-155 include the mismatch repair proteins Msh2, Msh6, and Mlh1 (130), or other proliferation-related genes (131), which could endow miR-155 with mutator activity. miR-155 is thus a miRNA with lymphomagenic potential, although the exact mechanism by which it promotes transformation is far from being understood and seems to involve several different targets and pathways. It also remains unknown whether AID and PU.1, known to be targeted by miR-155, play a negative or positive role in the development of miR-155-induced lymphomagenesis or, alternatively, if miR-155 regulates different targets at distinct developmental stages.

An interesting new concept in the oncomiR field arose from the work of Slack and collaborators (132), who showed that miR-21 contributes not only to the development of lymphoma but also to tumor maintenance. miR-21 is overexpressed in most tumor types, including B-cell malignancies (119, 133–135). A combination of Cre and Tet-off technologies was used to generate a mouse model that allowed conditional and inducible miR-21 overexpression in neural stem cells and the hematopoietic system (132). miR-21 overexpression in this mouse model promoted the generation of a transplantable pre-B-cell lymphoma (132). Notably, switching off miR-21 expression in established tumors caused a rapid tumor regression mediated by a combination of apoptosis and proliferative arrest (132). These results demonstrate that miR-21 is a genuine oncogene and present the first case of 'oncomiR addiction', which may open new avenues for therapy.

Other studies have evidenced the proto-oncogenic role of various miRNAs in B-cell lymphomas. miR-29, a miRNA whose expression is dysregulated in B-CLL, induces the generation of a $CD5^+$ B-CLL-like disease when overexpressed in Eμ-miR-29 transgenic mice (136). miR-125b, a GC miRNA that is overexpressed in B-cell precursor ALL and DLBCL

(115, 137, 138), induces clonal B-cell lymphomas in Eμ-miR-125b transgenic mice (137). Finally, miR-217, a positive regulator of the GC reaction, promotes the generation of mature B-cell lymphomas in a B-cell-specific overexpression mouse model, establishing a functional link between the physiology of this developmental program and the molecular events leading to lymphomagenesis (authors' unpublished results).

miRNA profiling in lymphomas reveals that particular miRNAs are located in genomic regions that are frequently deleted in cancer (139–141). However, the first evidence that miRNAs could function as tumor suppressors in B-cell lymphomas *in vivo* came from the work of Mendell and coworkers (20), who showed that c-myc-induced repression of a set of miRNAs contributed to lymphoma growth. These authors found that Myc induction in two models of B-cell lymphoma resulted in widespread downregulation of miRNA expression, presumably via direct binding to their promoters (20). Importantly, re-expression of a set of c-myc repressed miRNAs including mi-R34a, miR-150, miR-195/497, and miR-15a/16-1, abrogated the tumorigenic potential of B-cell lymphoma cells in SCID (sever combined immunodeficient) mice (20). Conditional knockout models have been used to directly assess the contribution to B lymphomagenesis of the minimal deleted region (MDR) within 13q14, which is deleted in more than 50% of B-CLL (142). MDR-13q14 encodes the DLEU2, a long non-coding RNA, and the miR15a/16 cluster (5, 139). Interestingly, mice in which only the miRNA cluster was deleted showed a clonal preleukemic expansion of $CD5^+$ B cells, whereas mice in which the MDR was deleted developed a more aggressive CLL-like disease (142). This study further showed that the miR15a/16-1 cluster limits the proliferation of B cells by targeting multiple genes involved in the G_0/G_1-S phase transition (142). However, the more aggressive phenotype of MDR-deleted mice suggests that additional genetic elements within the MDR locus contribute to the tumor suppressive function. Another study revealed a role for a set of p53-induced miRNAs in multiple myeloma (MM), a neoplasm of plasma B cells (143). The tumor suppressor p53 promotes the expression of miR-192, miR-194, and miR-215, which in turn directly target MDM2, a negative regulator of p53 (143). This regulatory loop could be valuable, as re-expression of these miRNAs in MM cell lines increased the therapeutic action of a MDM2 inhibitor *in vitro* and in a mouse xenograft model (143). In addition, this set of miRNAs impaired the migration and invasion of MM cell lines in NOD-SCID mice through the inhibition of IGF-1 and IGF1-R (143). Finally, miR-146a has been shown to function as a tumor suppressor miRNA for myeloid and B cells *in vivo* (144). miR-146a is expressed in various immune cell types, and its expression is deregulated in different cancers, including DLBCL and CLL B-cell lymphomas (115, 145, 146). Germline miR-146a-deficient mice develop a chronic inflammatory phenotype that progresses to splenic myeloid sarcoma and, less frequently, into B-cell lymphomas (144). The authors went on to show that this effect of miR-146a is mostly due to negative regulation of NF-κB by miR-146a, with deletion of the NF-κB p50 subunit effectively rescuing the myeloproliferative disease (144). These data provide a good example of a link between miRNA regulatory activity, inflammation, and cancer. Overall, these studies open a new perspective to the understanding of the molecular mechanisms underlying oncogenic transformation, in which miRNAs can play a fundamental, previously unforeseen role.

Concluding remarks

The last few years have seen an outburst of research into the regulation of diverse biological processes by miRNAs. Within the B-cell lineage, this effort has led to the identification of a number of miRNAs that impinge on critical differentiation or activation checkpoints, including miR-181, miR-17~92, miR-34, miR-150, and miR-155. A number of miRNAs are, moreover, now known to contribute to B-cell lymphoma development, either as oncogenes or as tumor suppressors. A considerable effort has been made in this and other fields to pinpoint individual mRNA targets that could account for the functional impact of a miRNA. However, it is already evident that miRNAs very often play pleiotropic roles in intertwined regulatory networks and that high-throughput approaches seem to be required to identify more complete sets of target genes at defined developmental stages. Continuing implementation of proteomics approaches, gene expression analysis by next-generation sequencing, and HITS-CLIP techniques will undoubtedly prove invaluable. Importantly, miRNAs are emerging as a new class of molecules with clinical potential. Their value as diagnostic and even prognostic markers is already a reality in cancer and other pathologies. Moreover, the possibility of manipulating the expression of miRNAs *in vivo* by the delivery of miRNAs or miRNA inhibitors has opened new and exciting therapeutic perspectives for the treatment of numerous diseases. We await new developments in this rapidly expanding field with anticipation.

References

1. Lee RC, Feinbaum RL, Ambros V. The C. elegans heterochronic gene lin-4 encodes small RNAs with antisense complementarity to lin-14. Cell 1993;**75**:843–854.
2. Wightman B, Ha I, Ruvkun G. Posttranscriptional regulation of the heterochronic gene lin-14 by lin-4 mediates temporal pattern formation in C. elegans. Cell 1993;**75**:855–862.
3. Reinhart BJ, et al. The 21-nucleotide let-7 RNA regulates developmental timing in Caenorhabditis elegans. Nature 2000;**403**:901–906.
4. Pasquinelli AE, et al. Conservation of the sequence and temporal expression of let-7 heterochronic regulatory RNA. Nature 2000;**408**:86–89.
5. Lagos-Quintana M, Rauhut R, Lendeckel W, Tuschl T. Identification of novel genes coding for small expressed RNAs. Science 2001;**294**: 853–858.
6. Lau NC, Lim LP, Weinstein EG, Bartel DP. An abundant class of tiny RNAs with probable regulatory roles in Caenorhabditis elegans. Science 2001;**294**:858–862.
7. Lee RC, Ambros V. An extensive class of small RNAs in Caenorhabditis elegans. Science 2001;**294**:862–864.
8. Bartel DP. MicroRNAs: target recognition and regulatory functions. Cell 2009;**136**:215–233.
9. Liu Q, Paroo Z. Biochemical principles of small RNA pathways. Annu Rev Biochem 2010;**79**:295–319.
10. Ebert MS, Sharp PA. Roles for microRNAs in conferring robustness to biological processes. Cell 2012;**149**:515–524.
11. Krol J, Loedige I, Filipowicz W. The widespread regulation of microRNA biogenesis, function and decay. Nat Rev Genet 2010;**11**:597–610.
12. Yang JS, Lai EC. Alternative miRNA biogenesis pathways and the interpretation of core miRNA pathway mutants. Mol Cell 2011;**43**:892–903.
13. van Kouwenhove M, Kedde M, Agami R. MicroRNA regulation by RNA-binding proteins and its implications for cancer. Nat Rev Cancer 2011;**11**:644–656.
14. Voinnet O. Origin, biogenesis, and activity of plant microRNAs. Cell 2009;**136**:669–687.
15. Pasquinelli AE. MicroRNAs and their targets: recognition, regulation and an emerging reciprocal relationship. Nat Rev Genet 2012;**13**:271–282.
16. Ozsolak F, et al. Chromatin structure analyses identify miRNA promoters. Genes Dev 2008;**22**:3172–3183.
17. Corcoran DL, Pandit KV, Gordon B, Bhattacharjee A, Kaminski N, Benos PV. Features of mammalian microRNA promoters emerge from polymerase II chromatin immunoprecipitation data. PLoS ONE 2009;**4**:e5279.
18. O'Donnell KA, Wentzel EA, Zeller KI, Dang CV, Mendell JT. c-Myc-regulated microRNAs modulate E2F1 expression. Nature 2005;**435**:839–843.
19. He L, et al. A microRNA component of the p53 tumour suppressor network. Nature 2007;**447**:1130–1134.
20. Chang TC, et al. Widespread microRNA repression by Myc contributes to tumorigenesis. Nat Genet 2008;**40**:43–50.
21. Ma L, et al. miR-9, a MYC/MYCN-activated microRNA, regulates E-cadherin and cancer metastasis. Nat Cell Biol 2010;**12**:247–256.
22. Melnyk CW, Molnar A, Baulcombe DC. Intercellular and systemic movement of RNA silencing signals. EMBO J 2011;**30**:3553–3563.
23. Valadi H, Ekstrom K, Bossios A, Sjostrand M, Lee JJ, Lotvall JO. Exosome-mediated transfer of mRNAs and microRNAs is a novel mechanism of genetic exchange between cells. Nat Cell Biol 2007;**9**:654–659.
24. Mittelbrunn M, et al. Unidirectional transfer of microRNA-loaded exosomes from T cells to antigen-presenting cells. Nat Commun 2011;**2**:282.
25. Mittelbrunn M, Sanchez-Madrid F. Intercellular communication: diverse structures for exchange of genetic information. Nat Rev Mol Cell Biol 2012;**13**:328–335.
26. Bernstein E, et al. Dicer is essential for mouse development. Nat Genet 2003;**35**:215–217.
27. Xiao C, Rajewsky K. MicroRNA control in the immune system: basic principles. Cell 2009;**136**:26–36.
28. Belver L, Papavasiliou FN, Ramiro AR. MicroRNA control of lymphocyte differentiation and function. Curr Opin Immunol 2011;**23**:368–373.
29. Cheloufi S, Dos Santos CO, Chong MM, Hannon GJ. A dicer-independent miRNA biogenesis pathway that requires Ago catalysis. Nature 2010;**465**:584–589.
30. Cifuentes D, et al. A novel miRNA processing pathway independent of Dicer requires Argonaute2 catalytic activity. Science 2010;**328**:1694–1698.
31. Yang JS, et al. Conserved vertebrate mir-451 provides a platform for Dicer-independent, Ago2-mediated microRNA biogenesis. Proc Natl Acad Sci U S A 2010;**107**:15163–15168.
32. Pritchard CC, Cheng HH, Tewari M. MicroRNA profiling: approaches and considerations. Nat Rev Genet 2012;**13**:358–369.
33. Mullokandov G, et al. High-throughput assessment of microRNA activity and function using microRNA sensor and decoy libraries. Nat Methods 2012;**9**:840–846.
34. de Yebenes VG, Ramiro AR. MicroRNA activity in B lymphocytes. Methods Mol Biol 2010;**667**:177–192.
35. de Yebenes VG, et al. miR-181b negatively regulates activation-induced cytidine deaminase in B cells. J Exp Med 2008;**205**:2199–2206.
36. Casola S. Mouse models for miRNA expression: the ROSA26 locus. Methods Mol Biol 2010;**667**:145–163.
37. O'Connell RM, Rao DS, Chaudhuri AA, Baltimore D. Physiological and pathological roles for microRNAs in the immune system. Nat Rev Immunol 2010;**10**:111–122.
38. Gentner B, et al. Stable knockdown of microRNA in vivo by lentiviral vectors. Nat Methods 2009;**6**:63–66.
39. Chaudhuri AA, et al. Oncomir miR-125b regulates hematopoiesis by targeting the gene Lin28A. Proc Natl Acad Sci USA 2012;**109**:4233–4238.
40. Rao DS, O'Connell RM, Chaudhuri AA, Garcia-Flores Y, Geiger TL, Baltimore D. MicroRNA-34a perturbs B lymphocyte development by repressing the forkhead box transcription factor Foxp1. Immunity 2010;**33**:48–59.
41. Chi SW, Zang JB, Mele A, Darnell RB. Argonaute HITS-CLIP decodes microRNA-mRNA interaction maps. Nature 2009;**460**:479–486.
42. Hafner M, et al. Transcriptome-wide identification of RNA-binding protein and microRNA target sites by PAR-CLIP. Cell 2010;**141**:129–141.
43. Dorsett Y, et al. MicroRNA-155 suppresses activation-induced cytidine deaminase-mediated Myc-Igh translocation. Immunity 2008;**28**:630–638.
44. Teng G, et al. MicroRNA-155 is a negative regulator of activation-induced cytidine deaminase. Immunity 2008;**28**:621–629.
45. Lim LP, et al. Microarray analysis shows that some microRNAs downregulate large numbers of target mRNAs. Nature 2005;**433**:769–773.
46. Baek D, Villen J, Shin C, Camargo FD, Gygi SP, Bartel DP. The impact of microRNAs on protein output. Nature 2008;**455**:64–71.
47. Selbach M, Schwanhausser B, Thierfelder N, Fang Z, Khanin R, Rajewsky N. Widespread changes in protein synthesis induced by microRNAs. Nature 2008;**455**:58–63.
48. Rajewsky K. Clonal selection and learning in the antibody system. Nature 1996;**381**:751–758.
49. Chen CZ, Li L, Lodish HF, Bartel DP. MicroRNAs modulate hematopoietic lineage differentiation. Science 2004;**303**:83–86.
50. Li QJ, et al. miR-181a is an intrinsic modulator of T cell sensitivity and selection. Cell 2007;**129**:147–161.
51. Ebert PJ, Jiang S, Xie J, Li QJ, Davis MM. An endogenous positively selecting peptide enhances mature T cell responses and becomes an autoantigen in the absence of microRNA miR-181a. Nat Immunol 2009;**10**:1162–1169.
52. Fragoso R, et al. Modulating the strength and threshold of NOTCH oncogenic signals by mir-181a-1/b-1. PLoS Genet 2012;**8**:e1002855.
53. Koralov SB, et al. Dicer ablation affects antibody diversity and cell survival in the B lymphocyte lineage. Cell 2008;**132**:860–874.
54. He L, et al. A microRNA polycistron as a potential human oncogene. Nature 2005;**435**:828–833.
55. Ventura A, et al. Targeted deletion reveals essential and overlapping functions of the miR-17 through 92 family of miRNA clusters. Cell 2008;**132**:875–886.
56. Chang TC, et al. Transactivation of miR-34a by p53 broadly influences gene expression and promotes apoptosis. Mol Cell 2007;**26**:745–752.
57. Raver-Shapira N, et al. Transcriptional activation of miR-34a contributes to p53-mediated apoptosis. Mol Cell 2007;**26**:731–743.

58. Hermeking H. The miR-34 family in cancer and apoptosis. Cell Death Differ 2010;**17**: 193–199.
59. Concepcion CP, et al. Intact p53-dependent responses in miR-34-deficient mice. PLoS Genet 2012;**8**:e1002797.
60. Hu H, et al. Foxp1 is an essential transcriptional regulator of B cell development. Nat Immunol 2006;**7**:819–826.
61. Martin F, Kearney JF. B1 cells: similarities and differences with other B cell subsets. Current Opin Immunol 2001;**13**:195–201.
62. Montecino-Rodriguez E, Dorshkind K. B-1 B cell development in the fetus and adult. Immunity 2012;**36**:13–21.
63. Thomas MD, Kremer CS, Ravichandran KS, Rajewsky K, Bender TP. c-Myb is critical for B cell development and maintenance of follicular B cells. Immunity 2005;**23**:275–286.
64. Monticelli S, et al. MicroRNA profiling of the murine hematopoietic system. Genome Biol 2005;**6**:R71.
65. Zhou B, Wang S, Mayr C, Bartel DP, Lodish HF. miR-150, a microRNA expressed in mature B and T cells, blocks early B cell development when expressed prematurely. Proc Natl Acad Sci USA 2007;**104**:7080–7085.
66. Xiao C, et al. MiR-150 controls B cell differentiation by targeting the transcription factor c-Myb. Cell 2007;**131**:146–159.
67. Mondol V, Pasquinelli AE. Let's make it happen: the role of let-7 microRNA in development. Curr Topics Cell Dev Biol 2012;**99**:1–30.
68. Thornton JE, Gregory RI. How does Lin28 let-7 control development and disease? Trends Cell Biol 2012;**22**:474–482.
69. Viswanathan SR, Daley GQ. Lin28: a microRNA regulator with a macro role. Cell 2010;**140**:445–449.
70. Buganim Y, et al. Single-cell expression analyses during cellular peprogramming reveal an early stochastic and a late hierarchic phase. Cell 2012;**150**:1209–1222.
71. Yuan J, Nguyen CK, Liu X, Kanellopoulou C, Muljo SA. Lin28b reprograms adult bone marrow hematopoietic progenitors to mediate fetal-like lymphopoiesis. Science 2012;**335**:1195–1200.
72. Busslinger M. Transcriptional control of early B cell development. Annu Rev Immunol 2004;**22**:55–79.
73. Allman D, Pillai S. Peripheral B cell subsets. Curr Opin Immunol 2008;**20**:149–157.
74. Carsetti R, Rosado MM, Wardmann H. Peripheral development of B cells in mouse and man. Immunol Rev 2004;**197**:179–191.
75. Wardemann H, Yurasov S, Schaefer A, Young JW, Meffre E, Nussenzweig MC. Predominant autoantibody production by early human B cell precursors. Science 2003;**301**:1374–1377.
76. Pillai S, Cariappa A. The follicular versus marginal zone B lymphocyte cell fate decision. Nat Rev Immunol 2009;**9**:767–777.
77. Li Y, Li H, Weigert M. Autoreactive B cells in the marginal zone that express dual receptors. J Exp Med 2002;**195**:181–188.
78. Martin F, Kearney JF. Positive selection from newly formed to marginal zone B cells depends on the rate of clonal production, CD19, and btk. Immunity 2000;**12**:39–49.
79. Stavnezer J, Guikema JE, Schrader CE. Mechanism and regulation of class switch recombination. Annu Rev Immunol 2008;**26**:261–292.
80. Di Noia JM, Neuberger MS. Molecular mechanisms of antibody somatic hypermutation. Annu Rev Biochem 2007;**76**:1–22.
81. Peled JU, et al. The biochemistry of somatic hypermutation. Annu Rev Immunol 2008;**26**:481–511.
82. de Yebenes VG, Ramiro AR. Activation-induced deaminase: light and dark sides. Trends Mol Med 2006;**12**:432–439.
83. Liu M, et al. Two levels of protection for the B cell genome during somatic hypermutation. Nature 2008;**451**:841–845.
84. Pasqualucci L, et al. Hypermutation of multiple proto-oncogenes in B-cell diffuse large-cell lymphomas. Nature 2001;**412**:341–346.
85. Ramiro AR, et al. AID is required for c-myc/IgH chromosome translocations in vivo. Cell 2004;**118**:431–438.
86. Ramiro AR, et al. Role of genomic instability and p53 in AID-induced c-myc-Igh translocations. Nature 2006;**440**:105–109.
87. Robbiani DF, et al. AID is required for the chromosomal breaks in c-myc that lead to c-myc/IgH translocations. Cell 2008;**135**:1028–1038.
88. Landgraf P, et al. A mammalian microRNA expression atlas based on small RNA library sequencing. Cell 2007;**129**:1401–1414.
89. Basso K, et al. Identification of the human mature B cell miRNome. Immunity 2009;**30**:744–752.
90. Kuchen S, et al. Regulation of microRNA expression and abundance during lymphopoiesis. Immunity 2010;**32**:828–839.
91. Belver L, de Yebenes VG, Ramiro AR. MicroRNAs prevent the generation of autoreactive antibodies. Immunity 2010;**33**:713–722.
92. Hobeika E, et al. Testing gene function early in the B cell lineage in mb1-cre mice. Proc Natl Acad Sci USA 2006;**103**:13789–13794.
93. Kil LP, et al. Btk levels set the threshold for B-cell activation and negative selection of autoreactive B cells in mice. Blood 2012;**119**: 3744–3756.
94. Honigberg LA, et al. The Bruton tyrosine kinase inhibitor PCI-32765 blocks B-cell activation and is efficacious in models of autoimmune disease and B-cell malignancy. Proc Natl Acad Sci USA 2010;**107**:13075–13080.
95. Xu S, Guo K, Zeng Q, Huo J, Lam KP. The RNase III enzyme Dicer is essential for germinal center B-cell formation. Blood 2012;**119**:767–776.
96. Rodriguez A, et al. Requirement of bic/microRNA-155 for normal immune function. Science 2007;**316**:608–611.
97. Thai TH, et al. Regulation of the germinal center response by microRNA-155. Science 2007;**316**:604–608.
98. Trotta R, et al. miR-155 regulates IFN-gamma production in natural killer cells. Blood 2012;**119**:3478–3485.
99. O'Connell RM, et al. Sustained expression of microRNA-155 in hematopoietic stem cells causes a myeloproliferative disorder. J Exp Med 2008;**205**:585–594.
100. O'Connell RM, Taganov KD, Boldin MP, Cheng G, Baltimore D. MicroRNA-155 is induced during the macrophage inflammatory response. Proc Natl Acad Sci USA 2007;**104**:1604–1609.
101. O'Connell RM, et al. MicroRNA-155 promotes autoimmune inflammation by enhancing inflammatory T cell development. Immunity 2010;**33**:607–619.
102. Eis PS, et al. Accumulation of miR-155 and BIC RNA in human B cell lymphomas. Proc Natl Acad Sci USA 2005;**102**:3627–3632.
103. Tili E, Croce CM, Michaille JJ. miR-155: on the crosstalk between inflammation and cancer. Int Rev Immunol 2009;**28**:264–284.
104. Costinean S, et al. Pre-B cell proliferation and lymphoblastic leukemia/high-grade lymphoma in E(mu)-miR155 transgenic mice. Proc Natl Acad Sci USA 2006;**103**:7024–7029.
105. Tam W. Identification and characterization of human BIC, a gene on chromosome 21 that encodes a noncoding RNA. Gene 2001;**274**:157–167.
106. Vigorito E, et al. microRNA-155 regulates the generation of immunoglobulin class-switched plasma cells. Immunity 2007;**27**:847–859.
107. Garrett-Sinha LA, et al. PU.1 and Spi-B are required for normal B cell receptor-mediated signal transduction. Immunity 1999;**10**:399–408.
108. Basso K, et al. BCL6 positively regulates AID and germinal center gene expression via repression of miR-155. J Exp Med 2012;**209**:2455–2465.
109. Victora GD, Nussenzweig MC. Germinal centers. Annu Rev Immunol 2012;**30**:429–457.
110. Sernandez IV, de Yebenes VG, Dorsett Y, Ramiro AR. Haploinsufficiency of activation-induced deaminase for antibody diversification and chromosome translocations both in vitro and in vivo. PLoS ONE 2008;**3**:e3927.
111. Takizawa M, et al. AID expression levels determine the extent of cMyc oncogenic translocations and the incidence of B cell tumor development. J Exp Med 2008;**205**:1949–1957.
112. O'Connell RM, Chaudhuri AA, Rao DS, Gibson WS, Balazs AB, Baltimore D. MicroRNAs enriched in hematopoietic stem cells differentially regulate long-term hematopoietic output. Proc Natl Acad Sci USA 2010;**107**:14235–14240.
113. Kim SW, Ramasamy K, Bouamar H, Lin AP, Jiang D, Aguiar RC. MicroRNAs miR-125a and miR-125b constitutively activate the NF-kappaB pathway by targeting the tumor necrosis factor alpha-induced protein 3 (TNFAIP3, A20). Proc Natl Acad Sci USA 2012;**109**:7865–7870.
114. Gururajan M, et al. MicroRNA 125b inhibition of B cell differentiation in germinal centers. Int Immunol 2010;**22**:583–592.
115. Malumbres R, et al. Differentiation stage-specific expression of microRNAs in B lymphocytes and diffuse large B-cell lymphomas. Blood 2009;**113**:3754–3764.
116. Chaudhuri AA, et al. MicroRNA-125b potentiates macrophage activation. J Immunol 2011;**187**:5062–5068.

117. Lu J, et al. MicroRNA expression profiles classify human cancers. Nature 2005;**435**:834–838.
118. Esquela-Kerscher A, Slack FJ. Oncomirs - microRNAs with a role in cancer. Nat Rev Cancer 2006;**6**:259–269.
119. Volinia S, et al. A microRNA expression signature of human solid tumors defines cancer gene targets. Proc Natl Acad Sci USA 2006;**103**:2257–2261.
120. Calin GA, Croce CM. MicroRNA signatures in human cancers. Nat Rev Cancer 2006;**6**:857–866.
121. Garzon R, Calin GA, Croce CM. MicroRNAs in Cancer. Annu Rev Med 2009;**60**:167–179.
122. Xiao C, et al. Lymphoproliferative disease and autoimmunity in mice with increased miR-17-92 expression in lymphocytes. Nat Immunol 2008;**9**:405–414.
123. Mu P, et al. Genetic dissection of the miR-17~92 cluster of microRNAs in Myc-induced B-cell lymphomas. Genes Dev 2009;**23**:2806–2811.
124. Olive V, et al. miR-19 is a key oncogenic component of mir-17-92. Genes Dev 2009;**23**:2839–2849.
125. Garzon R, Marcucci G, Croce CM. Targeting microRNAs in cancer: rationale, strategies and challenges. Nat Rev Drug Disc 2010;**9**:775–789.
126. Costinean S, et al. Src homology 2 domain-containing inositol-5-phosphatase and CCAAT enhancer-binding protein beta are targeted by miR-155 in B cells of Emicro-MiR-155 transgenic mice. Blood 2009;**114**:1374–1382.
127. Pedersen IM, et al. Onco-miR-155 targets SHIP1 to promote TNFalpha-dependent growth of B cell lymphomas. EMBO Mol Med 2009;**1**:288–295.
128. Dagan LN, Jiang X, Bhatt S, Cubedo E, Rajewsky K, Lossos IS. miR-155 regulates HGAL expression and increases lymphoma cell motility. Blood 2012;**119**:513–520.
129. Rai D, Kim SW, McKeller MR, Dahia PL, Aguiar RC. Targeting of SMAD5 links microRNA-155 to the TGF-beta pathway and lymphomagenesis. Proc Natl Acad Sci USA 2010;**107**:3111–3116.
130. Valeri N, et al. Modulation of mismatch repair and genomic stability by miR-155. Proc Natl Acad Sci USA 2010;**107**:6982–6987.
131. Tili E, et al. Mutator activity induced by microRNA-155 (miR-155) links inflammation and cancer. Proc Natl Acad Sci USA 2011;**108**:4908–4913.
132. Medina PP, Nolde M, Slack FJ. OncomiR addiction in an in vivo model of microRNA-21-induced pre-B-cell lymphoma. Nature 2010;**467**:86–90.
133. Fulci V, et al. Quantitative technologies establish a novel microRNA profile of chronic lymphocytic leukemia. Blood 2007;**109**:4944–4951.
134. Lawrie CH, et al. MicroRNA expression distinguishes between germinal center B cell-like and activated B cell-like subtypes of diffuse large B cell lymphoma. Int J Cancer 2007;**121**:1156–1161.
135. Jongen-Lavrencic M, Sun SM, Dijkstra MK, Valk PJ, Lowenberg B. MicroRNA expression profiling in relation to the genetic heterogeneity of acute myeloid leukemia. Blood 2008;**111**:5078–5085.
136. Santanam U, et al. Chronic lymphocytic leukemia modeled in mouse by targeted miR-29 expression. Proc Natl Acad Sci USA 2010;**107**:12210–12215.
137. Enomoto Y, et al. Emu/miR-125b transgenic mice develop lethal B-cell malignancies. Leukemia 2011;**25**:1849–1856.
138. Li C, et al. Copy number abnormalities, MYC activity, and the genetic fingerprint of normal B cells mechanistically define the microRNA profile of diffuse large B-cell lymphoma. Blood 2009;**113**:6681–6690.
139. Calin GA, et al. Frequent deletions and down-regulation of micro- RNA genes miR15 and miR16 at 13q14 in chronic lymphocytic leukemia. Proc Natl Acad Sci USA 2002;**99**:15524–15529.
140. Calin GA, et al. MicroRNA profiling reveals distinct signatures in B cell chronic lymphocytic leukemias. Proc Natl Acad Sci USA 2004;**101**:11755–11760.
141. Calin GA, et al. A MicroRNA signature associated with prognosis and progression in chronic lymphocytic leukemia. N Engl J Med 2005;**353**:1793–1801.
142. Klein U, et al. The DLEU2/miR-15a/16-1 cluster controls B cell proliferation and its deletion leads to chronic lymphocytic leukemia. Cancer Cell 2010;**17**:28–40.
143. Pichiorri F, et al. Downregulation of p53-inducible microRNAs 192, 194, and 215 impairs the p53/MDM2 autoregulatory loop in multiple myeloma development. Cancer Cell 2010;**18**:367–381.
144. Zhao JL, Rao DS, Boldin MP, Taganov KD, O'Connell RM, Baltimore D. NF-kappaB dysregulation in microRNA-146a-deficient mice drives the development of myeloid malignancies. Proc Natl Acad Sci USA 2011;**108**:9184–9189.
145. Visone R, et al. Karyotype-specific microRNA signature in chronic lymphocytic leukemia. Blood 2009;**114**:3872–3879.
146. Labbaye C, Testa U. The emerging role of MIR-146A in the control of hematopoiesis, immune function and cancer. J Hematol Oncol 2012;**5**:13.